TECHNISCHE UNIVERSITÄT ILMENAU
Fakultät für Informatik und Automatisierung
Fachgebiet Telematik/Rechnernetze

Dissertation

zur Erlangung des Akademischen Grades
Doktoringenieur (Dr.-Ing.)

Robust Distributed Resource Allocation for Cellular Vehicle-to-Vehicle Communication

---

vorgelegt von:	Philip Wendland
Datum der Einreichung:	2. Juli 2021
Datum der Verteidigung:	14. Februar 2022
Erster Gutachter:	Prof. Dr.-Ing. Günter Schäfer
Zweiter Gutachter:	Univ.-Prof. Dr. rer. nat. Jochen Seitz
Dritter Gutachter:	Prof. Dr.-Ing. Lars Wolf

DOI: 10.22032/dbt.51540
URN: urn:nbn:de:gbv:ilm1-2022000043

Abstract

Vehicular communication is envisaged to play a major role for the reduction of the number or severity of traffic accidents in the future. This can for example be realised by periodically exchanging status update messages to surrounding vehicles. Access technologies for this purpose based on wireless local area network (WLAN) have already been standardised and researched for years. Recently, wireless access technologies based on cellular technology gained more traction. Release 14 of the long term evolution (LTE) standard introduced support for vehicle-to-vehicle (V2V) communication. Using this long term evolution vehicle-to-everything (LTE-V2X) technology, vehicles can communicate directly without forwarding via the base station. This is important for example if no connection to the infrastructure is possible or if the desired communication distance can be reached by a local broadcast. In the distributed scheduling mode (Mode 4), vehicles select the radio resources autonomously and the base station is not involved. As single-carrier frequency division multiple access (SC-FDMA) is used at the physical layer, the media access control (MAC) protocol is different compared to WLAN-based technologies. The radio resources are divided into a fixed resource grid among the time (subframe) and frequency (subchannel) domain. Messages in V2V networks are typically periodically and locally broadcast. The MAC protocol leverages this periodicity by requiring the periodic reuse of radio resources for a certain number of times. This periodicity allows other terminals to estimate whether a radio resource will be occupied in the future.

While this MAC protocol shows some interesting performance benefits compared to access technologies based on WLAN, it has not been extensively researched yet. Recent related work as well as investigations in the context of this thesis show that LTE-V2X suffers from repeating radio frame collisions, incompatibilities with packet flows with different packet rates or sizes, ineffectiveness of distributed congestion control (DCC), and other issues. This indicates an urgent need for further improvements of this promising access technology. In addition to these issues, the new scheduling scheme potentially allows the development of new protocols that lead to additional improvements. For example, there are no mitigations for hidden-terminal effects due to the large overhead of request-to-send/clear-to-send (RTS/CTS) in broadcast scenarios.

This dissertation proposes scheduling based on acknowledgement feedback exchange (SAFE), a set of protocol enhancements that target the MAC and DCC protocol. SAFE is based on cellular technology and tries to solve the existing issues of LTE-V2X Mode 4. Moreover, it deploys a reactive and proactive mitigation for hidden-terminal effects. For this purpose, it introduces an efficient way to acknowledge radio resources. Acknowledged radio resources indicate to terminals further away that these resources are currently in use, which extends the sensing range. Unacknowledged radio resources, caused by collisions, motivate transmitters to stop reusing this radio resources and select new ones. SAFE also divides the reservations into multiple interleaved sub-reservations that use different radio resources. This allows for the use of packets of different sizes, different packet rates, and DCC without breaking the periodicity property.

The components of SAFE can be fine-tuned with various configuration parameters. Using multiple experimental designs, a set of good parameters for SAFE has been systematically determined. The subsequent evaluation shows that SAFE is able to reach a higher performance

both in terms of the packet delivery ratio (PDR) as well as under consideration of the application itself. An awareness metric that considers the application-oriented knowledge a vehicle can gain from cooperative awareness messages (CAMs) has been developed to evaluate this. Many different traffic scenarios have been studied in a system-level simulation approach. SAFE reaches higher PDR values especially in larger communication distances, indicating the benefits of the hidden-terminal mitigations. The DCC mechanism leads to higher increases of the PDR than the variant of LTE-V2X. Moreover, SAFE shows better compatibility with variable packet rates and sizes. The overhead that is necessary to transmit the acknowledgement feedback is very low and fits inside the padding bits in most situations. Hence, SAFE is a promising approach to further increase the reliability of V2V communication.

Zusammenfassung

Die Fahrzeugkommunikation wird als wichtige Komponente zur künftigen Reduzierung der Zahl oder Schwere von Verkehrsunfällen gesehen. Dies kann zum Beispiel durch ein periodisches Austauschen von Nachrichten über den aktuellen Status der Fahrzeuge realisiert werden. Funktechnologien für diese Anwendung, die auf Wireless Local Area Network (WLAN) basieren, wurden bereits vor einigen Jahren standardisiert und sind ausgiebig erforscht. Kürzlich wurden Funktechnologien vorgestellt, die auf zellulären Technologien basieren. Release 14 des Long Term Evolution (LTE) Standards führte die Unterstützung von Fahrzeug-zu-Fahrzeug-Kommunikation ein. Mit dieser Long Term Evolution Vehicle-to-Everything (LTE-V2X) Technologie können Fahrzeuge direkt miteinander kommunizieren, ohne dass dabei ein Weiterleiten über die Basisstation notwendig ist. Dies ist zum Beispiel in Fällen wichtig, in denen keine Verbindung zur Infrastruktur hergestellt werden konnte oder in denen die geforderte Kommunikationsreichweite durch einen lokalen Broadcast abgedeckt werden kann. In dem verteilten Scheduling-Modus (Modus 4) wählen die Fahrzeuge die Funkressourcen selbstständig aus und die Basisstation ist nicht involviert. Da Single-Carrier Frequency Division Multiple Access (SC-FDMA) in der physikalischen Schicht verwendet wird, ist das Media Access Control (MAC)-Protokoll anders als bei Technologien, die auf WLAN basieren. Die Funkressourcen sind in ein festes Raster in der zeitlichen (Subframe) Dimension und der Frequenz (Subchannel) eingeteilt. Nachrichten in Fahrzeug-zu-Fahrzeug-Netzwerken werden typischerweise periodisch als lokaler Broadcast verteilt. Das MAC-Protokoll nutzt diese Periodizität aus, indem es eine periodische Wiederverwendung von Funkressourcen vorschreibt. Diese Periodizität erlaubt es anderen Terminals, einzuschätzen, ob eine Funkressource in Zukunft von anderen Terminals verwendet werden wird.

Obwohl dieses MAC-Protokoll im Vergleich zu Technologien basierend auf WLAN einige interessante Vorteile hinsichtlich der Performanz aufweist, wurde es bisher noch nicht ausgiebig untersucht. Der Stand der Technik und Untersuchungen im Rahmen dieser Doktorarbeit zeigen allerdings, dass LTE-V2X unter Problemen wie sich wiederholende Kollisionen von Paketen, Inkompatibilitäten mit Paketflüssen mit variierender Paketrate oder -größe, Ineffektivität der verteilten Staukontrolle etc. leidet. Dies zeigt einen dringenden Forschungsbedarf nach Verbesserungen dieser eigentlich vielversprechenden Funktechnologie auf. Zusätzlich zu den genannten Problemen erlaubt das neue Schedulingverfahren womöglich, neue und verbesserte-Protokolle zu entwickeln, die darauf aufbauen. Zum Beispiel gibt es bei der Fahrzeugkommunikation keine Maßnahmen gegen Hidden-Terminal-Probleme, da der Kommunikationsoverhead von Request-to-Send/Clear-to-Send (RTS/CTS)-Protokollen bei Broadcast-Verkehr zu groß wird.

Diese Dissertation schlägt Scheduling based on Acknowledgement Feedback Exchange (SAFE) vor, eine Menge an Protokollverbesserungen, die sich auf das MAC- und Distributed Congestion Control (DCC)-Protokoll konzentriert. SAFE baut auf zellulären Technologien auf und versucht, die existierenden Probleme von LTE-V2X Modus 4 zu lösen. Darüber hinaus hat es eine proaktive und reaktive Gegenmaßnahme gegen Hidden-Terminal Probleme. Hierfür führt es ein effizientes Verfahren ein, um Funkressourcen mit Acknowledgements zu bestätigen. Bestätigte Funkressourcen implizieren für weiter entfernte Terminals, dass diese Ressource gerade in Verwendung ist. Dies erweitert die Reichweite des Sensing-Verfahrens. Nicht bestätigte Funkressourcen, die durch Kollisionen enstehen, motivieren Sender, diese nicht

weiter wiederzuverwenden und stattdessen neue auszuwählen. SAFE teilt eine Reservierung von Funkressourcen auch in mehrere, ineinander verschachtelte, Teil-Reservierungen auf. Diese nutzen andere Funkressourcen. Dadurch können Paketflüssen mit veränderlicher Paketrate oder -größe unterstützt werden. Außerdem kann dadurch die verteilte Staukontrolle die Periodizitätseigenschaft weiter gewährleisten.

Die Komponenten von SAFE können mit verschiedenen Konfigurationsparametern optimiert werden. Durch die Verwendung von mehreren experimentellen Designs wurde eine Menge an Konfigurationsparametern für SAFE systematisch ermittelt. Die darauf folgende Evaluierung zeigt, dass SAFE ein besseres Leistungsverhalten sowohl unter Metriken wie der Paketzustellrate als auch im Hinblick auf die Anwendung erzielen kann. Hierfür wurde eine Awareness-Metrik entwickelt, welche das anwendungsbezogene Wissen darstellt, das die Fahrzeuge aus den Cooperative Awareness Messages (CAMs) gewinnen können. Viele verschiedene Verkehrsszenarien wurden in einer Systemlevel-Simulation untersucht. SAFE erzielt eine höhere Paketzustellrate insbesondere bei längeren Kommunikationsdistanzen, was impliziert, dass die Gegenmaßnahmen gegen Hidden-Terminal-Probleme vorteilhaft sind. Die verteilte Staukontrolle von SAFE führt zu stärkeren Verbesserungen der Paketzustellrate im Vergleich zu LTE-V2X. Darüber hinaus zeigt SAFE, dass eine bessere Kompatibilität zu Paketflüssen mit variierender Paketrate oder -größe aufweist. Der Overhead, der notwendig ist, um die Acknowledgements zu übertragen, ist sehr gering. In den meisten Fällen dürften sie in die Padding Bits passen. SAFE zeigt sich somit als vielversprechender Ansatz, um die Leistungsfähigkeit der Fahrzeug-zu-Fahrzeug-Kommunikation weiter zu steigern.

Danksagung

Hiermit möchte ich mich von ganzem Herzen bei allen Personen bedanken, die mich bei der Anfertigung meiner Doktorarbeit unterstützt haben. Ganz besondere Erwähnung hat mein Doktorvater Prof. Dr.-Ing. Günter Schäfer verdient, der mich schon bereits im Informatik-Studium unterstützte. Während der Bearbeitung dieser Arbeit half er mir stets mit anregenden Fragen oder motivierender Unterstützung.

Mein besonderer Dank gilt auch allen Professoren, Doktoranden und sonstigen Beteiligten, die im Projekt *Kooperative Wahrnehmung und Situationserkennung in Mobilität und Logistik mittels Passiv-Radar (KoSiMoLo)* mitwirkten und/oder dieses auf den Weg brachten. Insbesondere sei hier Univ.-Prof. Dr.-Ing. habil. Reiner Thomä, Carsten Andrich, Andreas Schwind, Michael Döbereiner und Steffen Schieler genannt, die mir unermüdlich und geduldig zur Seite standen, wenn ich sie einmal wieder mit Fragen zu der Ausbreitung elektromagnetischer Wellen, Kanalmodellen, oder der physikalischen Schicht des LTE-Standards konfrontierte. Weiterhin gilt mein Dank Univ.-Prof. Dr.-Ing. Giovanni Del Galdo und Univ.-Prof. Dr. rer. nat. habil. Matthias Hein, die für die Entstehung und Durchführung des Projektes ebenfalls essentiell waren. Ohne die Anstellung in diesem Projekt wäre eine Fertigstellung dieser Arbeit schwerlich möglich gewesen. Mein Dank gilt auch den Mitgliedern des Unternehmensbeirats, die in halbjährlichen Workshops hilfreiche Anregungen und kritische Fragen äußerten.

Einen dankenden Gruß möchte ich ebenfalls den *Telenauten*, also allen Mitarbeitern des Fachgebiets Telematik/Rechnernetze, mitschicken. An den kollegialen Zusammenhalt, die anregenden Gespräche in der Kaffeeküche, Diskussionen während der *Teambesprechung* und das gesellige Zusammensein beim Grillen erinnere ich mich jetzt schon gerne. Martin Backhaus, Simon Buttgereit, Franz Girlich, Michael Pfeiffer, David Schatz, Dr.-Ing. Michael Roßberg und Markus Theil, danke für die schöne Zeit, in der ich mit euch zusammenarbeiten durfte.

Zu guter Letzt möchte ich mich herzlichst bei meiner Familie und meinen Freunden dafür bedanken, dass sie mir zeitweise den Rücken frei hielten, mich aufmunterten, oder auch mal verständnisvoll meine gedrückte Laune bei Rückschlägen aushielten.

Vielen Dank!

Contents

List of Tables

Chapter 1.

Introduction

Injuries caused by road traffic accidents are the eighth leading cause of death, and the first cause of death among 5 to 29 year old humans. In 2018, road traffic accidents lead to 1.35 million deaths and 50 million injuries [Wor18]. Many countries search for solutions to reduce the number and severity of these accidents. In Europe, the *Vision Zero* aims to reduce the number of traffic-related fatalities and severe injuries close to zero until 2050. Intelligent and connected vehicles are one of the main research areas to reduce these accidents.

The research activity regarding vehicle-to-vehicle (V2V) communication dates back as far as the fifth framework programme (FP5) in 1998 in Europe. In 2008, a bandwidth of $30\,\mathrm{MHz}$ in the $5.9\,\mathrm{GHz}$ was reserved for the V2V communication in Europe [Eur08]. Cooperative intelligent transport systems (C-ITS) is the framework developed by the European Telecommunications Standards Institute (ETSI) for V2V communication. The early research on the access technologies purely focused on technologies based on wireless local area network (WLAN). Institute of Electrical and Electronics Engineers (IEEE) 802.11p was developed as a standard for WLAN-based V2V communication. Notable changes were the abandonment of base stations and request-to-send/clear-to-send (RTS/CTS) protocols. IEEE 802.11p was originally designated as the main access technology for V2V communication in Europe. A few changes regarding distributed congestion control (DCC) were made and the technology was adopted as ITS-G5. The changes mean that the vehicles operate outside the context of a base station and there are no explicit mitigations for the hidden-terminal problem. The consequences are either put up with or mitigated to a certain degree by periodic and frequent repetitions of the transmitted messages. The characteristics of the wireless channel for vehicular communication are embossed by high Doppler shifts and spreads, as well as frequent interference through network congestion, and challenges for media access control (MAC) protocols imposed by the high terminal mobility. Consequently, MAC protocols for similar applications such as wireless sensor networks are hardly applicable, and the periodic transmission of messages is necessary to keep the communication reliability at a satisfactory level.

There are multiple applications for V2V communication such as internet-based services like over-the-air (OTA) updates or location-based services, tolling subscription and recording, traffic efficiency management, or road safety applications. The most important application is active safety. Most of the research regarding V2V communication focuses on this area. In Europe, two different message types are foreseen for this application: the cooperative awareness message (CAM) and decentralized environmental notification message (DENM). The CAM is a periodically transmitted status update message that includes the position, direction, speed, etc., of the vehicle. Despite the periodic transmission, the size and rate can vary depending on the movement of the vehicle and the presence of digital signature or additional information such as the past trajectory. The DENM is an event-based warning message, e.g. about a road hazard. This message is also repeated to increase the robustness and ensure reliable delivery.

Most of the time, the transmitted information is relevant for all surrounding vehicles and C-ITS stations. Hence, the vehicular communication is often broadcast locally. For some use cases, a connection to roadside infrastructure or the internet is required. Using ITS-G5, this is realized with dedicated roadside units (RSUs). The necessity to install RSUs with very limited geographic coverage at many places lead to debates regarding the required financial effort. A hybrid communication approach, using ITS-G5 for short and LTE for long range, was seen as a possible solution. In June 2017, support for direct vehicular communication was added to LTE with 3rd Generation Partnership Project (3GPP) Release 14.

With this new release, LTE now has a distributed mode that allows direct communication between the vehicles without involvement of the base station. This mode is called Mode 4 and is a direct competitor to ITS-G5. However, the MAC protocol of LTE Mode 4 is very different compared to ITS-G5 or IEEE 802.11p. Instead of the carrier sense multiple access/collision avoidance (CSMA/CA) protocol, LTE Mode 4 uses semi-persistent scheduling (SPS) and leverages the periodic nature of the exchanged messages. Using the assumption that every vehicle transmits the message periodically, typically with a packet rate of $10\,\mathrm{Hz}$, and the requirement to reuse radio resources at a fixed interval of typically $100\,\mathrm{ms}$ for a certain number of times, the MAC protocol can make predictions about the channel occupation based on observations made in the past. The use of single-carrier frequency division multiple access (SC-FDMA) at the physical layer stipulates the use of fixed time slots of $1\,\mathrm{ms}$, the so-called subframes, and one or multiple subchannels in the frequency domain. The channel allocation can be seen as a two-dimensional matrix that spans across the time and frequency domain. Vehicles have to use radio resources at a fixed interval for a random number of times (between 5 and 15). New radio resources are selected by random selection. However, those resources with a high collision risk are excluded from the set beforehand. This is done if no monitoring was possible due to half-duplex operation, if explicit reservations of other vehicles have been received, or if the average received signal strength indicator (RSSI) is high compared to the other resources.

Scope of this Work

In addition to the mentioned Mode 4, there is another mode for direct V2V communication with LTE: Mode 3. In Mode 3, the base station is responsible for the scheduling of radio resources. This leads to various technological and political challenges. Firstly, there is a high signalling overhead between the base station and the managed terminals. This is made even more complicated due to the fact that the base station has to select radio resources for terminals that are located further away. Hence, the base station might not know the exact interference situation at the managed terminals. Additional interference might for example arise due to communication that happens in Mode 4 because some terminals have lost the connection to the base station. Usually, the providers of the public land mobile network (PLMN) only have to manage their own radio frequencies. With the channels designated for V2V communication, the base stations of different providers must synchronise which radio resources are still free and can be used for the terminals managed by this provider. This requires coordination between the providers. In addition to the usual signalling and coordination overhead, the fail-over in case of an outage or in areas with no coverage is complex. Political considerations might further prevent Mode 3 from being used. For example, it might not be advisable to depend upon the operators to maintain the infrastructure for 20 years or longer. Due to these reasons, Mode 4 is considered the baseline and most important mode of LTE for V2V communication. Consequently, this dissertation focuses solely on Mode 4.

As main application and message format, the CAM will be used. This is the logical choice considering the optimisation of the MAC protocol of long term evolution vehicle-to-everything (LTE-V2X) Mode 4. The safety-related channel of the ITS band will likely predominantly be used for CAMs. However, in case of safety-critical events, the transmission of DENMs will be triggered. A master's thesis of Lucas Pförtner [Luc20] showed that these event-triggered DENMs do not significantly reduce the cooperative awareness when transmitted on the same channel as CAMs. One conclusion of this work can be that these DENMs can be transmitted along the CAMs even if the transmission is not periodic or does not follow the $100\,\mathrm{ms}$ interval. Hence, this dissertation focuses on the performance when CAMs are transmitted. Nevertheless, some of the improvements that are presented in this dissertation could be useful for traffic patterns with different rates or even non-periodic communication as well. This includes future technologies such as collective perception, i.e. sharing of sensor data.

Contributions and Objectives

Due to the recent release of LTE-V2X Mode 4, the new characteristics of the MAC protocol, and the special characteristics of V2V communication, there is only a limited amount of research available on this topic. However, it might be mandated to roll out V2V communication capabilities for every new vehicle in the coming years. Hence, there is an urgent need to research the performance of Mode 4. Specifically lacking in the existing research is the performance of LTE-V2X Mode 4 when using application-oriented metrics that consider the knowledge gained by the cars instead of simple and traditional metrics like the packet delivery ratio (PDR). Moreover, the requirement to reuse radio resources makes the allocation of resources inflexible. For example, the use of packet flows with varying sizes can be problematic if more subchannels are required to fit the packet. Additionally, SPS might not be compatible with a DCC mechanism that is based on packet dropping. These two issues require the development of additional or improved versions of the MAC protocol.

As this dissertation will show, the introduction of SPS opens the way for additional protocols that mitigate existing issues that have simply been accepted in existing protocols for V2V communication. Firstly, the hidden-terminal problem has been put up with for V2V communication due to the incompatibility of the RTS/CTS protocol with broadcast communication. The hidden-terminal mitigation developed in this dissertation leverages SPS and the periodicity properties of the resource allocation and solves this problem in an efficient way while being compatible with broadcast communication patterns. It works both by preventing hidden-terminal problems from occurring in the first place and preventing them from reoccurring due to SPS. Additionally, the developed protocol enhancements solve an additional problem of LTE-V2X Mode 4: the inability to detect collisions due to half-duplex operation which leads to repeating collisions due to radio resource reuse. The additional information that is exchanged due to the hidden-terminal mitigation is also used as input for the selection of radio resources, further increasing the performance of the system.

Specifically, the objectives of this dissertation are as follows:

- Perform an investigation of the special properties of LTE-V2X Mode 4 using application-oriented metrics and other analysis techniques.
- Develop a mitigation for the issue of repeating collisions due to resource reuse.
- Create a mechanism to enable the compatibility of SPS for the use of packet flows with varying packet rates and/or sizes.
- Invent a DCC mechanism that is compatible with periodicity requirements of SPS.

- Leverage SPS and the resource reuse to develop an efficient hidden-terminal mitigation that is compatible with broadcast communication.
- Evaluate the developed concepts and protocol extensions and compare the performance to standard LTE-V2X Mode 4 both under traditional metrics and in terms of the actual application performance.

Document Structure

Chapter 2 gives an overview of the relevant background information upon which this dissertation builds upon. This includes a description of the most prevalent types of crashes in intersections or highway scenarios. The typical reaction time of humans in traffic situations is investigated in order to be able to compare the latencies of V2V communication and driver assistance systems. The future developments that could impact the way V2V communication is used are also described. Next, the communication patterns and characteristics typical for V2V communication are presented. This includes fading characteristics, the Doppler effect, as well as the hidden and exposed terminal effect. Subsequently, the architecture of the ETSI C-ITS stack for connected and intelligent vehicles is presented. This includes a detailed description of the MAC protocol of LTE-V2X Mode 4 and the corresponding DCC algorithm. The last part of the chapter introduces experimental designs, an evaluation technique that will be used later to find a good set of configuration parameters for the developed system.

Chapter 3 first establishes a set of functional and non-functional requirements for MAC and DCC protocols, which motivate the design and classification of related work, and the evaluation focus later on. The Chapter continues with an overview of the current state of the art regarding the topic of this dissertation. This includes papers that present evaluations of existing standards, with a focus on the performance of LTE-V2X Mode 4 and comparisons to ITS-G5 or IEEE 802.11p. Moreover, modifications for LTE-V2X Mode 4 or protocols compatible with SC-FDMA are also considered, including proposals for DCC mechanisms.

Chapter 4 analyses several aspects and weaknesses of LTE-V2X Mode 4. The candidate resource selection process, SPS, and DCC mechanism are investigated in detail. The findings of these investigations motivate the development of improved protocols that mitigate the identified weaknesses.

The developed MAC protocol and DCC component, named scheduling based on acknowledgement feedback exchange (SAFE), is presented in Chapter 5. SAFE has four components: reservation splitting, acknowledgement feedback for radio resources, a newly developed radio resource selection component, and a new DCC mechanism. These components have configuration parameters that need to be set in order to achieve a good performance.

The architecture of the simulation framework used in this dissertation for evaluation and optimisation purposes is described in Chapter 6. This includes the traffic scenarios and a set of default simulation parameters.

Chapter 7 uses experimental designs in order to find a good set of configuration parameters for SAFE. Three large $2^4 \times 32$ or $2^{7-3} \times 32$ experimental designs are used to identify good values for the parameters and to identify the parameters with the largest impact. Separate studies with multiple parameter values are performed for the most influential system parameters.

The actual evaluation takes place in Chapter 8. The chapter starts with a qualitative discussion of the requirements. Additionally, an analytic evaluation of selected aspects is performed. This includes the interpretation of the acknowledgement feedback by the wrong terminals, as well as the probability of safety-critical situations due to collisions. The main quantitative evaluation is performed using a system-level simulation approach. SAFE has to prove itself in different configurations, with settings beneficial for standard LTE-V2X Mode 4, in scenarios with explicit obstacle shadowing, with limited number of available bits for the required acknowledgments, and with different packet rates.

Chapter 9 concludes this thesis with a summary. Lastly, future research and additional possible enhancements of SAFE are presented.

Chapter 2.

Background Information

This chapter describes background information relevant for this dissertation. It starts with the characteristics of vehicular traffic and accidents, including rare, but important edge cases. Additionally, the specific properties of vehicular communication are described. The chapter continues with an overview of the European approach for intelligent vehicles: C-ITS. This includes a description of the access technologies, most importantly ITS-G5 and LTE-V2X. The last part of this chapter deals with experimental design, an analysis technique used later in this dissertation.

2.1. Vehicular Traffic

This section gives an overview of the characteristics of vehicular traffic: common traffic scenarios, edge cases, and characteristics of traffic accidents. This information could be used for selecting or weighing evaluation metrics, design decisions regarding quality of service (QoS) aspects, selection of simulation scenarios, etc.

2.1.1. Characterisation of Traffic Accidents

In this section, the most frequent and most severe types of traffic accidents will be briefly characterized. This helps the decision process on which traffic scenarios should be used for evaluation purposes. Another important factor are pre-crash conditions. Specifically, the reaction time of humans and vehicular components is an important factor that decides whether a crash can be mitigated.

2.1.1.1. Safety-Critical Scenarios

The safety-critical traffic scenarios that are most relevant for this dissertation are traffic jams and accidents in highway scenarios, and intersection-related crashes that mostly occur in urban areas.

Highway Traffic Jams Common safety-critical traffic scenarios are traffic jams, especially on highways. Accidents or dangerous situations often occur at the end of a traffic jam due to the large speed difference between the stationary and arriving vehicles. This situation is highly relevant as an evaluation scenario because it has unique features. It endangers human lives due to the high speed difference. This difference also allows for less time to communicate, and less times for the MAC protocol to reach convergence. From a QoS perspective, it is detrimental that vehicles reaching the end of the traffic jam can receive warning messages.

Additionally, it is important that emergency vehicles can distribute warning messages to vehicles far ahead, so that they can prepare a corridor for emergency vehicle access. This means that it is likely important that the communication system is able to quickly, i.e. with minimal delay, forward messages even at high traffic speeds.

Traffic jams often travel upstream as *shockwaves*, even if the initial disturbance is already gone. A common goal of traffic flow management is to prevent or eliminate shockwaves. This can be achieved with electronic speed signs, which enable dynamic and variable speed limit assignment. In future, variable speed limits could be disseminated via infrastructure-to-vehicle (I2V) communication to the vehicles. The importance of direct V2V communication depends on the presence of such intelligent roadside infrastructure because these visual hints can be enough to prevent severe accidents. The most dangerous situations are those in which such infrastructure is not available. Therefore, a traffic jam scenario without roadside variable speed signs was chosen as one of the simulation scenarios.

Intersection-Related and Urban Crashes The U.S. Department of Transportation and National Highway Traffic Safety Administration reported that 2.6 million crashes occurred at intersections in the United States of America in 2015 [fSoT17]. A further 2.8 million crashes were intersection-related. Crashes at intersections account for about $23\,\%$ of all crashes, intersection-related crashes for an additional $25\,\%$. Therefore, almost half of all crashes are at or in the vicinity of intersections. Consequently, it is important to also use urban traffic scenarios that include intersections for the evaluation of vehicle-to-everything (V2X) communication systems.

2.1.1.2. Human and System Reaction Times

The reaction time of human drivers is usually modelled with the perception-intellection-emotion-volition (PIEV) theory [LD12]. Perception is the time the driver needs to perceive the dangerous situation. This includes time delays due to processing of the visual and acoustic signals in the organs and human brain. Intellection is the time required by the driver to compare different variants of interpretation and to understand the perceived situation. Afterwards, the human driver might need additional time due to cognitive or emotional disturbance. Lastly, reacting (e.g. pressing the brake pedal) requires additional time (volition).

All those delays are often combined into a single, larger delay: the human reaction time. Early studies on human reaction times showed that it depends mainly on whether the human anticipates an imminent need for a reaction, e.g. a braking maneuver. It can vary between around 0.4 and 0.8 seconds if the driver anticipates the situation, or otherwise be around 0.9 seconds up to 2 seconds in outliers [JR71]. Later, more refined analysis showed that the reaction time depends on a lot of influences like age, cognitive load, and urgency [Gre00, Sum00], but the most important factor is still reported to be driver expectation. This is an indicator that advanced driver assistance system (ADAS) systems that proactively warn the human driver of a potentially dangerous traffic situation are an essential component of future intelligent vehicles.

Various components of the vehicle itself also lead to additional reaction time. This includes time necessary to apply the brake pads to the disks by hydraulic pressure, suspension travel and dynamic weight transfer, etc. The maximum deceleration time is obviously limited by the condition of the brakes and tires, road and weather conditions, and the laws of physics. Modern cars are able to pre-charge the braking system if they perceive an imminent danger (e.g. Volvo's *collision warning with auto brake* system [CJLL07]), which decreases this system reaction time. Such systems could also be triggered by received warning messages.

Should an (automatic or human-induced) reaction to an event be due to information received via V2X communication, the latency required to distribute this message is an additional relevant delay. Compared to delays introduced by the MAC protocol or congestion control, other delays such as processing times or propagation times on the wireless medium are negligible. MAC delays add up multiple times if a message is being forwarded via multiple hops in order to reach its destination. This delay needs to be considered for time-to-crash considerations or can just be compared to reactions solely done by humans. In practice, not the MAC delay, i.e. the delay between the message generation and begin of transmission is relevant, but the update delay. The update delay measures the delay until a receiver successfully receives a status update. The MAC delay does not differentiate between successful and unsuccessful transmissions.

2.1.2. Future Technologies, Developments, Use Cases and Implications

In this section, current and future technologies that might have an influence on the way V2X communication is used will be briefly demonstrated.

2.1.2.1. Platooning and Autonomous Driving

Autonomous driving is a huge trend in research and for vehicle manufacturers and suppliers. Usually, autonomous vehicles will only depend upon their own sensors for the detection of the environment: radio detection and ranging (radar), light detection and ranging (lidar), stereo cameras, and ultrasonic sensors. Hence, a distinction between the term *autonomous vehicle* and *cooperative vehicle* can be made. While V2V communication can help to increase the reliability and reduce the risk of traffic accidents, it is not a necessary requirement for autonomous driving per its definition. While it might be hard to predict, the impact that autonomous driving has on V2V communication might be limited. However, new V2V use cases such as collective perception (see the following section) might still be used to increase the reliability of the sensor information. The combination of autonomous driving and communication is often referred to as connected and autonomous vehicles (CAVs).

Platooning means that multiple vehicles, e.g. trucks, follow a leading vehicle. The leading vehicle might be driven by a human driver or it might be driving autonomously. The requirements regarding the capabilities and sensors for the following vehicles are less strict. This is because the functionality mainly restricts itself to follow the vehicle that is ahead in the platoon. V2V will likely be used to realize platooning or increase its reliability by reducing delays due to the latency to detect braking manoeuvres by the vehicles themselves. Protocols for different platooning tasks are necessary. These include booking and joining, maintaining the platoon, and leaving. While joining and leaving a platoon happens comparatively rarely and thus only has a small impact on the V2V communication, the maintenance of a platoon requires repeated exchange of distance information. According to Vinel et al. [VLL15], minor extensions to CAM or DENM messages might suffice for the realisation of platooning. In order to reach acceptably small distances between the members of the platoon, the authors propose to remove the variable CAM rate for platoons and to fix the CAM rate to its maximum value, i.e. $10\,\mathrm{Hz}$. Hence, platooning does not require extensive modifications to the existing message types. However, the information age of the received data is highly relevant for the successful and safe realisation of platooning.

2.1.2.2. Collective Perception and Sensor Data Sharing

The idea of collective perception and sensor data sharing is that the range of the sensors of a vehicle is limited, either by the range of the sensor itself or by obstructions such as buildings or vehicles in between. Günther et al. [GTW15, GRWF16, GMT+16] performed early research on collective perception, with a focus on the European C-ITS stack. If the vehicles shared their sensor readings in a compressed format, other vehicles would be able to detect obstacles behind these obstructions, which would increase the safety. This can also increase the safety of autonomous driving by providing a better data basis for the algorithms.

The generation rules and contents for the collective perception message (CPM) is published by ETSI in a first proposal for standardisation [ETS19b]. The CPM contains information about the detecting vehicle and its sensors and about the detected object, e.g. its position, size, or speed. New CPMs should be generated if a new object is detected, or if already reported objects changed its position by more than $4\,\mathrm{m}$, its speed by more than $0.5\,\mathrm{m\,s^{-1}}$, its orientation by more than $4°$, or it has not been reported for more than one second. A new CPM may only be issued every $0.1\,\mathrm{s}$ to $1\,\mathrm{s}$, which is managed with the DCC component of ITS-G5 and LTE-V2X, respectively. Objects can be omitted in messages for reasons of redundancy prevention.

Thandavarayan et al. [TSG20] recently showed that the initial message generation rules by ETSI leads to a high number of messages that are only about a small number of objects, which is an inefficient use of the channel capacities. They propose a modified algorithm to tackle this problem. Regardless of changes to the CPM and the service, the communication requirements are likely to be similar to the requirements for CAMs.

2.1.2.3. Passive Coherent Location for Vehicular Scenarios

Unlike active radar, which transmits dedicated radar signals, passive coherent location (PCL) or passive radar makes secondary use of radio signals that are already being transmitted for reasons of communication. This might also be feasible in the area of V2V or V2X communication, leveraging the corresponding messages.

Radar can be (pseudo-) monostatic or bistatic/multistatic. Monostatic radar means that the transmitter and receiver are located at the same place or in the same device. In a bistatic radar, the receiver is at a different location than the transmitter. The receiver only knows the position of the transmitter and itself, as well as the additional propagation time of the signal reflected at the target object. Hence, the detected object can be at any location on an ellipse with the transmitter and receiver as focal points. In three dimensional scenarios, e.g. the detection of aircrafts, the target can be on an ellipsoid. Bistatic radar hence requires the use of directional antennas or antenna arrays in order to estimate the direction of arrival of the reflected signal. In a V2X scenario, the base station could be used for this, given that the angular resolution is sufficient.

Multistatic radar does not have this requirement but uses multiple transceivers to resolve the uncertainty by overlaying multiple ellipses. If all the receivers detected the same target object, it must be positioned at the intersection point of all ellipses. In general, three ellipses are required for a definite result. This means that at least four transceivers must cooperate in order to resolve all uncertainties if some of the intersection points cannot be ruled out due to other factors. An example of such a constellation can be seen in Figure 2.1. In reality, the ellipses are subject to uncertainties and the resulting intersection area will be larger. The ellipse parameters must be available at a single vehicle or central instance in order to perform this calculation.

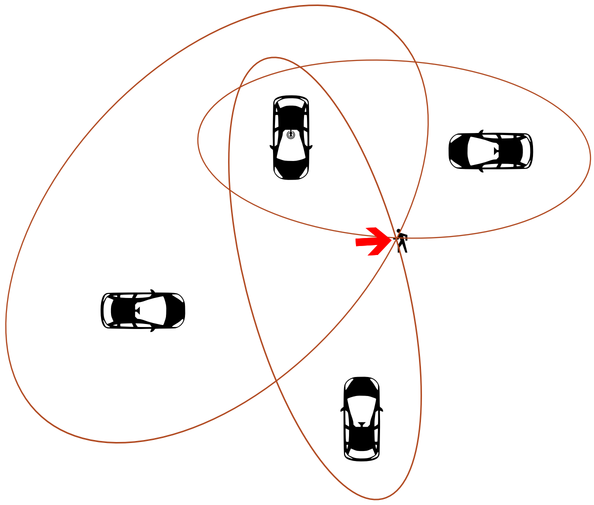

Figure 2.1.: Visualisation of ellipse intersections for multistatic radar in benign constellations.

This dissertation was developed in a research project that targeted cooperative passive coherent location (CPCL) [TAG+19], a version of PCL that additionally relied upon cooperation between multiple transceivers that are already part of a network (e.g. LTE). Multiple publications regarding CPCL have been made during this project, e.g. [TAG+19, SSH18, SAW+19, SSA+19, SDA+20]. The cooperation can be the adjustment of transmission parameters or simply the sharing of the result in order to determine the position of a detected obstacle. The intended goal of the protocol enhancements of this dissertation was to increase the reliability and accuracy of CPCL in an unmanaged LTE network consisting of vehicles, i.e. LTE-V2X Mode 4. For example, CPCL might benefit from a functional DCC that is configurable with a single parameter, a reduction of interference due to hidden-terminal mitigations, etc. All of the proposed modifications have been developed with the requirement that the communication performance may not be sacrificed, and should be increased, if possible.

Various uncertainties make the quantification of the intended benefits for CPCL difficult to predict at the current state of research of CPCL. The impact of interference caused by other transmitters still needs to be determined in realistic measurement campaigns before a scientific model can be developed. Therefore, the evaluation, motivation, and discussion of the methods of this dissertation are limited to communication-related aspects only. In particular, the following uncertainties currently make a realistic and real-time deployment of CPCL in a measurement campaign impossible:

- The difference between the energy of the line-of-sight signal and the reflected signal is high. The spurious free dynamic range of typical transceivers might not be sufficient to support the extraction of the reflected signal.

- The range resolution is a function of the signal bandwidth and the bistatic angle. The currently available bandwidth on the sidelink is not enough to support a reliable location and separation of target objects.

- Similarly, the Doppler processing to isolate moving targets from static clutter is a function of the integration time and bistatic angle. The signal duration might not be enough to separate the clutter sufficiently. Moreover, it is unclear how clutter from static objects is separated with Doppler processing when one or more transceivers move themselves. Static objects might be filtered as static clutter, even though they might be a road hazard that is not moving.

- The aforementioned limitations indicate that high-resolution parameter estimation might be necessary. The required processing power might prevent the operation in real time and with sufficiently low processing times.

- Ambiguities in regard to the mapping of ellipses to objects are likely to exist. This might lead to the intersection of ellipses for different target objects, resulting in false positives and negatives.

- The time difference of the reflected path is estimated under the assumption of the presence of a line-of-sight signal. This line-of-sight connection is a requirement for the correct operation. Moreover, it is important to detect situations in which this requirement is not fulfilled. It is unclear how and whether this can be performed with sufficient reliability in practical scenarios.

- The target may reside in the line-of-sight between two transceivers. In this case, there would be no deviation of the propagation time and the calculation of ellipses would not be possible. Forward scattering approaches could possibly be applied in this case.

- A line-of-sight connection needs to be present between all transmitters, receivers, and the connection to the target.

- Small intersection angles of ellipses result in large uncertainties of the target position due to the geometric dilution of precision.

The geometric dilution of precision and blockage of the line-of-sight connection is visualized in Figure 2.2.

2.2. Characteristics of Vehicular Communication

This section deals with the characteristics and special features of vehicular communication. At first glance, vehicular communication has properties like the ones of wireless sensor networks (WSNs): The purpose of WSNs is to wirelessly share sensor data and the MAC protocol usually works in a distributed way without involvement of a central infrastructure. However, there are distinct and important differences. For example, a main optimisation goal for sensor networks is energy efficiency. Specific MAC protocols have been developed and proposed for the purpose of saving energy and extending battery life. Additionally, reliability and time constraints are likely less strict for WSNs than for vehicular networks. Vehicular networks also suffer from different wireless channel conditions than WSNs. Therefore, many parts of the communication architecture, including MAC protocols and physical layer mechanisms, need to be developed or derived specifically for V2V communication.

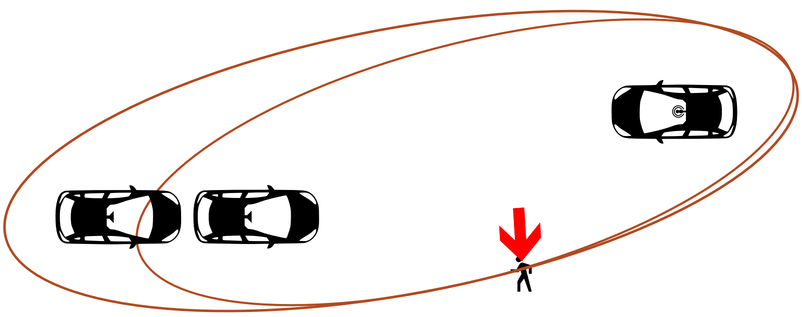

Figure 2.2.: Visualisation of ellipse intersections for multistatic radar in adverse constellations.

2.2.1. Communication Patterns and Characteristics

V2X communication can involve only vehicles, infrastructure, or even pedestrians. The former is called V2V communication. If infrastructure is involved, I2V or vehicle-to-infrastructure (V2I) is used. Communication between vehicles and pedestrians is abbreviated as vehicle-to-pedestrian (V2P). The communication between vehicles is usually locally constrained, most often it is just a local, single-hop broadcast. This means that a transmitter usually targets all surrounding vehicles and only rarely a single specific vehicle. There are exceptions to this, for example warning messages or other message types that are being forwarded to specific targets or areas. Details of this geographical routing will be given in Section 2.3.2.3.

V2V messages are generally either periodic status updates or event-driven warning messages. These warning messages can also include the shared sensor data, for example road hazards detected by radar sensors. They are usually periodically repeated for reasons of robustness. Vehicles can communicate with each other or target the roadside or PLMN infrastructure to reach local services or the internet. This enables other possible applications such as tolling or entertainment services, which are however not the focus of this dissertation.

2.2.2. Typical Effects in Wireless Communication

This section deals with a selection of effects typical for (vehicular) wireless communication. These effects should be considered when designing medium access control algorithms. This likely increases the performance of the communication system.

2.2.2.1. Hidden and Exposed Terminal

The hidden-terminal effect is a problem that negatively impacts the performance of all sensing-based collision-avoidance MAC protocols if no successful mitigations are deployed. This effect occurs if a terminal is inside the interference or communication range of other transmitters that are not able to receive packets or detect the signal power of each other. Therefore, the transmitters are unable to notice one another if no explicit mitigation techniques are used. Figure 2.3 visualizes this constellation. If these transmitters use the same frequency, the terminal or vehicle in between will not be able to receive any of the messages. The hidden-terminal problem also illustrates that a *collision* of radio frames is an effect that can be highly dependent on the position of the receiver. Depending on the location of the transmitter, receiver and interferers, a packet could be decodable in one area, and collisions might only

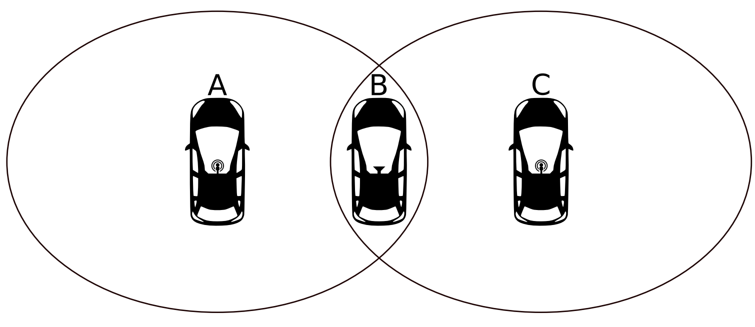

Figure 2.3.: Visualisation of the hidden-terminal effect. Vehicle B is unable to decode packets from either vehicle A or C because of interference. Still, vehicles A and C cannot detect each other's interference.

occur in some areas. From a MAC protocol perspective, there is another interesting dimension to this problem, especially for protocols based on carrier sensing such as CSMA/CA or Mode 4 of LTE-V2X. The assessment whether the wireless channel is free is done from the perspective of the transmitter. Therefore, it cannot detect interference caused by the other transmitter and will assess the channel as free. This makes the occurrence of hidden-terminal problems relatively likely if no mitigations are applied.

Such mitigations are often RTS/CTS protocols, in which a transmitter explicitly asks the receiver if it senses the channel as free. RTS/CTS is used in normal WLAN, but not in IEEE 802.11p, i.e. not for the vehicular configuration. However, due to the local broadcast nature of the communication, multiple vehicles are potential receivers of a message. Therefore, explicit mitigations for hidden-terminal situations like RTS/CTS mechanisms would incur a high overhead because a RTS/CTS dialog would need to be carried out with every potential receiver before the actual transmission. Moreover, every potential receiver might not be known to the transmitter in advance, especially with local broadcast communication. Another assumption of RTS/CTS in traditional WLAN is that the RTS/CTS packets are small in comparison to the actual data packets. This assumption also might not be true in vehicular communication, as often only small status update messages are transmitted. The access technologies for V2V communication usually do not include such mechanisms and accept the risk of collisions due to hidden-terminal effects. Specifically, neither IEEE 802.11p (including dedicated short range communication (DSRC) and ITS-G5) nor LTE-V2X Mode 4 use special hidden-terminal mitigations. In order to reach acceptable reliability, the messages are often either sent periodically with updated contents or at least being repeated for a given number of times.

The exposed terminal problem is the problem contrary to the hidden-terminal problem. It also appears with MAC protocols based on carrier sensing. Figure 2.4 visualizes a situation in which a vehicle senses the channel as occupied and is prevented from transmitting even though the other receiver would not be affected by the transmission. Hence, the exposed terminal problem prevents terminals from using the channel even if it would be possible to reach a specific receiver. This reduces the spatial reuse.

However, the exposed terminal problem becomes less likely with a larger amount of broadcast-type communication patterns because every vehicle in the vicinity is interested in the transmitted packets. In the example of Figure 2.4, vehicle B would also be interested in the transmission of vehicle C. Hence, it is the correct reaction of vehicle C to defer the transmission. As most of the V2V communication is a local broadcast, the exposed terminal problem is deemed to be a much less relevant problem than the hidden-terminal problem.

In conclusion, the hidden-terminal problem leads to an erroneous transmission attempt, while the exposed terminal problem wrongly prevents an otherwise feasible transmission. The

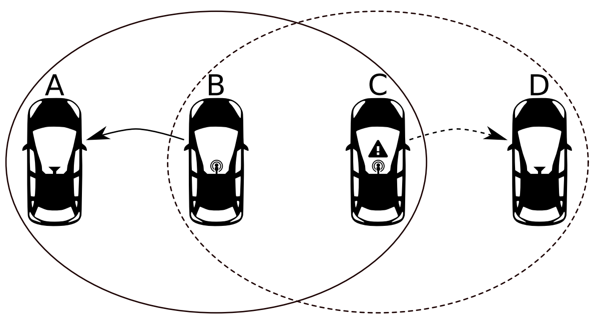

Figure 2.4.: Visualisation of the exposed terminal effect. Vehicle C is unable to transmit due to perceived channel occupation. However, the reception process at vehicle A would not be interrupted by vehicle C's transmission.

exposed terminal problem is less frequent if most of the communication is broadcast locally.

2.2.2.2. Capture Effect

Even if a terminal is affected by two interfering transmissions, it is still possible to detect and decode the stronger signal if the power difference is high enough. A terminal is also able to switch to a stronger transmission if it is currently receiving a signal with significantly lower power. This is called the *capture effect*. The inverse problem is called the *near-far problem*. This happens when a stronger signal completely blocks weaker signals. This issue is more important in code-division multiple access (CDMA) systems but can for example also occur in SC-FDMA systems through adjacent-channel interference.

2.2.2.3. Wireless Channel Conditions of Vehicular Communication

In comparison to many other wireless systems, the high terminal mobility and variability of the channel conditions of vehicular communication systems are a significant difference. In heavily built-up areas such as street canyons or cities, even a small variation of the receiver's or transmitter's position can lead to strong changes of the reception power, e.g. by moving destructive interference to constructive interference.

Especially on highways with high relative speeds, in extreme cases up to $500\,\mathrm{km\,h^{-1}}$, high Doppler shifts can cause adjacent-channel interference and reception problems. The Doppler effect is a change in frequency of a signal. It can be intuitively explained by considering a single sinus signal with a given phase, i.e. wavelength. If a transmitter moves towards a receiver during a transmission, it will be at a different distance to it at the end of a phase compared to when it transmitted the beginning of the phase. As this movement occurred during transmission, the wavelength was effectively shortened, slightly increasing the frequency of the transmitted signal. This effect also occurs if a receiver moves and in case of multipath propagation if a scattering object has a relative movement to the transmitter or receiver. When a transmitted signal reaches a target via several propagation paths, the Doppler shift of the single paths can be different. Hence, the receiver experiences multiple Doppler shifts at once, which is called *Doppler spread*. The high relative speeds of vehicles can cause significant Doppler spread, which needs to be accounted for when designing wireless access technologies. This, however, is merely a physical layer problem.

2.3. ETSI Cooperative Intelligent Transport Systems

The European *Vision Zero* is to move close to zero traffic fatalities and serious injuries by 2050. C-ITS is the complete communication stack for V2X communication in Europe, and is assumed to help reach the goal of this vision.

2.3.1. Regulatory Background

Research in Europe on C-ITS began with the fifth and sixth framework program (FP5 and FP6) [Eur09], starting in 1998 and 2002, respectively. Early on, the industry formed consortia on V2V communication.

In 2006, the European Commission presented COM (2006) 59, which is a policy framework for the *intelligent car initiative*. The goal of this initiative is to coordinate the work on intelligent cars, support research and development and create acceptance by the citizens [Eur06]. Subsequently, a 30 MHz frequency band was set aside for intelligent transport systems (ITS) by Commission Decision 2008/671/EC [Eur08] in 2008. The Comité Européen de Normalisation (CEN), Comité Européen de Normalisation Électrotechnique (CENELEC) and ETSI have been invited to develop, publish and maintain according standards by the Standardisation Mandate M/453 EN of October 2009 [Eur09]. In August 2010, the *ITS Directive* 2010/40/EU [Off09] of the European Parliament and Council came into effect. This directive provides a legal framework for the deployment of interoperable, intelligent transport systems.

The following years, many technical specifications and standards regarding C-ITS have been published by the ETSI. For a long time, it seemed clear that ITS-G5, a modified version of IEEE 802.11p would be used as communication technology. However, with a long delay, the 3GPP became interested in V2X communication and started developing a PLMN based solution: LTE-V2X. In 2016, the European Commission presented COM (2016)766 to address, among others, security, privacy and fragmentation concerns [Eur16]. Notably, a *hybrid communication approach*, consisting of ITS-G5 for short communication and traditional LTE for long range communication, was now favoured. With the LTE Release 14 in June 2017, support for V2V and V2I communication has been added to LTE. The ETSI and its partners noticeably worked to provide compatibility between the C-ITS framework and LTE-V2X. This goes as far as introducing a DCC algorithm for LTE-V2X in November 2018 [ETS18c]. Meanwhile, a debate on which technology is best suited emerged.

In March 2019, the commission adopted new rules for the deployment of C-ITS. The act still favours a hybrid approach consisting of ITS-G5 for small range and cellular technology for long range communication. Up until its effectiveness, expert groups will be consulted to evaluate potential benefits of competing access technologies such as LTE-V2X or fifth generation (5G). The preferred way of deploying C-ITS is to make them mandatory by Europe-wide legal regulation [Eur19]. The delegated act is based on the ITS Directive 2010/40/EU and passed the European Parliament on April 30. However, it was stopped by the majority of the member states due to concerns regarding the commitment towards ITS-G5[1]. This shows that there is still uncertainty about which access technology should be used or even mandated in Europe. The Federal Communications Commission (FCC) withdrew the reserved bandwidth for IEEE 802.11p in the United States of America in October 2020[2] [Fed20], paving the way for a full transition to cellular vehicle-to-everything (C-V2X). It is possible that Europe will follow this decision.

2.3.2. Architecture

The European C-ITS stack consists of four *horizontal* layers (applications, facilities, networking and transport, access layer) and two cross-layer, *vertical* entities (management and security). These layers are shown in Figure 2.5 along with the interfaces between them. Those interfaces are called service access points (SAPs).

2.3.2.1. ITS Applications Layer

The applications in the ITS applications layer just use the communication stack and provide features like cooperative safety, traffic management, infotainment or business systems. Those

[1] `https://heise.de/-4464225`, accessed December 9, 2020
[2] `https://heise.de/-4966174`, accessed December 16, 2020

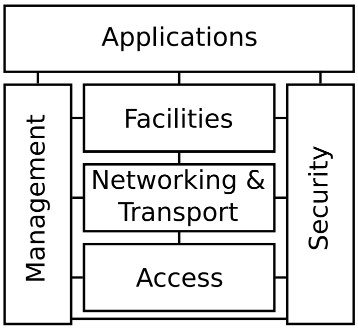

Figure 2.5.: Layers of the European C-ITS stack according to [ETS10].

applications are not necessarily standardised as part of the C-ITS framework and can also be proprietary services of car manufacturers that simply use the connectivity to access back-end servers.

While the various applications themselves are not the focus of this document, an understanding of the use cases is important to derive communication patterns and requirements that are relevant in practice. ETSI technical report (TR) 102 638 contains a basic set of applications [ETS09], which are partitioned into the following categories:

Active road safety: These applications provide driving assistance and increase the cooperative awareness, or warn about road hazards. The cooperative awareness use cases include warnings about approaching emergency vehicles, slow and crossing vehicles, motorcycles, etc. Additionally, warnings about road hazards like stationary vehicles, cars driving in the wrong direction, traffic conditions, signal violations, etc., are issued.

Cooperative traffic efficiency: This category serves speed management and cooperative navigation purposes. The uses cases include speed limit notifications, speed advisories, in-vehicle signage or traffic and navigation information dissemination.

Cooperative local services: These are location-based services such as notifications about points of interests or parking management.

Global internet services: These services are for example used for fleet and loading zone management or OTA software updates.

The most important and interesting application category is of course road safety. As safety-critical messages are likely to be transmitted using designated channels (e.g. the G5-CCH channel), they are treated in an isolated way in this dissertation.

2.3.2.2. ITS Facilities Layer

The facilities layer, corresponding to the Open Systems Interconnection (OSI) application, presentation and session layers, provides support for applications, information retrieval and storage, communication and session management. Additionally, it has interfaces to the communication and security entities of the C-ITS stack [ETS10].

The local dynamic map (LDM), which will be described in more detail in the following, is the main data storage for static and dynamic objects and events in the environment surrounding the vehicle. The facilities layer additionally provides different message formats for service, event, and periodic update messages. The standardised message formats ensure that vehicles can cooperate with one another.

Local Dynamic Map The LDM contains information about objects obtained by different sensors, e.g. radar, or ITS applications like CAMs or DENMs. Objects inside the LDM are location-referenced. There are many challenges of such a central data storage. Firstly, a life cycle management needs to be implemented. In the ETSI LDM, objects are timestamped and garbage-collected [ETS14a]. For example, CAMs have a lifetime of one second [ETS19c]. Secondly, a de-duplication mechanism should exist if it is possible that multiple reports from different information sources are about the same object, e.g. a vehicle detected by radar and its own CAMs. The LDM is also responsible for verifying new information, e.g. based on digital signatures.

Cooperative Awareness Basic Service CAMs are used to periodically broadcast status update information [ETS19c]. An ITS station that broadcasts CAMs does not need to send separate beacon messages because the CAM also serves this purpose. The CAM is the message related to the *cooperative awareness basic service*. It includes the current position, speed, direction and basic attributes of a vehicle. There are different aspects of traffic safety that can be accomplished with CAMs: warnings about emergency vehicles or slow vehicles, (intersection) collision warnings, etc.

The packet rate varies between one and ten Hertz, depending on DCC restrictions. A CAM is always transmitted over one hop, i.e. never forwarded by other ITS stations. Application-layer parameters are used to trigger the generation of a new CAM: A change of $4°$ in heading, $5\,\mathrm{m}$ in position or $1\,\mathrm{m\,s^{-1}}$ in speed. The desired maximum generation time is $50\,\mathrm{ms}$, the maximum communication latency is $100\,\mathrm{ms}$. Each dataset in a CAM includes a $95\,\%$ confidence interval, so that other vehicles are informed about uncertainties. An important aspect for MAC protocols is the varying size. Every $500\,\mathrm{ms}$, a CAM contains a *lowfrequencyContainer*, which contains information that is less time-critical such as the exterior lights of the vehicle, the role and the past trajectory [ETS19c]. The size of the packet also depends on the type of vehicle and the presence of a digital signature. The *Car 2 Car Communication Consortium* performed an analysis on the size of CAMs and concluded that it depends on various factors, including the speed of the vehicle, at least for ITS-G5 [MB18]. The smallest CAM size, around 190 to $300\,\mathrm{B}$ occurred for about $30\,\%$ of the packets. More than $30\,\%$ of the packets are above $450\,\mathrm{B}$, with packet sizes reaching over $800\,\mathrm{B}$.

As LTE-V2X Mode 4 is built upon the idea of periodic packet flows, it is unclear whether the variable CAM rate will be used. The DSRC standard in the United States of America does not stipulate a variable packet rate for basic safety messages (BSMs). If variable CAM rates are used in conjunction with LTE-V2X Mode 4, some of the resources will be left unused. If a certain number of consecutively unused resources is exceeded ($\mathrm{sl{-}reselectAfter}$ [ETS20]), new resources have to be selected. However, the variable CAM rate has been developed with an access technology in mind that handles variable packet rates better. Some of the approaches developed for this thesis mitigate this deficiency of LTE-V2X. However, in general it is conceivable that the feature of variable CAM rates will not be enabled when using unmodified LTE-V2X as access technology, increasing the channel load compared to ITS-G5. Regardless of the access technology, there are other reasons to disable the variable CAM rate in general. Firstly, if there is channel capacity available, there is hardly any reason not to use it (except for a small safety margin for DENMs). The restriction of the channel load should be the task of a DCC algorithm and should depend upon the current channel load. Secondly, the consideration of the change of position and speed can lead to dangerous situations in practice. For example, a vehicle that is stationary at a dangerous spot at an intersection uses the lowest possible CAM rate as it does not change its position. However, it is important that vehicles that are approaching with high speed notice the stationary road hazard. Hence, the stationary vehicle should transmit with the highest rate possible in order to prevent collision accidents.

Decentralized Environmental Notification Basic Service The DENM message type is used for event-driven communication, such as a warning of a road hazard. DENMs are meant to be sent as long as the detected event persists. This aspect is important for MAC protocol considerations: Just like CAMs, DENMs can also require periodic reuse of radio resources. Information about non-communicating objects can be shared by *hazardous location – obstacles on road* message types.

Service messages A service message is either used for session management or to transport protocol data units (PDUs) from applications that are not directly standardised, but still use the C-ITS communication stack.

2.3.2.3. ITS Network and Transport Layer

The network and transport layer of the C-ITS stack provides reliable data transfer and congestion avoidance mechanisms if necessary. It is subdivided into an upper layer, corresponding to the transport layer of the OSI model, and into a lower layer, corresponding to the network layer. The transport layer part supports the transmission control protocol (TCP), user datagram protocol (UDP) and basic transport protocol (BTP), which is closely related to GeoNetworking. The network layer supports modes of GeoNetworking and additionally, internet protocol version 6 (IPv6). IPv6 support is realized by IPv6 with mobility support by communications access for land mobiles (CALM) and using an IPv6 adaptation sub-layer called *GN6ASL* on top of GeoNetworking [ETS10, ETS14d].

GeoNetworking Protocol GeoNetworking is an ad-hoc and connectionless protocol to support sophisticated communication requirements even without the involvement of a central infrastructure. Nevertheless, it can leverage an intermittent coordinating infrastructure. One of the main features is the ability to use multi-hop communication and geographic positions for addressing and forwarding. Geographic forwarding decisions are made without the need for special routing tables. GeoNetworking supports the following addressing schemes [ETS13a]:

Point-to-point: This means communication that is potentially multi-hop between two stations. GeoUnicast forwarding [ETS14b] can be used to route the message to its destination.

Point-to-multipoint: This is an addressing scheme to distribute a message from one station to multiple other stations. A special case is single-hop broadcast, which is a simple local broadcast without further forwarding.

GeoAnycast: This can be used to address an arbitrary, single station in a specified area.

GeoBroadcast: If all stations in a given geographic area should be addressed, GeoBroadcast can be used.

For the location of target nodes and geographic forwarding decisions, nodes need a limited and local knowledge of the positions of other nodes, which is facilitated by the cooperative awareness basic service. The GeoNetworking protocol defines data fields in the header that contain the position of the current transmitter and, if GeoCast is used, of the source and destination node or target area [ETS11c]. Additionally, GeoNetworking implements mechanisms to detect duplicate packets and prevent routing loops. For GeoUnicast forwarding, two different algorithms can be used: a greedy algorithm, which selects the node that has the smallest geographical distance to the destination, or a contention-based forwarding algorithm, which lets the receiver decide whether it should be the next hop. The latter algorithm leads to a larger delay and processing time but ensures that a packet reaches its destination [ETS14b].

For GeoBroadcast, a simple, line-based forwarding algorithm and two different advanced algorithms, both based on the contention-based forwarding algorithm mentioned earlier, are envisaged.

The forwarding strategies and GeoNetworking overhead could be considered for DCC. The channel load could be decreased by choosing forwarding strategies with less communication overhead. Additionally, the information value in relation to the used wireless resources decreases with the number of hops. Therefore, dropping GeoCast packets early when applying DCC restrictions can be very effective. GeoNetworking additionally needs to support prioritisation of packets [ETS14b]. For the application of a DCC mechanism, this requirement needs to be considered – if DCC restrictions lead to packet dropping, lower-priority packets should be preferred for dropping if possible.

As most of the aspects of the GeoNetworking protocol are not relevant for this dissertation, only a high-level overview was given. The reader is also kindly referred to the ETSI standards and specifications regarding GeoNetworking: requirements [ETS14b], scenarios [ETS13a], network architecture [ETS14c], media-independent functionality [ETS11c], media-dependant functionalities for ITS-G5 [ETS13b], BTP [ETS19d], GeoNetworking protocols [ETS14d] and amendments for LTE-V2X [ETS19e, ETS19f].

Basic Transport Protocol The BTP protocol is used to deliver packets like CAMs or DENMs to the facilities layer. It uses GeoNetworking as transport protocol. The protocol is very lightweight. The protocol header is only 4 B long and contains the source and destination port, or the destination port and additional information if the non-interactive version of the header is chosen [ETS19d].

2.3.2.4. ITS Access Technologies Layer

The access technology is responsible for the reception and transmission of packets. As the upper layers are as access-technology-agnostic as possible, it is possible to use different wireless access technologies to transmit the messages to other vehicles or the roadside infrastructure. The two major competing access technologies are ITS-G5 and LTE-V2X (or its successor, 5G). Additionally, conventional WLAN or LTE can also be used. A hybrid approach consisting of ITS-G5 for V2V communication and LTE for V2I communication was also proposed before LTE-V2X has been published with Release 14 of the LTE standard. The focus of this dissertation is however on the direct V2V communication. The existing access technologies for V2V communication will be described in more detail in Section 2.4.

2.3.2.5. ITS Management Layer

The ITS management layer is a cross-layer entity that is used for the configuration of the ITS station and cross-layer information exchange [ETS12a]. It specifies, among others, an interface to read and write communication interface parameters such as the transmission power, reception sensitivity or data rate. Access technologies need to inform the management entity about received and transmitted frames [ETS12b].

2.3.2.6. ITS Security Layer

The security layer manages identities and credentials and is an entity used by multiple layers to secure or verify messages. Upon reception or transmission of a packet, each vertical layer will use a horizontal interface to the security layer to perform security-related actions before passing the packet to the next vertical layer [ETS16].

2.4. Wireless Access Technologies for Vehicle-to-Vehicle Communication

It is likely that a single access technology cannot fulfil all requirements of C-ITS. Various access technologies can be used for ITS communication. This is in fact very likely, as seen in Section 2.3.1.

2.4.1. ITS-G5

ITS-G5 is the access technology initially developed and foreseen for the European C-ITS framework. ITS-G5 uses the MAC and physical layer of IEEE 802.11p [oES16, ETS19a] and is therefore based on WLAN. The technology is also very similar to the solution taken in the United States of America with DSRC or wireless access in vehicular networks (WAVE), which also uses IEEE 802.11p. ITS-G5 is mainly suited for low to medium range communication and is, besides a communication with special RSUs, mainly used for direct V2V communication.

The communication happens outside a basic service set (BSS). An access point is not present. ITS-G5 requires that transceivers are capable of transmitting and receiving at a rate of 3, 6 and $12\,\mathrm{Mbit\,s^{-1}}$, which corresponds to binary phase shift keying (BPSK), quadrature phase shift keying (QPSK) or 16-quadrature amplitude modulation (QAM) with a coding rate of 0.5. As it is a variant of WLAN, it uses orthogonal frequency division multiplex (OFDM) as modulation scheme, and enhanced distributed coordination access (EDCA), which is an enhanced version of CSMA/CA with QoS support [oES16], as MAC protocol. The principal mode of operation of CSMA/CA is as follows: if a station is willing to transmit a packet, it first checks whether the wireless channel is occupied. If it is free, the station can start transmitting right away. If not, it must wait a random time and perform sensing again [oES16], the so-called arbitration inter-frame spacing (AIFS). This AIFS is larger for packets with lower priority, which realises QoS. Standard WLAN optionally supports a RTS/CTS mechanism, which is used to limit the hidden-terminal problem by explicitly asking the receiver if a sender is allowed to transmit. This works well in traditional WLAN because even if stations cannot see each other, almost all stations can see the access point. In V2V communication however, the communication is typically defined by local broadcast to many receivers (see Section 2.2.2.1). A RTS/CTS protocol is not used and there are no specific mitigations for hidden or exposed terminal problems [oES16].

CSMA/CA protocols merely reduce the probability of a radio frame collision. If the channel load is very high, it is almost inevitable that collisions happen. The most notable difference between ITS-G5 and IEEE 802.11p is the introduction of a DCC mechanism, which limits the channel load and ensures that the MAC protocol works as intended.

2.4.2. LTE-V2X

Support for vehicular communication by the PLMN was introduced in 2017 with Release 14 of the LTE standard. It is built upon device-to-device (D2D) capabilities already existing in previous versions. The modifications for vehicular communication are part of the official LTE standard. Nevertheless, the name LTE-V2X is often used to emphasize the capabilities for vehicular communication of LTE Release 14 or newer. A more general term is C-V2X, which denotes V2X communication based on cellular infrastructure and technology and can therefore also be used to refer to 5G.

2.4.2.1. Overview

LTE uses specific abbreviations and names for many components of the standard. For example, a LTE-capable terminal is called user equipment (UE). The cellular base station is called evolved node B (eNodeB). There are three different communication channels in LTE-V2X. The *Downlink* channel stands for the communication from the eNodeB to the UE. The *uplink* channel is the reverse direction. Communication between UEs without forwarding via the base station is performed on the so-called *sidelink* channel. Figure 2.6 gives an overview of the three communication patterns. The focus of this dissertation is the sidelink.

The LTE radio interface protocol architecture [ETS19g] corresponds to the lowest two layers of the OSI model, the data link and physical layer. Layer 2 consists of various *sublayers*: the packet data convergence protocol (PDCP) [ETS19i], radio link control (RLC) [ETS19m] and MAC [ETS20] layer. The physical layer [ETS19j, ETS19h, ETS19l, ETS19k] is not further subdivided. Besides this vertical structure, the non-access stratum (NAS) [ETS19p] and radio resource control (RRC) [ETS19n] components are cross-layer entities. A visual overview is given in Figure 2.7.

The main functionality of the aforementioned components and protocols is as follows:

PDCP: The PDCP is a protocol for the transfer of user and control plane data. Other features are the compression of (internet protocol (IP)) headers, ciphering and deciphering, integrity protection and verification [ETS19i].

RLC: The RLC layer can operate in a transparent, acknowledged and unacknowledged mode. Unless the transparent mode is being configured, the main tasks of the RLC layer are the segmentation, re-segmentation, reassembly and duplicate detection of RLC PDUs. If the acknowledged mode is used, the RLC layer is additionally responsible for error correction

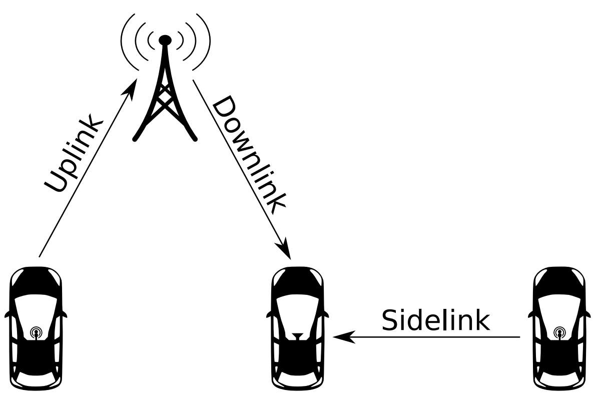

Figure 2.6.: Visualisation of downlink, uplink and sidelink communication.

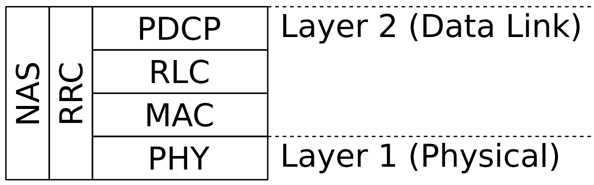

Figure 2.7.: Structure of LTE layers.

using automatic repeat request (ARQ) and for indicating successful transmissions to upper layers [ETS19m]. In V2V communication, the transparent mode will be used.

NAS: The NAS layer is responsible for session, call, and mobility management. Mobility management means the seamless handover between the entities of two different serving cells [ETS19p].

RRC: The RRC protocol has the following main features: broadcast of system information, RRC connection control and mobility support [ETS19n]

The MAC and physical layer will be described in more detail in the following sections.

2.4.2.2. Physical Layer

LTE-V2X uses SC-FDMA as waveform for the sidelink, which is and has previously also been used in the uplink. SC-FDMA is a modified version of orthogonal frequency division multiple access (OFDMA), which in turn is based upon OFDM. Due to its low peak-to-average power ratio (PAPR), the requirements regarding the linearity of the power amplifier can be relaxed and the power consumption can be reduced, making it well suited for mobile, battery-powered devices such as mobile phones [ESAKAND16]. It was hence chosen for the uplink in LTE. SC-FDMA is also used for the later introduced sidelink, i.e. D2D communication, of LTE and has also found its way into the up- and sidelink for V2V communication.

Determining the maximum allowed transmit power for an UE, i.e. a vehicle, is not as straightforward as with ITS-G5. In a normative annex of ETSI Technical Specification 103 613 [ETS18a] and in the LTE standard itself [ETS19o, Section 6.2.2G and Table 6.2.2-1], the transmit power is specified to be $23\,\mathrm{dBm}$ with a tolerance of $\pm 2\,\mathrm{dB}$. Unlike in WLAN standards, which use the effective isotropic radiated power (EIRP) for power thresholds, the maximum output power is specified as the power at the antenna connector, i.e. the gain of the transmitting antenna is not included in the LTE transmit power specification. This maximum output power is valid for transmissions of any bandwidth within the channel [ETS19o, Section 6.2.2]. As the transmit power is distributed over the effective bandwidth, the spectral density for a single UE will be higher if it uses a smaller part of the channel bandwidth. Therefore, if multiple UEs transmit on single, different subchannels at the same time, there will be more power introduced to the channel than if a single UE transmits over the whole channel bandwidth. However, this maximum transmit power is subject to additional restrictions. Firstly, the maximum spectral density for the V2X channels ($5855 - 5925\,\mathrm{MHz}$) is specified as $23\,\mathrm{dBm/MHz}$ EIRP [ETS19o]. This means if an UE has an antenna with a maximum gain of $3\,\mathrm{dB}$ and transmits using a single subchannel of $2\,\mathrm{MHz}$, a maximum output power of $23\,\mathrm{dBm}$ can be used. If the antenna gain is higher, the spectral power density requirement can only be fulfilled by reducing the transmit power.

If the UE requires power reductions, e.g. to meet additional spurious emission requirements, i.e. emissions into other frequencies, it has the following possibilities. There is a mechanism called maximum power reduction (MPR) for an additional power restriction, which depends on the modulation and number of used resource blocks, i.e. subchannels. If only a single subchannel is used in a $10\,\mathrm{MHz}$ channel along with QPSK modulation, MPR leads to no additional restrictions. For multiple subchannels using QPSK or a single subchannel using 16-QAM, the MPR reduction is less than or equal to $1\,\mathrm{dB}$. The MPR is less than or equal to $2\,\mathrm{dB}$ if multiple subchannels are used along with 16-QAM modulation [ETS19o]. The other cases are likely not relevant for the V2V use case. Lastly, there is another power reduction mechanism besides MPR, called advanced maximum power reduction (A-MPR). A-MPR is a complex formula which depends on the post antenna connector gain, the adjacency of the resource pool, the carrier frequency, the number of used resource blocks and the start position of the first resource block. The A-MPR value consists of the sum of a base value and a step value, which is multiplied by the antenna gain before adding it. At the time of writing, the A-MPR step values are not yet defined for the V2V communication in the ITS-G5A band ($5875 - 5905\,\mathrm{MHz}$) [ETS19o, Table 6.2.4G-2]. The base value is $3.5\,\mathrm{dB}$ (one subchannel), $2.5\,\mathrm{dB}$ (two to four subchannels) or $3\,\mathrm{dB}$ (all subchannels).

The use of SC-FDMA as waveform leads to an interesting effect in practice. As the wireless channel is further subdivided into subchannels, multiple UEs can transmit at the same time without causing collisions if they chose different subchannels. Receiving UEs that are not involved in the transmission are able to receive these messages at once, leveraging the multiple access capabilities of SC-FDMA. However, this is not the case for transmitting UEs. Due to leakage of power from the transmit components into the receiver side, a terminal is usually either capable of receiving, which includes sensing, or transmitting, but not both simultaneously, even if it would have been performed on different subchannels. Hence, wireless transceivers typically operate in a half-duplex fashion. Therefore, the transmitting UEs are unable to receive messages distributed via other subchannels during the time they transmit. In the following, this limitation will be described as the *half-duplex problem*.

2.4.2.3. MAC Layer

There are four different modes of operation for D2D communication:

Mode 1: This mode uses the base station to centrally schedule radio resources.

Mode 2: If configured this way or if the base station is not available, a very basic random access scheme without involvement of the base station is used.

Mode 3: Like Mode 1, Mode 3 is centrally scheduled by the base station, but intended for V2X use cases. The LTE standard specifies the actual protocol to inform terminals about scheduling decisions, but the actual scheduling algorithm is up to the integrator or operator.

Mode 4: Like Mode 2, Mode 4 is a distributed mode. It is optimized for V2V communication, which does not rely on the presence of a base station.

For various reasons, it is unclear whether Mode 3 will be deployed in Europe, should LTE-V2X be chosen as access technology for V2V communication. Those reasons are a high signalling overhead as every terminal needs to inform the base station about the channel conditions at its location, possibly a lack of motivation between providers to coordinate the resource allocation between different base stations, complex failovers in case of (partial) outages or lack of coverage, and political considerations. For example, it is unclear whether the PLMN operators are willing or able to support and maintain the LTE infrastructure for as long as necessary to maintain connectivity to older vehicles in future. The focus of this dissertation is the distributed mode for V2V communication. Therefore, only Mode 4 will be described in detail.

Compared to IEEE 802.11p or the European variant ITS-G5, LTE-V2X Mode 4 has some important differences: SPS, which requires transmitters to periodically reuse radio resources, a resource reselection mechanism that leverages the periodicity of the transmitted packets, and an additional scheduling domain due to the division of the channel into subchannels by SC-FDMA [ETS19l]. The additional scheduling domain has implications on the MAC protocol, which are visualized in Figure 2.8.

From a MAC protocol perspective, the main difference to 802.11p is the introduction of subchannels, which allow to use the frequency domain as additional scheduling possibility [ETS19l]. The MAC protocol is slotted in time and LTE-V2X requires the clocks of terminals to be tightly synchronized, preferably by global navigation satellite system (GNSS) [ETS18a]. Another option is to use base stations to synchronize the clocks. It is likely that the terminals can keep the synchronisation for some time even if they cannot receive the synchronisation signal at all times. The scheduling granularity is one subframe (one millisecond) and one or more subchannels (frequency domain) [ETS19j]. The total number of subchannels is not fixed by the LTE standard itself, but the ETSI specified it to be five per $10\,\mathrm{MHz}$ channel [ETS18a]. Transmitters typically operate in half-duplex fashion, which makes it is impossible to receive or sense on other subchannels while transmitting. A transmission in LTE-V2X always consists of a sidelink control information (SCI), which is transmitted via the physical sidelink shared channel (PSSCH) and one or more transport blocks (TBs), which are transmitted using the PSSCH. The physical sidelink control channel (PSCCH) and PSSCH can be adjacent or nonadjacent [ETS19l], but the ETSI recommends the former [ETS18a]. The SCI contains additional scheduling and control information, while the TBs contain the actual data, i.e. the MAC PDU [ETS20].

The distributed MAC protocol of Mode 4 leverages the periodicity of messages exchanged in V2V communication to make predictions about future channel allocations. This mechanism requires transmitters to behave predictably, which is achieved by SPS. Transmitters are required, once they have chosen a new radio resource, to reuse it according to a *resource reselection counter*, which is a random number between 5 and 15, drawn each time a new resource has been selected. The lower and upper boundary of the reselection counter will be called $\mathrm{resel}_{\mathrm{min}}$ and $\mathrm{resel}_{\mathrm{max}}$, respectively. At the end of this reuse interval, the radio resource can be further reused with a given probability, which is called $\mathrm{probResourceKeep}$ and is not fixed by the LTE standard, but can be between zero and $80\,\%$. In this case, the resources are being reused (without re-evaluating the channel conditions or occupation) and a new reselection counter is randomly drawn [ETS19l]. Each reuse of existing radio resources happens blindly, i.e. without evaluating the current channel conditions. This procedure is visualized in Figure 2.9.

Once a terminal cannot keep re-using existing radio resources or if the currently reserved resources cannot fit the new packet, it must select new ones. The selection procedure makes predictions about future channel occupations based on the past. A terminal starts by selecting a selection window, which can be between 20 and $100\,\mathrm{ms}$, depending on latency requirements by upper layers. For CAMs, the latency requirement is $100\,\mathrm{ms}$ [ETS11b]. This time window, in conjunction with the subchannels, spans a two-dimensional matrix of candidate resources. The goal of the resource selection procedure is to exclude $80\,\%$ of the candidate resources, so that the $20\,\%$ with the lowest collision probability remain. From those $20\,\%$, the radio resource is chosen randomly [ETS19l]. There are three conditions that lead to the exclusion of candidate resources, which are visualized in Figure 2.10.

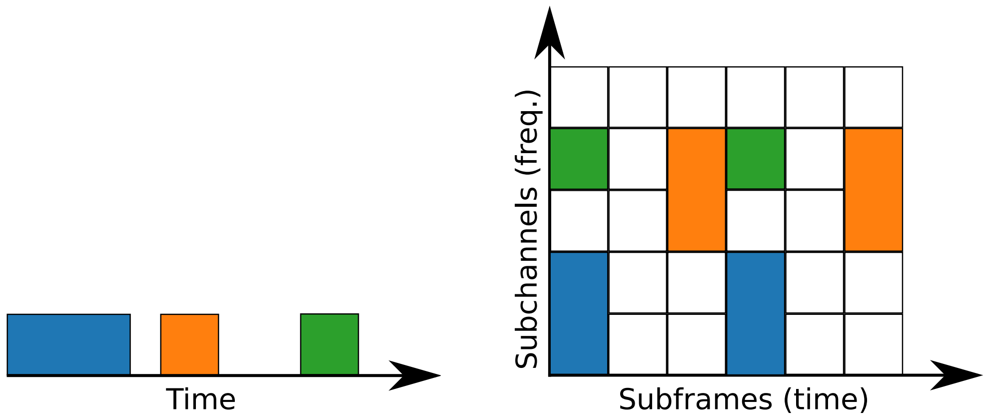

(a) OFDM. (b) SC-FDMA/OFDMA.

Figure 2.8.: Scheduling possibilities of OFDM and SC-FDMA/OFDMA.

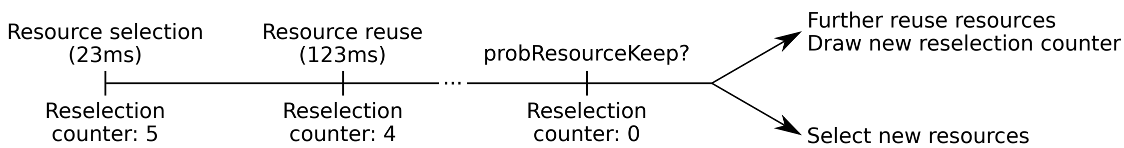

Figure 2.9.: Visualisation of SPS in LTE-V2X Mode 4 by example.

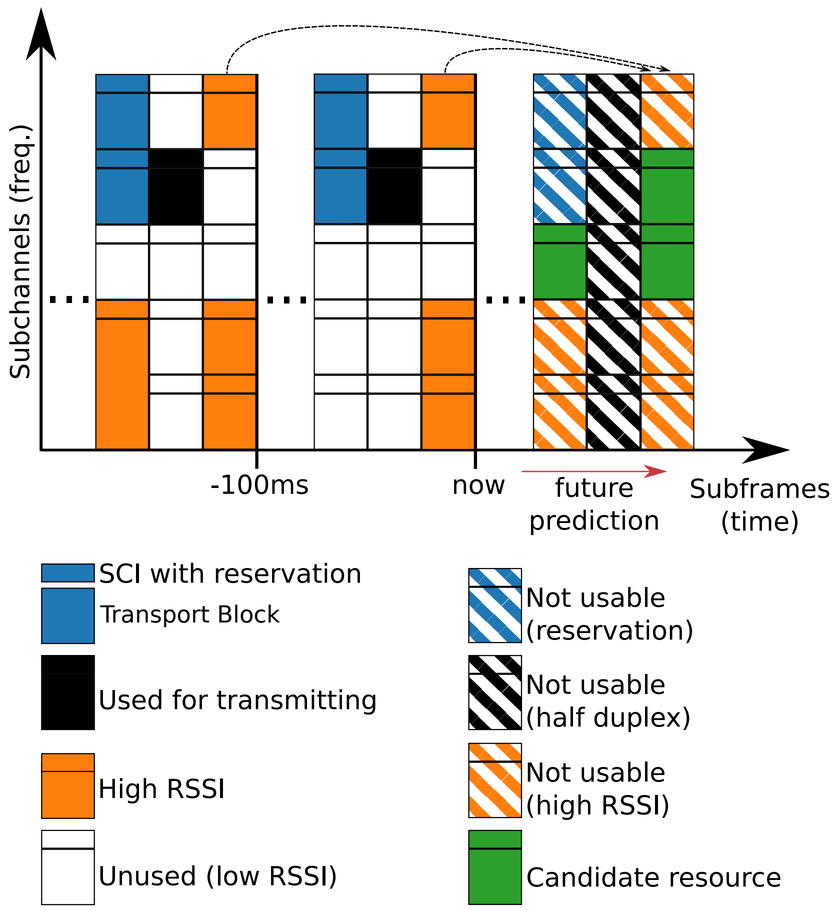

Figure 2.10.: Simplified visualisation of radio resource allocation in LTE-V2X Mode 4.

Explicit reservations: The SCI contains explicit reservations of other transmitters for the following transmission. If a terminal can receive and successfully decode this SCI and the measured reference signals received power (RSRP) is above a given threshold called $\mathrm{Th}_{a,b}$, it will exclude the resource in order to avoid collisions with this transmitter. The RSRP is the reception energy only measured over the reference symbols. If more than $80\,\%$ of the candidate resources are excluded, the procedure will be repeated with $\mathrm{Th}_{a,b}$ increased by $3\,\mathrm{decibels}$. This is done as often as necessary to reach the target number of candidate resources.

The $\mathrm{Th}_{a,b}$ depends on the priority of the received and transmitted packet. An index is built using the formula $i = a * 8 + b + 1$, where a is the priority of the packet to be transmitted and b is the priority of the received packet. This index is then used to look up the $\mathrm{Th}_{a,b}$ from the *SL-ThresPSSCH-RSRP-List* [ETS19l]. The first entry, i.e. with an index equal to zero, is minus infinity dBm. The last entry, corresponding to index value 66, is infinity dBm. Values in between are calculated as $(-128 + (\mathrm{index} - 1) * 2)$ dBm [ETS19n].

Half-duplex precaution: As previously noted, when a terminal is transmitting on a subchannel, it cannot simultaneously perform sensing or receive on other subchannels. This means that any other prediction of future channel allocations will not work for subframes that were used for transmission. Additionally, preventing the re-selection of the same subframe makes it less likely that half-duplex effects with the same transmitters carry on. Therefore, a terminal will exclude the whole subframe as a precaution if it has been using a corresponding resource in the past for transmission.

RSSI-based exclusion: There might be interference from transmitters that are further away, so that explicit reservations cannot be decoded or the reception energy is below the $\mathrm{Th}_{a,b}$ threshold, but the reception energy is still high enough to cause significant interference. The objective of the RSSI-based mechanism is to reduce the number of collisions with transmitters outside the communication range, but inside the interference range. The terminal calculates a linear average of the RSSI over the last ten repetitions of a resource, i.e. the last second. This is the mean value of the resource reselection counter. It will then exclude candidate resources with the highest RSSI until the $20\,\%$ target is met.

2.4.2.4. Distributed Congestion Control

DCC is a necessary tool to prevent channel overload and congestive collapse. It also keeps some radio resource unoccupied so that they can be used in emergency situations, e.g. for DENMs. It is mandatory for LTE-V2X Mode 4 in Europe [ETS18c]. The DCC algorithm works by mapping the priority of a packet and the current channel busy ratio (CBR) to allowed channel occupancy ratio (CR) values. This mapping is shown in Table 2.1. A CAM has a

Table 2.1.: ETSI DCC CR Limits Depending on CBR and PPPP [ETS18c]

CBR Range	PPPP $1-2$	PPPP $3-5$	PPPP $6-8$
$0 \leq \mathrm{CBR} \leq 0.3$	none	none	none
$0.3 < \mathrm{CBR} \leq 0.65$	none	0.03	0.02
$0.65 < \mathrm{CBR} \leq 0.8$	0.02	0.006	0.004
$0.8 < \mathrm{CBR} \leq 1$	0.02	0.003	0.002

proximity services per-packet-priority (PPPP) of five. Therefore, the CAM rate will only be reduced if the CBR is above $80\,\%$.

The CR is defined as the ratio between radio resources (i.e. subchannels per subframe) that have been used by the terminal itself divided by the totally available radio resources of the channel. Therefore, it is the portion of the channel that is occupied by the terminal. The CR is measured over one thousand subframes, i.e. one second. The measurement interval can be completely in the past, or reach up to $500\,\mathrm{ms}$ in the future, if the currently configured grant for radio resources reaches this far [ETS18c]. However, it is compliant to the specification if the CR measurement window never reaches into the future. The simulation framework developed for this dissertation follows this approach.

The CBR is defined for LTE-V2X by the ratio of resources with an RSSI above $-94\,\mathrm{dBm}$ during the last 100 subframes. An additional offset of four subframes is allowed so that there is time to perform the calculation.

It is not specified how a reduction of the CR has to be realized. A wireless terminal has the following possibilities to reduce its CR in order to comply with the current limit:

Dropping packets: This is the most straightforward way to reduce the number of used radio resources. Using this possibility, a terminal will just not use a reserved radio resource. There is a configurable number of consecutively unused radio resources after which a reservation needs to be discarded and new resources have to be selected using the sensing-based mechanism described earlier. This number is called *sl-ReselectAfter* [ETS20]. A default configuration or recommended value of this parameter is not specified yet. In the simulation framework for this dissertation, a value of nine was configured. Dropping resources can also mean to disable retransmissions, which are optional until a speed of $160\,\mathrm{km\,h^{-1}}$ and mandatory above this threshold [ETS18a].

Using more efficient modulation and coding schemes: A terminal can use less radio resources to transmit the same amount of data by increasing the modulation and coding scheme (MCS) index, i.e. by using more efficient modulation and coding schemes. However, this method makes the transmission more susceptible to interference and propagation issues, neglecting the benefits of a reduced channel load. Hence, the benefits of this method are debatable.

A reduction of the transmit power also reduces the channel load from a global point of view. However, it does not reduce the CR according to the definition given by the ETSI. Hence, it does not help in reaching a compliance with the CR limit.

2.4.3. Outlook for 5G

The PLMN technology is continuously evolving. 5G is the name of the successor to LTE. At the time of writing, the features specific for V2V are still a work in progress. The parts most interesting for this dissertation, the link layer and distributed MAC protocol have not been specified yet. In the 3GPP `RAN1#94` meeting, it was agreed upon two different modes for V2V sidelink communication: Mode 1, which is controlled by the base station, and Mode 2, in which the UE determines the radio resources by itself or with the help of other UEs or the base station.

Mode 2 is subdivided into four different modes:

Mode 2a: This mode is a completely autonomous resource selection mode.

Mode 2b: UEs can assist each other with resource selection in this mode.

Mode 2c: Pre-configured grants are used in this mode.

Mode 2d: A designated UE performs resource scheduling.

In the RAN1#95 meeting, studies and support for Mode 2b are dropped. It was however not ruled out that UEs can assist other UEs in other modes. LTE-V2X's Mode 4 can be found in Mode 2a. RAN1#95 also lead to the conclusion that a semi-persistent scheme and a dynamic scheme for resource allocation need to be further investigated [Cor19] and are therefore candidates for inclusion in the standard. In RAN1#97, the subchannel was agreed upon as the smallest granularity for the frequency domain for the PSSCH [Pro19a]. The RSRP threshold for considering reservations was looked at in RAN1#98 and it was stipulated that it depends at least on the priority of the transmitted packet [Pro19b]. RAN1#98b determined that the threshold should also depend on the priority of the received packet as in LTE-V2X. Moreover, the $20\,\%$ threshold for the ratio of candidate resources, as well as the repeated selection procedure with a RSRP threshold increased by $3\,\mathrm{dB}$ was also defined. Terminals could perform a reselection if they received a reservation that (partially) overlaps with the reserved resources [Pro19c]. RAN1#99 posted the working assumption that the resource selection mechanism of LTE-V2X Mode 4 will be reused. However, no ranking based on the RSSI should be performed. This illustrates that many concepts and ideas of LTE-V2X Mode 4 will likely be reused. This makes the research and improvements of this technology even more relevant for the future [Pro20].

2.5. Experimental Design and Analysis

Aside from the metrics mentioned previously, which are mostly relevant for the evaluation of the system in Chapter 8, Chapter 7 is dedicated to finding the optimal configuration parameters beforehand. In this chapter, experimental designs and analysis of variance will be performed using the procedure described by Raj Jain [Jai91]. This section introduces the general concept and procedure.

The goal of these experimental designs is to understand how important each configuration parameter is. Additional, isolated studies that vary only important parameters can then help to determine the optimal values of the important parameters. Confidence intervals determine whether the impact of a configuration parameter is statistically significant. Additionally, dependencies between configuration parameters can be determined. Understanding those can help when developing a set of parameter values for the configuration.

2.5.1. Terminology

In the analysis of the designs, various terms will be used. Those are precisely defined. In accordance with [Jai91], the following terminology will be used:

Response variables: These variables are the results of an experiment using a given metric, e.g. the PDR.

Factors: These are the (configuration) parameters of the system and experiment. Factors can be *primary*, which means that the effect of the factors are of interest and these factors will be varied during the experiment. There can also *secondary* factors, which are of no further interest.

Levels: The values that factors can take are called levels. A level can be an alternative hardware, e.g. a different processor model. It can also be a setting that is turned on or off, or multiple possible values of a tuneable parameter.

Interaction: This means that the effect of one factor depends on the level of another factor. For example, processor A might benefit more from faster memory than processor B.

Replication: A replication is a repetition of an experiment. This replication is subject to different random influences.

Design: This term is used to describe the specification of the number of experiments and replications, and the factor level combinations that are being evaluated.

2.5.2. Factorial Designs

Usually, the number of parameters of a system and the values that these parameters can take make it impossible to explicitly test all possible combinations of values. Full factorial designs use all possible values of a factor. A reduction of the levels per factor is recommended to decrease the number of necessary experiments [Jai91, Sec. 16.3.2]. The use of two levels per factor is very popular. It allows to determine which factors are especially effective or relevant. Further studies can be conducted to find the optimal value for the important parameters. This design is called the 2^k design (with k factors). If the experiments are repeated, i.e. have r replications, the design is called $2^k \times r$.

An additional method to reduce the number of necessary experiments is to use fractional designs. Fractional designs do not explicitly test all possible combinations of factor levels. Using the previous notation, the number of necessary experiments can be reduced to 2^{k-p} or $2^{k-p} \times r$, respectively. For example, a $2^7 \times 32$ design requires 4096 different experiments. Depending on the effort that is necessary to carry out a single experiment, this number of experiments is likely too high. Using a fractional design, it could be reduced, for example to $2^{7-4} \times 32 = 256$. Fractional designs also have an important disadvantage: the reduced resolution. This leads to a situation in which multiple combinations of factors *confound* with one another. Only the sum of the effects of confoundings can be determined. However, the exact confoundings can be determined before carrying out the experiment.

The responses subject to the factor levels are regressed on the primary factors using nonlinear regression. For example, the model for a 2^2 design is [Jai91, Sec. 17.2]:

$$y = q_0 + q_A x_A + q_B x_B + q_{AB} x_A x_B$$

A 2^2 design uses four experiments because it has two primary factors A and B with two levels each. Hence, there are four different equations with a different response y_i. The resulting set of equations can be used to determine q_0, q_A, q_B and q_{AB}. Now, q_0 represents the average response, q_A the effect of factor A, and so forth. The values of the factors are substituted with 1 and -1.

If repetitions are being used, the regression model is extended to

$$y = q_0 + q_A x_{Ai} + q_B x_{Bi} + q_{AB} x_{Ai} x_{Bi} + e_{ij}$$

where i is the experiment and j is the replication. Hence, e_{ij} is the error for the jth replication of the ith experiment.

Table 2.2.: Example of a Sign Table [Jai91]

I	A	B	AB	Mean $\bar{y}$
1	-1	-1	1	15
1	1	-1	-1	45
1	-1	1	-1	25
1	1	1	1	75
160	80	40	20	Total
40	20	10	5	Total/4

2.5.3. Sign Table Method

In order to handle the large number of different equations, the sign table method is generally used. The example for a 2^2 design from [Jai91, Sec. 17.3] is shown in Table 2.2. The first column, which is labelled as I, contains all ones. The columns A and B contain all possible combinations of A and B. The AB column is the product of A and B. The column y contains the result of the experiment with the configuration of the previous columns in this row. If multiple repetitions were made, it contains the mean value. The Total and Total/4 rows contain the mean response in column I or the effect of the factors or factor interactions in the other columns. These total values are obtained by multiplying the value of the column A with the mean response y and adding these values. For example, for column A, $-1 \times 15 + 1 \times 45 + (-1) \times 25 + 1 \times 75 = 80$. Hence, the last row contains the coefficients for the regression model.

2.5.4. Allocation of Variation

The importance of a factor is assessed with the fraction of the total variation that is due to this factor. The total variation or sum of squares total of a $2^k \times r$ design is [Jai91]:

$$SST = \sum_{i,j} (y_{ij} - \bar{y}_{..})^2$$

where y_{ij} is the response of the ith experiment and the jth replication. A dot indicates that the average is built across this dimension. Hence, $y_{..}$ is the mean response of all experiments and replications.

For a $2^2 \times r$ design, the variation explained by factor A can be calculated as $2^2 r q_A^2$, and so forth. The variation explained by errors is $SSE = \sum_{i,j} e_{ij}^2$. The percentage of variation is then easily calculated as $^{SSA}/_{SST}$, for example.

2.5.5. Calculating Confidence Intervals for Effects

When assuming that the errors are normally distributed, the confidence intervals for the effects can be calculated. This assumption should be verified by evaluating the distribution of the errors, e.g. by using quantile-quantile plots. An additional visual test is to plot the residuals against the predicted responses in a scatter plot in order to rule out any visible trend.

The variance of the errors can be estimated with [Jai91, Sec. 18.5]:

$$s_e^2 = \frac{SSE}{2^2 (r-1)}$$

The estimated variance for any effect is:

$$s_{q_i} = {}^{s_e}\!/\!\sqrt{2^2 r}$$

As the errors add up to zero, there are $r-1$ degrees of freedom. The confidence interval for any effect is hence:

$$q_i \pm t_{[1-\alpha/2;2^2(r-1)]} s_{q_i}$$

If the confidence interval of a effect does not include zero, it can be concluded that the effect is statistically relevant.

2.5.6. Confounding Factors and Factor Level Combinations

Despite restricting the number of primary factors and using only two possible values per factor, the experimental design might still be too large in many situations in practice. As previously mentioned, fractional designs can be used in these situations. These designs have a lower resolution. This shows in confounding factors, so that only the sum of these confounding effects can be determined. It can be determined which factors or factor level combinations confound with one another prior to carrying out the experiments.

In fractional designs, the last columns in the sign table are usually replaced by additional factors. The reason is that the last columns represent factor interactions with a high order, which are generally considered to be low. For example, a 2^4 design can be turned into a $2^{(5-1)}$ design by replacing ABC with D. The resulting confoundings depend on which of the columns have been replaced. In the previous example, D replaces ABC, hence $D = ABC$. Using I as the unity leads to the generator polynomial $I = ABCD$. By multiplying both sides of the polynomial with A, B, C, D, respectively and removing quadratic terms, more confoundings of the design can be calculated [Jai91, Sec 19.2–19.4]. For example, multiplying with A:

$$\begin{aligned} I &= ABCD \\ A &= A^2BCD \\ A &= BCD \end{aligned}$$

Hence, A confounds with BCD. Performing this step for the other factors leads to the additional confoundings $B = ACD$, $C = ABD$ and $D = ABC$.

When replacing more than one column, the generator polynomial consists of multiple entries, e.g. $I = ABD = ACE = BCF = ABCG$. As the product of any subset of this polynomial is also equal to I, it needs to be further expanded by considering all combinations of products before determining the confoundings. This is not further pursued here, but carried out in full for the $2^{7-3} \times 32$ design in Section 7.2.2. Depending on how large p is and which effects are being replaced by new primary factors, different confoundings exist. The confounding with the lowest number of factors determines the minimum resolution of a fractional experimental design.

Summary

This chapter started with an analysis of vehicular traffic. Traffic jams, in particular the end of a jam due to the high accident risk, and urban scenarios due to the importance of intersection-related traffic accidents, were identified as the most important simulation scenarios. The reaction times relevant for pre-crash situations depend on the human and vehicle itself. Human reaction times mainly depend on whether the driver anticipates the reaction and is usually below one second but can be higher in outliers. Communication-based driver assistance systems can help to prevent accidents or limit the negative consequences. Those systems can also be of simple and non-intrusive nature, e.g. by pre-charging brakes. Latencies introduced by MAC protocols can lead to an additional increase of the total reaction time. When forwarding warning messages, those latencies delay the message at every hop. Driving automation and platooning, as well as collective perception, are future developments that might lead to additional requirements for the access technologies. However, the currently predictable communication patterns do not indicate so. CPCL makes secondary use of radio signals for the location of objects. However, the application to V2V networks is in its early stages and the benefits of modified protocols are currently not quantifiable.

V2X communication can be between vehicles only (V2V), between vehicles and the infrastructure (V2I, I2V), or even between vehicles and pedestrians (V2P). Between vehicles, periodic local broadcast of typically short packets is usually used. Another important communication pattern are event-driven warning messages, which are sometimes forwarded via GeoNetworking (in Europe). They are also periodically repeated for increased robustness. Hence, most of the V2V communication is periodic.

The hidden-terminal effect is relevant for V2V communication and can severely limit the communication performance. Due to the broadcast nature of most of the communication, there are multiple potential receivers in the surroundings. Therefore, the potential receivers are not known to the transmitter and traditional mitigations for the hidden-terminal effect are likely costly. None of the currently standardised wireless access technologies with distributed scheduling and stochastic channel access deploy mitigations for hidden-terminal situations. The exposed terminal situation is less relevant for broadcast communication. The high mobility of terminals and subsequent variability of channel conditions can be an additional challenge for V2X communication, including MAC protocols.

C-ITS is the term used for intelligent and communication-enabled vehicles in Europe. Applications of this technology include active road safety, cooperative traffic efficiency, local services, and internet services. The standards are developed by the ETSI. Unlike the traditional OSI architecture, C-ITS uses four horizontal layers (applications, facilities, networking and transport, access layer) and two cross-layer, vertical entities (management and security). The facilities layer incorporates the cooperative awareness basic service, which periodically transmits CAMs, which contain the current speed, position, direction, etc. The decentralized environmental notification service is responsible for event-driven warning messages, e.g. about obstacles on the road. This information is stored in the LDM, also part of the facilities layer. The LDM also contains other information about the environment, e.g. objects detected with radar sensors. The network and transport layer contains various technologies relevant for this thesis, most importantly congestion avoidance mechanisms and the GeoNetworking protocol. This protocol enables message dissemination via point-to-point, point-to-multipoint, GeoAnycast and GeoBroadcast mechanisms. The access technologies layer can use different wireless technologies for communication, e.g. ITS-G5, LTE-V2X, or traditional WLAN.

There are various competing wireless access technologies for vehicular communication. ITS-G5, based on WLAN, uses a distributed, listen-before-talk MAC protocol (EDCA, i.e. a CSMA/CA variant). The RTS/CTS mechanism of normal WLAN is not used. A DCC mechanism is introduced, which limits the channel load to levels in which the MAC protocol can function properly.

The competitor to ITS-G5 and the focus of this dissertation is LTE-V2X. Vehicles can communicate with the base station, but also among themselves without any forwarding (sidelink). The base station can be responsible for scheduling the radio resources for the sidelink (Mode 3).

However, it is also possible that terminals are required to choose them by themselves (Mode 4). This can be due to lack of coverage of the base station, interference, downtime, denial-of-service (DoS) attacks, or even regulation – it is possible that Mode 4 will be the only deployed mode in unlicensed bands. The ideas developed in this dissertation are targeting Mode 4. The sidelink uses SC-FDMA as waveform, which enables scheduling possibilities both in the time (subframe) and frequency (subchannel) domain. This means that traditional CSMA/CA MAC protocols will not work. While a terminal is transmitting, it cannot receive messages from other terminals, even if they are on different subchannels (half-duplex problem). Mode 4 instead leverages the periodicity of the messages typically used in V2V communication and requires transmitters to periodically reuse radio resources (SPS). This enables terminals to extrapolate the resource use by others into the future when selecting radio resources. Radio resources which are reserved by others, were affected by half-duplex operation, or had a high average reception power in the past, will not be used because of the high risk of collisions. Mode 4 also has a DCC mechanism. 5G, the successor to LTE-V2X will also have distributed scheduling modes, which will likely be similar to LTE-V2X.

Lastly, a short overview of experimental design has been given. Experimental designs are a method to systematically manage the evaluation of systems with a larger set of configuration or system parameters. The goal of the designs is to reduce the number of necessary experiments to manageable numbers while retaining as much accuracy as possible. As this technique will be used in later chapters of this dissertation, an overview over the terminology, full and fractional factorial designs, the sign table method, allocation of variation, confidence intervals for effects, and confoundings has been given. The experimental design method is often used to determine which parameter of a system has the largest amount of influence and which parameters interact with one another. Further studies about the identified important parameters should then be carried out afterwards.

Chapter 3.

Requirements and State of the Art

In this chapter, requirements for MAC protocols and congestion control mechanisms in the vehicular environment will be presented. The current state of the art will then be investigated with those requirements in mind.

3.1. Requirements

This section deals with requirements both for MAC protocols as well as DCC. Even though an integrated solution for MAC and DCC has been developed for this thesis, the functional requirements in this section are subdivided into requirements for medium access control and for congestion control, because they differ significantly. The non-functional requirements for MAC and DCC are very similar and can be described in a single section. All requirements have been established while considering the vehicular communication scenario.

3.1.1. Functional Requirements for Medium Access Control

The main functional requirements for MAC protocols for V2V communication systems are as follows:

Coordination of resource allocation and scheduling: The main functional requirement of MAC protocols is the allocation of communication resources to nodes, i.e. multiplexing the transmission medium. With wireless communication, these communication resources are slices of the shared radio medium. Depending on the capabilities of the physical layer, such a slice can be a time slot, a frequency slot, or a combination of both. When using multi-user multiple-input and multiple-output (MIMO), an additional geometric dimension can be introduced. This is out of scope for this dissertation due to the broadcast-nature of the V2V communication. The main goal is to prevent a double use of such radio resources that would cause radio frame collisions. If there is no central scheduling entity, i.e. base station, this task has to be carried out with distributed MAC protocols.

Detection of collisions by the transmitter itself: A terminal should have the ability to detect whether its transmissions are successful or not, and whether other vehicles are able to react to the transmitted message. As indicated below, this information can be used to react to unsuccessful transmissions.

Reaction to detected collisions: If a terminal notices that its currently used radio resources resulted in collisions on the medium, it should react to it. This is even more important in the context of SPS, where it might not be advantageous to keep reusing resources which lead to bad performance. There can be different ways to react to such a situation, e.g. retransmissions, or a selection of new radio resources ahead of time. In any case, *congestive collapse*, or any other effect that is adverse to the initial intention of the reaction, should be prevented.

Prevention of Hidden-Terminal-Effects The hidden-terminal effect (see Section 2.2.2.1) can cause severe problems for the performance of a broadcast and unicast communication system. For V2V communication, the effective communication range can be severely impacted. Therefore, it is desirable that a V2V communication protocol is able to detect, prevent, and/or react to hidden-terminal situations.

3.1.2. Functional Requirement for Distributed Congestion Control

The main functional requirement of congestion control is to limit the channel load. The DCC component has to be able to limit the channel load even in extreme scenarios. There are two main arguments for this requirement. Firstly, there should be always some unused capacity available in case vehicles need to transmit warning messages at short notice. This underlines the importance of this functional requirement instead of only using quantifiable, non-functional metrics to assess the performance in general. Secondly, the performance of stochastic MAC protocols deteriorates at a certain threshold of the channel load. This is because many terminals contest for few radio resources in those situations. A terminal has at least three possibilities to limit the channel load: by reducing the packet transmit rate, decreasing the transmission power (so that the spatial reuse increases), and by transmitting the same amount of data using a more efficient MCS. The use of more efficient MCSs makes the communication less robust at the physical layer, while making it more robust at the MAC layer. The overall advantage is unclear, but it is certain that a range penalty will occur, similarly to the case of reducing the transmit power.

3.1.3. Non-Functional Requirements

The following non-functional requirements can be identified both for MAC protocols and DCC mechanisms in V2V communication.

High packet delivery ratio: One of the main non-functional requirements is a low number of radio frame collisions. Using a simple definition, the PDR is the ratio of successfully transmitted packets. However, it is often unclear which set of transmitted packets should be included in the *divisor* of the fraction. If the PDR is used to evaluate the MAC protocol or DCC components, and to draw conclusions from comparisons between different versions of these mechanisms, some physical layer effects are not relevant. For example, it is not necessary to include packets that are physically impossible to decode due to the long range and corresponding low reception power. Doing so would mean that the PDR value correlated heavily with the size and composition of the evaluated scenario. Additionally, the maximum achievable value might be very low and/or unknown. Therefore, it would be better to only include packets that would be decodable in the absence of interference. This is however impossible when stochastic receiver models are used, which map the success of the receive operation to a probability that depends on the signal-to-interference-plus-noise ratio (SINR). In addition to that, channel models usually also model fast fading effects with a random variable, which influences the reception energy. As a conclusion, it might be best to create different results for different ranges of the communication distance. This has the additional advantage that conclusions about the more safety-critical low distances can be drawn. As seen in Section 6.6, the way the PDR is calculated also has an effect on the expressiveness of the result. The main conclusion of the previous discussion is that PDR values in papers cannot directly be compared to one another because they depend upon the exact definition of the term by the authors.

Low Overhead: MAC protocols and transmitted meta-information can introduce overhead to each transmission, which decreases the amount of channel capacity that can be used to transmit the actual payload data. These overheads should be kept as low as possible. However, accepting some additional overhead in order to increase the overall communication performance might be justified.

Application performance: Traditional metrics such as the PDR are important for the evaluation of communication systems and MAC protocols in general. However, the application-oriented performance should be considered as well, as it is the *real* requirement of the complete system. There are scenarios in which the classical metrics show good results, but the communication system still has undetected disadvantages when used for the desired application. Therefore, it is important to use application-oriented metrics in order to be able to determine the performance from the point of view of the intended application. For example, the goal of the cooperative awareness basic service is that vehicles gain knowledge about the vehicles in their surroundings. Therefore, an application-oriented metric could quantify this knowledge. Compared to this, traditional metrics such as the ratio of successful transmissions might not be as important. For example, there might be a single vehicle that is unknown to the others, but all other vehicles know about each other and the mean PDR is very high. The lack of knowledge about that single car can lead to severe traffic accidents because such accidents are often the result of a combination of multiple unfortunate events.

Latency and Inter-Packet Gap: The MAC protocol should enable the delivery of messages according to the latency requirements of the applications. This non-functional requirement can be quantified if the message type is known. For example, a CAM has a maximum allowable latency of $100\,\mathrm{ms}$ [ETS11b] and the MAC protocol needs to support this. Some DENM message types such as the pre-crash sensor warning have an even lower latency requirement of $50\,\mathrm{ms}$ [ETS09]. DCC by itself increases the latency, or at least the inter-packet time gap, by design. The DCC mechanism should still ensure that there are no extreme outliers in the inter-packet delay. Such gaps could occur if the DCC protocol favoured or enabled situations in which a high number of successive packets would be suppressed, followed by longer packet bursts. In this situation, there would be a long time interval in which other vehicles would not receive updates from the affected vehicle.

Quality of service: QoS aspects, with the meaning of traffic prioritisation, can be implemented both in the MAC layer and DCC component. For example, packets with a higher priority can preferably be allowed to use radio resources with the lowest collision risk. This scenario is relevant in the V2V scenario. Usually, there is a constant stream of CAM packets, and it is usually tolerable if a vehicle cannot receive such a message once because the previous and subsequent CAM is only $100\,\mathrm{ms}$ in the past or future. However, a low delay and reliable transmission of warning messages, i.e. DENMs, is very important to prevent accidents. Therefore, ETSI assigns higher priorities for DENMs than for CAMs. In case of ITS-G5, these priorities translate to the contention window [ETS13b]. In case of LTE-V2X Mode 4, the threshold $\mathrm{Th}_{a,b}$ is influenced [ETS18a, ETS19l, ETS19n]. As any intervention of DCC penalizes the affected packet, QoS control can be implemented by focusing on packets with low priority. QoS changes the reliability of a transmission depending on the priority. When comparing two different access technologies, the overall performance is more important than the impact of QoS. In particular, the general performance of a competing protocol might be so much higher that even packets prioritised by QoS cannot reach the baseline performance of the competing protocol.

Fairness: Both MAC and DCC mechanisms should ensure that no terminal is substantially preferred or hindered. Assigning the same amount of radio resources to each terminal is however impossible, simply due to quantisation effects or incomplete knowledge in a distributed system. It should however be prevented that some terminals are completely hindered and unable to transmit safety-critical messages while others are not.

Scalability: The MAC protocol and DCC mechanism need to be able to cope with extreme scenarios and high channel load, for example in scenarios with a high vehicle density such as traffic jams on highways. The DCC mechanism is likely more affected by this requirement, as it needs to be able to reduce the packet rate of each terminal by a significant amount.

Generality: The system should be able to function in many different scenarios, e.g. urban traffic scenarios, suburban and rural roads, highways with a low to high amount of traffic. This can be validated by using various traffic scenarios for the evaluation. To prevent over-fitting of parameters, not all evaluation scenarios should be used for the design and optimisation of the system or its parameters in addition for its evaluation.

Reliability and robustness: The reliability requirement is related to the generality and adaptability requirements. Still, the vehicular scenario leads to additional requirements, mostly related to the quick changes due to moving terminals and heavy shadowing effects. Vehicles can move quickly, but there is generally a correlation between the movement of different vehicles, because they need to follow the road network. Many vehicles move in the same direction along the road and a group of potentially similar size moves exactly in the opposite direction on the oncoming lane. This means that the MAC and DCC protocols of the terminal in a vehicle will need to cooperate with a set of vehicles that move in the same direction and are not likely to change, and with a set of vehicles that move in the opposite direction, i.e. might get inside or outside the communication and interference range more quickly. Additionally, shadowing effects might lead to a quick appearing and disappearing of communication partners and hence, sources of interference. The protocols should be able react to those situations in adequate manner. Otherwise, effects on quantifiable requirements and metrics such as the PDR and awareness metrics might emerge.

Autonomous operation: Central instances in general are a single point of failure. The risk of losing the availability of critical services is often reason enough to forgo such architectures. Widespread outages have already affected the PLMN of different operators in the past. Single points of failures are often also chosen by attackers. In the cellular infrastructure case, the base station can be targeted by various attacks. Attackers could create DoS attacks, e.g. by physical destruction, or jamming of the radio medium at a position close to the base station. This would hinder the base station from receiving any other signal, which increases the range of the attack beyond the potentially shorter range of the jamming signal. Moreover, there are more sophisticated attacks that target the integrity and authenticity, confidentiality, etc. of the transmitted data.

For infrastructure services, the base station is obviously essential. Still, it is possible to build peer-to-peer (P2P) components in a way that they do not rely on this infrastructure, avoiding the aforementioned disadvantages. This also means that there should be no designated wireless terminals with special features, even temporarily, e.g. single terminals that are responsible for the scheduling of radio resources for surrounding terminals.

Compatibility: The protocols developed in this thesis are based on cellular technology. As modifications to the MAC and DCC components are being developed, it is inevitable that the performance of some protocol features depends upon the fact that every terminal follows the same protocol. However, the protocol should not substantially deviate from LTE-V2X Mode 4. For example, protocol modifications should still be compatible with the hardware, physical layer procedures, and general ideas and assumptions made in the MAC layer. These features are primarily the SPS, and the resource grid scheme and SC-FDMA.

3.2. State of the Art

This section deals with the current state of the art regarding the MAC protocols and DCC in vehicular communication, as well as the evaluation methodologies and metrics currently in use. It only deals with results published by other researchers. A detailed problem analysis follows in Chapter 4.

3.2.1. Evaluations of Existing Standards

This section gives an overview of research related to the performance of existing standards that are relevant for V2V communication. This includes LTE-V2X Mode 4, its DCC method, and comparison studies between LTE-V2X and ITS-G5 or IEEE 802.11p.

3.2.1.1. Performance of LTE-V2X Mode 4

An analysis of the state of the art regarding the performance of LTE-V2X Mode 4 is advantageous by identifying potential existing deficiencies and starting points for further improvements and modifications. Additionally, recommendations about the configuration of parameters of LTE-V2X could be derived. This section only deals with the performance of the distributed scheduling mode of LTE-V2X (Mode 4).

Molina-Masegosa et al. [MG17] present a system-level evaluation of LTE-V2X Mode 4 in urban scenarios. They use a Manhattan grid scenario. The packet rate of the periodic packets is $10\,\mathrm{Hz}$. One of five packets has an increased size of $300\,\mathrm{B}$, the other packets are $190\,\mathrm{B}$ large. Some of the simulation and system parameters are different to the ones preferred by ETSI [ETS18a]: in the paper, four subchannels per subframe are assumed instead of five. This means that the small packets can fit into one subchannel instead of two. Moreover, the RSRP threshold $\mathrm{Th}_{a,b}$ was apparently not yet specified at the time of writing. Hence, the authors assumed $-110\,\mathrm{dBm}$, which is significantly lower than the value to be expected in practice (see Section 4.1.1.1). The results indicate that the sensing-based SPS leads to an increase of the PDR compared to random selection. However, these improvements become smaller if retransmissions are enabled. If one of the two redundant transmissions are not decodable, the transmission is still counted as successful when evaluating retransmissions. The authors analyse which errors are the causes for the transmission errors. The analysed errors are half-duplex, propagation, collision errors, and errors due to inability to decode the SCI. Collisions are the dominant reason for transmission errors until a transmission distance of about $250\,\mathrm{m}$, after which errors due to propagation effects become more likely. The SCI can be received at larger distances, which can be attributed to the more robust modulation and coding scheme. The authors conclude that further enhancements or even alternative schemes should be investigated to improve the performance of LTE-V2X Mode 4, especially in situations with a high vehicle density or traffic load.

Toghi et. al [TSM+18] publish simulation results of LTE-V2X Mode 4 in highly congested highway scenarios. The authors use packet sizes of 190 B and 300 B and apparently only two subchannels per subframe. One of the goals of the paper is to determine the best configuration parameters for Mode 4. In the study, a lower probResourceKeep value leads to a higher PDR and a lower inter-packet gap. It is difficult to derive an optimal value for the RSRP threshold, however. This is due to the non-linear response of the PDR and inter-packet gap metrics. In general, the trend of better performance with a lower energy threshold can be observed.

Mansouri et al. [MMH19] present a performance analysis of LTE-V2X Mode 4 by simulation in a slow and fast highway scenario. The authors use the uncommon configuration of only three subchannels per subframe. The results indicate that LTE-V2X Mode 4 leads to significant increases of the PDR compared to a random selection of the radio resources. They also determine the necessity of a DCC algorithm and evaluate a first model, which will be described in Section 3.2.1.2.

Nabil et al. [NKDM18] determine the influence of configuration parameters of LTE-V2X Mode 4. The authors select three major configuration parameters: the resource pool configuration, the resource reservation interval, and the probResourceKeep parameter. The resource pool configuration states how many radio resources of a channel are dedicated for V2X communication. In practice, it can be assumed that complete channels will be dedicated for this, making this parameter less relevant. Unfortunately, the first and second parameter of those have secondary influences on the available bandwidth or the packet rate, and hence, the channel load. This means that mostly the effect of a higher or lower channel load is evaluated. The investigation of the probResourceKeep parameter however, is highly relevant. The authors evaluate LTE-V2X Mode 4 in a freeway traffic scenario with simple vehicle mobility patterns. They use the same packet sizes like in the papers described previously: four out of five packets are 190 B large, while one is 300 B large. The results show that the probResourceKeep parameter has a negligible impact on the PDR. A small tendency that a higher value leads to a lower PDR can be seen. With other problems of this mechanism (see Section 4.2.1), the best configuration of this parameter seems to be 0 %. Furthermore, the authors conclude that the performance of LTE-V2X Mode 4 has room for further improvement. Additionally, they state that more research on DCC is necessary.

Molina-Masegosa et al. [MGS18a] also investigate the impact of various parameters of LTE-V2X Mode 4 in different traffic patterns and with different channel loads. The different scenarios have a significant impact on the performance and optimal configuration. A configuration of four subchannels and a packet transmission pattern of either solely 190 B packets or a mixture of 190 B and 300 B packets is used. In the latter case, one of five packets has the larger size. The authors investigate the influence of the probResourceKeep parameter, the length of the sensing window, the initial RSRP threshold, and the size of the set of valid candidate resources. Of those, only the probResourceKeep parameter is not explicitly defined in the standard. Even the $\mathrm{Th}_{a,b}$ threshold is currently fixed by the *SL-ThresPSSCH-RSRP-List* [ETS19l]. Nevertheless, the results are still relevant. The probResourceKeep parameter leads to conflicting results. Increased values can lead to PDR improvements in scenarios with low channel load. However, the effect is negative in scenarios with high load. Additionally, high values increase the inter-packet reception delay due to reoccurring collisions. A shortening of the sensing window can lead to an increased PDR. However, this makes the performance more reliant on the RSRP method for candidate resource exclusion. The initial threshold of this mechanism only has an impact if the channel load is high. In these cases, a low threshold is beneficial. Generally, changing the size of the valid candidate resource set, which is 20 % by default, has no significant impact on the performance. This is because changes in both directions have individual disadvantages that seem to balance out. Specifically, a low channel load benefits from a larger value and a higher channel load from a lower value as fewer resources are actually free. This indicates that it might be beneficial to determine this parameter depending on the current channel load.

3.2.1.2. Distributed Congestion Control of LTE-V2X Mode 4

This section specifically deals with related work about the DCC algorithm that is part of the LTE-V2X standard and ETSI [ETS18c]. Additionally, other DCC approaches are included if the conclusions are useful and a comparison is applicable. Unfortunately, there is only a limited amount of research available regarding DCC for LTE-V2X.

Mansouri et al. [MMH19] presented the first analysis of a DCC mechanism for LTE-V2X Mode 4. The DCC model is close to the version specified by ETSI [ETS18c]. However, the mapping of CR limits to the current CBR parameters were not fixed at the time of writing and were based on 3GPP working group contributions. This mapping is more restrictive than the values subsequently published [ETS18c]. Additionally, the authors use only three subchannels per subframe instead of five. Nevertheless, this paper gives a relevant insight into the performance and compatibility of DCC with LTE-V2X Mode 4. The authors determine that the DCC algorithm of LTE-V2X Mode 4 leads to a reduction of the PDR, even though the CBR decreases. This counter-intuitive result is attributed to the fact that the reservations of old messages are invalid if a packet is dropped, tricking other terminals into thinking that this resource will be used when it is not. Additionally, the first packet after the drop of a previous one will not be announced by reservations. This shows that the current DCC version is incompatible with SPS from a performance point of view. The authors propose to select completely new radio resources after each resource drop to prevent this. This however is not evaluated. The lack of periodicity of the use of radio resources could lead to additional performance problems. The authors also note that the CBR is subject to relatively large amounts of oscillation and propose a method to reduce those by a more fine-grained CR mapping and a hysteresis method.

Toghi et al. [TSFM19] present an analysis of a custom DCC algorithm standardised by Society of Automotive Engineers (SAE), which has rate- and range-control components. This DCC variant has been originally developed for DSRC but has been adopted by the authors of the paper to be used with LTE-V2X Mode 4. The authors only use two subchannels per subframe and multiple configurations of a twelve-lane highway traffic scenario with different traffic densities. Rate-based congestion control sacrifices throughput in closer ranges in order to increase the effective communication range. The DCC mechanism increases the PDR without sacrificing latency or throughput. The authors note the interesting observation that LTE's fixed mapping of the CBR value to allowed CR values is not capable of correctly restricting the channel load in scenarios with high congestion because the channel load cannot increase past a certain value even if more and more transmissions are carried out.

Toghi et al. [TSMF19] also investigate the spatio-temporal dynamics of LTE-V2X Mode 4, with special focus on DCC variants. They use different traffic scenarios, but simple models for the behaviour of vehicles. The authors note concerns about the compatibility with SPS and a range-based DCC. Range-restriction is realized by reducing the transmit power. This reduced transmit power could impact the sensing-based SPS. However, the authors note that range-control has a quicker response time than rate-control. According to the authors, SPS and rate-based DCC are compatible from a functional perspective.

3.2.2. Comparative Analysis

In this section, related work that compares the performance of IEEE 802.11p and LTE-V2X Mode 4 is presented. The goal is to help understand the implications and differences of the more random CSMA/CA algorithm of IEEE 802.11p compared to the more persistent allocation scheme of LTE-V2X Mode 4. In this section, the nomenclature of the papers is kept. There are only few differences between IEEE 802.11p, DSRC, or ETSI ITS-G5.

Hu et al. [HCZ+17] performed an early simulation study to compare the link-level performance of LTE-V2X to DSRC. Only the impact of the physical layer is considered in this study. Hence, differences in the MAC protocol are not of concern for this paper. The authors show that LTE-V2X is able to reach the same block error rate (BLER) than DSRC with a lower signal-to-noise ratio (SNR). The reason for this improved performance lies in the differences in the coding and channel estimation. LTE-V2X uses turbo coding, an advanced and more robust scheme compared to DSRC. The channel estimation of DSRC is performed using the long and short training sequence in the preamble. Afterwards, only four subcarriers are used as pilots during the complete duration of the signal. This might not be enough to keep a accurate channel estimation during the transmission. LTE-V2X uses four dedicated demodulation reference symbols (DMRSs), which occupy all subchannels, i.e. the complete transmission frequency.

Mannoni et al. [MBSP19] perform a comparison study that considers aspects of the physical as well as the MAC layer. The simulation scenario is rather unrealistic for V2V communication because vehicles follow specific routes on roads in reality, but the study assumes a random placement of the nodes. Only a single communication link is observed in this study. The authors only evaluate Mode 4 of LTE-V2X with $\mathrm{probResourceKeep}$ set to zero. The results show that the cellular technology has advantages in low-density scenarios, while ITS-G5 takes the lead in scenarios with high network density. From a perspective of the physical layer, it can be seen that LTE-V2X requires less SINR in order to reach the same packet delivery ratio. ITS-G5 requires significantly less time for the channel access, which can be explained by the selection window of LTE-V2X. However, the practical update delay of LTE is better at distances larger than $300\,\mathrm{m}$.

Nguyen et al. [NSS+17] publish a simulation study that compares LTE-V2X Mode 4 to DSRC in a highway and urban scenario. Interestingly, triggering conditions for the generation of messages have been used, so that the CAM rate can be seen as variable. Additionally, the authors note that assumptions regarding the characteristics of the physical layer performance of the terminals have been made that are disadvantageous towards LTE-V2X. For example, it is assumed that the first symbol of each subframe is lost due to automatic gain control. The authors show the PDR subject to the transmission range. The results indicate that LTE-V2X can reach a higher PDR in both traffic scenarios, however especially in higher ranges and in the highway scenario. In the highway scenario, this advantage gets better with increasing vehicle speed. One of the reasons is that the average CBR decreases and LTE-V2X terminals are allowed to use double transmissions in such conditions. The packet is recorded as successfully transmitted even if only one of those transmissions is decoded.

Vukadinovic et al. [VBM+18] compare IEEE 802.11p and LTE-V2X in a platooning scenario. Both Mode 3 and Mode 4 of LTE-V2X are evaluated. However, idealistic assumptions are made about Mode 3 and collisions on the sidelink or transmission errors to the base station do not occur. For Mode 4, the authors deviate from the standard and use a reselection counter range between one and three to prevent repeating collisions. The authors use the CAM latency and reception ratio as traditional metrics. The latency only includes the channel access and transmission latency. It is hence not relevant whether this message has in fact been received or not. The interesting unique feature of this paper is the application-oriented metric for the evaluation. In order to evaluate the platooning scenario, they use the achievable average inter-truck spacing as metric. The requirement is that the crash probability is below $99\,\%$, which could be increased to practical levels with other technologies as additional safety mechanisms. As Mode 3 is assumed to function without errors, it outperforms the other technologies. The authors note that 802.11p scales poorly with increasing channel load and leads to an increased number of collisions, apparently caused by hidden-terminal effects. LTE-V2X Mode 4 performs better than 802.11p and can reach a lower inter-truck spacing in all scenarios in which there is background traffic from vehicles outside the platoon.

3.2.2.1. Conclusion

In the previous sections, related work regarding the performance of LTE-V2X Mode 4, its DCC mechanism, and comparisons with IEEE 802.11p has been reviewed.

Comparison studies often attribute a better performance to LTE-V2X Mode 4 than to IEEE 802.11p. However, LTE-V2X has special issues, which are discussed by other papers. In multiple papers, the issue of reoccurring collisions is noted. Once radio resources collide in LTE-V2X Mode 4, it is likely to repeat as both transmitters are likely to reuse the same radio resources in the future due to the reselection counter. This was also discovered during the work on this dissertation and published in [WST19b]. The $\mathrm{probResourceKeep}$ parameter has a significant influence on the length of these reoccurring collisions. In papers that use the inter-packet gap as metric, an increase of the extreme outliers is reported when $\mathrm{probResourceKeep}$ is increased. The half-duplex issues can persist in time due to the same reasons. A more detailed analysis is presented in Section 4.2.1. The parameter also influences the PDR in some papers. However, these results are inconclusive. In general, configuring this parameter to zero for a reduced period of blindness due to the reocurring collision issue seems to be the only viable option. This configuration often also showed better PDR result. An additional problem of LTE-V2X Mode 4 is the inflexibility of the resource allocation. If packets of a packet flow vary their rate or packet sizes, the semi-persistent resource allocation might not be suitable anymore.

The need for DCC is clearly documented in the current research, but not much research is available on the topic. Interestingly, while the DCC mechanism of LTE-V2X Mode 4 is able to reduce the CBR, it also reduces the PDR. An incompatibility between SPS and DCC has been noted as the possible reason. A different publication notes that the fixed mapping of the DCC mechanism can lead to an insufficient reduction of the CBR, which means that it cannot fulfil the functional requirement noted in Section 3.1.2. Different authors share the concern that DCC based on transmit power reduction is not compatible with SPS.

Many of the currently published studies do not set the RSRP threshold according to the *SL-ThresPSSCH-RSRP-List* [ETS19l], but set arbitrary, fixed values instead. This might have an impact on the reported performance.

3.2.3. Media Access Control Proposals for LTE-V2X Mode 4

This section gives an overview of the current state of the art regarding proposed improvements or protocols for LTE-V2X Mode 4, i.e. protocols that work with SC-FDMA.

Abd El-Gawad et al. developed, evaluated [EGEK19b] and tested [EGEK19a] HCMAC, a hybrid cooperative MAC protocol for IEEE 802.11p. This protocol also uses time slots. A time slot cannot be used by more than one vehicle. Each terminal attaches the list of one-hop neighbouring terminals to each beacon message, which also includes the time slot that is used by this terminal. Protocols that depend on the exchange of one-hop neighbour information have already been investigated in the area of WSNs [ROGLA03]. Before acquiring a new slot, a terminal has to listen for a given period of time to receive enough information about the neighbouring vehicles. Afterwards, a free slot is chosen randomly. Collisions can be detected by checking whether the terminal is in the received neighbour list, i.e., if other vehicles recognized the vehicle. HCMAC uses additional, more advanced collision detection methods. These include a random backoff inside the slot before the transmission to enable carrier sensing. In addition to the list of neighbours and slots, terminals also attach a list of slots that were affected by collisions. This is detected at the physical layer by assuming that a packet that is not recoverable despite a high RSSI indicates a collision. The approach is also evaluated with real measurements, in which not many vehicles can be used for testing. The overhead related to the explicit naming of terminals and slots increases with the number of terminals in the one-hop neighbourhood. In realistic scenarios, this overhead can grow too high and the practicability of the approach can thus be debated. Nevertheless, a unique feature of HCMAC is the possibility to prevent hidden-terminal situations.

Jeon et al. [JKK18] propose *reservation lookahead*, which means that the next starting resource is indicated in the current transmission, even if the next resource is different from the current one. As the next resource has to be known prior to sending the last packet of the old resource set, the new resources have to be chosen earlier than with standard LTE-V2X Mode 4. This might increase performance disadvantages. The authors use a very simple simulation model that neglects all effects at the physical layer and use a disk model for the distribution of terminals. Effects like propagation, coverage, path loss, fading, or hidden-terminal effects are not considered in this model. The proposed approach leads to significantly reduced probability of collision for the newly selected radio resources. A very similar idea has been developed by the author of this dissertation at the same time [WST19b]. However, this idea is not incorporated in this dissertation as the performance of the approach has not been found to be satisfactory in system-level simulations.

Jung et al. [JCK19] published a resource selection algorithm that reserves two sets of radio resources per packet flow. Afterwards, one of the resources is used for the transmissions in which the reselection counter is an odd number, the other one for even numbers. Hence, the two radio resources alternate periodically. The number of times that one of those resources is being repeatedly used is effectively cut in half with this approach. However, the duration remains the same. This approach solely focuses on repeating collisions, which are a special consequence of the SPS in Mode 4. In the paper, the authors state that new resources are used at the end of the reselection counter with probability p_{keep}, which is incorrect. Moreover, a RSRP problem is sketched that leads to unrecoverable transmissions if the RSRP is above a certain threshold. However, a high energy level is actually beneficial for decoding. The authors use a system-level simulation approach for the evaluation of the proposed resource allocation algorithm. This algorithm can increase the message reception reliability and decrease the severity of consecutive collisions. Unfortunately, the simulated scenario only leads to a very small channel utilisation. The traffic scenario is a freeway segment with a length of $2\,\mathrm{km}$. Only 240 vehicles spread across this distance. Additionally, the authors assume that four subchannels are used. With the message size of $190\,\mathrm{B}$, a CAM should fit into a single subchannel. This further contributes to the low utilisation of the channel. There is one disadvantage of the proposed resource allocation algorithm that is likely only relevant in scenarios with higher load. A single terminal only uses half of the resources for one radio resource due to the distinction between even and odd reselection counter values. Which one of those is used or not depends on the value that has been initially drawn for the reselection counter and the time point at which the new resources are used. Hence, it is random and uniformly distributed. This means that it is left to chance whether two terminals use the same half of the resources or a distinct set of them. In the first case, a repeating collision will occur until one of the terminals selects new radio resources. In the second case, no collision will occur between these terminals. This flaw can potentially significantly reduce the performance of the proposed algorithm by introducing a large number of collisions in high-load scenarios, in which a majority of the available channel resources are occupied.

He et al. [HTFZ18] propose a modification of LTE-V2X Mode 4 that increases the redundancy of scheduling announcements. Instead of only announcing the next packet of the same resources that are reused, the authors propose the use of additional separate scheduling packets that contain the location of the next scheduling packet and data transmissions. These packets seem to be transmitted in a separately contained set of resource blocks like the PSCCH, i.e. SCI. Moreover, they are transmitted in subframes different to the ones of the data transmissions. The authors claim an increase of $17\,\%$ of the network capacity in terms of supported terminals and show that the PDR is increased when using the modification. However, this modification can lead to an increased number of wasted resource blocks due to inflexibility of the distribution of radio resources. Moreover, the range of the mechanism is limited as it is necessary to decode the scheduling announcement packets. Hence, this approach is still affected by the hidden-terminal problem.

Zhao et al. [ZHW+19] developed a cluster-based approach that works without involvement of the base station. Vehicles create clusters with other vehicles in the surroundings. One cluster head per cluster is responsible for the radio resource scheduling. It determines one resource set that consists of multiple radio resources. Among those, subsets are assigned to the individual terminals in the cluster. Vehicles that are looking for clusters to join can only do so if the reception energy of the cluster head is above a certain threshold. This threshold can be adjusted to tune the size and range of clusters. If all clusters are already full or if there is no cluster, a vehicle may become the cluster head of a new cluster. It has to select a new resource set in this case. If there is no free resource set, the vehicle will perform sensing individually. This could lead to a performance degradation in scenarios with high network load. Vehicles can also change the current cluster if they find transmissions of other cluster heads that have a higher reception energy. The authors do not state how unnecessary changes to clusters of vehicles that drive on the oncoming lane are prevented. Cluster heads can detect collisions within their own cluster or transmissions that have not been scheduled by themselves. In this case, the resource set is abandoned and a new one is chosen. It is likely that both cluster heads abandon the resources in this case. The selection of resource sets works by averaging the RSSI of all resources in each set. This could be problematic of only a part of the radio resources in a set are actually occupied. This average is allowed to be below a certain adaptive threshold, which controls the spatial reuse of radio resources. For the performance evaluation, the authors chose to calculate use the average global PDR as metric. The proposed approach outperforms LTE, especially in the highway scenario. CAMs are typically periodically transmitted. The authors also investigate aperiodic packet flows and present large performance increases in such scenarios. However, they assume that LTE resorts to a random selection of radio resources in this case. Additionally, it is unclear which application is simulated by the aperiodic traffic model chosen by the authors.

Campolo et al. [CMR+19] present modifications to the MAC protocol of LTE-V2X Mode 4 that require a full duplex transceiver. Full duplex transceivers potentially enable a terminal to detect collisions with other terminals while transmitting themselves. In the paper, a comparison with the expected RSSI and the measured RSSI is proposed as a method to detect collisions. The full duplex capability is then leveraged to make the sensing more accurate by monitoring the resources that a terminal has used for transmission itself. Additionally, the $\mathrm{probResourceKeep}$ parameter is adjusted depending on the number of detected collisions. A low number of collisions indicates that this resource can be further reused. The full duplex operation additionally allows a terminal to decode transmissions on other subchannels while transmitting. Hence, the half-duplex problem is mitigated. In the evaluation, a highway scenario with many vehicles is used. Two different CAM sizes, $300\,\mathrm{B}$ and $1000\,\mathrm{B}$, are used. The proposed scheme reaches PDR results similar to standard LTE-V2X Mode 4 with $\mathrm{probResourceKeep}$ set to $80\,\%$ and with $300\,\mathrm{B}$ packets. With $1000\,\mathrm{B}$ packets, the PDR is increased. At the same time, the severity of repeating collisions is reduced due to the dynamic adaption of the $\mathrm{probResourceKeep}$ parameter. Still, update delays of $10\,\mathrm{s}$ are observed. Additionally, the approach only reacts to collisions at the end of a reuse interval. This could be done earlier after detecting collisions. In direct V2V communication, the benefits of full duplex transceivers are small if the MAC protocol itself is able to reduce the impact of repeating collisions and half-duplex effects. Hence, the increased complexity and cost of those receivers might not be justified and there is a possibility that they will not be used in practice due to cost pressure.

Kang et al. [KJB18] investigate the impact of the transmit power on the performance of LTE-V2X Mode 4. A reduced transmit power inevitably leads to a decreased PDR in higher communication distances. The authors notice that a lower transmit power can however lead to an increased PDR in lower ranges if the channel load is high. Hence, they propose an algorithm that reduces the transmit power depending on the RSSI of resources within the same subframe that a terminal uses for transmission. Due to the half-duplex operation, this transmit power value needs to be determined and fixed at the time the resources are selected. Only looking at the same subframe might introduce large inequalities between terminals, leading to fairness problems. The proposed scheme seems to be a middle ground between a static $10\,\mathrm{dBm}$ and $23\,\mathrm{dBm}$ transmit power. However, the reduction of the communication robustness in ranges over $140\,\mathrm{m}$ might increase the risks of traffic accidents. This approach significantly increases the PDR compared to standard LTE-V2X Mode 4. Still, it does not address issues such as packet flows with varying packet sizes, half-duplex problems, or the hidden-terminal effect. Moreover, the performance of the protocol in extreme scenarios is not clear but should be further investigated because the approach completely eliminates the sensing aspect of LTE-V2X Mode 4 and solely relies on decoded announcements.

Sabeeh et al. [SSW19] propose a modified MAC protocol for LTE-V2X Mode 4. The idea is that beginning at a reselection counter value of five, each vehicle transmits the next resource in time that will be occupied and have the same reselection counter. At subsequent transmissions, i.e. lower reselection counter values, this resource can change to a different vehicle if this vehicle has entered the awareness range. When selecting resources, the initial value of the reselection counter is not determined randomly. Instead, the vehicle tries to choose the same reselection counter that is currently used by other transmitters in the same subframe. This can lead to a reduced number of reselections on average. This protocol requires the reselection counter and some additional information to be included in the SCI.

Masegosa et al. [MGS18b, MSG19] present a geographically assisted, distributed scheduling scheme for LTE-V2X Mode 4 in two publications. The first publication [MGS18b] focuses on intersection scenarios and requires all vehicles to be equipped with both LTE-V2X and IEEE 802.11p transceivers. This leads to increased costs. The beacon messages are transmitted with 802.11p. The information about the locations of surrounding vehicles is needed by the proposed scheduling scheme. The description of the protocol focuses on intersection scenarios. The radio resources are divided into multiple pools and a pool is assigned to a lane arriving at an intersection. Vehicles on this lane calculate the order of the vehicles on this lane and derive a queue index for themselves based on the order in the lane. This index determines the subframe within the pool that this vehicle can use for transmission. The subchannel in this subframe is chosen randomly. This is quite inflexible and can sooner lead to network congestion issues if the channel load is high. The assignment of resource pools to intersection lanes can lead to similar problems in heterogeneous scenarios, e.g. a small lane crossing a larger lane with significantly more traffic. The protocol is based on the assumption that the severity of interference is solely based on distance. This assumption is wrong in many real-world scenarios, as antenna patterns, constructive and destructive interference, and other effects occur. Situations with oncoming traffic might be problematic, as the queue index needs to be updated multiple times. In a second publication [MSG19], the authors give more detail about the protocol or a similar protocol. The necessity for IEEE 802.11p is not mentioned in this paper. The vehicles attach their queue index to their message. This allows a quick update if the neighbour transmits the same index as the vehicle itself. In this case, the index is incremented, and the change propagates along the lane. Moreover, additional radio resources are now designated solely for an additional random allocation, which improves the communication robustness. The evaluation shows that the proposed resource allocation scheme outperforms LTE-V2X Mode 4 in the selected highway scenario. However, there is an alarming decrease of the PDR between a communication distance of $250\,\mathrm{m}$ to $350\,\mathrm{m}$.

Conclusion There are interesting approaches related to distributed resource allocation and SPS for SC-FDMA and LTE-V2X Mode 4. The hidden-terminal effect is even targeted by the protocol proposed by Abd El-Gawad et al. [EGEK19b, EGEK19a]. However, like many other proposals, this incurs a high overhead. Campolo et al. [CMR+19] present a protocol that even requires the use of full duplex transceivers. In addition to the above, there are concerns that some of the approaches do not work correctly in some safety-critical scenarios in real world deployments.

In general, none of the related works solve all of the issues of SPS at once. The main issues are inflexibility regarding different packet sizes and rates, incompatibility with DCC variants that are based on rate control, hidden-terminal effects, reoccurring collisions and half-duplex problems. The related work also shows that some additional protocol overhead might be justified by the potential performance increase. In conclusion, there is a need to carefully investigate which further potential modifications and extensions are necessary to improve the general performance and solve existing issues of LTE-V2X Mode 4.

3.2.4. Distributed Congestion Control Proposals for LTE-V2X Mode 4

As C-ITS is a broadcast-type system and the number of potential receivers is constantly changing, the use of acknowledgements has not been considered. Therefore, explicit feedback is typically not used for DCC in C-ITS networks. The research regarding DCC differs depending on the access technology. For IEEE 802.11p based systems, a reduction of the packet rate or packet dropping can be implemented without side effects. Hence, the research focuses on the actual control algorithms and protocols. As this access technology is significantly older, more research is available in this area.

Presumably due to the relatively recent release of LTE-V2X, there is almost no research available that propose new approaches for DCC. Most of the research regarding DCC for LTE-V2X Mode 4 targets the evaluation of the standardised approach, as it was seen in previous sections in this chapter. It is clear that dropping a number of packets of a periodic flow is not an optimal approach. Still, Bazzi et al. [Baz19] showed that power variation is ineffective and that the maximum transmit power should always be used with LTE-V2X Mode 4. Moreover, MCS tuning has a very small impact. This leaves packet dropping as the only remaining effective mechanism to reduce the channel load. However, the SPS of LTE-V2X Mode 4 complicates the integration of DCC based on packet dropping because the resource allocation scheme depends upon periodic traffic patterns. Hence, DCC algorithms and protocols developed for other access technologies should not be applied to LTE-V2X Mode 4 without adjustment. The approaches described in the following have been specifically developed for LTE-V2X Mode 4.

Yoon et al. [YK20] present an approach to balance the packet rate and power control for cellular V2X communication. Despite contradicting findings in related work regarding the inefficiency of power control for C-V2X, the authors show that power and rate control show improved performance under the inter-packet gap metric when utilized equitably. Moreover, the CBR is more effectively reduced. The presented approach applies an algorithm for congestion control named *J2945/1* to LTE-V2X Mode 4. This algorithm stipulates a linear reduction of the transmit power between $10\,\mathrm{dBm}$ to $23\,\mathrm{dBm}$ depending on the CBR along with a linear reduction of the packet rate depending on the vehicle density. Yoon et al. find that the power control hardly ever engages due to the quick and strong reaction of the rate control mechanism, which itself reduces the CBR that is used as input parameter for the power control. Hence, the authors suggest that the rate control should be relaxed. This modification leads to a better PDR for vehicles in close proximity because the transmit power can be reduced, limiting the interference from transmitters further away.

Haider et al. [HH19] propose another approach for DCC based on power control. The idea is to determine the (expected) interference by other vehicles when new resources are selected. Depending on the MCS, only a certain interference and noise level is allowed in order to guarantee the message delivery. The algorithm increases the transmission power stepwise from $10\,\mathrm{dBm}$ to $23\,\mathrm{dBm}$ of the current interference level is below a certain threshold. The performance evaluation of this approach only shows moderate benefits in high-load scenarios for communication distances below about $220\,\mathrm{m}$. Moreover, the way the transmission power is allocated leads to a high reaction time of the DCC mechanism. This could lead to dangerous situations when the channel load abruptly increases, e.g. when multiple vehicles issue DENMs due to dangerous conditions on the road.

Conclusion Due to the unique features of SPS and SC-FDMA, existing work on DCC, e.g. in the area of IEEE 802.11p, cannot be applied. Unfortunately, there is hardly any research that proposes DCC algorithms specifically for SPS. Moreover, the available research draws a conflicting picture of the effectiveness of power control. Still, power control seems to be a popular choice in the current state of the art. This can be explained by the potential incompatibility between packet dropping and SPS, which arises from the fact that SPS requires packets to be transmitted periodically. However, transmit power control can lead to dangerous situations because the transmission range is reduced for every packet. This can make it impossible to react early enough for an emergency braking maneuver. In conclusion, there is a huge necessity for further research on this issue. The main goal should be to develop an approach that retains the compatibility between SPS, i.e. retains some form of periodicity. At the same time, the main method to reduce the channel load should be packet dropping.

Summary

At the beginning of this chapter, a set of functional and non-functional requirements has been established. The main functional requirement of any MAC protocol is the scheduling of radio resources and the channel access so that no or as few collisions as possible occur. Another requirement for MAC protocols can be the detection of collisions. This enables the terminals to react to these events, e.g. by issuing retransmissions or by selecting new radio resources ahead of time. The main functional requirement of DCC is the reduction of the channel load. One potential benefit of this can be reflected in quantifiable metrics to assess non-functional requirements such as the PDR. Aside from this, it is advantageous to always have a small portion of the channel available in order to be able to react to suddenly occurring dangerous situations, e.g. by transmitting DENMs.

There are numerous non-functional requirements for V2V access technologies. These include a high PDR, a low protocol overhead if possible, and a good application performance. Application-oriented metrics can be used to assess this. Moreover, the latency introduced by the MAC protocol should be low enough so that the latency requirements of the applications can be met. For CAMs, this is $100\,\mathrm{ms}$. For most DENM types, a latency requirement of $100\,\mathrm{ms}$ is also foreseen, even though there are use cases with lower minimum latencies like the pre-crash sensor warning with $50\,\mathrm{ms}$ [ETS09]. The MAC and DCC protocols should also ensure that there are as few outliers of the inter-packet gap as possible. Other requirements are QoS control, which can be realized in the MAC or DCC component, fairness, scalability, generality, and reliability. The requirement of autonomous operation for the V2V communication has also been stipulated due to concerns about single points of failure, among others. Modified protocols should still be compatible with SC-FDMA and potentially existing hardware components.

The review of the state of the art has been categorized into papers assessing the performance of LTE-V2X Mode 4 and its DCC, comparison studies with IEEE 802.11p, and new MAC as well as DCC proposals. In general, a better performance is attributed to LTE-V2X Mode 4 compared to IEEE 802.11p. However, LTE-V2X Mode 4 has multiple other issues that do not necessarily express themselves in the PDR metric. These include reoccurring collisions and half-duplex problems, and incompatibility with packet flows with varying packet sizes and rates.

The hidden terminal problem has usually been accepted in existing standards as it was perceived that it is impossible to solve for broadcast traffic and with small packet sizes. It is hence not mitigated in any of the existing standards for V2V communication. Many of enhancements and modifications of LTE-V2X Mode 4 proposed in papers do not consider the hidden-terminal problem. Those that implicitly or explicitly limit the occurrence of hidden-terminal situations have other significant disadvantages. From a point of view of the state of the art, this problem is not completely solved and further protocol modifications that target this problem should be investigated.

Proposals for MAC protocols based on SPS and SC-FDMA only target some of these design problems. Additionally, there are various other concerns about the protocols proposed in related work, such as the scalability and protocol overhead, as well as the generality. However, as long as the scalability requirement can still be fulfilled, some additional protocol overhead might be justified if it is beneficial for the overall performance.

The related works agree that there is a need for DCC for LTE-V2X Mode 4. However, only a limited amount of research in this area is available. There are conflicting results regarding the efficiency of power control, but the reduced transmission range might be dangerous in practice. Hence, packet dropping should be used to reduce the packet rate. This is however incompatible with the assumptions about periodicity that are made by SPS. There is no approach that targets this issue and tries to retain this compatibility.

Chapter 4.

Problem Analysis

SPS and SC-FDMA as deployed in LTE-V2X Mode 4 come with certain advantages, but also introduce new challenges compared to the simpler random access technologies like CSMA/CA. The goal of this chapter is to analyse the consequences of SPS and SC-FDMA using theoretical and analytic considerations. Section 4.1 will begin with the candidate resource selection process, while Section 4.2 is about the special features resulting from SPS.

4.1. LTE-V2X Mode 4: Candidate Resource Selection Process

This section analyses the properties of the candidate resource selection process of LTE-V2X Mode 4. The most important features of this component are the calculation of the average RSSI of candidate resources, the threshold for respecting explicit reservations $\mathrm{Th}_{a,b}$, the size of the candidate resource set, and the subchannel allocation scheme. All of these components will be looked at in detail in the following.

4.1.1. Reception-Energy Dependant Consideration of Reservations

As described in Chapter 2, LTE-V2X Mode 4 uses a minimum RSRP threshold to determine whether a terminal should respect an explicit reservation of another terminal or whether this reservation should be ignored, meaning that the same resource could be used and a radio frame collision can be risked. This threshold is called $\mathrm{Th}_{a,b}$ and is dependent on the priority of the received packet (the packet that contained the reservation) and the packet to be sent using the newly selected resource. In this section, reasons for and possible disadvantages of the use of such a reception-energy dependant consideration of radio resource reservations will be deduced.

When determining the energy threshold $\mathrm{Th}_{a,b}$ with LTE, a refers to the priority of the packet to be transmitted and b refers to the priority of the received packet, which would use the same radio resource. The $\mathrm{Th}_{a,b}$ threshold is specified as the *i-th* entry in the *SL-ThresPSSCH-RSRP-List*, where $i = a \times 8 + b + 1$ [ETS19l]. This list can be generated with the following algorithm [ETS19n]:

$$\text{SL-ThresPSSCH-RSRP}_{\text{dBm}}(i) = \left\{ \begin{array}{ll} -\infty, & \text{if } i = 0 \\ -128 + (i-1) \times 2, & \text{if } 1 \leq i \leq 65 \\ \infty, & \text{if } i = 66 \end{array} \right\} \tag{4.1}$$

4.1.1.1. The RSRP Threshold for CAMs

In order to understand the intended behaviour of the threshold $\mathrm{Th}_{a,b}$, scenarios with CAMs and high-priority DENMs will be depicted. The first scenario considers two CAMs that compete for the same radio resource. As the ETSI specifies the PPPP of CAMs to be five [ETS18a], the resulting index i for two CAMs is $5\times8+5+1 = 46$ and the resulting $\mathrm{Th}_{5,5}$ is $-128+(46-1)\times2 = -38\,\mathrm{dBm}$. This represents a high reception energy. The corresponding distance between a transmitter and receiver required to reach this reception power is low. As a coarse indication, the free-space path loss model can be used to estimate the distance. The channel attenuation in decibels according to the free-space path loss model is [Gol05]

$$\mathrm{F_{dB}}(r,\lambda) = 20\log_{10}\left(\frac{r}{\mathrm{m}}\right) - 20\log_{10}\left(\frac{\lambda}{\mathrm{m}}\right) + 20\log_{10}(4\pi) \tag{4.2}$$

where r is the distance between the transmitter and receiver, λ is the wavelength, and m stands for the unit of meters. Assuming a transmission power of $23\,\mathrm{dBm}$ and a reception power of $-38\,\mathrm{dBm}$, the path loss would be $61\,\mathrm{dB}$. The resulting distance under the assumption of the free space path loss model can be calculated as follows:

$$\begin{aligned}
\mathrm{PL} &= 20\log_{10}\left(\frac{r}{\mathrm{m}}\right) - 20\log_{10}(\lambda) + 20\log_{10}(4\pi) \\
-20\log_{10}\left(\frac{r}{\mathrm{m}}\right) &= -20\log_{10}(\lambda) + 20\log_{10}(4\pi) - \mathrm{PL} \\
\log_{10}\left(\frac{r}{\mathrm{m}}\right) &= \frac{-20\log_{10}(\lambda) + 20\log_{10}(4\pi) - \mathrm{PL}}{-20} \\
\log_{10}\left(\frac{r}{\mathrm{m}}\right) &= \log_{10}(\lambda) - \log_{10}(4\pi) + \frac{\mathrm{PL}}{20} \\
\frac{r}{\mathrm{m}} &= \frac{\lambda}{4\pi}\times10^{\frac{\mathrm{PL}}{20}} \\
r &= \frac{\lambda}{4\pi}\times10^{\frac{\mathrm{PL}}{20}}\,\mathrm{m}
\end{aligned} \tag{4.3}$$

When assuming a centre frequency of $5.9\,\mathrm{GHz}$, resulting in a wavelength $\lambda = 0.050\,812\,\mathrm{m}$, and a path loss of $61\,\mathrm{dB}$ as calculated above, the corresponding maximum distance at which the threshold can still be fulfilled is $r \approx 4.54\,\mathrm{m}$. Thus, beyond a distance of about $5\,\mathrm{m}$, the explicit reservations are being ignored for CAMs. Considering the size of vehicles and the typical distance between them in traffic, it is safe to assume that explicit reservations are being completely ignored in almost all cases if the prevalent occupation of the channel is by messages with a PPPP of five, such as CAMs. This scenario is likely prevalent in the G5-CCH channel. This means that the RSRP threshold below which reservations are ignored might need to be set to a lower value.

4.1.1.2. The Quality-of-Service Aspect of the RSRP Threshold

If the PPPP of the received reservation and the packet to be sent are different, the $\mathrm{Th}_{a,b}$ threshold behaves differently, likely with the goal to provide some form of QoS. In order to further understand the reasoning of the $\mathrm{Th}_{a,b}$ threshold, the behaviour for packets with different priorities should be investigated. In order to do this, the following scenario is pictured: the G5-CCH channel is mostly congested by CAMs. A vehicle detects a road hazard with its own sensors (e.g. radar sensors) and is about to issue a DENM for the first time to warn surrounding vehicles. In order to do this, it needs to reserve new resources. A DENM has a PPPP of two or four, depending on whether it is a high priority DENM or not [ETS18a]. A lower priority number means that the packet is more important. In this case, as it is a time-critical warning message to prevent accidents, the priority of the message is two. If the DENM to be sent is competing for radio resources reserved by CAMs with a priority of five, the corresponding index i for the transmitter is $i = 2 \times 8 + 5 + 1 = 22$, resulting in a $\mathrm{Th}_{2,5} = -128 + (22 - 1) \times 2 = -86\,\mathrm{dBm}$. This value is relatively close to the sensitivity of LTE-V2X terminals, so that most of the reservations should be respected in practice. In the opposite case, i.e. a less important message competing with more important reservations, the effect is not as strong because the index *i* is more affected by the priority of the packet to be transmitted: The factor of variable a is 8, of b only 1 when calculating the index *i*. This observation is also visible in Figure 4.1, which shows all $\mathrm{Th}_{a,b}$ values subject to different priorities of received and to-be-transmitted packets. To continue the example, a CAM competing with more important DENMs results in $i = a \times 8 + b + 1 = 5 \times 8 + 2 + 1 = 43$. The corresponding $\mathrm{Th}_{a,b}$ is $-44\,\mathrm{dBm}$, a reception power that is again going to hardly be reached in practice. This means that less important messages likely ignore reservations of more important messages, which can result in a higher collision risk for more important messages.

In summary, when less important packets contest for radio resources with packets of the same priority, reservations are likely to be ignored and the terminals fall back to the RSSI-based exclusion mechanism. If a terminal is about to send a more important packet, it will respect the explicit reservations of less important messages and the collision risk will be lower. However, less important packets are likely to ignore reservations of high-priority messages. The intention of this protocol seems to have been to leave some unique resources for important messages by requiring less important messages to use resources that have a higher collision risk. The risk of less important packets colliding with high priority messages might offset some or all of this intended advantage.

As previously mentioned, the prevalent reason for introducing the RSRP threshold $\mathrm{Th}_{a,b}$ seems to have been to provide a form of QoS. Considering the risks of this protocol, it might be beneficial to investigate other possibilities to prioritise individual packets. ETSI specified a version of DCC for LTE-V2X Mode 4 in the Technical Specification 103 574 [ETS18c]. This DCC mechanism restricts packets with a lower priority more aggressively. Solely relying on this QoS mechanism might be a valid alternative.

4.1.2. RSSI Averaging When Selecting Resources

The target size of the candidate resource set is $20\,\%$ of the total resources in the selection window. When explicit reservations of other terminals affect less than $80\,\%$ of the future resources, the target size is reached by only selecting the resources with the lowest average RSSI. This RSSI is averaged over the last ten repetitions, i.e. one second. This second is equal to the mean value of the resource selection counter range of 5 to 15 multiplied by the packet interval of $100\,\mathrm{ms}$.

This section investigates how this averaging window affects reservations of different ages. In order to understand the following analysis, the workings of the SPS need to be recalled (see Section 2.4.2.3). As the number of data points for the averaging of the RSSI-based exclusion of resources is exactly the mean value of the reselection counter range (10) and the reselection counter is randomly chosen from this range, almost half of the resources will actually be used for a shorter time interval if $\mathrm{probResourceKeep}$ is zero. On average, if $\mathrm{probResourceKeep}$ is zero, once a resource is *established* in the sense that it stretches across the RSSI averaging window (one second) when selecting candidate resources, it will not be reused further. Additionally, this mechanism does not work well at the beginning of a resource

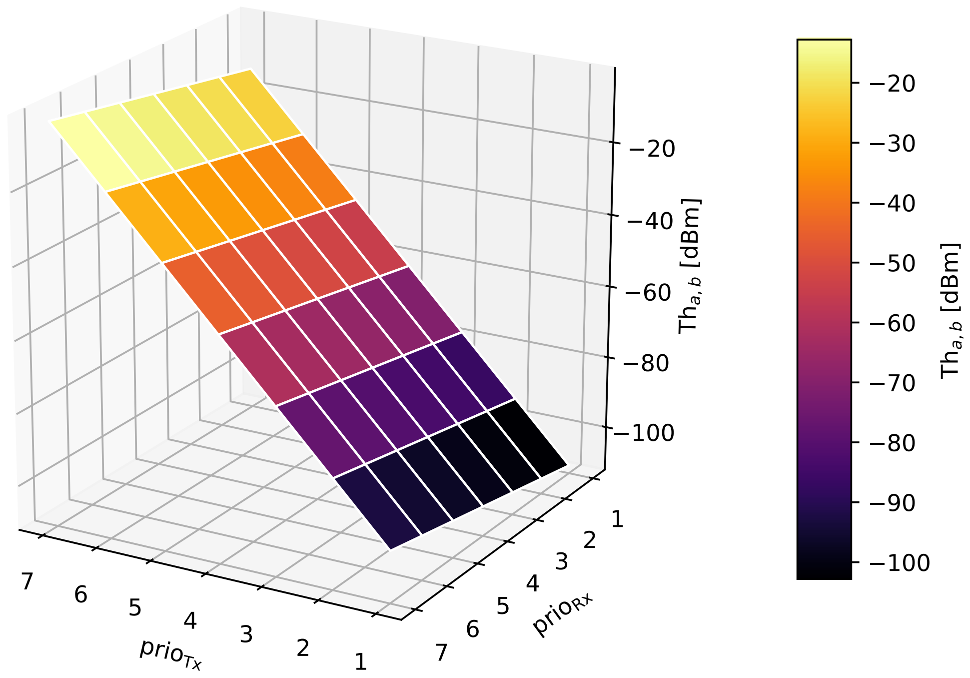

Figure 4.1.: Visualisation of $\mathrm{Th}_{a,b}$ values, depending on the priority of the received packet and of the packet to be sent.

usage, i.e. when the resource has not been reused often. In this case, other terminals will average the RSSI by including resources that have not been used by the terminal at all. This leads to a lower average RSSI than the current resource allocation would cause. Consequently, if new resources have to be selected for newly generated event-type warning messages such as DENMs, this message will be discriminated against other, repeating resource allocations. This is problematic because the importance of warning messages is likely significantly higher than a single message that is part of periodic status updates. This effect is visualized in Figure 4.2 in the horizontal dimension.

Consequently, there are reasons and situations that suggest that it might be disadvantageous to use the mean resource reuse interval for averaging the RSSI in order to determine if the resource will be reused again. It could be better to use mechanisms that retain the correlation with the resource allocations of strongest interferer of that resource: Firstly, if this interferer just started using this resource, the resources in the past that have not been used by this interferer cannot be used in order to make predictions of future resource allocations. In fact, averaging over these irrelevant resources might be harmful because the determined average reception energy will be lower than the actual interference that will likely reoccur for a longer period.

Figure 4.2 also shows in the vertical dimension that such a misalignment can occur in the frequency domain, i.e. with subchannels. The effects of this are similar: the average RSSI that is used to predict the severity of future interference will be lower than it actually is for some of the resources. Therefore, the decision which resources to use for transmission is based on skewed data, potentially increasing the probability of collisions. In practice, it does hardly matter *how many* resources are affected by a collision because the complete set of resources is likely necessary to decode the packet. It is unlikely that a potential receiver is able to recover

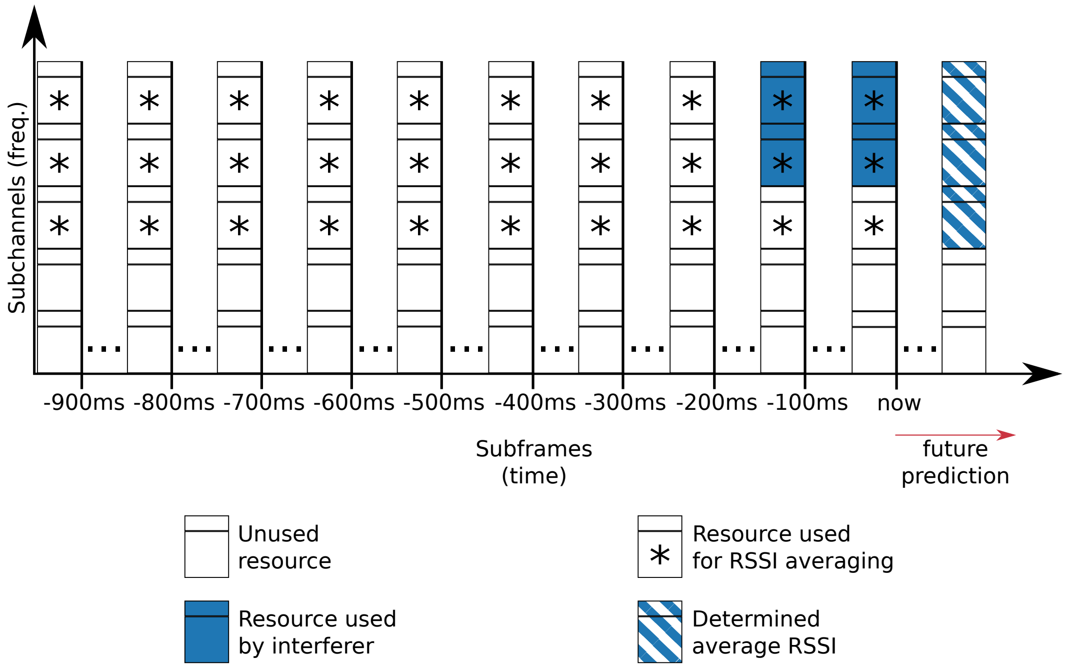

Figure 4.2.: Visualisation of potential misalignment between the RSSI averaging interval and actual resource allocation by an interferer. The transmitter requires candidate resources with three subchannels.

a message with forward error correction (FEC) that was affected by strong interference on some subchannels. In conclusion, it might be beneficial to only consider the average RSSI of the strongest subchannel.

With the addition of DCC to LTE-V2X Mode 4 (Section 2.4.2.4), another facet of this problem has been created. This DCC mechanism drops packets of a reservation if the CBR is above a given threshold. As the measurement of the CBR is done locally and from the perspective of the terminal only, some terminals might be restricted by DCC, while some terminals in the interference range might not be. The average RSSI of resources that are restricted by DCC is lower because the average is also calculated from resources that have actually not been used due to DCC restrictions. This is visualized in Figure 4.3. The resources that are already restricted by DCC are now additionally more likely to be affected by collisions because the

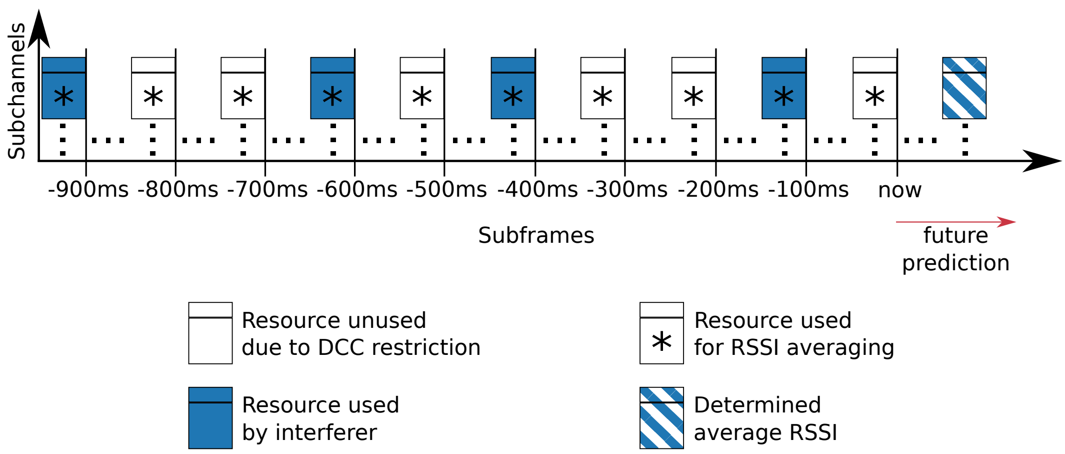

Figure 4.3.: Visualisation of potential misalignment between the RSSI averaging and resources by an interferer restricted by DCC.

average RSSI is lower if not all of the resources are used. On the other hand, the interferer potentially only uses a portion of this resource as well. Therefore, some of the resources could successfully be used by the transmitter. There are three different cases when resources overlap and both transmitters are restricted by DCC:

- None of the potential transmitters use the resource and it is unoccupied.
- Both transmitters use the same resource and a collision occurs.
- Exactly one of the two potential transmitters uses the resource, the other transmitter is restricted by DCC.

Only the last option is desirable. However, the DCC implementation leaves it to chance. Moreover, in practice, it might even be more likely that the use of resources is correlated in a disadvantageous way. Oscillations of the CBR are geographically correlated and might affect both terminals. This can lead to situations in which both of them perform the same action simultaneously, i.e. they either do or do not use the resource at the same time.

Even with the mentioned disadvantages of the RSSI averaging, there might be beneficial properties as well. The RSSI averaging mechanism only affects resources that are not excluded for other reasons such as the half-duplex precaution or explicit reservations. As deduced in Section 4.1.1.1, due to the $\mathrm{Th}_{a,b}$ threshold, only a part of the received explicit reservations are actually respected. This increases the number of resources that are affected by the RSSI averaging mechanism. It is possible that the averaging of the reception energy limits the effect of small-scale fading effects or hardware limitations. For example, there might be constraints of the transceiver devices themselves so that the averaging of these energies makes the energy detection more reliable solely from a physical layer perspective. Also, some resources might actually not be used due to varying packet rates or DCC. As the physical-layer constraints of the hardware are not known, it might still be a feasible decision to not modify the averaging interval of the RSSI at the current state of research.

4.1.3. Size of the Candidate Resource Set

In LTE-V2X Mode 4, a new candidate resource is chosen randomly from the $20\,\%$ of the resources with the lowest predicted collision probability ($20\,\% \times M_{\mathrm{total}}$). This short section discusses the fixed size of this set.

In low-load situations, more than $20\,\%$ of the resources might be unoccupied. Hence, the probability that two or more transmitters choose the same radio resource and cause a collision could be lowered by using a larger part of the total set of candidate resources. On the contrary, in high-load scenarios, the majority of the $20\,\%$ might already be occupied. Still, reducing the ratio might also lead to additional collisions because many transmitters likely compete for a few free resources. The task of the DCC component of LTE-V2X is to limit the channel load to a degree at which the MAC protocol can function. The aforementioned considerations indicate that the size of the candidate resource set should be adjusted depending on the current channel load.

4.1.4. Subchannel Granularity and Transport Block Padding

The granularity of the radio resource allocation of LTE-V2X is significantly lower than with ITS-G5. While ITS-G5 always uses the complete channel bandwidth and can use an arbitrary number of symbols in the time domain (constrained by the channel coherence time), a transmission of LTE-V2X is always one millisecond or subframe long. Instead of changing the transmit duration, the number of subchannels is varied for differently sized packets. A transmission is hence always one millisecond long and consists of one to five subchannels.

In the sidelink, a fragmentation of MAC PDUs and the spreading of one PDU over multiple radio resources is not viable, because only few messages will be transmitted. In most situations, only CAMs will be transmitted. The only other potential option to reduce the number of padding bits is to decrease the MCS index, i.e. to use a more robust and less efficient modulation and coding scheme. However, this approach does not use the channel more efficiently, i.e. it does not use less radio resources. Instead, the transmission is just made more robust. Depending on the application scenario, this might not be feasible or even allowed. For example, the allowed range of the MCS index for transmissions on the PSSCH by non-RSU stations below $160\,\mathrm{km\,h^{-1}}$ ranges from 0 or 3 (depending on whether multiple subchannels are used) to 11 [ETS18a]. An MCS index of six represents QPSK with a coding rate of approximately 0.5 [ETS19l]. It is possible that many implementations of the LTE standard just use this value for the transmission of CAMs.

For a V2V sidelink transmission, the MAC header is $11\,\mathrm{B}$ long [ETS20], the RLC likely operates in transparent mode and has thus no header [ETS19m], and the PDCP header is likely only $1\,\mathrm{B}$ long. After this, non-IP headers and GeoNetworking follow. This MAC PDU has to fit inside the TB. The capacity of a TB depends on the number of used resource blocks (RBs) (and hence, the number of used subchannels), and the MCS index. For the V2V sidelink with $10\,\mathrm{MHz}$ and five subchannels, the number of RBs are multiples of ten. For example, one subchannel uses ten RBs. The capacity of the transport blocks is specified in [ETS19l, Table 7.1.7.2.1–1]. Table 4.1 shows the most relevant values for all configurations with QPSK modulation. If the capacity of the chosen TB exceeds the size of the message, the unused bits will be padded, i.e. unused. This is almost always the case. For example, if using a MCS index of six and two subchannels (i.e. 20 RBs), the corresponding TB has a capacity of $2088\,\mathrm{bit}$. As the overhead due to the cyclic redundancy check (CRC) is already subtracted from those and the other header information of the physical layer is included in the SCI, the $2088\,\mathrm{bit}$ can be fully used for the MAC PDU. When assuming a CAM size of $200\,\mathrm{B}$, i.e. $1600\,\mathrm{bit}$, $488\,\mathrm{bit}$ of padding are necessary. Still, this message does not fit into a single subchannel with an MCS index of six, which would have a TB size of $1032\,\mathrm{bit}$.

Depending on the reliability requirements, some of the higher MCS indices might not be available. Nevertheless, Table 4.1 shows that jumps of 300 to 400 bits are the norm between the next higher index. This means that there is a high probability that a packet sent with LTE-V2X Mode 4 has to use large amounts of padding in order to completely full the subchannel.

4.2. LTE-V2X Mode 4: Semi-Persistent Scheduling

This section investigates consequences of SPS in LTE-V2X Mode 4.

4.2.1. Repeating Collisions

In centrally scheduled modes of LTE, SPS leads to reduced scheduling overhead because radio resource grants can be issued in bulk by the base station, i.e. the base station issues a grant for multiple radio resources. In those modes, the risk of radio frame collisions is low.

The idea of SPS was also adopted for the distributed Mode 4, which is the focus of this dissertation. The reasoning for the adoption of SPS is slightly different in this mode because there is no explicit scheduling overhead by the base station as it is not involved. The anticipated

Table 4.1.: Transport Block Sizes (in Bit) for Different MCS Indices and Number of Subchannels

Subchannels MCS index	1	2	3	4	5
0	256	536	808	1096	1384
1	344	712	1064	1416	1800
2	424	872	1320	1800	2216
3	568	1160	1736	2344	2856
4	696	1416	2152	2856	3624
5	872	1736	2664	3496	4392
6	1032	2088	3112	4136	5160
7	1224	2472	3624	4968	6200
8	1384	2792	4264	5544	6988
9	1544	3112	4776	6200	7992
10	1736	3496	5352	6968	8760

advantage was to reduce the number of radio frame collisions by making radio resource selections by terminals more predictable, which should help to make better decisions about which radio resources will likely be occupied in future. For a detailed description of the SPS and radio resource selection in Mode 4, please see Section 2.4.2.3.

While SPS might help to increase the PDR, it might also have disadvantageous properties. This section investigates the probability and severity of potentially reoccurring radio frame collisions. As all radio resources are reused in fixed intervals, collisions of radio frames are likely to repeat at the next resource reservation intervals. The transmitters cannot detect that they are causing collisions because they operate in a half-duplex fashion. Thus, the repeating collisions can only end when at least one of the transmitters selects new resources because the reselection counter reached zero and the probabilistic resource reuse method with $\mathrm{probResourceKeep}$ did not trigger. A repeating collision between overlapping resources is visualized in Figure 4.4.

In a safety-critical environment such as vehicular traffic, it is important that every vehicle can distribute its status update in a given time interval. Re-occurring collisions can impede this goal. Due to the way SPS works in Mode 4, the time period in which resources overlap and collisions reoccur is potentially infinite if the $\mathrm{probResourceKeep}$ parameter is larger than zero. Of course, radio frame collisions can stop to reoccur when terminals move away from each other and are outside of their interference range. However, this time span is very large, therefore this case will be ignored in the following analysis.

In order to theoretically determine the impact of this potential problem, the time interval of resource reuse in LTE-V2X Mode 4 will be investigated first. The $\mathrm{probResourceKeep}$ parameter will subsequently be denoted as P. Even without resource reselection ($P = 0$), it can take up to 1.5 seconds for a vehicle to give up its periodic resource ($r = 15$, CAM rate: $10\,\mathrm{Hz}$). The mean reservation interval can be determined for different $\mathrm{probResourceKeep}$ values P using an analytical approach. For $P = 0$ or a single resource selection, it is one second:

$$\mu_{\mathrm{RI}}(P = 0) = \frac{\sum_{r=5}^{15} r}{\sum_{r=5}^{15} 1} \times 0.1\,\mathrm{s} = \frac{110}{11} \times 0.1\,\mathrm{s} = 1\,\mathrm{s}$$

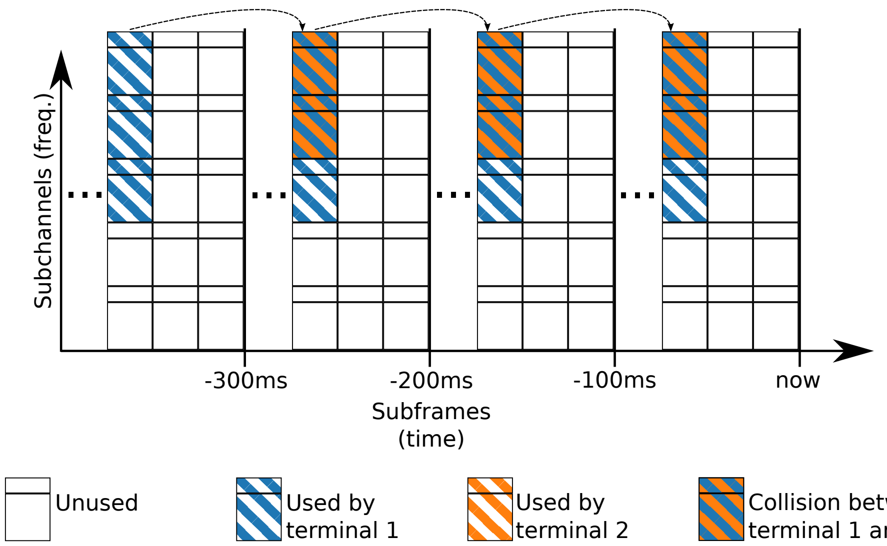

Figure 4.4.: Visualisation of reoccurring collisions.

In general, the mean reservation interval for the same resource subject to P can be calculated by:

$$\mu_{\mathrm{RI}}(P) = \lim_{n\to\infty} \sum_{m=0}^{n} P^m \times \mu_{\mathrm{RI}}(P=0) = \frac{1}{1-P} \times 1\,\mathrm{s} = \frac{1\,\mathrm{s}}{1-P}$$

Figure 4.5 visualizes the mean reuse interval subject to $\mathrm{probResourceKeep}$. The mean reusage interval of a specific resource is at most five seconds, when using $P = 0.8$, which is the maximum reselection probability allowed in the standard. Therefore, in a period of five seconds on average, there cannot be a reaction to channel conditions or packet collisions. Assuming a CAM rate of $10\,\mathrm{Hertz}$, this equals 50 packets. In this comparably long period of time, it is possible that collisions and the inability to receive due to half-duplex persist. In the worst case, the maximum overlapping time is infinite, so that vehicles will potentially never find out about one another. This happens when both transmitters reselect their resources over and over again, which is possible if $\mathrm{probResourceKeep}$ is larger than zero.

Figure 4.6 visualizes how many resource overlaps and possibly reoccurring collisions can happen for a reselection counter of $r = 5$ for both resources and when $\mathrm{probResourceKeep}$ is set to $P = 0$. If it is not considered that resources that have been used multiple times already are less likely to be affected due to collisions (see Section 4.1.2), each case visualized in Figure 4.6 is equally likely. In order to analytically derive statistics about the severity, i.e. duration of a resource overlap, every combination of possible resource selection counters needs to be considered. Without loss of generality, it is assumed that the first of the colliding radio resources has the shorter or an equal validity period r_{min}, the second one r_{max}. In order to determine the average number of resource overlaps of two colliding resource allocations, the number of overlap configurations needs to be determined. This value will be in the denominator. The numerator will contain the sum of single radio resources that overlap for each of the aforementioned configurations. It can be seen in Figure 4.6 that partially overlapping resources occur $2 \times (r_{\mathrm{min}} - 1)$ times. Fully overlapping resources occur $r_{\mathrm{max}} - r_{\mathrm{min}} + 1$ times, so that the number of overlap configurations can be expressed as:

$$\begin{aligned} \mathrm{n}_{\mathrm{overlap}}(r_{\mathrm{min}}, r_{\mathrm{max}}) &= 2 \times (r_{\mathrm{min}} - 1) + r_{\mathrm{max}} - r_{\mathrm{min}} + 1 \\ &= 2\, r_{\mathrm{min}} - 2 + r_{\mathrm{max}} - r_{\mathrm{min}} + 1 \\ &= r_{\mathrm{max}} + r_{\mathrm{min}} - 1 \end{aligned} \tag{4.4}$$

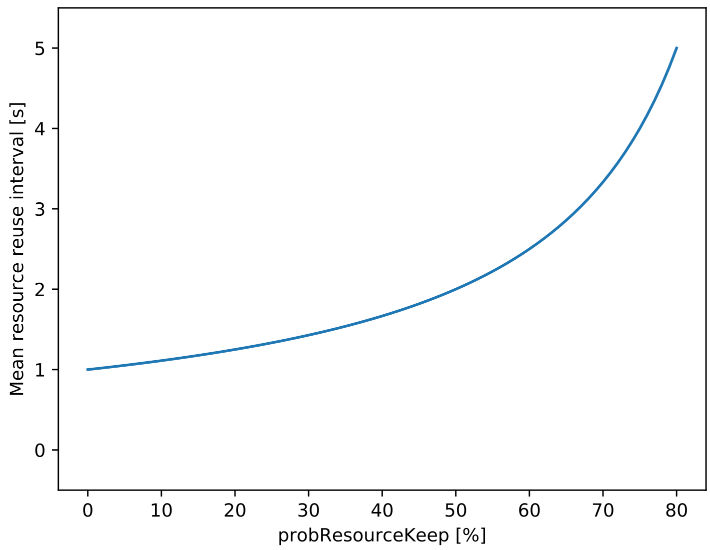

Figure 4.5.: The mean resource reuse interval subject to the probResourceKeep parameter.

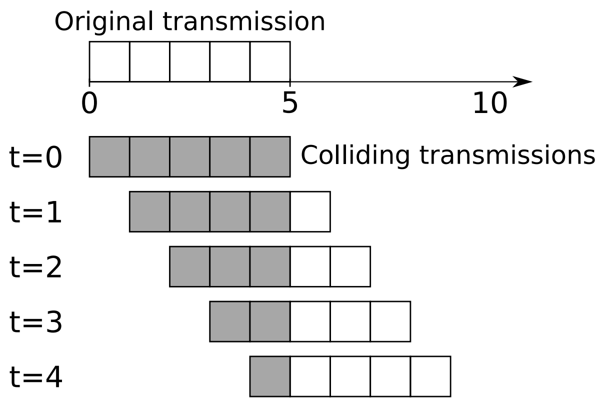

Figure 4.6.: Number of repeating collisions for reselection counters of five.

Fully overlapping resources account for r_{min} overlaps of single resources each, so that they account for $r_{\text{min}} \times (r_{\text{max}} - r_{\text{min}} + 1)$ overlaps in total. Partially overlapping resources account for

$$2 \times \sum_{i=1}^{r_{\text{min}}-1} i$$

overlaps, so that the sum of single-resource overlaps can be expressed as:

$$\begin{aligned}
\text{s}_{\text{overlap}}(r_{\text{min}}, r_{\text{max}}) &= r_{\text{min}} \times (r_{\text{max}} - r_{\text{min}} + 1) + 2 \times \sum_{i=1}^{r_{\text{min}}-1} i \\
&= r_{\text{min}} \times r_{\text{max}} - r_{\text{min}}{}^2 + r_{\text{min}} + 2 \times \sum_{i=1}^{r_{\text{min}}-1} i \\
&= r_{\text{min}} \times r_{\text{max}} - r_{\text{min}}{}^2 + r_{\text{min}} + 2 \times \left(\frac{(r_{\text{min}} - 1) \times r_{\text{min}}}{2} \right) \\
&= r_{\text{min}} \times r_{\text{max}} - r_{\text{min}}{}^2 + r_{\text{min}} + r_{\text{min}}{}^2 - r_{\text{min}} \\
&= r_{\text{min}} \times r_{\text{max}}
\end{aligned} \tag{4.5}$$

Therefore, for two overlapping resources with reservation intervals r_{min} and r_{max}, the average number of single-resource overlaps results from Equations 4.4 and 4.5 and is:

$$\mu_{\text{resOverlap}} (r_{\text{min}}, r_{\text{max}}) = \frac{r_{\text{min}} \times r_{\text{max}}}{r_{\text{max}} + r_{\text{min}} - 1} \tag{4.6}$$

The distinction between r_{min} and r_{max} does not matter in the resulting formula, they can be swapped without altering the result:

$$\mu_{\text{resOverlap}} (r_1, r_2) = \frac{r_1 \times r_2}{r_1 + r_2 - 1} \tag{4.7}$$

The resulting overlap factor can be seen as *average worsening factor of collisions* compared to wireless access technologies with (mostly) uncorrelated collision behavior such as ITS-G5. For example, a factor of ten means that if there is a collision of radio resources, the average number of occurrence of collisions of these resources is ten, which lasts one second with a resource reservation interval of $100\,\text{ms}$.

Figure 4.7 visualizes the outcomes of all possible combinations of r_1 and r_2. It can be seen that the average overlap of single resources increases more steeply when both reselection counters take on larger values. As the reselection counters are random numbers, the global average can easily be calculated:

$$\mu_{\text{resOverlap,global}} = \frac{\sum_{r_1=5}^{15} \sum_{r_2=5}^{15} \frac{r_1 \times r_2}{r_1 + r_2 - 1}}{\sum_{r_1=5}^{15} \sum_{r_2=5}^{15} 1} \approx 4.88 \tag{4.8}$$

This means that if there is a collision, it will repeat itself with the same vehicles for almost half a second on average. This amount of time can make the difference in vehicular traffic, potentially deciding the occurrence or outcome of traffic accidents. As previously mentioned, this analysis was made under the assumption that probResourceKeep is configured to $P = 0$. For other values, the overlap of resources increases as the reuse interval increases significantly. Additionally, outliers and maximum values increase heavily as resource reservation counters

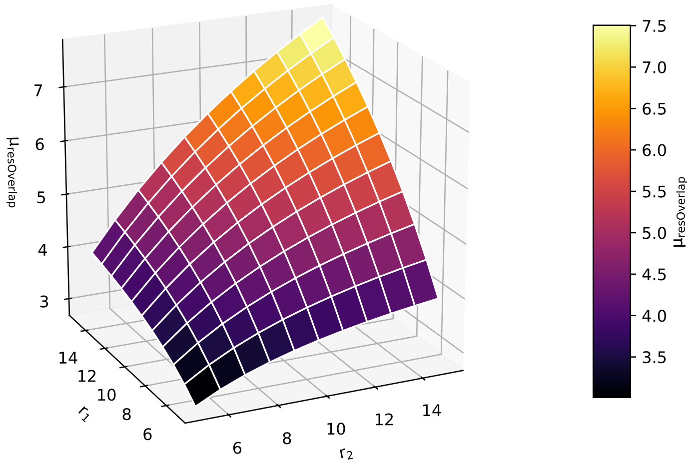

Figure 4.7.: Visualisation of the average number of single-resource overlaps between two overlapping radio resources with reselection counters r_1 and r_2.

can be re-drawn for the same resources repeatedly. An additional factor has not been considered in this theoretical analysis: in practice, the overlap configurations are potentially not equally likely. This is due to the operation of the MAC protocol, especially the RSSI based averaging mechanism. The mechanism makes the selection of resources less likely if they show a high reception energy in the last second. However, it means that collisions are probably more likely to occur at the beginning of a reservation as the average reception energy is the lowest at this point. This is because the resource has not been repeatedly reused yet. In turn, it means that the average number of resource overlap in case of collisions should even be higher in practice, resulting in an even worse result. The analysis performed here is therefore an upper boundary to the performance, and it might be even worse in practice.

Aside from the average, outliers and maximum values are important to look at as well. These heavily depend on the configuration of $\mathrm{probResourceKeep}$. If it is zero, the maximum number of times resources overlap is 15, the maximum number of the reselection counter. If $\mathrm{probResourceKeep}$ takes any other value, the number of resource overlaps can potentially be infinite, as there is a possibility that terminals keep on reusing resources forever. With larger values of $\mathrm{probResourceKeep}$, the probability of seeing such larger periods of resource reuse increases.

In conclusion, it can be said that the issue of reoccurring collisions poses a major risk to traffic safety. This problem of LTE-V2X Mode 4 should be mitigated before a large-scale deployment. This issue also outlines that classical evaluation methods, such as simply considering the PDR as single metric, are not sufficient to assess the performance of such safety-critical technologies. These metrics count every lost packet as *equal*. From a safety and application-oriented perspective, a single unsuccessful transmission between two vehicles might not be detrimental. However, it is significantly more dangerous if the transmissions of the same vehicles collide repeatedly and no information about the two vehicles can be distributed for long periods of time. Therefore, additional, application-oriented metrics should be used for the evaluation of V2V protocols.

4.2.2. Half-Duplex Transceiver Operation

SC-FDMA makes it possible to further subdivide the channel into so-called subchannels. In the case of the sidelink of LTE, one transmission can consist of multiple contiguous subchannels if larger packets need to be transmitted. However, a transmission is always one subframe long, which equals one millisecond. Subchannels allow more granularity when allocating radio resources.

One disadvantage of the use of subchannels results from the half-duplex limitation of the transceivers. Crosstalk between the transmitting and receiving parts of a transceiver prevent it from simultaneously transmitting and receiving. This also applies to radio frames on different subchannels. Therefore, a radio terminal cannot receive packets on other subchannels during the time it transmits itself, as shown in Figure 4.8. This limitation is subsequently called the *half-duplex* problem.

In the following, an analytical approach is used to investigate the half-duplex problem in a theoretical way. The goal is to have an idea of the severity and likelihood of this issue. For this analysis, some idealistic assumptions are made. Firstly, it is assumed that no collisions of radio frames happen. This also implicates that the wireless channel capacity is never completely exhausted. This simplification means that the specific algorithm and complex interactions of the MAC protocol do not need to be considered. Secondly, it is assumed that each terminal has the same communication patterns, including a fixed number of subchannels required for each transmission and a fixed packet rate. Table 4.2 gives an overview of the variables and constants used in this section, including a description. This section continues with an assessment of the effects of the half-duplex effect on a single terminal (Section 4.2.2.1). Afterwards, a global analysis of the probability of occurrence of the half-duplex effect and the average number of affected terminals depending on the number of terminals in the transmission range is presented (Section 4.2.2.2).

4.2.2.1. Effect of Half-Duplex Operation on a Single Terminal

The number of packets that a terminal cannot receive due to the half-duplex effect depends on the current allocation of radio resources and the size of each transmission. This number is higher if each transmission only consists of one subchannel. In this case, four subchannels and radio frames can be affected by the half-duplex effect. If terminals transmit ten packets per second, i.e. one packet in $100\,\mathrm{ms}$, only one subframe can be affected per terminal in $100\,\mathrm{ms}$ because only the subframe that the terminal used for transmission is affected. Only a part of the subframe can be occupied by other transmitters. Thus, less than $1\,\%$ of resources can

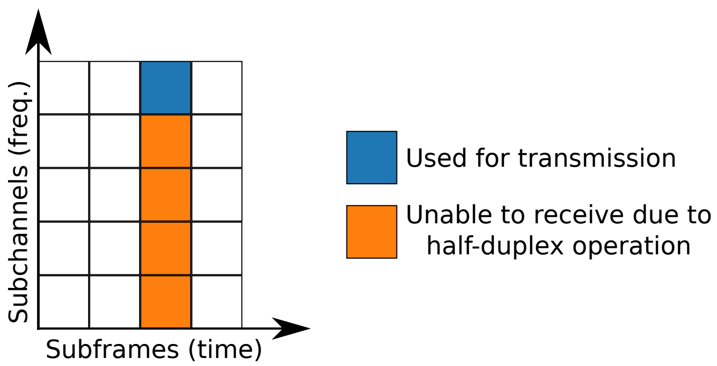

Figure 4.8.: Visualisation of the half-duplex effect.

Table 4.2.: Overview of Variables and Constants Used for the Analysis of the Half-Duplex Effect

Variable	Default Value	Description
n_{SF}	1000	Number of subframes in one second (LTE default)
$n_{SC,\ TOT}$	5	Total number of subchannels (LTE default)
$n_{SC,\ REQ}$	2	Number of subchannels required for one transmission
r_{PKT}	10 Hz	Packet rate
n_{TX}	—	Number of transmitters in transmission range
$n_{TX,\ HD}$	—	Minimum number of transmitters in transmission range so that at least one terminal is guaranteed to be affected by half-duplex problems
$n_{TX,\ ALL\ HD}$	—	Minimum number of transmitters in transmission range so that all terminals are guaranteed to be affected by half-duplex problems

be affected by the half-duplex problem in any case if only one packet is transmitted every 100 ms. However, the severity of the half-duplex problem is also related to SPS. Not only collisions with the same terminals can repeat, but also half-duplex problems. This also means that any access technologies affected by the half-duplex effect can reach a perfect PDR only in situations with low load.

4.2.2.2. Probability of Occurrence and Average Number of Affected Terminals

The goal of this analysis is to determine under which conditions and how often half-duplex problems occur. Firstly, the minimum number of terminals in the transmission range is determined so that at least one of them is guaranteed to be affected by the half-duplex problem even in the best case. Secondly, the number of terminals so that every one of them is affected in the best case will also be derived. Lastly, as a more general case, the average case will be analysed. This includes the probability of occurrence of the half-duplex effect depending on the number of terminals in the transmission range and average number of terminals affected by half-duplex problems.

Impairment of a Single Terminal in the Best Case If all the subframes are only occupied by a single terminal, half-duplex problems cannot happen. In a best-case scenario, the resource allocations are spread out evenly over time. Nevertheless, if the channel load is higher than a certain threshold, half-duplex problems are guaranteed to occur even under idealized conditions. This threshold depends on the number of vehicles in the transmission range $n_{TX,\ HD}$, the number of subframes n_{SF}, and the packet rate r_{PKT}. It is not dependent on the number of subchannels required for one transmission, as long as a transmission does not fully occupy a subframe, as half-duplex effects cannot occur otherwise. When the number of terminals in the transmission range is larger than the number of subframes per second divided by the packet rate, at least one terminal is affected by the half-duplex problem:

$$n_{\text{TX, HD}}(n_{\text{SF}}, r_{\text{PKT}}) > \left\lceil \frac{n_{\text{SF}}}{r_{\text{PKT}}} \right\rceil$$

$$n_{\text{TX, HD}}(n_{\text{SF}}, r_{\text{PKT}}) = \left\lfloor \frac{n_{\text{SF}}}{r_{\text{PKT}}} \right\rfloor + 1$$

For the default configuration of one thousand subframes per second and a packet rate of $10\,\text{Hertz}$, $n_{\text{TX, HD}}$ is 101: one hundred terminals occupy all of the subframes if they transmit ten packets per second. The next terminal needs to use subframes that are already occupied on other subchannels and cannot receive the packet transmitted with those. This number can easily be reached in congested traffic. DCC will hardly help with this problem as the unused subchannels likely make up more than half of the totally available channel capacity. Figure 4.9 shows the results for different packet rates. Starting from packet rates around $5\,\text{Hz}$ to $10\,\text{Hz}$, it is likely that enough vehicles can be in the transmission range in many situations so that half-duplex problems occur regardless of the resource scheduling.

Impairment of Every Terminal If the channel load is high enough so that every subframe is being used by more than one terminal, the half-duplex effect affects every terminal. A resource allocation that would prevent half-duplex problems would first need to fill all available subframes. The next transmission would inevitably cause a half-duplex problem. Further transmissions might fill subframes with one transmission or more transmissions. In the first case, both terminals are now affected by half-duplex problems. In the second case, the three terminals in the subframe cannot receive messages from each other. Hence, not all terminals are affected by half-duplex problems, but there are terminals that are unable to receive messages of at least two other terminals due to the half-duplex operation. The safety implications of both of those cases are similar. Therefore, it can be concluded that the question when and whether every single transceiver is affected by half-duplex problems is not really relevant in practice. The allocation of radio resources does not make a large difference if every subframe is already occupied by at least one transmission, which inevitably occurs if 100 transmitters with a packet rate of $10\,\text{Hz}$ are in the transmission range of each other.

Probability of Occurrence of Half-Duplex Problems The previous analysis assumed the best case. In the worst case, however, half-duplex effects can occur with only two terminals in the transmission range. In this case, both terminals are unable to receive any message. The likelihood for this to happen is very low. Half-duplex effects that are not collisions can only happen if both packets fit into a single subframe. Therefore, the following constraint needs to hold for the determination of the probability for the worst case:

$$n_{\text{SC, REQ}} \leq \left\lceil \frac{n_{\text{SC, TOT}}}{2} \right\rceil$$

In general, there are $n_{\text{SC, TOT}} - n_{\text{SC, REQ}} + 1$ possibilities to allocate a packet that allocates $n_{\text{SC, REQ}}$ subchannels into a subframe with $n_{\text{SC, TOT}}$ subchannels. In the following, it is assumed that the terminals try to prevent a fragmentation of the subframe at the beginning and the end. For example, they do not allocate the second and third subchannel if the first one is also free. If a subframe is already occupied with one packet, the second terminal has

$$n_{\text{SC, TOT}} - n_{\text{SC, REQ}} + 1 - n_{\text{SC, REQ}} = n_{\text{SC, TOT}} - 2 \times n_{\text{SC, REQ}} + 1$$

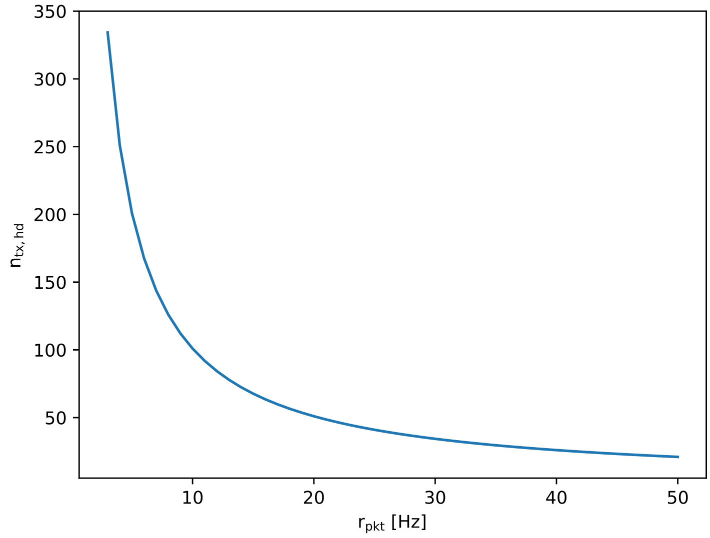

Figure 4.9.: Relation between the packet rate r_{PKT} and number of terminals in the transmission range so that half-duplex effects are guaranteed to occur even with ideal resource allocation ($n_{SF} = 1000$).

possibilities to select a resource from the same subframe without causing collisions. For the subframes that are not occupied, there are

$$(n_{SC,\ TOT} - n_{SC,\ REQ} + 1) \times \left(\frac{n_{SF}}{r_{PKT}} - 1\right)$$

possibilities to choose resources without causing half-duplex effects. Therefore, the possibility to choose the resources that cause half-duplex effects when only two terminals are in the transmission range is:

$$\begin{aligned}
&\frac{n_{SC,\ TOT} - 2 \times n_{SC,\ REQ} + 1}{(n_{SC,\ TOT} - 2 \times n_{SC,\ REQ} + 1) + (n_{SC,\ TOT} - n_{SC,\ REQ} + 1) \times \left(\frac{n_{SF}}{r_{PKT}} - 1\right)} \\
&= \frac{n_{SC,\ TOT} - 2 \times n_{SC,\ REQ} + 1}{-n_{SC,\ REQ} + (n_{SC,\ TOT} - n_{SC,\ REQ} + 1) + (n_{SC,\ TOT} - n_{SC,\ REQ} + 1) \times \left(\frac{n_{SF}}{r_{PKT}} - 1\right)} \\
&= \frac{n_{SC,\ TOT} - 2 \times n_{SC,\ REQ} + 1}{\frac{n_{SF}}{r_{PKT}} \times (n_{SC,\ TOT} - n_{SC,\ REQ} + 1) - n_{SC,\ REQ}}
\end{aligned}$$

For the default configuration with $n_{SC,\ TOT} = 5$, $n_{SF} = 1000$, $r_{PKT} = 10\,\text{Hz}$, and $n_{SC,\ TOT} = 2$ the probability that there are half-duplex problems if only two terminals are in the vicinity is only $2/398 \approx 0.5\,\%$.

However, in the general case, there are usually more than two terminals in the transmission range. The calculation of the probability that at least two of them are affected by half-duplex problems is more complex. The opposite approach than the one above is taken. If n terminals are present in the vicinity, the event that at least one half-duplex problem occurred is complementary to the case with no half-duplex problems. Hence, the probability that at least one half-duplex problem occurred when n vehicles are in the transmission range is:

$$\begin{aligned}
P_{\text{h-d}}(n) &= 1 - P_{\text{noh-d}}(n) \\
&= 1 - \prod_{i=1}^{n-1} P\left(i \text{ selects free subframe} \mid \text{all before } i \text{ selected free subframes}\right) \\
&= 1 - \prod_{i=1}^{n-1} \frac{\left(\frac{\mathrm{n_{SF}}}{\mathrm{r_{PKT}}} - i\right) \times \left(\mathrm{n_{SC,\,TOT}} - \mathrm{n_{SC,\,REQ}} + 1\right)}{i \times \left(\mathrm{n_{SC,\,TOT}} - 2 \times \mathrm{n_{SC,\,REQ}} + 1\right) + \left(\frac{\mathrm{n_{SF}}}{\mathrm{r_{PKT}}} - i\right) \times \left(\mathrm{n_{SC,\,TOT}} - \mathrm{n_{SC,\,REQ}} + 1\right)}
\end{aligned}$$

Figure 4.10 shows the results for different values of n, i.e. vehicles in the transmission range, using the equation above. It can be seen that the probability of half-duplex problems is close to $100\,\%$ beginning at 30 to 40 vehicles in the transmission range. Hence, half-duplex problems are very likely to occur and need to be considered as potential safety-critical problem, even though only two terminals are affected by a single hidden-terminal effect.

Average Number of Affected Terminals Resource allocations with more than one half-duplex problems are more complicated to analyse with an analytical approach because of many different possible allocations and interactions caused by the MAC protocol. Hence, more simplifications are made for the analysis of the average number of affected terminals. In the following analysis, it is neglected that there is a lower probability to choose a subframe that is already occupied. Additionally, there are no restrictions as to how often a subframe can be chosen. These simplifications make it more probable that an occupied subframe is chosen and hence make half-duplex problems more common. Hence, this model can be understood as a upper boundary for the performance of LTE-V2X Mode 4.

With these simplifications, the probability that two or more vehicles choose the same subframe is equivalent to the occurrence of a half-duplex effect. The probability of the occurrence of a half-duplex effect can now be calculated using a modified version of the generalized birthday paradox. Firstly, α is defined as the number of subframes between two consecutive packets of the same packet flow of a transmitter. All transmitters are assumed to transmit one packet flow with rate r. As there are a thousand subframes per second in LTE, $\alpha(r) = \frac{1000\,1/\mathrm{s}}{r}$. Consequently, the probability that two or more of n vehicles choose the same subframe is:

$$p_{\text{anyCol}}(n, r) = \left\{ \begin{array}{ll} 1 - \prod_{k=1}^{n-1} \left(1 - \frac{k}{\alpha(r)}\right), & \text{for } n \leq \alpha(r) \\ 1, & \text{for } n > \alpha(r) \end{array} \right\}$$

Assuming a packet rate of $r = 10\,\mathrm{Hz}$, for 12 vehicles in the communication range, it is already approximately $50\,\%$, for 30 cars it is $99\,\%$.

The events are now independent of each other due to the simplifications that have been made. This enables the calculation of the expected number of simultaneously chosen subframes. The probability that the kth vehicle will select a subframe that has been previously selected by the $k-1$ vehicles before it is:

$$p_{\text{kCol}}(k, r) = 1 - \left(\frac{\alpha(r) - 1}{\alpha(r)}\right)^{k-1}$$

For example, for a packet flow with a rate of $10\,\mathrm{Hz}$, $\alpha(r = 10) = 100$ and

$$p_{\text{kCol}}(k, r = 10) = 1 - \left(\frac{100 - 1}{100}\right)^{k-1} = 1 - 0.99^{k-1}$$

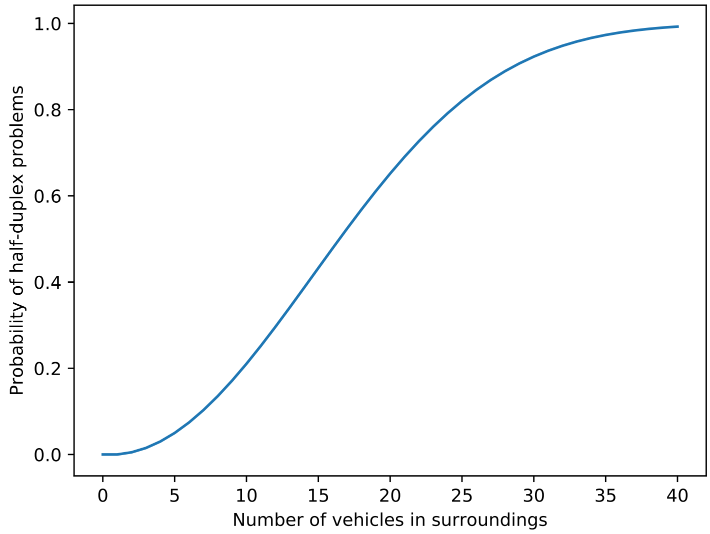

Figure 4.10.: Probability of occurrence of half-duplex problems subject to the number of terminals in the transmission range ($\mathrm{n_{SF}} = 1000, \mathrm{r_{PKT}} = 10, \mathrm{n_{SC,\ TOT}} = 5, \mathrm{n_{SC,\ REQ}} = 2$).

Subsequently, the expected number of simultaneously chosen subframes is the summation of additional matches for any $k \in [1, n]$ vehicle:

$$\mu_{col}(n, r) = \sum_{k=1}^{n} p_{\text{kCol}}(k, r)$$

As Figure 4.11 shows, for 50 vehicles and a packet rate of $r = 10\,\text{Hz}$, the expected number of simultaneously chosen subframes is 10.5, for 100 vehicles it is 36.6.

This simplified analysis illustrates that the problem of persisting half-duplex effects and collisions is not negligible. Measures to protect vehicles, especially from the effects of half-duplex effects that repeat with the same vehicles due to SPS should be deployed.

Summary

In this chapter, a problem analysis of LTE-V2X Mode 4 has been performed. Various special features and properties of the candidate resource selection process and SPS have been investigated.

The candidate resource selection process has multiple potential issues. Firstly, depending on the priorities of the received packet and the packet to be transmitted, the explicit reservations are often ignored because of an extremely high RSRP threshold ($\mathrm{Th}_{a,b}$). This serves as a QoS mechanism but can lead to an increased number of collisions.

Secondly, the way the average RSSI is estimated leads to a discrimination of radio resources that have not yet been used often. This is because the average over the last second is used to calculate the RSSI. If a resource has been reused less than this time, the average RSSI will be lower than the actual reception energy. This is also the case if a resource is subject to packet drops due to DCC or if a smaller number of subchannels are used compared to the interfering packet.

Thirdly, the fixed size of the candidate resource set has been identified to be potentially disadvantageous. In situations with low load, more than $20\,\%$ of the resources might be

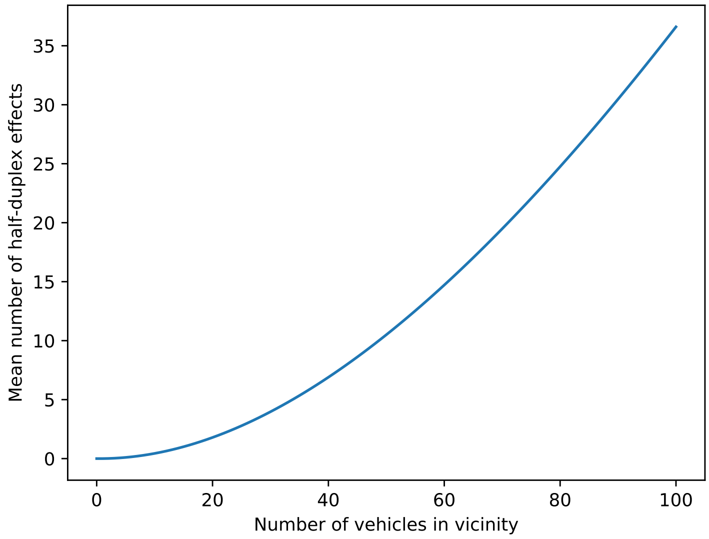

Figure 4.11.: Mean number of half-duplex problems for a packet rate of 10 Hz.

available, i.e. the size of the set should be increased. In situations with high load, the opposite might be necessary. Lastly, due to the low granularity of the subchannels, many padding bits are often necessary. These padding bits waste transmission resources because they do not carry information.

The SPS also leads to disadvantageous effects. While it decreases the number of packet collisions by enabling a forecast about the future allocation of radio resources, it also leads to reoccurring radio frame collisions. This issue can lead to extended periods in which vehicles might not be known to other vehicles. In a safety-critical situation, this could lead to accidents.

Due to the half-duplex effect, terminals cannot receive messages transmitted in the subframe that the terminal used for transmission itself on a different subchannel. This problem is less severe because only the terminals that transmit in this subframe are affected. However, the half-duplex problem is also intensified due to the resource reuse dictated by SPS. The consequences of these reoccurring issues should be prevented with improved MAC protocols if possible.

Chapter 5.

Scheduling Based on Acknowledgement Feedback Exchange (SAFE)

After identifying potential design problems through the analysis of related work (Chapter 3) and a detailed problem analysis (Chapter 4), a set of protocol modifications for MAC and DCC is developed and presented in this chapter. These modifications are subsequently called scheduling based on acknowledgement feedback exchange (SAFE) in their entirety. This architecture consists of various mechanisms that work together to provide a more robust method to control the access on the wireless medium in V2X scenarios. The presented approach is not reliant on a base station or RSU that would be able to centrally schedule radio resources. Hence, the mechanisms work in a distributed way. In short, the mechanisms comprise a more collision-robust radio resource allocation scheme by splitting resource reservations, an acknowledgement feedback mechanism for radio resources, a DCC component that is designed to work well together with SPS and that leverages reservation splitting and the acknowledgement feedback, and a newly developed candidate resource selector that leverages the additional information and possibilities provided by the other mechanisms. Many of the mechanisms have configuration options or parameters. While some predictions about the impact can be made in this chapter, the optimal values of these configuration options will be systematically determined in Chapter 7.

This chapter continues with an overview of the complete architecture, including the single components and the interactions and synergy effects of the combined approach in Section 5.1. Afterwards, the individual components will be described in more detail in Sections 5.2 to 5.5.

5.1. Overview and Interaction of Components of SAFE

The physical layer of the communication system is assumed to be compliant or similar to the sidelink of LTE-V2X (Release 14). Therefore, radio resources can be scheduled both in the time and frequency domain. The LTE standard specifies the time domain as one subframe, which is one millisecond long. The layout of the physical channels is specified in ETSI TS 103 613 [ETS18b], i.e. a single 10 MHz channel is subdivided into five subchannels. While the presented approach works with different values for the channel bandwidth, number of subchannels, and length of a subframe, the standard values will be used for the explanation and subsequent evaluation. The components described here target an improvement compared to LTE-V2X Mode 4. More details on the wireless access technology that is used as basis for the following concepts can be found in Chapter 2.

There are four major components, which will be described in detail in following sections individually. In this section, only a high-level overview is given. While some modifications can work independently of the others, the full potential can only be realized with a combination of them. Moreover, some components require other components to function. The focus of this section is to give an overview, lay out interdependencies between the mechanisms, and show the benefits of an integrated system in which all four components can work with each other. The following four components form the central parts of SAFE:

Reservation Splitting: (Section 5.2) This modification splits one reservation of periodically reused radio resources into multiple, interleaved reservations. These are subsequently called sub-reservations. Due to the splitting, the reuse interval between the uses of the sub-reservations becomes longer. The main anticipated advantage and motivation behind this design is that the impact of the reoccurring collisions and half-duplex effects outlined in Chapter 4 can be limited by this modification. The reasoning is that while these effects will still reoccur, it will only be for the affected sub-reservation. The vehicle will only be completely unable to distribute status updates if all sub-reservations are affected at the same time. If a single sub-reservation is affected by repeating collisions, the next sub-reservation with different radio resources still has a high probability of successful transmission. An additional advantage is that periodic packet flows with varying packets sizes, e.g. short and long CAMs, can now be supported without losing the periodicity property because some of the sub-reservations can reserve more subchannels and support larger packets. This idea has been proposed and investigated in [WST19a].

Acknowledgement Feedback for Radio Resources: (Section 5.3) As seen in Chapter 4, LTE-V2X might use large amounts of padding in order to comply with the relatively low granularity of the resource allocation by subchannels. There might also be free channel capacity that can be explicitly used to improve the performance of the MAC protocol. RTS/CTS mechanisms are not used in ITS-G5 or LTE-V2X, most likely because they scale badly with the broadcast communication typically present in V2V communication. Hidden-terminal problems can heavily impede the performance of the communication system.

The idea of the explicit acknowledgement feedback is to leverage the periodicity of SPS for an additional use: while the goal of RTS/CTS in conventional CSMA/CA systems is to prevent hidden-terminal problems *before they appear*, SPS in LTE-V2X allows to use a reactive approach. Terminals can explicitly report which radio resources could have been successfully decoded in the past, which gives transmitters an indication about the packet delivery ratio of their used and about to be reused resources. The acknowledgement of radio resources instead of packets leverages the periodicity and is an efficient way to provide a mitigation for hidden-terminal situations. An adequate reaction to low acknowledgement ratios would be to select new resources ahead of time, which prevents these collisions from occurring in the future. This idea has been proposed and investigated in [WS20].

Custom Candidate Resource Selector: (Section 5.4) Chapter 4 showed that the candidate resource selection process of LTE-V2X Mode 4 has various possibly disadvantageous features, such as the RSRP threshold $\mathrm{Th}_{a,b}$, the fixed size of the candidate resource set ($20\% \times \mathrm{M}_{\mathrm{total}}$), or the lack of distinction between power levels at different subchannels. The goal of the new candidate resource selector is to rectify these issues and also leverage the additional possibilities that the other three mechanisms give. A rating will be built for each candidate resource. This rating indicates the predicted collision probability. The acknowledgement feedback mentioned above will be leveraged to extend the sensing range. This is a secondary use of this information and an additional *proactive* mechanism to prevent hidden-terminal problems.

Semi-persistent DCC: (Section 5.5) Related work already showed that the channel load can quickly reach high levels and a form of DCC is necessary. However, the current DCC implementation in LTE-V2X Mode 4 is not beneficial. This is because the periodicity property of the radio resource allocations is lost when using this form of DCC. The subdivision of reservations by reservation splitting mentioned above is leveraged by the DCC mechanism of SAFE. It is now possible to reduce the packet rate without losing the periodicity property due to the resource reuse. This is achieved by semi-persistently, i.e. for a given duration, disabling one or multiple of the *sub-reservations*. The other, still active sub-reservations are not affected by this rate-limiting approach. Thus, they are still used periodically. An earlier and similar version of semi-persistent DCC is published in [WST19a].

There are various synergy effects that occur when combining the four previously mentioned approaches with each other in an integrated approach. These benefits and new dependencies are visualized in Figure 5.1.

Reservation splitting is a pre-requisite for the semi-persistent DCC mechanism because it allows to rate-limit one packet flow while retaining a periodic reuse of sub-reservations. The candidate resource selector has an additional DCC component. If all of the available candidate resources have a rating below a certain threshold, the reservation of new radio resources can be aborted. This prevents collisions due to high channel load from occurring in the first place.

When splitting reservations, the sub-reservations use different resources. Therefore, the sub-reservations can potentially have different size, enabling support for varying packet sizes within one packet flow. This is a crucial improvement over the standard LTE-V2X Mode 4, which is incompatible with such traffic characteristics. In practice, even CAMs will have different sizes, depending on the presence of the low frequency container, i.e. the recent path of the vehicle, or digital signatures. Thus, even though LTE-V2X Mode 4 has been designed for periodic traffic, it is incompatible with CAM packet flows due to the varying packet sizes or rates. Using the new candidate resource selector, this requirement can be considered.

The acknowledgement feedback is used to select new radio resources for a sub-reservation if the acknowledgement ratio has been low. Using different resources for sub-reservations also creates the possibility to compare the acknowledgement ratio of each sub-reservation with one another. Hence, the relative performance compared to other resources can be used as indicator. This is advantageous compared to fixed thresholds because the average performance or acknowledgement ratio depends on various parameters, such as the channel load. There are additional uses of the acknowledgement feedback. Firstly, it is used inside the DCC component to disable sub-reservations with bad performance ahead of time. Secondly, the candidate resource selector uses the acknowledgement feedback to prevent hidden-terminal situations. This is done by assuming that they will be reused due to SPS. Hence, if a terminal further away acknowledges a radio resource, it is likely to be occupied in future.

The following sections in this chapter describe the individual mechanisms in more detail.

5.2. Reservation Splitting

As indicated in Chapter 4, SPS itself leads to collisions and half-duplex effects that are likely to repeat for the following reuses of a configured resource. This is detrimental for safety-critical applications such as traffic safety. A simple mitigation for this problem would be to reduce the number of repeated reuses of a radio resource, i.e. reduce the upper and potentially lower boundary of the reselection counter range. Decreasing the number of resource reuses leads to an increased scrambling of radio resources used by the terminals and thus, would limit the negative effects of SPS, i.e. repeated half-duplex limitations and radio frame collisions

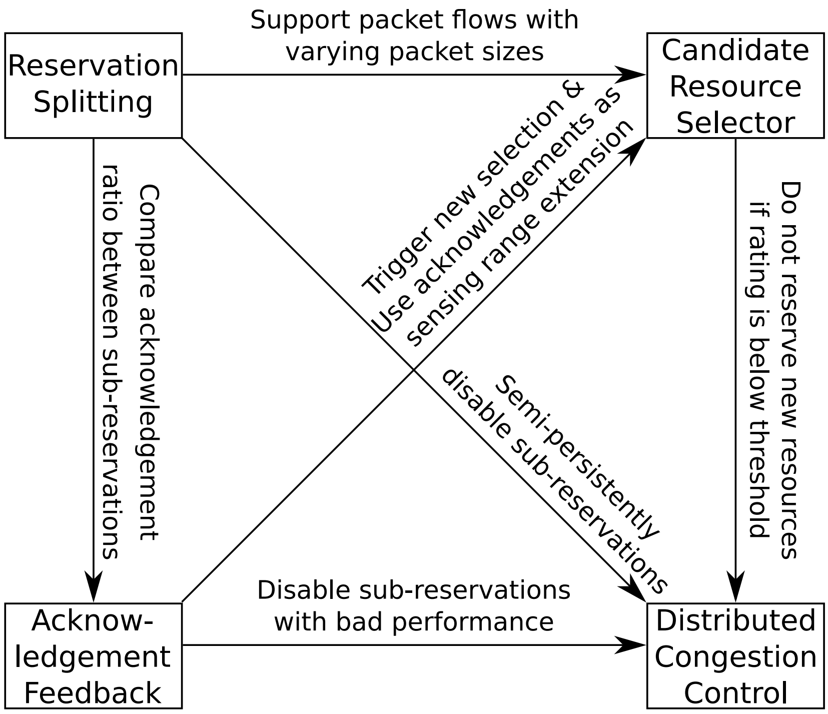

Figure 5.1.: Overview of interdependencies and synergies between reservation splitting, the acknowledgement feedback, the newly designed candidate resource selector, and the semi-persistent DCC variant.

between the same transmitters. However, it would also probably increase the likelihood of collisions by decreasing the predictability of transmitters. Additionally, there is still the problem of supporting packet flows with packets of varying sizes, e.g. short and long CAMs, and with varying packet rates. This is normally also the case for CAMs, which can be triggered by changes in the speed, direction, etc. A reservation scheme that supports varying packet rates could at least to some extent support these traffic patterns.

5.2.1. Overview

A different, more elaborate method to scramble resource allocations could retain this predictability. This can be achieved by splitting one allocation into multiple, interleaved *sub-reservations* with a longer time period between reuses. This means that a single sub-reservation has a lower packet rate, but the overall rate of the packet flow is unchanged as it is being transmitted using multiple sub-reservations. The new sub-reservations with a larger interval between reuses need to be interleaved, so that the required packet transmit rate can be met. For example, one $10\,\mathrm{Hz}$ reservation can be split into two $5\,\mathrm{Hz}$ or five $2\,\mathrm{Hz}$ reservations. The former is visualized in Figure 5.2. With this change, there need to be collisions for every of the sub-reservations for the issues of SPS to gain significant impact. At the same time, the predictability of the behaviour of transmitters is maintained, leveraging advantages of SPS.

There are different possibilities to split a single reservation of standard LTE-V2X. The simplest scheme is a division by two, which is visualized in most figures in this section. A division by two means that there are now two sub-reservations with a reservation interval that has doubled, i.e. is $200\,\mathrm{ms}$. Consequently, two sub-reservations with a packet rate of $5\,\mathrm{Hz}$ replace a single reservation with a packet rate of $10\,\mathrm{Hz}$. The most important feature is that each sub-reservation uses different radio resources, so that repeating collisions do not affect all packets.

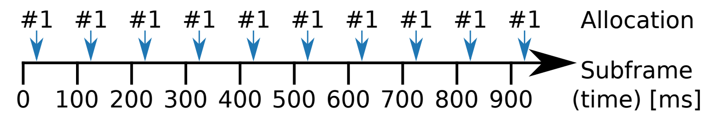

(a) Standard LTE-V2X behavior with a packet rate of 10 Hz.

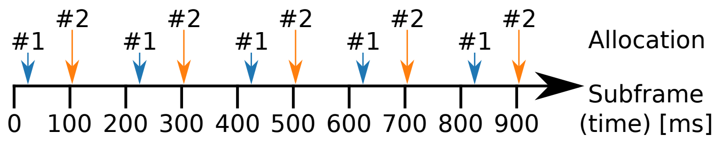

(b) Packet rate of 10 Hz split into two 5 Hz resource allocations.

Figure 5.2.: Standard LTE-V2X resource assignment and proposed reservation splitting scheme. Sub-reservation #1 uses different radio resources, i.e. subframes and/or subchannels than sub-reservation #2.

Table 5.1 summarizes various possible configurations of reservation splitting. The number of sub-reservations is a configurable parameter called $\mathrm{num}_{\mathrm{sub\_res}}$. As it can be seen, increasing the number of sub-reservations also increases the reservation interval. Additionally, the granularity at which packet flows can be rate-limited becomes finer. Higher packet rates can always be supported by using more sub-reservations in the same time interval.

5.2.2. Resource Selection and Reuse with Reservation Splitting

Splitting a reservation has various effects on the MAC protocol and the way the predictions about future channel conditions have to be made when selecting new candidate resources. The reservation splitting scheme maintains the periodicity of resource reuse, but the reuse patterns are different. This is visualized in Figure 5.3.

With this modification, an additional scheduling domain is introduced by subdividing the time domain into further interleaved *sub-slots*. As multiple reservations with lower frequency are now used, the interval between the reuse of sub-reservations will increase accordingly. For example, when splitting one 10 Hz reservation into five 2 Hz reservations, the interval is being multiplied by five (five sub-reservations every 500 ms instead of one reservation every 100 ms). Now it takes 500 ms instead of 100 ms until a resource is reused. The effects of this interval lengthening need to be considered in order to prevent introducing additional disadvantages. However, the resource selection window is still 100 ms. This means that a terminal needs to determine the collision risk for the same amount of candidate resources in the future. The only difference is that the repetition interval is longer. For example, if five sub-reservations are used, they are repeated every 500 ms instead of every 100 ms. For the estimation of candidate resources, it is not relevant whether the sub-reservations are interleaved or not because the

Table 5.1.: Reservation Splitting Strategies

Sub-Reservations $\mathrm{num}_{\mathrm{sub\_res}}$	Reservation Interval	Supported Packet Rates [Hz]
1 (default)	100 ms	10
2	200 ms	5 and 10
3	300 ms	$3\frac{1}{3}$, $6\frac{2}{3}$, and 10
5	500 ms	2, 4, 6, 8, and 10
10	1000 ms	1, 2, 3, 4, 5, 6, 7, 8, 9, and 10

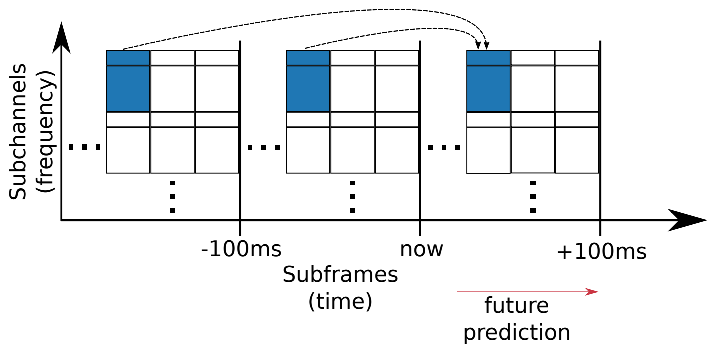

(a) Standard LTE-V2X behavior.

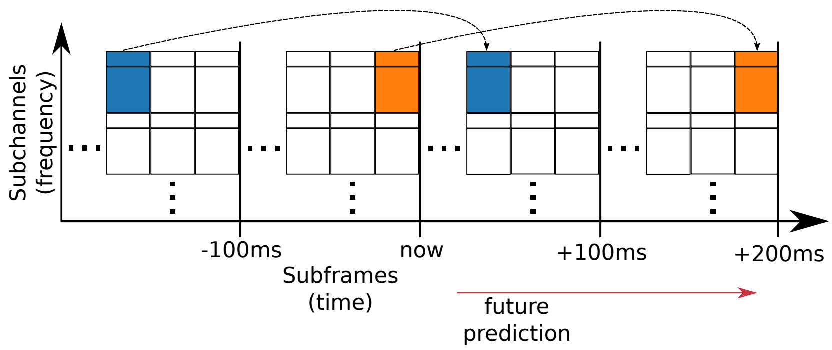

(b) Packet rate of 10 Hz split into two 5 Hz resource allocations.

Figure 5.3.: Implications of reservation splitting on the future prediction of the MAC protocol.

reuse pattern of a single sub-reservation is evaluated. Only the time interval between the reuses increases. The number of sub-reservations, i.e. the repetition interval is a global system parameter that has to be known to all terminals.

In summary, various effects of reservation splitting on the MAC protocol can be seen in comparison to standard LTE-V2X:

Longer reuse time of a resource: Reservation splitting leads to a higher average time interval of resource reuses. This is because the repetitions are not determined by a fixed time interval, but by the reselection counter. With the longer time interval between reuses of the same sub-reservation, the total duration of the resource reuse is increased accordingly.

Longer reservation interval: The information in explicit reservations is older, i.e. the reservation interval until the next resource of the same sub-reservation is longer.

Longer prediction time horizon: Due to the longer interval between repetitions of the same sub-reservation, the time horizon for RSSI-based predictions is lengthened.

The longer reuse time of a resource can be counteracted by reducing the number of resource reuses, either by reducing the reselection counter range or by decreasing $\mathrm{probResourceKeep}$. This is another argument to set $\mathrm{probResourceKeep}$ to zero when using SAFE. For aforementioned reasons, ten sub-reservations should not be used, and five sub-reservations are seen as the highest possible configuration. The prediction time horizon would be increased to 1000 ms instead of 100 ms, and the sub-reservations would be used ten times longer. This cannot sufficiently be counteracted by a decrease of $\mathrm{probResourceKeep}$.

The longer reservation interval could be mitigated by indicating the next resource in time, i.e. of the next sub-reservation. This leads to a slightly increased overhead, because the next sub-reservation in time likely uses a different time slot (i.e. not a fixed 100 ms reuse interval) and different subchannels. Therefore, in this case, the subchannels and subframe of the next reservation need to be transmitted via the SCI as well. In order to encode the subchannels, 4 bit suffice when using five subchannels. This is because there are 15 different allocations possible. In order to encode the subframe, 7 bit to 10 bit are additionally necessary, in order to be able to express between 128 and 1024 subframes. This modification is not enabled for SAFE because it did not show performance benefits. Hence, the additional overhead is not justified.

The longer time horizon for the RSSI prediction cannot be fully eliminated. While more sub-reservations are expected to increase the robustness, they also increase the prediction time interval, which might cause a drop of the PDR. The effects can be limited by choosing the best compromise for configuration of the reservation splitting scheme.

5.2.3. Support for Varying Packet Sizes and Rates

In this section, possibilities and constraints to support packet flows with varying packet sizes and rates will be outlined. In principle, there are two possibilities to consider. Firstly, different sub-reservations can be disabled, reducing the overall packet rate. This can also happen with a DCC component, but in the case of CAMs, the packet rate could also be influenced by considerations in the application layer, e.g. the change in speed or heading. The allocation with reservation splitting enables the immediate reduction of the packet rate by stopping transmissions using some sub-reservations and dropping the reservations for radio resources. However, it is advantageous to maintain some periodicity of the resource use of sub-reservations. In the case of CAMs, this could mean that a higher packet rate could be maintained at least for the current reservation. This makes sense in practical considerations, because it increases the reliability of the transmission of the new and important information.

Different packet sizes can always be supported by increasing the MCS index or using previously unused padding bits. This is also possible with standard LTE. However, the effect of this is limited. Reservation splitting enables the possibility to use different numbers of subchannels for each sub-reservation. Consequently, packet flows with larger variations in the packet size can be respected. CAMs are a good example for this, as short and long messages are usually sent. The long CAMs could be sent with a sub-reservation of four or five subchannels, and the other, shorter CAMs should fit into sub-reservations with two subchannels. This allocation assumes that the longer packets occur at predictable and constant intervals. This is often the case. However, the possibilities to schedule these messages are dependent on the number of sub-reservations. For example, assuming a CAMs packet flow with ten packets per second, and five sub-reservations, one of the sub-reservation is used every 500 ms. Hence, two of the ten packets per second need to be long CAMs. This is a reasonable assumption. Additionally, the equidistant spacing of the long messages in the time domain is an additional implicit advantage.

Figure 5.4 shows an example for a resource allocation when using five split reservations. The third and fifth sub-reservation is disabled, indicating that the current packet rate is only six packets per second ($3/5 \times 10\,\mathrm{Hz}$). The fourth sub-reservation carries the long CAM, once every 500 ms, i.e. twice per second.

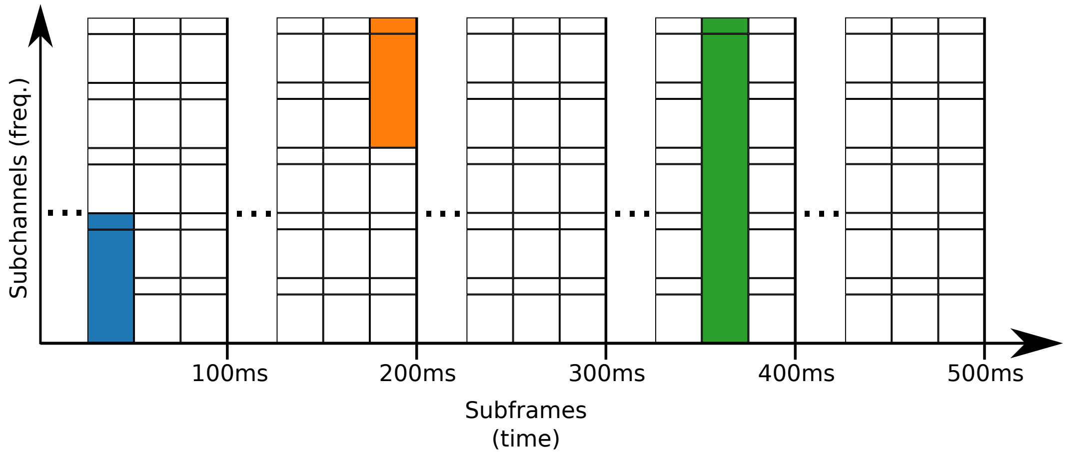

Figure 5.4.: Example resource allocation for the use of reservation splitting with varying packet sizes and rates. In this example, a packet rate of 6 Hz is shown. Every third packet is larger and occupies the complete subframe.

5.3. Acknowledgement Feedback for Radio Resources

As it has been seen in previous chapters, RTS/CTS is not suitable as a hidden-terminal mitigation for V2V communication. This is because it is not applicable for the often local broadcast that is predominantly used in V2V communication. Hence, a more efficient, potentially heuristic approach needs to be developed for this type of communication. The high overhead of RTS/CTS for broadcast traffic can only be mitigated by not explicitly asking each potential receiver beforehand. A mechanism that uses more aggregated data is necessary. Moreover, as every potential receiver might not be known to the transmitter beforehand, it might not be the best practice to address each one individually. In conclusion, a distributed, indirect procedure is most promising.

Just as with the resource selection, the SPS and periodic reuse of resources can be leveraged for this approach. As resources are likely to be reused, *resources in the resource grid* instead of transmissions can be addressed by acknowledgement feedback. This is the most important idea behind the acknowledgement feedback of SAFE and enables a very efficient encoding and addressing.

The acknowledgement feedback can be represented in a (flattened) bitmap, using only a single bit per radio resource. The data format represents a two-dimensional matrix. The number of rows is equal to the number of subchannels in the channel. The number of columns can vary, depending on how much history should be reported. The latest entry in the matrix is always the most recent subframe. It is important to notice that *radio resources* are acknowledged instead of *packets*. Other terminals can aggregate this information and know the number and ratio of the reported successful and unsuccessful receptions. This ratio is called the acknowledgement ratio of a radio resource.

This feedback mechanism fulfils the efficiency requirements mentioned above. There is no need to address individual transmitters or receivers. The feedback has a constant overhead of only one bit per radio resource, regardless of the number of surrounding terminals. The acknowledgement feedback does not have complete coverage nor does the addressing scheme claim that the feedback reaches the correct transmitter in every corner case. Hence, it can be seen as a heuristic. Specifically, terminals might not be able to transmit all acknowledgements for the complete resource repetition interval, maybe due to a high channel load or overhead constraints. In this case, there is only an incomplete picture about a single terminal's history of radio resource receptions. However, due to the large number of terminals in the vicinity that goes along with the high channel load, it is likely that there is still enough information in order to make radio resource scheduling decisions. The acknowledgements are meant to be transmitted in the padding bits, of which LTE-V2X Mode 4 uses plenty due to the large granularity of the resource allocation by subchannels. Still, there are different possibilities to increase the number of bits to be used for acknowledgements. Firstly, additional subchannels could be allocated. Secondly, the data could be transmitted using a higher MCS index. Thirdly, separate acknowledgement packets with the aggregated information could be sent. This is reflected by the factor or configuration parameter $\mathrm{ack}_{\mathrm{sep\_pkts}}$. The benefits of such decisions compared to the disadvantages due to the increased overhead remain to be evaluated in subsequent chapters.

The second reason why this mechanism is a heuristic is due to the fact that radio resources are acknowledged instead of packets. It is hence possible that a transmitter receives acknowledgements for radio resources that it used for transmission, but the receivers intended to acknowledge the transmission from another terminal. This occurs in asymmetric hidden-terminal situations in which the receiver is still able to decode one of the transmissions despite interference. However, these asymmetric hidden-terminal situations happen due to the capture effect and only occur in limited areas. It is hence likely that there are more receivers close to both transmitters, which would report non-acknowledgements back to them. Moreover, it is debatable whether this is actually a desirable feature. Essentially, receivers that were not disturbed by more distant transmitters, report this non-disturbance back to both transmitters and potentially increase the spatial reuse of the wireless medium. It might also happen that a receiver is not able to reach a transmitter even though the transmitter was able to reach the receiver. This seems to be counterintuitive at first because wireless channels are always assumed to be reciprocal. However, as the receiver aggregates the acknowledgements and transmits them at a later point in time, the positions and multipath propagation might be slightly changed. Moreover, the interference situation at the transmitter might be different.

The acknowledgement feedback has two components to mitigate hidden-terminal problems: a reactive and proactive one. For the reactive hidden-terminal mitigation to work, the terminals need to remember which radio resources they have been using in the past. With the acknowledgement feedback from others, they now know the acknowledgement ratio for radio resources that they have been using. The approach works as a hidden-terminal mitigation because of SPS: if the terminals notice that the acknowledgement ratio is too low (below the value of the configuration parameter $\mathrm{ack}_{\mathrm{min}}$), there was a collision or hidden-terminal problem. Due to SPS, they must reuse those radio resources, just as the other terminal that was also affected by this collision. Hence, the hidden-terminal effect would reoccur. The proposed idea is to drop the current radio resources of this sub-reservation and select new ones ahead of time in these situations. Hence, this is a reactive component of the hidden-terminal mitigation.

This mechanism works well together with reservation splitting because a transmitter can compare the acknowledgement ratio to other sub-reservations. This is implemented by calculating an exponential moving average of the acknowledgement ratio across all used radio resources (with a configurable $\mathrm{ack}_{\mathrm{avg},\alpha}$ parameter) and reacting to collisions if the current acknowledgement ratio is below the moving average minus a delta parameter $\mathrm{ack}_{\mathrm{avg},\delta}$, which acts as hysteresis component. The exponential moving average is calculated as

$$m(t) = \alpha \times x(t) + (1 - \alpha) \times m(t - 1)$$

where α is $\mathrm{ack}_{\mathrm{avg},\alpha}$, and $x(t)$ is the acknowledgement ratio of the most recently used resource. This method eliminates the need to set arbitrarily high thresholds for the absolute minimum acknowledgement ratio $\mathrm{ack}_{\mathrm{min}}$, below which new radio resources need to be selected ahead of time. This is beneficial because the acceptable or achievable acknowledgement ratio might depend on the current channel conditions, especially the channel load. The exponential moving average is beneficial compared to a linear average because it avoids dependencies to configuration parameters such as the number of sub-reservations, packets dropped due to DCC, packet flows with different packet rates, etc. When reservation splitting is not used, this mechanism will still work and detect suddenly decreasing acknowledgement ratios that occur when another transmitter causes a collision. There is an additional advantage of reservation splitting when combined with the acknowledgement feedback. As the reuse interval of the sub-reservations is longer, there is more time to receive or transmit the feedback. Thus, if a terminal transmits a packet with a large amount of padding, all of it can be used for the transmission of acknowledgement feedback that is still relevant.

In order to prevent overreactions of SAFE and still ensure the periodicity of resource allocations, an additional hysteresis time period is introduced. It determines the minimum time between dropping radio resources due to acknowledgement feedback and is called $\text{ack}_{\text{hysteresis}}$.

In the following, the proactive component of the hidden-terminal mitigation will be described. It is also based on the acknowledgement feedback and also leverages the periodicity of resource allocations due to SPS. The idea is to use the acknowledgements as a mechanism to extend the sensing range with feedback from other terminals. This idea is visualized in Figure 5.5. As the acknowledgements are transmitted by the receivers and not the original transmitter, they can reach terminals further away. Due to the periodic resource reuse, other terminals can assume that the resource is being reused. Therefore, resources marked with acknowledgements are likely to be occupied in the future, potentially by terminals outside the sensing range. By excluding those resources from the candidate resource set, hidden-terminal effects with these transmitters are prevented from occurring in the first place.

The acknowledgements need to be considered when selecting radio resources. Hence, a modification of the candidate resource selector is necessary. This modified candidate resource selector will be described in detail in the following section.

Another previously not mentioned advantage of the acknowledgement feedback is that a transmitter knows how many receivers were able to receive its message. This is especially relevant for safety-critical messages such as high-priority DENMs. If the delivery ratio is determined to be too low, the transmitter could additionally react, e.g. by increasing the packet rate to increase the robustness.

(a) Transmission. (b) Acknowledgement.

Figure 5.5.: Visualisation of the proactive hidden-terminal mitigation. At first, vehicle A transmits a CAM that can only be received at vehicle B, which acknowledges the successful reception of this particular radio resource. Vehicle C will avoid this resource because it now knows that it will likely be occupied in the future (due to SPS) by a transmitter that it cannot detect itself.

5.4. Radio Resource Selection Mechanism

The proactive hidden-terminal mitigation, i.e. considering acknowledgements when selecting radio resources, has already been mentioned in the previous section. The details of the technical realisation still need to be explained. Additionally, several deficiencies of the candidate resource selection process of standard LTE-V2X mode have been outlined in Chapter 4. For example, the threshold $\mathrm{Th}_{a,b}$ is often not considered at all, the candidate resource is chosen from only $20\,\%$ of the total resources, and the RSSI is averaged over multiple subchannels, of which some might not be occupied at all. Additionally, while introducing new data input such as acknowledgements, the design of the candidate resource selector should be simplified by eliminating logical interdependencies between the reasons for the exclusion of candidate resources.

The new candidate resource selector builds a single rating for each candidate resource. This rating indicates the predicted collision probability if this resource had been chosen for transmission. The rating is a number between zero and one thousand. A higher rating (or score) is better, i.e. indicates a lower predicted collision probability.

Various factors can influence the rating of a candidate resource. Just like in standard LTE-V2X Mode 4, some of those factors depend on reception energies, e.g. the RSRP or RSSI. This energy needs to be converted to a rating factor. A simple linear interpolation (in the logarithmic domain) from $-110\,\mathrm{dBm}$ to $0\,\mathrm{dBm}$ is used for this conversion:

$$\mathrm{interp}(p\,[\mathrm{dBm}]) = \left\{ \begin{array}{ll} 0, & p < -110\,\mathrm{dBm} \\ \frac{p}{110\,\mathrm{dBm}} + 1, & -110\,\mathrm{dBm} \leq p \leq 0\,\mathrm{dBm} \\ 1, & p > 0\,\mathrm{dBm} \end{array} \right\}$$

The lower boundary of $-110\,\mathrm{dBm}$ is close to the theoretical noise floor per subchannel of $-111\,\mathrm{dBm}$, assuming $-174\,\mathrm{dBm/Hz}$ of thermal noise over a subchannel that occupies $2\,\mathrm{MHz}$.

Algorithm 1 describes how the rating of a candidate resource is calculated. The functions `getRssiFactor()` and `getRsrpFactor()` use the `interp()` function from above to calculate the factor from the energy levels. One aspect that is not shown is how candidate resources with multiple subchannels, i.e. for larger packets, are handled. In this case, the single-subchannel resources of the candidate resource with the highest negative impact is chosen for each of the conditions. For example, the subchannel with the highest average RSSI is chosen for the RSSI calculation. For the calculation of the impact of the acknowledgement ratio, the subchannel with the highest acknowledgement ratio is chosen, and so forth. As it can be seen in Algorithm 1, there is a static penalty for the presence of reservations ($\mathrm{crs}_{\mathrm{reservation\_penalty}}$) and for the presence of acknowledgements ($\mathrm{crs}_{\mathrm{ack\_penalty}}$). Additionally, there are weighted penalties for the average RSSI ($\mathrm{crs}_{\mathrm{rssi\_weight}}$), the RSRP of resources that contain reservations ($\mathrm{crs}_{\mathrm{reservation\_weight}}$) and the acknowledgement ratio ($\mathrm{crs}_{\mathrm{ack\_weight}}$). The optimal values for these parameters will be determined in Chapter 7. The parameters that influence the rating of a candidate resource should add up to one thousand, so that the whole range of the rating (between zero and one thousand) can be used. If SAFE is configured with penalties that do not add up to one thousand, they will automatically be scaled accordingly.

Once a rating is calculated for every possible candidate resource, the actual candidate resource needs to be chosen. In standard LTE-V2X Mode 4, it is randomly chosen from the $20\,\%$ of the candidate resources that remain after the exclusion of resources with reservations, a high average RSSI, etc. In situations with a low channel load, more than $20\,\%$ of the candidate

Algorithm 1 Calculate candidate resource rating

Require: candidate resource cr
  rssiPenalty = $\mathrm{crs}_{\mathrm{rssi\_weight}} \times$ cr.getRssiFactor()
  if cr.isReservationPresent() **then**
    reservationPenalty = $\mathrm{crs}_{\mathrm{reservation\_penalty}} + \mathrm{crs}_{\mathrm{reservation\_weight}} \times$ cr.getRsrpFactor()
  else
    reservationPenalty = 0
  end if
  if cr.isAckPresent() **then**
    ackPenalty = $\mathrm{crs}_{\mathrm{ack\_penalty}} + \mathrm{crs}_{\mathrm{ack\_weight}} \times$ cr.getAckRatio()
  else
    ackPenalty = 0
  end if
  rating = 1000 − rssiPenalty − reservationPenalty − ackPenalty
  return rating

resources might be a good choice. On the other hand, in situations with high channel load, there might be candidate resources among those 20 % that might have an almost guaranteed chance of collision. Therefore, a different approach has been chosen. This approach can leverage the rating mechanism of a candidate resource by restricting the candidate resource set to those with a rating above a certain threshold. This threshold is called $\mathrm{crs}_{\mathrm{min\_rating}}$. In order to prevent collisions that would occur if many transmitters would have to choose a resource from a very small set, it should still be ensured that at least 20 % of the candidate resources are available. There are two possibilities to facilitate this. Firstly, the selection of a new candidate resource could be prevented, i.e. no candidate resource could be returned to the higher layer. This would prevent the transmission of the packet, which would act as a DCC component. The other possibility is to fall back to the behavior of standard LTE, i.e. to use the 20 % of the candidate resources with the highest rating. SAFE supports both of these options. This is configured with the boolean $\mathrm{crs}_{\mathrm{min\_rating\_dcc}}$ parameter.

Another benefit of this rating-based approach is that it can incorporate a QoS aspect: candidate resources with the highest rating could be reserved for packets with a higher priority. Alternatively, packets with different QoS classes could have different minimum ratings (i.e. $\mathrm{crs}_{\mathrm{min\_rating}}$).

5.5. Semi-Persistent Distributed Congestion Control

The performance of MAC protocols for wireless access technologies can be severely impacted by a high channel load. Most wireless MAC protocols essentially work by reducing the likelihood of a collision (*"collision avoidance"*). However, this likelihood inevitably increases as the channel becomes fully occupied. Therefore, DCC has been introduced in ITS-G5 [ETS11a] and LTE-V2X Mode 4 [ETS18c]. The purpose of DCC is to prevent terminals from transmitting if the channel busy ratio is already high, which ensures that MAC protocols can continue to work as intended.

There are different ways to restrict the channel load:

Using a more efficient modulation and coding scheme: It might be possible to reduce the number of subchannels required for the transmission of a packet by using a higher MCS index. However, this requires a higher SINR at the receiver and thus, is more likely to be affected by collisions, especially at higher transmission ranges.

Decreasing the transmission power: Another possibility to reduce the channel load is to use a lower transmission power. This also decreases interference range. Like the possibility of a higher MCS index, it also increases the spatial reuse.

Restricting the packet rate: Reducing the packet rate, either by dropping at the MAC layer, or even in the application layer, is another method to reduce the channel load.

Limiting the packet rate is the reaction that is typically referred to when speaking of DCC. The other methods are orthogonal to this, but decrease the reliability and/or range of transmissions and are not discussed further due to the potentially dangerous safety implications.

DCC, if improperly implemented in conjunction with SPS, breaks assumptions made in the MAC layer about periodic behaviour of transmitters. As shown in Chapter 4, this is the case with the standard version of DCC for LTE-V2X Mode 4. This version also has the disadvantage that restricted packet flows that only use a part of their radio resources have a lower average RSSI and are therefore additionally more likely to be affected by collisions, as other transmitters might preferably choose those candidate resources. When splitting reservations, this disadvantage could be circumvented: as packet flows are already split across multiple reservations, some of them can be semi-persistently disabled when required by DCC. With this method, the packet rate of a single packet flow can be reduced with a granularity restricted by the number of sub-reservations. For example, splitting a reservation into five allows to regulate the packet rate to $0\,\%$, $20\,\%$, $40\,\%$, $60\,\%$, $80\,\%$, and $100\,\%$. Other transmitters are than more likely to choose resources of this disabled sub-reservation because it is completely and persistently unoccupied. This is in line with the original design goal of DCC in general – limit the packet rate so that the performance of the MAC protocol does not deteriorate. By predominantly disabling resources with bad performance, as indicated by low acknowledgement ratios, the DCC component of SAFE has an additional positive influence on the communication reliability.

This method retains the predictability, i.e. periodicity of transmitter behaviour. Therefore, it should make the predictions about future channel allocations more reliable. Various technical aspects still need to be considered, which will be presented in the following.

5.5.1. Preventing Oscillations of Packet Rate and Channel Busy Ratio

In order to maintain predictability, any kind of *nervous* behaviour, i.e. an under- or overreaction should be prevented. In other words, it is disadvantageous that every vehicle reacts instantly to changing conditions regarding the channel occupation. In this case, if the channel load was too high, this overreaction would likely lead to a sharp decrease of the channel load, further motivating terminals to increase the transmit rate again, and so forth. This kind of oscillation of the transmit rate and hence, the channel load, introduces unnecessary unpredictability for the MAC protocol and needs to be prevented.

The chosen solution for this problem is to *semi-persistently* disable sub-reservations. This means that one of the sub-reservations of a packet flow is disabled for a consecutive number of times. In order to prevent synchronisation effects and oscillations of the channel load, a sub-reservation is disabled for a specified time period, which is a configurable parameter $\mathrm{dcc}_{\mathrm{disable\_time}}$ in seconds.

5.5.2. Selection of Sub-Reservations for Restriction

Up until now, it has been described how sub-reservations are disabled in a semi-persistent manner while preventing overreactions and oscillations of the channel load. It remains to be specified which sub-reservations are disabled and under which conditions this happens.

A packet with a bad acknowledgement ratio will already be dropped along with the associated radio resources as long as the hysteresis time period ($\mathrm{ack}_{\mathrm{hysteresis}}$) is not exceeded (see Section 5.3). Moreover, the DCC component when selecting new radio resources (Section 5.4) can also limit the current packet rate. However, this might not be enough, as this only affects newly selected resources and resources are reused often.

Sub-reservations are disabled depending on the current CBR, i.e. channel load. The CBR is determined by building the ratio of radio resources of the last $100\,\mathrm{ms}$ with an RSSI above $-94\,\mathrm{dBm}$. Hence, this follows the standard definition of the CBR by ETSI [ETS18c].

For this approach, there are two different stages of a high CBR. The first, mild condition triggers if the CBR is in the normal working range of the DCC component. The CBR target is a parameter called $\mathrm{dcc}_{\mathrm{cbr\_target}}$. If it is within a margin (plus/minus $\mathrm{dcc}_{\mathrm{cbr\_margin}}$), only a mild reaction is triggered. This means that the current sub-reservation is only disabled if its acknowledgement ratio is low. Like in Section 5.3, the acknowledgement ratio of the sub-reservations is compared by using the exponential moving average with $\alpha = \mathrm{ack}_{\mathrm{avg},\alpha}$. The DCC mechanism is only carried out in this case if the acknowledgement ratio of the sub-reservation under consideration below the moving average minus $\mathrm{ack}_{\mathrm{avg},\delta}$, or additionally, below $\mathrm{ack}_{\mathrm{min}}$. The hysteresis time ($\mathrm{ack}_{\mathrm{hysteresis}}$) is not relevant for DCC. Resources are dropped when the sub-reservation is disabled due to DCC. Using this approach, only sub-reservations with a bad performance are disabled, if the CBR is only slightly above the target value. The second condition triggers if the current CBR is above the target CBR $\mathrm{dcc}_{\mathrm{cbr\_target}}$ plus the margin $\mathrm{dcc}_{\mathrm{cbr\_margin}}$. In this situation, sub-reservations are dropped regardless of their acknowledgement ratios. Both of these reactions disable the sub-reservations semi-persistently.

5.5.3. Fairness and Prevention of Starvation

The DCC component and the restriction of new candidate resources based on the minimum rating can both lead to unfair conditions and starvation of terminals in extreme cases. It should be prevented that a terminal is completely unable to distribute status updates due to DCC restrictions, as this might lead to dangerous situations.

For both DCC mechanisms, i.e. the DCC mechanism itself and the DCC component in the candidate resource selector, minimum CR values or number of sub-reservations are specified. This means that the DCC mechanism cannot restrict terminals below a certain threshold regardless of the current channel load. The restriction in the candidate resource selector works by only considering conditions relevant for the complete terminal. A minimum CR of 0.0024 is conceded to each terminal. Thus, each terminal is always allowed to use at least twelve single-subchannel resources during one second. For example, at minimum, a terminal is able to transmit six packets that occupy two subchannels each in one second. This is equal to three sub-reservations if only a single packet flow and five sub-reservations are used. Therefore, it might be necessary to sacrifice some of the resources of CAMs for DENMs in extreme scenarios.

The minimum CR value described above affects all packet flows of this terminal together. For each packet flow, the DCC component does not restrict it below two sub-reservations, regardless of the current CBR.

These mechanisms ensure that there are no terminals that are significantly more impacted by DCC than others. Hence, this ensures the fairness of the protocol. Secondly, every terminal is still able to distribute potentially safety-critical packets with redundant radio resources.

Summary

The design of the MAC and DCC protocols developed for this thesis have been described in this chapter. It is comprised of four components, which create synergy effects when working in conjunction, or even depend upon each other. The first component is reservation splitting, which subdivides the resource allocation into independent sub-reservations. Each sub-reservation has its own radio resources, and a longer resource repetition interval. By using multiple sub-reservations per packet flow, the same packet rates can be reached. Terminals need to respect the longer interval between repeating resources, which also increases the total duration of a reservation. The advantage of this approach by itself is that it limits the effect of reoccurring collisions and half-duplex problems.

The second component is the acknowledgement feedback for radio resources. The difference to traditional acknowledgements is that radio resources instead of individual packets are acknowledged. This leverages the periodic resource reuse and enables the efficient encoding of the feedback in a simple bitmap. As resources are periodically reused, the same resource is likely to be used by the same transmitter in future. Transmitters can remember which resources they used in the past and know which acknowledgement feedback is relevant for them. If two transmitters use the same radio resources, some of the acknowledgement feedback might be addressed incorrectly. The probability and consequences of this need to be investigated in the evaluation of SAFE. The acknowledgement feedback can be used in conjunction with SPS to select new radio resources ahead of time, if the old ones performed badly. If reservation splitting is used, the acknowledgement ratio of the sub-reservations can be compared to one another, which is implemented by using an exponential moving average.

The third component also leverages the acknowledgement feedback. It is a newly designed candidate resource selector. By considering the acknowledgement feedback, the sensing range of a terminal is effectively extended. This acts as proactive hidden-terminal mitigation. The candidate resource selector also eliminates complex interdependencies between reasons for excluding candidate resources and eliminates other disadvantages of LTE-V2X Mode 4. By building a rating for each candidate resource, the pool of resources from which the actual resource is randomly chosen can be of variable size. Additionally, packet flows can be rate-restricted by setting limits for the lowest allowable rating of a candidate resource that is selected.

The main DCC component, as fourth component, leverages reservation splitting and disables sub-reservations semi-persistently for a configurable duration. This limits the packet rate while retaining the periodicity property of the resource allocation or usage. The DCC mechanism only disables sub-reservations with a bad performance under normal conditions, which is indicated by a low acknowledgement ratio. This ensures that the main goal of DCC is considered: to limit the packet rate in order to ensure that the MAC protocol can perform at its best potential. Still, the DCC component is able to disable any sub-reservation in situations with an extremely high channel load, while still ensuring fairness.

Chapter 6.

System-Level Simulation Framework

The preferred method to evaluate link layer protocols in general and for vehicular ad hoc network (VANET) scenarios in particular are simulations. This is due to the complexity of the scenarios, which makes a comprehensive analytical approach infeasible. Additionally, large-scale real-world measurement campaigns are highly expensive and impractical. Firstly, a large number of testing vehicles is necessary to reach a meaningful and realistically distributed channel load. Secondly, real-world measurements are difficult to reproduce and analyse.

No publicly available simulator for LTE-V2X Mode 4 was available at the beginning of the research for this dissertation. Hence, a simulation framework had to be developed. This chapter describes this simulation framework. Simulation results are used for the optimisation of configuration parameters (Chapter 7) and the evaluation of SAFE (Chapter 8). Simulations have also been used during the development of the approach presented in this dissertation in order to identify deficiencies of LTE-V2X Mode 4. These deficiencies were motivated in Chapter 4 using analysis techniques instead of simulation results. This allowed the quantification of the individual impact in an isolated way and helps with the understanding of the dependencies between the mechanisms of LTE-V2X Mode 4.

This chapter also serves as a description of the simulation setup with all of its parameters and is hence part of the specification of the experiment setups.

6.1. Overview

From a high-level perspective, the simulation framework is a combination of a traffic simulator coupled with a network simulation. The traffic simulation uses Simulation of Urban Mobility (SUMO), an existing microscopic simulator and newly created as well as existing traffic scenarios.

The network simulation for this dissertation builds upon the Objective Modular Network Testbed in C++ (OMNeT++), which is a framework for discrete event simulation that is typically used for network simulations. OMNeT++ provides the basic functionality and data structures to handle the discrete events and offers an integrated development environment (IDE), while the domain-specific functionality is implemented in separate modules.

The simulation framework developed for this dissertation leverages various additional modules and external libraries:

INET: The most widely known module for OMNeT++ is the INET module[1]. Without this model, OMNeT++ is just a framework for discrete event simulation. INET adds functionality for network simulations across all OSI layers. At the physical layer, it provides models for

[1] https://inet.omnetpp.org

background noise, antenna patterns, reception error models, wireless channel propagation, and shadowing models. Additionally, there are implementations of the physical layer of different access technologies, e.g. IEEE 802.11 or 802.15.4. The physical layer can be simulated with different granularities, e.g. with packet-, bit- or symbol-level models. Some features of the more fine-grained models are not complete, and the execution of the simulation takes considerably longer, to a point that makes it infeasible to simulate larger scenarios.

The link layer consists of various access-technology-agnostic parts and specific implementations, e.g. for Ethernet or IEEE 802.11. As part of the network layer, INET contains many different protocols such as internet protocol version 4 (IPv4) and IPv6, address resolution protocol (ARP), multi-protocol label switching (MPLS), etc. The transport layer contains implementations of TCP and UDP, among others. INET also includes various applications, a model for the physical environment, node mobility, power consumption, and visualisation features.

Veins: Vehicles in network simulation (Veins)[2] [SGD11] is a simulation framework based on OMNeT++ for V2V communication. It is bidirectionally coupled with SUMO via traffic command interface (TraCI). This means that SUMO and the Veins simulation run in parallel and can influence each other. For example, a DENM issued by a vehicle might cause other vehicles to slow down. Veins provides additional features such as a model for the carbon dioxide emissions of vehicles or the controlling of traffic lights. However, these features are not relevant for this dissertation. Veins leverages features of the MiXiM[3] model, which itself is a combination of several other OMNeT++ modules. Many parts of the MiXiM code have been integrated into the INET module in 2014. Veins is still mostly built upon the older MiXiM code, while INET-based simulations are also possible.

Vanetza: The European C-ITS stack is implemented in Vanetza[4], which is a standalone C++ library. The most important features comprise of the GeoNetworking protocol and BTP, DCC for ITS-G5, security features and abstract syntax notation one (ASN.1) support for CAMs and DENMs. Vanetza can be leveraged to provide C-ITS support in V2V simulations. It can also be used with real devices such as Cohda wireless modules like the MK5 to perform for real-world tests with C-ITS.

Artery: Being the counter-part for Vanetza, Artery[5] [RGFW15] is an OMNeT++ module for V2V simulations for C-ITS and specifically, the ITS-G5 access technology. Artery also makes use of Veins, but adds additional features such as an environment model, a holistic architecture to support multiple V2V applications in heterogeneous deployments, or a possibility to manipulate vehicle dynamics with a custom TraCI implementation for the SUMO integration. Artery couples INET, Veins and Vanetza and is the basis for the extensions that have been made for this dissertation.

The simulation software used for the evaluation in this dissertation is a combination of SUMO, OMNeT++, INET, Veins, Vanetza and Artery. SUMO and OMNeT++ have not been modified and are used as is. The simulation only uses a very small part of Veins, namely the code for coupling the network simulation with the traffic simulation carried out by SUMO. The simulation updates the position of vehicles every $100\,\mathrm{ms}$. There are some small modifications to INET, which are mostly for fixing bugs. Most of the developed features build upon Artery. Firstly, the INET-based simulation model has been extended to support

[2] https://veins.car2x.org
[3] https://mixim.sourceforge.net
[4] https://github.com/riebl/vanetza
[5] https://github.com/riebl/artery

communication via Mode 4 of LTE-V2X. Artery focuses on ITS-G5 as access technology and does not support communication via LTE. Therefore, the LTE features have been developed from scratch, requiring the re-writing of many INET modules due to the special features of SC-FDMA. Various other bugfixes and performance optimisations have been integrated into Artery, which are however of no concern for the outcome of simulation results. Other important modifications are the introduction of statistics recording modules, e.g. for application-oriented metrics or range-restricted PDR statistics, and the implementation of additional INET-based channel models that are better suited to simulate V2V communication. Moreover, additions for the simulation of obstacle shadowing have been implemented, including the parsing of building outlines and the consideration of the vehicles as obstacles that can shadow wireless propagation. The relevant extensions and modifications will be described in more detail later.

6.2. Traffic Simulation

The traffic simulation is performed by the widely known tool SUMO in conjunction with various traffic scenarios.

6.2.1. SUMO

There are various methods to simulate vehicular traffic, which are divided into the following three categories:

Macroscopic simulations: If only coarse averages over larger scenarios are required as simulation results, a macroscopic simulation might suffice. Often, models for fluid dynamics are used to perform macroscopic simulations, whose most important feature is the execution speed.

Mesoscopic simulations: By combining macroscopic and microscopic approaches, e.g. by simulating clusters or platoons of vehicles at once, mesoscopic models try to find a middle ground between granularity and execution speed.

Microscopic simulations: If the actions and behaviour of single vehicles need to be modelled separately, microscopic models are required. Those models are often used for combined simulations with network functionality because the computation of the communication and wave propagation is usually multiple times more time-consuming.

SUMO[6] [LBB+18] uses a microscopic approach, i.e. simulates each vehicle separately. In recent versions of SUMO, a mesoscopic model has been added. While the execution time is about one hundred times faster, the model does not support TraCI[7]. It supports public transport or even pedestrians. It has an interface to influence the simulation in real time and obtain information about it via a TCP socket. This interface is called TraCI and enables to bi-directionally couple SUMO with network simulations. There are implementations of this interface in python, C++ and other languages. SUMO is used for various applications, e.g. optimisation of traffic light programs, routing algorithms for vehicle navigation or forecasts of traffic volume during large events. SUMO also provides a graphical user interface (GUI) and other tools for the creation, import (e.g. from OpenStreetMap) and modification of traffic scenarios and routes.

[6] https://sumo.dlr.de
[7] https://sumo.dlr.de/wiki/Simulation/Meso

While SUMO can calculate the routes itself, traffic demands need to be specified beforehand. This is part of the *traffic scenario*. A demand is specified by a start and destination position and mode of transportation, e.g. vehicles or buses. Demands can also be specified as specific routes, i.e. by including waypoints [LBB+18]. SUMO uses an extended version of the Stefan-Krauß car following model [KWG97, Kra98].

6.2.2. Traffic Scenarios

As it is detrimental that a MAC protocol or DCC works flawlessly in many different scenarios, it is important to use different traffic scenarios for the evaluation. The protocol additions and modifications in this dissertation are evaluated in various traffic scenarios, either based on real-world locations or synthetically created, which will also be presented in this section.

In some of the scenarios, a smaller area of the complete scenario is used for the network simulations as the number of vehicles in the complete scenario is too large for detailed network simulations. Due to the geographic restriction, there are no vehicles and thus transmissions outside of the restricted area. This is unrealistic, because in reality, terminals that are further away would cause additional interference for the vehicles at the borders of the restricted area. Hence, in addition to the geographic restriction, an additional, smaller region of interest is used in these cases. This means that statistics are only taken of vehicles that are at least $300\,\mathrm{m}$ away from the borders of the geographic restriction. This ensures that every vehicle that contributes to the recorded statistics is also subject to realistic interference patterns.

The traffic scenarios that are used for this dissertation are described in the following.

6.2.2.1. Luxembourg

The Luxembourg scenario [CFFE17] is a realistic traffic scenario for SUMO, based on the real road network of the city of Luxembourg. It includes over $900\,\mathrm{km}$ of road and uses an area of $155\,\mathrm{km}^2$. The traffic demands are based on extensive real data about the demographics, which are available online due to large investments in traffic research by Luxembourg. The scenario models a complete day, from 0:00 to 24:00. It has a very high quality, as a lot of manual checks have been performed in order to ensure that there are no unrealistic bottlenecks at intersections.

In the simulations performed in this dissertation, only a subset of the geographic region of about $5.4\,\mathrm{km}^2$ is used, depicted in Figure 6.1. The exact coordinates for the geographic restriction are $(5500, 5200) - (7850, 7500)$ in the format of OMNeT++ or $(5500, 3955) - (7850, 6255)$ in SUMO's representation. The difference is due to the different points of origin of the coordinate systems. In the area close to the borer of the scenario $(300\,\mathrm{m})$, the vehicles will be simulated, but no statistics are recorded. This is to ensure that there are no border effects due to missing interference from areas outside the restricted range. The restricted region still contains over one thousand vehicles at rush hour. It eliminates some special features of the Luxembourg traffic patterns and makes the evaluation more universal and comparable to other large cities. Two different times are used for the evaluation: 8:00, which is the rush hour, and 11:30, which sees significantly less traffic activity.

For the simulation of scenarios with obstacle shadowing, a smaller area had to be chosen. The simulated area can be seen in Figure 6.2. The coordinates are $(6400, 3755) - (7400, 5155)$ or $(6400, 6300) - (7400, 7700)$, respectively.

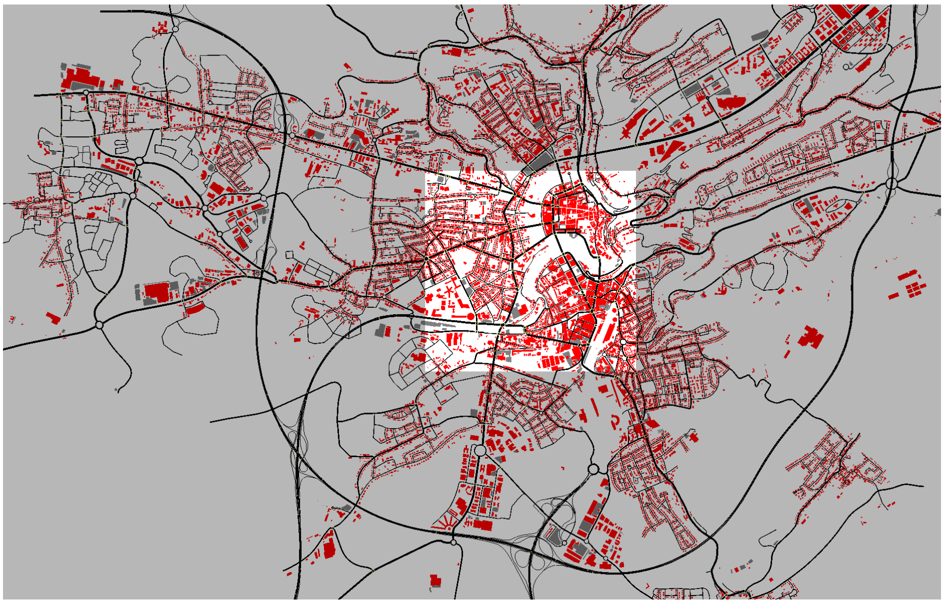

Figure 6.1.: Simulated area of the Luxembourg scenario.

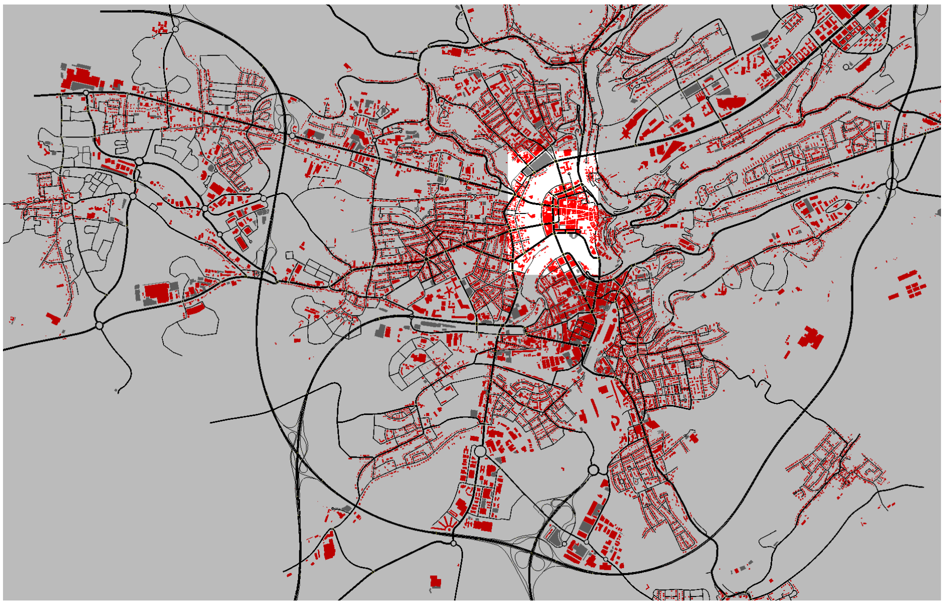

Figure 6.2.: Simulated area of the Luxembourg scenario with obstacle shadowing.

6.2.2.2. Autobahn

The Autobahn scenario is one of the two synthetic scenarios specifically created for this dissertation. It encompasses a straight road segment with three lines per direction, i.e. six lanes in total. Vehicles travel with a maximum speed of $130\,\mathrm{km\,h^{-1}}$ if the traffic situations allows it. The scenario models trucks, standard passenger cars and sporty vehicles. The whole traffic scenario is over $10\,\mathrm{km}$ long. For the network simulation, only $2.5\,\mathrm{km}$ are used. The region of interest for the recording of statistics is the inner segment with a $300\,\mathrm{m}$ margin to the borders.

This scenario is interesting because of the high relative speeds of the vehicles that travel in different directions. This might stress the semi-persistent scheduling and other mechanisms, as the channel condition might quickly change simply due to the quick relative movement of the vehicles.

Additionally, the scenario allows for the simulation of traffic jams. A scenario in which one direction is completely blocked has been chosen for this purpose. The line of stationary vehicles expands about $1.3\,\mathrm{km}$. This scenario results in extreme traffic densities while there are still very quick vehicles traveling in the other direction and it is thus certainly a stress-test for any MAC and DCC protocol.

6.2.2.3. Manhattan Grid

A synthetic Manhattan-style grid scenario is often used as traffic scenario. This is because it is homogeneous and easy to reproduce and set up. Therefore, results from such scenarios are more likely to be comparable to other results that use different implementations of simulators.

The Manhattan grid scenario, which was created for this dissertation, uses ten by ten streets, i.e. is quadratic. The distance between the intersections is $100\,\mathrm{m}$. Hence, the scenario is $900\,\mathrm{m}$ by $900\,\mathrm{m}$ large. It contains 500 vehicles in its default configuration. Using SUMO's *scale* parameter, the traffic load can easily be adjusted. A higher *scale* means that more vehicles are spawned. In the following discussion, this parameter is referred to as *traffic scale*. Table 6.1 shows the median CBR values for different configurations of the SUMO scale parameter. The default configuration, i.e. $100\,\%$ traffic scale, results in a median CBR of $49.7\,\%$ when transmitting CAMs with a packet rate of $10\,\mathrm{Hz}$ and two subchannels per CAM. At $125\,\%$ traffic scale, it increases to $58.2\,\%$. Further increasing the traffic scale to $150\,\%$ leads to a further increase of the median CBR to $65.1\,\%$. When interpreting these CBR values, the following needs to be considered. Firstly, the energy threshold for the classification of resources as occupied is relatively high compared to the noise that is to be expected at this bandwidth.

Table 6.1.: Median CBR for the Manhattan Grid Traffic Scenario at Different Traffic Load Settings

SUMO Traffic Scale	Median CBR [%]
$50\,\%$	28.1
$75\,\%$	39.4
$100\,\%$	49.7
$125\,\%$	58.2
$150\,\%$	65.1

ETSI specifies the CBR threshold to be $-94\,\mathrm{dBm}$ per radio resources of $2\,\mathrm{MHz}$. The theoretical thermal noise at this bandwidth would be $-174\,\mathrm{dBm\,Hz^{-1}} \times 2\,\mathrm{MHz} = -101\,\mathrm{dBm}$. Secondly, it is not always possible to completely fill all subchannels of a subframe without causing collisions. This is even more the case when all transmissions occupy two subchannels and there are five subchannels in total. Thirdly, random-access-based MAC protocols fail to work optimally significantly before a total utilisation of the channel is reached. A traffic scale of $125\,\%$ or $150\,\%$ is hence ideal for the evaluation of DCC components, depending on how severe the channel load should be.

6.3. Application and Facilities Layer

The simulator uses the default cooperative awareness basic service implementation of Artery. This service generates realistic CAMs and fills the data structures according to the data available. Various modifications to the implementation have been made. For example, an interface that allows the service to specify the usual communication patterns to lower layers has been implemented. This allows the service to tell the MAC layer the typical size and rate of the packets, which in turn allows the MAC layer to reserve radio resources for the future. The interface also considers the PPPP and maximum MCS index. The service can work in dynamic and static mode, meaning the CAMs are generated either according to the triggering rules or at a fixed interval. Different sizes for CAMs can now also be specified, which allows an investigation of the performance of LTE-V2X and other implementations when variable CAM sizes are used.

6.4. Data Link Layer

At the data link layer, the most important part is the implementation of the MAC protocol of LTE-V2X Mode 4. The selection of the candidate resource set is part of the physical layer. The MAC implementation is mostly responsible for the resource reuse according to the reselection counter and $\mathrm{probResourceKeep}$. For this, it has to keep track of reserved resources and packet flow characteristics of higher-level services. The implementation supports the $\mathrm{sl{-}reselectAfter}$ mechanism. The MAC module also has to create the sidelink control information for transmitted packets and evaluate it from received packets.

The data link layer also hosts the DCC component. Different DCC implementations follow a common interface and can be swapped out easily. For example, there is a standard-compliant implementation and one that implements the version of SAFE. The current CBR is periodically updated. Depending on the priority, CBR and CR, it decides whether it is allowed to transmit a packet under the current circumstances. The calculation of the CR can also include predictions for the future according to the standard (see Section 2.4.2.4). However, the implementation of the simulator only uses the history of the most recent transmissions for consistency.

6.5. Physical Layer

Various enhancements at the physical layer had to be made in order to support SC-FDMA and LTE-V2X. These include the support for subchannels and the physical-layer procedures of the terminals according to the LTE standard.

6.5.1. Implementation

For the LTE implementation, an early prototype based on the SimuLTE[8] package had been created. However, this prototype could not satisfy all requirements of the simulation framework. Hence, a more detailed implementation building upon INET has been developed.

As SC-FDMA introduces subchannels, the modelling of transmissions needs to be modified to support this. INET supports both scalar and multi-dimensional transmissions. Both versions have been implemented as choice to support SC-FDMA. The multi-dimensional implementation is simpler and uses existing features of INET more extensively. However, the performance is insufficient for the amount of simulation runs that are necessary for the parameter optimisation and evaluation. Hence, the scalar architecture has also been enhanced to support subchannels. At various locations, adjustments had to be made to ensure that the reception energy is calculated correctly. These includes the radio medium, background noises, representations of transmissions and interference, calculation of reception energies, transmission formats, transceiver implementations, etc.

The implementation of the physical layer procedures of the LTE terminals had to be made from scratch as there are no existing LTE implementations in INET. Each terminal stores the history of the last one thousand subframes. This is necessary in order to calculate the average RSSI over the last ten repetitions, which are $100\,\mathrm{ms}$ apart each. In case of SAFE, more history needs to be recorded. It is stored in a dictionary with the subframe number as key. The dictionary uses the standard implementation, i.e. a red-black tree. The recorded activity includes the following history per resource:

- The RSSI and RSRP of the resource
- Whether it has been correctly received
- Whether it was used for transmission by this terminal
- In case of SAFE, the number of received acknowledgements and non-acknowledgements for this resource
- A set of resources (subframe and subchannel) that made reservations for this resource. The channel history also extends into the future in order to be able to consider explicit reservations.

If packets with different priorities are to be sent during the simulation, the channel history also needs to store the priority of received packets in order to calculate $\mathrm{Th}_{a,b}$.

The standard-compliant implementation of the candidate resource selector uses this history to calculate the half-duplex restrictions, average RSSI and $\mathrm{Th}_{a,b}$ threshold for each candidate resource in the resource selection window. The candidate resource selector is a encapsulated component and can easily be swapped with other implementations, e.g. the one of SAFE. Before reporting the candidate resource set to higher layers, the candidate resource selector shuffles it using the Fisher-Yates algorithm in order to prevent synchronisation effects and unwanted correlations. Whenever a random number is used in the simulation code, it is ensured that a new random number generator is used. In total, 16 independent random number generator instances are used in a single simulation run.

[8]https://simulte.com

6.5.2. Wireless Channel Modeling

There are different concepts that can or need to be applied when modelling wireless channels. Fading, subdivided into large-scale and small-scale fading, describes the influence of the wireless channel on the signal power at the receiver. Large-scale fading describes the loss of signal power just by the effect of the distance travelled by the signal or a blockage, e.g. by buildings [Zaj12]. In urban V2V scenarios, obstacle shadowing is a very common cause of reception errors. Small-scale fading is related to shorter fluctuations of the signal power caused by interference through multipath propagation. For example, a reflection at a building causes a multipart component to arrive at the receiver slightly delayed, and most likely with less energy. Small scale fading can be *fast*, i.e. happen from one symbol to the next one, or slow, for longer durations [Zaj12]. The interference can be destructive or constructive, depending on the difference of the phase.

6.5.2.1. Channel Models in INET

INET divides the wireless channel model into a path loss component and an optional obstacle loss component. The path loss components are not subdivided into fast and slow fading. However, INET also includes fast fading path loss models. If a fast-fading model is selected, a free-space path loss model for slow fading is automatically used, i.e. the architecture of the INET framework does not allow the combination of a fast fading model with a slow fading model other than free-space path loss. INET provides the following slow fading path loss models:

Free-space path loss: A simple model for slow fading is the free-space path loss model, which just computes the signal attenuation depending on the travelled distance. Hence, it assumes that there is no ground reflection and no shadowing by obstacles. The signal propagates as a *straight line* between the transmitter and receiver. The free space path loss is expressed as

$$\frac{P_r}{P_t} = \left(\frac{\lambda}{4 \times \pi \times d}\right)^2$$

where P_r is the reception power, P_t is the transmit power, λ is the wavelength of the signal and d is the distance between the transmitter and receiver [Gol05]. Often, the distance is weighted, depending on the propagation characteristics of the simulated scenario. For example, the distance will be weighted more if a free-space path loss model is used to model wireless channels in urban areas. In this case, a new variable is used to increase the influence of the distance from its default inverse square root influence. The path loss is then calculated as

$$\frac{P_r}{P_t} = \left(\frac{\lambda}{4 \times \pi \times d^\alpha}\right)^2$$

where α is the weighting factor of the distance. The free-space path loss model of INET allows for such an adjustment.

Breakpoint or dual-slope path loss: A breakpoint or dual-slope path loss model is very similar to the free-space path loss model. The only difference is that a dual-slope model has two different path loss factors, depending on the distance that the signal travelled. This distance is called the breakpoint distance. The idea of such a path loss model is based on measurement observations. In many experiments, the path loss initially follows a free-space path loss with a flatter path loss curve, i.e. slope, and continues to follow a free-space model with a more steep slope, i.e. higher path loss.

Log-normal shadowing: A log-distance path loss model is used to model signal propagation inside buildings or in densely populated areas with communication ranges over larger distances [Sin10]. The path loss of this model is usually expressed in the logarithmic domain as

$$\mathrm{L_{dB}}(d) = \mathrm{PL}_0 + 10 \times \gamma \times \log\left(\frac{d}{d_0}\right) + X_g$$

where PL_0 is the path loss at the reference distance in decibels, γ is the path loss propagation constant, d is the distance between the transmitter and receiver and d_0 is the reference distance. X_g denotes attenuation caused by flat fading. It depends on the scenario and is zero in case of no fading, usually a Gaussian distribution with standard deviation in decibels in case of only slow fading. It can also have a Rayleigh or Rician distribution in case of only fast fading [Sin10].

Two-ray ground reflection model: This model can be used if a single ground reflection dominates the multipath effect. In this model, the received signal consists of the direct, line-of-sight part, and the reflection off the ground. The two-ray ground model is a very basic variant of raytracing [Gol05]. Considering the phase difference of the two signal paths leads to complex computations, which are not beneficial for large-scale network simulations. Therefore, Rappaport, among others, presented simplifications of the two-ray ground reflection model [Rap96], which are commonly used. For the far field and under the assumption of perfect polarisation and reflection at the ground, the path loss can then be calculated as

$$\frac{P_r}{P_t} = \left(\frac{h_r \times h_t}{d^2}\right)^2$$

where h_r is the height of the receiving antenna and h_t of the transmitting antenna, respectively. To comply with the far-field assumptions, network simulators usually use a crossover distance at which they switch from a free-space path loss model to a two-ray ground reflection model. However, Giordano et al. showed that the two-ray ground reflection should not be used for V2V models if large-scale obstacle shadowing effects, e.g. through buildings, are present [GFG$^+$09].

Two-ray interference model: Investigations of Sommer et al. showed that the use of a two-ray ground reflection model does not lead to more precise channel modelling for V2V communication. One of the reasons is that the crossover distance can hardly be reached with V2V communication [SJD12, SD11]. They showed that a two-ray interference model without simplifications is significantly more exact than the simplified two-ray ground reflection models.

INET contains additional path loss models such as the Stanford University Interim model for worldwide interoperability for microwave access (WiMAX) or a model for ultra-wideband infra-red communication. These models are however not relevant for this dissertation.

Besides the slow-fading models, INET also contains the following fast-fading models with free space path loss as slow fading:

Rayleigh fading: Rayleigh fading is typically used in heavy multipath scenarios without the presence of a line-of-sight connection.

Rician fading: The main difference between Rayleigh and Rician fading is that Rician fading is suited for multipath situations with a single strong signal, while Rayleigh fading prohibits the presence of a strong signal.

Nakagami fading: Some empirical measurement data does not fit well into a Rayleigh or Rician distribution. Nakagami fading is a more general model that can be configured to match a more variety of empirical data [Gol05].

The following obstacle-shadowing models are included in INET:

Idealized obstacle shadowing: This simple shadowing model completely blocks the signal if an obstacle is blocking the optical line-of-sight connection between a transmitter and receiver. This is a very significant simplification and is most likely not valid for many communication systems.

Dielectric obstacle shadowing: INET also includes a second, more elaborate model for obstacle shadowing, which models the dielectric properties of the materials. It computes the energy lost by reflection and the dielectric loss, e.g. by heat, and subtracts this lost energy from the signal power. However, the parameterisation is likely scenario-specific and requires elaborate measurement campaigns.

6.5.2.2. Custom Channel Models

The pre-existing channel models of INET are hardly usable to model the wireless channel for V2V communication. While some of the slow fading models might be applicable, the obstacle loss models in particular are not appropriate. They completely neglect the effects of multipath propagation, which plays a very important role for V2X communication, especially in urban scenarios. In V2V communication, the optical line-of-sight connection is often obstructed by buildings or other vehicles, but communication is often still possible due to strong multipath components, i.e. signals reflected off other buildings, vehicles or even large traffic signs.

For the simulative evaluation in this dissertation, new channel models based on existing work have been implemented. Existing INET-based models could not have been used due to lack of flexibility or features. In order to have the best option depending on the traffic and geographic scenario, three different channel models have been chosen. These channel models will be described in the following, ordered by the complexity and computational cost.

The first path loss model is based on work by Cheng et al. [CHS+07]. The model is a log-distance, dual-slope path loss model designed for V2V communication at $5.9\,\mathrm{GHz}$. Cheng et al. present two different data sets from different vehicle routes. As this path loss model combines a log-distance model with two different slopes, the path loss can be calculated by [ASKT15, CHS+07]

$$\mathrm{L_{dB}}\left(d; \mathrm{PL}_0, d_0, d_b, n_1, n_2, \sigma_1, \sigma_2\right) = \left\{ \begin{array}{ll} \mathrm{PL}_0 + 10 \times n_1 \times \log_{10}\left(\frac{d}{d_0}\right) + X_{\sigma_1}, & \text{if } d_0 \leq d \leq d_b \\ \mathrm{PL}_0 + 10 \times n_1 \times \log_{10}\left(\frac{d_b}{d_0}\right) + 10 \times n_2 \times \log_{10}\left(\frac{d}{d_b}\right) + X_{\sigma_2}, & \text{if } d > d_b \end{array} \right\} \tag{6.1}$$

where PL_0 is the reference path loss in decibel at the validity distance d_0, d is the distance between the transmitter and receiver, d_b is the breakpoint distance, n_1 and n_2 is the first and second path loss exponent, and X_σ is a random variable from a Gaussian distribution with a mean of zero and standard deviation σ. This model uses a breakpoint distance $d_b = 100\,\mathrm{m}$. The reference distance is not specified. A value of $d_0 = 10\,\mathrm{m}$ was used. The reference power level was derived from the reception power plots [CHS+07]. The parameters for the two different datasets from [CHS+07] are documented in Table 6.2.

The first dataset can be characterized as a longer driving route that includes some country roads without buildings in the vicinity. The second dataset was recorded using a route

Table 6.2.: Parameters for the Channel Model from [CHS+07]

Dataset	n_1	n_2	σ_1	σ_2
1 (suburban)	-2.1	-3.8	2.6	4.4
2 (urban)	-2	-4	5.6	8.4

that only included built-up areas. This dataset of this model is used in simulations using the Luxembourg and Manhattan grid scenario. This channel model includes the effects of shadowing by buildings and other vehicles statistically, but not deterministically. This is both an advantage and a disadvantage. It is beneficial for the application-oriented evaluation methodology with awareness metrics because it ensures that the awareness results correlate with the performance of the protocols, but not with shadowing situations caused by other vehicles or buildings. When using this channel model, it is ensured that changes in the simulation results are caused by the performance of the evaluated protocols, and not the traffic situation on the road. On the other hand, in practice, shadowing effects occur deterministically and correlated in geographical areas. This could have secondary effects on the behaviour of protocols, such as MAC or DCC protocols. It is important to also investigate such effects. For this reason, more deterministic channels models are additionally used for the evaluation.

As a second channel model, a custom implementation of an empirical log-distance, dual-slope path loss model based on a measurement campaign by Abbas et al. was used [ASKT15]. The measurements have been carried out in urban and highway scenarios. The data is further subdivided into the following categories: line-of-sight, line-of-sight obstructed by vehicles and line-of-sight blocked by buildings. For the *line-of-sight* and *obstruction by vehicles* cases, the path loss is described as log-distance, dual-slope path loss model [ASKT15]. The same formula as in the first channel model described above (Equation 6.1) is used to calculate the path loss. The path loss model of Abbas et al. uses a reference distance d_0 of $10\,\mathrm{m}$ and a breakpoint distance d_b of $104\,\mathrm{m}$. For the sake of completeness and documentation, the parameters of the channel models are copied from [ASKT15] and shown in Table 6.3.

The channel model does not model line-of-sight obstructed by vehicles on the highway for distances below $80\,\mathrm{m}$. In this case, the line-of-sight model was used. For the situations in which the line-of-sight is blocked completely by buildings, the authors derive a model from

Table 6.3.: Parameters for the Channel Model from [ASKT15]

Line-of-Sight Obstruction	Scenario	n_1	n_2	PL_0	σ
None	Highway	-1.66	-2.88	-66.1	3.95
None	Urban	-1.81	-2.85	-63.9	4.15
Vehicles	Highway	—	-3.18	-76.1	6.12
Vehicles	Urban	-1.93	-2.74	-72.3	6.67

other models. It is given as

$$\mathrm{L_{dB}}\left(d_r, d_t, d_b, w_r, x_t, i_s, \lambda; n_{\mathrm{NLOS}}\right) = 3.75 + 2.94 \times i_s + \left\{ \begin{array}{ll} 10 \times \log_{10}\left(\left(\frac{d_t^{0.957}}{(x_t \times w_r)^{0.81}} \times \frac{4 \times \pi \times d_r}{\lambda}\right)^{n_{\mathrm{NLOS}}}\right), & \text{if } d_r \leq d_b, \\ 10 \times \log_{10}\left(\left(\frac{d_t^{0.957}}{(x_t \times w_r)^{0.81}} \times \frac{4 \times \pi \times d_r^2}{\lambda \times d_b}\right)^{n_{\mathrm{NLOS}}}\right), & \text{if } d_r > d_b. \end{array} \right\} \tag{6.2}$$

where d_r is the distance between the receiver and the intersection centre, d_t is the distance between the transmitter and the intersection centre, d_b is the breakpoint distance, w_r is the width of the street in which the receiver is, x_t is the distance of the transmitter to the wall, $n_{\mathrm{NLOS}} = 2.69$ is the path loss exponent, λ is the wavelength, and i_s takes the value one for suburban environments and zero for urban environments. The calculation of the non-line-of-sight path loss is hardly compatible with the interface for path loss or obstacle loss models of INET. Additionally, the model requires knowledge about the street widths and distances to the intersection centre, which is difficult to determine for heterogeneous traffic scenarios such as the Luxembourg scenario of SUMO. Therefore, the non-line-of-sight part of the model seems to be more applicable to Manhattan-grid type traffic scenarios. Abbas et al. present probabilities with which the presence of a line-of-sight condition shall be derived statistically. This approach is not used for this dissertation. Instead, the actual positions of the vehicles and buildings in the simulation are used to deterministically identify the presence of line-of-sight, or obstruction by vehicles or buildings. For multiple obstructions by vehicles, the situation is classified as line-of-sight obstructed by vehicles. If a single building blocks the line-of-sight, the situation is classified as non-line-of-sight and use Equation 6.2 to calculate the channel attenuation. Multiple buildings on the theoretical line-of-sight cause the signal to be lost completely. This channel model is used for the Autobahn scenario.

Michael Schubert developed a (shooting and bouncing rays) raytracing-based channel model that is accelerated by graphics processing units (GPUs) [Sch18] in a master's thesis. This prototype has been specifically developed for the simulation framework used in this dissertation. The parameterisation of the prototype could not be performed due to the effort required for multiple measurement campaigns. Still, the required angular resolution for longer transmission distances requires a huge computational effort, which was prohibitive. Therefore, a different approach to model obstacle shadowing needed to be taken. The third and last channel model used in this dissertation has been developed and published by Sommer et al [SJS+15]. It considers the distance that the theoretical line-of-sight would have travelled through buildings and the number of penetrated buildings. This distance and number of buildings are used to statistically derive a channel model that correlates with the number and size of obstructing buildings. The path loss is calculated as $L_{\mathrm{static}}\left(n, d_m; \beta, \gamma\right) = \beta \times n + \gamma \times d_m$, where n is the number of penetrated buildings, d_m is the distance travelled through buildings, and $\beta = 9.6\,\mathrm{dB}$ and $\gamma = 0.45\,{}^{dB}/_{\mathrm{m}}$ are empirically determined constants [SJS+15]. For the shadowing effects of vehicles in this channel model, a knife edge model is used. If only a single obstacle crosses the line-of-sight, a single-knife edge model is deployed. At first, a geometrical parameter, which describes how far the obstacle gets into the Fresnel zone, is calculated as [SJS+15]

$$\mathrm{v}\left(h, d_1, d_2; \lambda\right) = h \times \sqrt{\frac{2}{\lambda} \times \left(\frac{1}{d_1} + \frac{1}{d_2}\right)} \tag{6.3}$$

where h is the height of the obstacle, d_1 is the distance between the transmitter and obstacle, d_2 is the distance between the obstacle and receiver, and λ is the wavelength. If v is greater than -0.7, the obstacle shadowing is calculated as [SJS+15]

$$L_{\mathrm{dB}}\left(v\right) = 6.9 + 20 \times \log_{10}\left(\sqrt{\left(v - 0.1\right)^2} + v - 0.1\right) \tag{6.4}$$

where v is obtained with Formula 6.3. For multiple obstacles, a multi-knife edge model considers different heights of obstacles and computes a bounding box on top of the obstacles that are between the transmitter and receiver. This can be visualized as *laying a rope* from the transmitter to the receiver. Large obstacles will be in contact with the rope or bounding box while smaller obstacles will be *hidden* in the shadow area of larger neighbours, which do not necessarily have to be direct neighbours. Those large obstacles are classified as *major obstacles*, others as *minor obstacles*. While the attenuation is summed up for every major obstacle, only the largest minor obstacle between two major obstacles is counted. The final attenuation then consists of the sum of attenuation by major and minor obstacles and a correction term. For details about the correction term, the reader is kindly referred to [SJS+15]. This channel model is used for investigations of obstacle shadowing in the Luxembourg scenario.

6.5.3. Antenna Model

The type and position of the antenna determines the direction-dependent antenna gain, which can have an influence on the performance. Therefore, a realistic antenna model should be considered in simulative evaluations. In order to reduce the number of simulations and to be able to focus on evaluating different approaches and parameter sets, only one antenna model was used. This model assumes a single dipole antenna with half the length of the wavelength, i.e. a *half-wave dipole antenna*, mounted to the roof the vehicles.

6.5.4. Reception Model

The reception model describes whether a reception of a packet was successful or not. The granularity and complexity of this model can be very simplistic, i.e. a simple SINR threshold and a binary decision. The most complex models simulate the complete digital signal processing chain, which also requires sophisticated channel models that model the variation of the signal power over time, with a granularity of a single transmitted symbol or higher. This is not applicable to system-level type simulations, in which many transmitters are simulated simultaneously.

For the evaluation in this thesis, a BLER table originating from a 3GPP work contribution of Huawei and HiSilicon [HH16] was used. A BLER table maps probabilities of successful reception to different input parameters, commonly the SINR. The tables are dependent on the SINR, coding and modulation scheme, vehicle speeds and packet size.

6.6. Statistic Collection and Metrics

In this section, the statistic collection methods and metrics used and developed in this dissertation are explained.

6.6.1. Aggregation of Results

For each result in this dissertation, multiple experiments (*runs*) are usually performed. A result can be one value per experiment that is already aggregated, which depends upon the exact definition of a metric. Alternatively, each vehicle in each experiment might produce a result. In this case, these values are first aggregated over all vehicles for each run, giving one value per run. Whether the median or mean is used depends upon the statistical distribution of the results. If they follow a normal distribution, the mean is used and the confidence interval over all runs can be easily calculated using the normal or Student's t-distribution. Unless otherwise specified, the confidence level is $95\,\%$ in this dissertation.

If the results do not approximately follow a normal distribution, they can be plotted using quantile function plots. However, if a single indicator value is necessary for easy comparison, the median is used. This dampens the impact of outliers. This means that the median across all runs is used, and no assumptions are made about the statistical distribution of the medians. This complicates the calculation of confidence intervals. In this case, the method outlined in [HM11] is used:

$$P(X_l \leq m \leq X_h) \geq 0.5^n \times \sum_{i=l}^{h} \binom{n}{i}$$

X_l and X_h are the results of two experiments and form the lower and upper boundary of the confidence interval. They need to be chosen manually (along with l and h) in this case, so that the resulting confidence level is high enough. This means that the confidence interval can be asymmetric. Additionally, the resulting confidence level might not be a round value as it is not pre-determined. The confidence level is explicitly stated in this case.

The metrics that were added to the simulation framework and used for the evaluation of concepts in this thesis are described in the following.

6.6.2. Packet delivery ratio

The packet delivery ratio determines the ratio of packets that have been successfully received by the terminals. The PDR is a very common metric used to compare the performance of different MAC protocols. Despite the simple and intuitive definition, there are various details that need to be defined and considered so that the PDR is comparable and meaningful.

Firstly, terminals that are physically unable to receive a message, e.g. due to the large distance to the transmitter, should be excluded from the statistics. Otherwise, the PDR would not be comparable between different scenarios because it would mainly correlate with the size of the scenario. The main measured effect would be the distribution of the geographical positions of the nodes. Larger scenarios would result in a significantly lower PDR because many terminals would be out of the transmission range of the transmitters. If the wireless channel models include a random component, which is often the case in order to model fast fading effects, there is no exact distance at which a receiver would be unable to receive messages. In the simulation performed for this thesis, the PDR will always be for a specified range, e.g. from $0\,\mathrm{m}$ to $300\,\mathrm{m}$. Arbitrary distances for the PDR statistics could be chosen, e.g. to determine the PDR at the safety-critical lower distances, or to investigate the performance with larger communication distances.

Secondly, it must be considered how exactly the ratio is built. The global goal of a MAC protocol should be to ensure that as many packets as possible can be successfully received. The throughput is not meaningful as evaluation metric for vehicular communication because it is highly dependent on the traffic scenario and not a relevant goal for the traffic safety application. It will be higher in a dense traffic scenario because there will be more receivers per transmission for broadcast packets and more transmitters in general. When using the PDR to prevent this, the delivery ratio of each transmitted packet could be determined and the mean of those could be calculated. This method would however calculate the mean of ratios with different bases, which is a common mistake in performance analysis [Jai91, Section 12.4]. Therefore, the number of successful receptions and potential receivers should be counted in global variables per simulation run, and the ratio should be calculated at the end of the run. This ensures that the PDR is representative of the real performance of the MAC protocol.

6.6.3. Cooperative awareness

Application-oriented metrics are rarely used for the evaluation of communication systems. This is unfortunate, because they can help to uncover design issues, which could even lead to injury or deaths in the case of safety-critical systems such as V2V communication. The results regarding repeating collisions of LTE-V2X Mode 4 from Chapter 4 and the current state of the art described in Chapter 3 clearly indicate that there is a need for more application-oriented metrics when evaluating V2V protocols.

Such a metric is developed and applied for CAMs in this dissertation. Awareness metrics have already been used in proposals for IEEE 802.11p, e.g. in [SLL+10]. The awareness metric and visualisation in this dissertation are a further enhancement compared to earlier research. The application-oriented metric means that instead of simply calculating a PDR or packet error ratio (PER), the actual knowledge of vehicles about their surroundings is quantified. This is performed every $100\,\mathrm{ms}$ for each vehicle in the simulation and for different, configurable ranges. For a vehicle to be *aware* of another, it must have received a valid CAM from it. *Valid* CAM implies that the lifetime of the CAM is not exceeded. The default lifetime is $1000\,\mathrm{ms}$, but it can be configured specifically for the calculation of the awareness metric, i.e. independently of other applications. The exact definition of the awareness ratio of a vehicle for a given range is as follows: let A be the set of vehicles that it received valid CAM from. Let B be the set of vehicles in the surroundings of the vehicle for the given range. Then, the awareness ratio of this vehicle is:

$$\alpha = \frac{|A \cap B|}{|B|}$$

A variation of the awareness metric is the *percentage of time with ideal awareness*. As there are very strict requirements regarding the cooperative awareness of vehicles, an awareness requirement of $100\,\%$ can be defined. Other minimum awareness requirements are possible, e.g. the *percentage of time with at least* $95\,\%$ *awareness*. The distribution of these values across the vehicles for a single simulation run are expected to be heavy-tailed. Hence, the *mean percentage of time with ideal awareness* might not be completely significant. At least, the median or different percentiles should be used in order to get an idea of the underlying distribution. A better approach would be to use quantile function plots or similar visualisation methods. This visualisation shows how many vehicles have been able to meet the awareness requirement during which amount or percentage of time. The awareness requirement in conjunction with the visualisation using quantile function plots are therefore an additional methodical contribution of this dissertation.

6.7. Default Simulation Parameters

Subsequent chapters use the simulation framework described in this chapter. The default configuration parameters are summarised in Table 6.4. Those will be used in subsequent system-level simulations unless noted otherwise. The parameters regarding the message size and rate are set according to design motivations of LTE-V2X Mode 4. A fixed message rate is used. The $\mathrm{probResourceKeep}$ parameter is set to zero according to observations in the state of the art in Chapter 3 and the problem analysis in Chapter 4. The reselection counter range follows the LTE standard and is between 5 and 15. The simulation setup uses a standard setup of a 10 MHz wide channel at the 5.9 GHz ITS band. As five subchannels are used, the subchannel bandwidth is one fifth of the total channel bandwidth, i.e. 2 MHz.

The transmission power is 23 dBm at the antenna connector. The simulation assumes a half-wave dipole antenna mounted at the roof of the vehicles. If necessary, the power is reduced in order to comply with the maximum spectral density of the channel. Please also see the description of the MPR and A-MPR mechanisms in Section 2.4.2.2. As background power, the default $-174\,\mathrm{dBm\,MHz^{-1}}$ over 10 MHz have been used, which results in -104 dBm over the channel bandwidth of 10 MHz. A special background model has been implemented in the simulator that ensures that the background noise scales with the number of used subchannels. The default energy threshold to detect resources as occupied for DCC has been used. The simulation assumes a low transceiver sensitivity of -101 dBm. However, this is only because the performance of the simulator allows for fine-grained calculations that take the background noise, interference, and the error model into account. A further simplification for receptions with a low reception power to increase the simulator performance is not necessary.

For each experiment, 32 runs are carried out. The seed value is equal to the run number, which is the default behaviour of OMNeT++. A warmup period of 10 s is used to exclude the transient phase in which the simulation has not yet reached a steady state. It has been verified that this warmup period is sufficiently long.

Summary

In order to evaluate VANET networks, simulations are often used. The microscopic traffic simulator SUMO is commonly used in combination with a network simulator. A combination with SUMO, OMNeT++, the INET project, Artery, Veins, Vanetza, and a custom implementation of LTE-V2X Mode 4 will be used for simulation-based evaluations in this thesis.

Various traffic scenarios, based on real-world traffic, or artificial scenarios, can be used. These include a central part of the Luxembourg scenario, an Autobahn scenario, and a standard Manhattan grid scenario.

Beside traditional evaluation metrics such as the PDR, application-oriented awareness metrics will be used. The awareness metric shows precisely how many vehicles were able to reach the awareness requirement during which amount of time.

In many scenarios, a dual-slope wireless channel model specifically tailored for V2V scenarios and 5.9 GHz will be used. However, a density-based obstacle loss model has also been implemented so that simulations with obstacle shadowing can also be used. The reception model is taken from a 3GPP contribution from Huawei and should model the receiver behaviour with adequate accuracy.

The simulator models each vehicle, i.e. terminal, separately. This includes the movement and LTE terminal. Each terminals has to keep a history of the activity on the wireless channel separately like in deployments in practice. The implementation of the MAC and physical layer procedures follow the LTE standard. The default simulation parameters are specified in this chapter and will be referenced in subsequent chapters.

Table 6.4.: Common Configuration Parameters in System-Level Simulations

Parameter Name	Comment	Default Value
CAM message size	See Sec. 2.3.2.2 (p. 17)	200 B
CAM rate	See Sec. 2.3.2.2 (p. 17)	10 Hz
$\mathrm{probResourceKeep}$	See Sec. 2.4.2.3 (p. 24)	0
$\mathrm{resel}_{\mathrm{min}}$	See Sec. 2.4.2.3 (p. 24)	5
$\mathrm{resel}_{\mathrm{max}}$	See Sec. 2.4.2.3 (p. 24)	15
$\mathrm{sl-reselectAfter}$	See Sec. 2.4.2.4 (p. 27)	5
Center frequency		5.9 GHz
Channel bandwidth		10 MHz
Subchannels		5
Subchannel bandwidth		2 MHz
Transmission power	at antenna connector	23 dBm
Antenna	at vehicle roof	half-wave dipole
Max spectral density	EIRP	23 dBm MHz^{-1}
Background power	−174 dBm MHz^{-1} over 10 MHz	−104 dBm
DCC: CBR threshold	ETSI TS 103 574 [ETS18c]	−94 dBm
Sensitivity	also limited by error model	−101 dBm
Error Model	See Sec. 6.5.4 (p. 100)	BLER table [HH16]
Seed	run number	1 to 32

Chapter 7.

Optimisation of Configuration Parameters

This chapter deals with finding the best set of configuration parameters for SAFE. Various experiments are carried out for this purpose. These are done by simulation using the setup described in Chapter 6. The experiments have multiple goals. Firstly, the importance and significance of the individual configuration parameters should be assessed. Secondly, as the name of this chapter indicates, optimal values for the configuration parameters should be determined. The success of this influences the performance of the approach in the evaluation in Chapter 8. Thirdly, dependencies between configuration parameters, i.e. interactions of factors, should be determined, if possible. This helps to understand how SAFE works and to draw meaningful conclusions.

An overview of all the factors related to SAFE is given and external influences are explained and listed in Section 7.1. Afterwards, three different experimental designs are used to incrementally parameterise SAFE: The first one is to determine the most important configuration parameters for reservation splitting and the radio resource selection mechanism (Section 7.2). The second one is for the additional use of the reactive hidden-terminal mitigation using the acknowledgement feedback (Section 7.3), and the third one is for the parameters related to DCC (Section 7.4).

7.1. General Overview and Factors

In this section, the factors for various experimental designs will be developed. However, it is important to prevent a combinatory explosion of simulation and configuration parameters. Hence, only a single traffic scenario is chosen. The Manhattan Grid scenario described in Section 6.2.2 will be used as traffic scenario. This is because it contains situations with different vehicle speeds and network loads depending on the local traffic situation. It is also easily reproducible and requires a shorter time to compute than the more extensive scenarios. For the actual performance evaluation in Chapter 8, additional traffic scenarios will be used. Details about the simulator have been described in Chapter 6. This includes a set of default simulation parameters in Section 6.7.

The mean PDR has been chosen as response variable. While it is clear from Chapter 4 that many of the modifications developed for this thesis, especially reservation splitting, aim to benefit the cooperative awareness, choosing the PDR as optimisation goal ensures that the solutions are applicable for many different applications other than CAMs. If reservation splitting does not have a high negative impact on the PDR, a large number of sub-reservations might be chosen regardless in order to ensure a highly reliable communication and to increase the cooperative awareness by mitigating the effects of reoccurring collisions.

Table 7.1 gives an overview of the factors for SAFE that have been explained in Chapter 5. Table 7.2 lists additional factors that are related to standard LTE parameters or the simulation setup.

The parameters in Table 7.2 either already exist in the LTE standard, or are related to the simulation setup. For example, different *workloads* could be simulated by varying the traffic density (with SUMO's *scale* parameter), the message sizes, or the packet rate. Additionally, a variable CAM rate could be used. The total number of factors is 23. It is clear that the number of primary factors or factor combinations needs to be significantly reduced. Even with only two levels per factor, a full factorial design without replications would result in 2^{23}, i.e. over eight million different experiments. As 32 runs are performed per configuration in order to be able to estimate the influence of experimental errors, the required number of experiments increases to 2^{28}, i.e. over 268 million.

Hence, a reduction of the primary factors is necessary, which is realised using the following approach. Firstly, the additional factors in Table 7.2 are considered to be secondary. Still, a reasonable choice of the parameters should be made. The characteristics of the CAM packets are chosen to be oriented towards design motivations of LTE-V2X, as motived in Section 2.3.2.2. A fixed CAM rate of $10\,\mathrm{Hz}$ is used and CAM messages have a fixed size of $200\,\mathrm{B}$. The traffic load should also be carefully chosen. As the DCC component is being parameterised in a separate experiment, the channel load will vary depending on the experiment. Pre-existing parameters of the LTE standard in Table 7.2 are considered to be secondary. The $\mathrm{probResourceKeep}$ parameter will be set to zero, according to the results from related work (Chapter 3) and the problem analysis (Chapter 4).

Secondly, some factors in Table 7.1 also need to be classified as secondary factors. They are further subdivided using three different experimental designs. Each experiment only considers a subset of the factors to be primary, depending on the goal of the design. The purpose of the first experimental design is to find parameters for the candidate resource selection process. The second design is for the reaction to acknowledgement feedback. The last and third design is to find optimal parameters for the DCC component. The reasoning for this approach is that the components can mostly operate by themselves and can hence be well optimized step by step. At first, the candidate resource selection process is parameterised (Section 7.2). This component needs to select good radio resources regardless of a later reaction to acknowledgement feedback or the presence of DCC. Afterwards, the reaction to low acknowledgement ratios will be looked at (Section 7.3). The parameters found with the previous design can be used. Lastly, the DCC component is investigated (Section 7.4), using the previous parameters and results to configure the candidate resource selector and acknowledgement reaction.

7.2. Experimental Design for the Candidate Resource Selection Process

The goal of the first experimental design is to find optimal configuration parameters for the candidate resource selection process.

7.2.1. Factor Levels and Level Combinations

In this design, no separate acknowledgement packets will be used. The benefit of these acknowledgement packets will be evaluated in Chapter 8. The traffic load, i.e. the scale

Table 7.1.: Factors Related to SAFE for the Experimental Design

Factor Name	Comment	Explained in Section
$\mathrm{num}_{\mathrm{sub\_res}}$	Number of sub-reservations	5.2 (p. 73)
$\mathrm{ack}_{\mathrm{avg},\alpha}$	Ack ratio exp. average alpha	5.3 (p. 78)
$\mathrm{ack}_{\mathrm{avg},\delta}$	Ack ratio exp. average delta	5.3 (p. 78)
$\mathrm{ack}_{\mathrm{min}}$	Min. allowed acknowledgement ratio	5.3 (p. 78)
$\mathrm{ack}_{\mathrm{hysteresis}}$	Hysteresis time period	5.3 (p. 78)
$\mathrm{ack}_{\mathrm{sep\_pkts}}$	Use separate ack. packets	5.3 (p. 78)
$\mathrm{crs}_{\mathrm{min\_rating}}$	Candidate resource rating threshold	5.4 (p. 81)
$\mathrm{crs}_{\mathrm{min\_rating\_dcc}}$	DCC component in resource selector	5.4 (p. 81)
$\mathrm{crs}_{\mathrm{rssi\_weight}}$	Weight for average RSSI	5.4 (p. 81)
$\mathrm{crs}_{\mathrm{reservation\_penalty}}$	Static penalty for reservations	5.4 (p. 81)
$\mathrm{crs}_{\mathrm{reservation\_weight}}$	Weight for RSRP of reservations	5.4 (p. 81)
$\mathrm{crs}_{\mathrm{ack\_penalty}}$	Static penalty for acknowledgements	5.4 (p. 81)
$\mathrm{crs}_{\mathrm{ack\_weight}}$	Weight for acknowledgement ratio	5.4 (p. 81)
$\mathrm{dcc}_{\mathrm{cbr\_target}}$	Target CBR	5.5 (p. 82)
$\mathrm{dcc}_{\mathrm{cbr\_margin}}$	CBR margin ($\pm$)	5.5 (p. 82)
$\mathrm{dcc}_{\mathrm{disable\_time}}$	Sub-reservation disabling time	5.5 (p. 82)
$\mathrm{dcc}_{\mathrm{min\_subres}}$	Min. number of enabled sub-res.	5.5 (p. 82)

Table 7.2.: Additional Factors for the Experimental Design

Factor Name	Comment	Explained in Section
$\mathrm{probResourceKeep}$	Std. LTE parameter (default $\in [0; 0.8]$)	2.4.2.3 (p. 24)
$\mathrm{resel}_{\mathrm{min}}$	Std. LTE parameter (default 5)	2.4.2.3 (p. 24)
$\mathrm{resel}_{\mathrm{max}}$	Std. LTE parameter (default 15)	2.4.2.3 (p. 24)
Traffic density	SUMO scale parameter	6.2.2 (p. 90)
CAM message size	—	2.3.2.2 (p. 17)
Variable CAM rate	—	2.3.2.2 (p. 17)

parameter of SUMO, needs to be chosen so that the channel load is not high enough to require the use of DCC, but still high enough so that collisions are likely to appear so that a better MAC protocol can make a difference. Considering the results and discussion from Section 6.2.2, the scale parameter is left at its default value of $100\,\%$ for this design. Additionally, DCC will be disabled and the dcc_* parameters are irrelevant or secondary. This includes $\mathrm{crs}_{\mathrm{min\_rating\_dcc}}$, which is set to `false`. Moreover, the reactive hidden-terminal mitigation, i.e. dropping radio resources if the acknowledgement ratio is too low, will be disabled. The motivation for this decision is as follows. Firstly, the candidate resource selector is an independent component that might be used without acknowledgement feedback, or without the reactive hidden-terminal mitigation. Secondly, the channel load might not be very high in most situations in practice. Therefore, it is detrimental that the candidate resource selector performs well in these situations. Thirdly, the approach of finding parameters for each component individually has the advantage that the number of factor level combinations remains manageable and interactions between the primary factors of this component can be accurately determined. This confinement of factors leaves seven primary factors, which are mapped to single letters as shown in Table 7.3. The configuration parameters for the candidate resource selector (A to E) are assigned 0 or 100, respectively. The value of the high number does not make a difference if each value is the same. This is because the total sum is scaled to 1000 by SAFE as described in Section 5.4. The minimum rating for the candidate resource selector $\text{crs}_{\text{min\_rating}}$ can neither be zero nor one thousand. The former would mean that every candidate resource is usable, regardless of the prior calculations. The latter means that no candidate resource is applicable. Therefore, 800 and 400 are used for the configuration of this parameter. The low value for the number of sub-reservations $\text{num}_{\text{sub\_res}}$ is one, which means that reservations are not split. Five sub-reservations have been chosen as maximum value. This means that the time period in which a radio resource is reused is increased five times. This can be mitigated by setting probResourceKeep to zero, which reduces the average resource reuse by the same factor compared to $80\,\%$. Moreover, the reliability gain from five to ten sub-reservations is marginal as the inter-packet gap of the packets in these situations is already quite high. Lastly, the granularity for DCC with five sub-reservations is deemed to be sufficient.

A 2^7 experimental design would still require too many experiments: 128 or 128×32 with replications. A 2^{7-4} design would only require eight experiments. However, not even all single-level interactions of factors could be considered. For this reason, a $2^{7-3} \times 32$ design was chosen, requiring 16 different experiments with 32 replications each. This design is a one-eighth replicate of the full $2^7 \times 32$ design. A complete analysis of the confounding factors and the resolution of this design is performed in Section 7.2.2. The sign table and results for this design can be seen in Table 7.5. A discussion of the results takes place in Section 7.2.3.

7.2.2. Analysis of the Design

The design in Table 7.5 has been created by using a 2^4 design and replacing the rows ABD, BCD, and $ABCD$ by E, F, and G, respectively. 32 replications are used per configuration. Hence, it is a $2^{7-3} \times 32$ design. The following confoundings exist:

$$E = ABD \qquad F = BCD \qquad G = ABCD$$

Or, related to the mean:

$$I = ABDE \qquad I = BCDF \qquad I = ABCDG$$

Which is equal to:

$$I = ABDE = BCDF = ABCDG$$

Table 7.3.: Mappings for Reservation Splitting and Resource Selection

Mapping	Parameter	Low Value (-1)	High Value (1)
A	$\text{crs}_{\text{reservation\_penalty}}$	0	100
B	$\text{crs}_{\text{reservation\_weight}}$	0	100
C	$\text{crs}_{\text{ack\_penalty}}$	0	100
D	$\text{crs}_{\text{ack\_weight}}$	0	100
E	$\text{crs}_{\text{rssi\_weight}}$	0	100
F	$\text{crs}_{\text{min\_rating}}$	800	400
G	$\text{num}_{\text{sub\_res}}$	1	5

The complete generator polynomial is obtained by multiplying each possible combination of the above terms with each other [Jai91, Sec. 19.3]:

$$\begin{aligned} I &= ABDE = BCDF = ABCDG \\ &= ABDEBCDF = ABDEABCDG = BCDFABCDG \\ &= ABDEBCDFABCDG \end{aligned}$$

By re-ordering, the equation becomes:

$$\begin{aligned} I &= ABDE = BCDF = ABCDG \\ &= AB^2CD^2EF = A^2B^2CD^2EG = AB^2C^2D^2FG \\ &= A^2B^3C^2D^3EFG \end{aligned}$$

Erasing terms with a power of two [Jai91, Sec. 19.3] gives the final form of the generator polynomial:

$$\begin{aligned} I &= ABDE = BCDF = ABCDG \\ &= ACEF = CEG = AFG \\ &= BDEFG \end{aligned}$$

This polynomial can be multiplied by the factors on both sides to determine with which factor interactions the factor confounds. Those results are displayed in Table 7.4. It can be seen that there are first-order effects that are confounded with second-order terms. Hence, this design has a resolution of three, and is called a R_{III} or 2^{7-3}_{III} design.

The following tests were carried out to validate the assumptions about the model. Firstly, the range of the lowest and highest response (y_{min} and y_{max}) is small. Secondly, the scatter plot of the residuals (Figure 7.1) versus the predicted responses does not show any trend in the errors.

Thirdly, a normal-quantile quantile plot has been created in order to perform a visual test whether the errors follow a normal distribution (Figure 7.2). The shape of the curve indicates that the residuals have slightly longer tails to the left (negative residuals). However, the smallest value is very close to the normal distribution. Given the extremely low values of the residuals in general and the fact that there are very few of those extreme values compared to the number of responses (512), the model seems to be an adequate fit and can be used to estimate the importance of the factors for further optimisation.

Table 7.4.: Confoundings for the Candidate Resource Selector Experimental Design

Factor	Confounds with
A	$FG = BDE = CEF = BCDG = ACEG = ABCDF = ABDEFG$
B	$ADE = CDF = ACDG = BCEG = ABFG = DEFG = ABCEF$
C	$EG = AEF = BDF = ACDG = ACFG = ABCDE = BCDEFG$
D	$ABE = BCF = CDEG = ADFG = BEFG = ABCG = ACDEF$
E	$CG = ABD = ACF = AEFG = BDFG = BCDEF = ABCDEG$
F	$AG = ACE = BCD = BDEG = CEFG = ABDEF = ABCDFG$
G	$AF = CE = ABCD = BDEF = ABDEG = BCDFG = ACEFG$

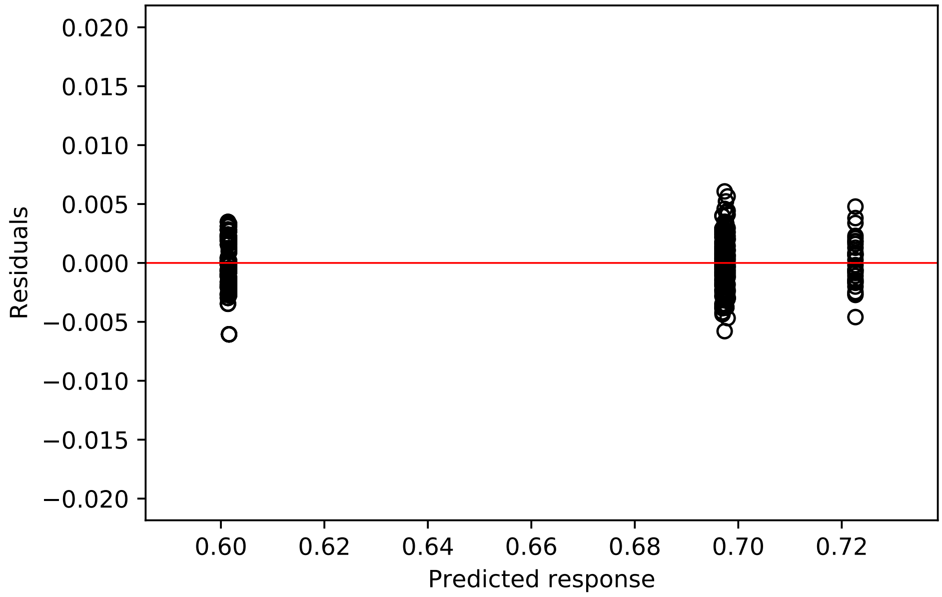

Figure 7.1.: Scatter plot of the residuals versus the predicted responses for the candidate resource selection experimental design.

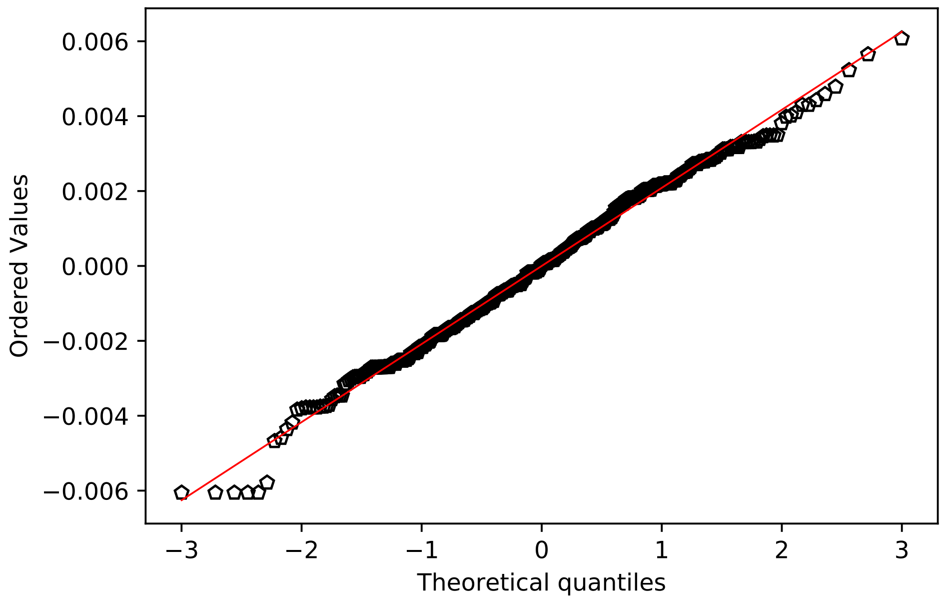

Figure 7.2.: Normal quantile quantile plot of the residuals for the candidate resource selection experimental design.

7.2.3. Analysis and Discussion of the Results

Table 7.5 shows the effects that the different primary factors and combinations thereof had on the mean response. The most important observations are the mean effect (*total/16* column) and whether this effect is positive or negative. The percentage of variation gives an indication as to the strength of the effect.

The confidence intervals have been calculated using the following approach. At first, the variance of the errors needs to be determined:

$$s_e^2 = \frac{\text{SSE}}{2^2\ (r-1)}$$

The number of repetitions is $r = 32$. SSE, the sum of squared errors, is approximately $0.002\,217$. The estimated variance of the effects is:

$$s_{q_0} = s_{q_A} = \dots = s_{q_G} = \frac{s_e}{2\sqrt{r}}$$

The confidence intervals for the effects are then calculated with the t-distribution:

$$q_i \pm t_{[1-0.5\,\alpha;\ 2^2\,(r-1)]} \times s_{q_i} \approx q_i \pm 1.26 \times 10^{-8}$$

In this calculation, a confidence level of $95\,\%$ was used ($\alpha = 0.05$). For each row, the confidence interval does not include the number zero. Hence, each effect, i.e. any row, is statistically significant.

The following conclusions can be drawn from Table 7.5:

- The parameter $\text{crs}_{\text{reservation\_penalty}}$, as a remnant of standard LTE, has a slight negative impact. The effect is low and could also be explained by confounding interactions. Still, this feature will be disabled, i.e. $\text{crs}_{\text{reservation\_penalty}}$ will be set to zero. Reservations will be considered solely with $\text{crs}_{\text{reservation\_weight}}$, which factors in the reception energy.
- The parameters $\text{crs}_{\text{reservation\_weight}}$, $\text{crs}_{\text{ack\_penalty}}$, $\text{crs}_{\text{ack\_weight}}$ are important parameters with significant positive influence. As the influence of each parameter is very similar, they will all be set to 100. Using $\text{crs}_{\text{ack\_penalty}}$ enables SAFE to consider hidden-terminal effects even if only few transmitters report that they are affected.
- The parameter $\text{crs}_{\text{rssi\_weight}}$ is neither important nor has it a negative influence. It will be set to 100, so that it can serve as fall-back for cases in which not much acknowledgement feedback can be sent.
- The parameter $\text{crs}_{\text{min\_rating}}$ has a very strong negative influence. This indicates that $\bar{F}$ ($\text{crs}_{\text{min\_rating}} = 800$) performs significantly better than F ($\text{crs}_{\text{min\_rating}} = 400$). Subsequently, the parameter is very important, and should be significantly higher than 400. The effect is so large that further studies on this parameter are justified. These will be performed in Section 7.2.4 to determine the optimal value.
- The parameter $\text{num}_{\text{sub\_res}}$ has a slight negative impact. This effect is small and could for example be explained by confounding factor combinations. A negative impact on the PDR can still be explained by the larger time horizon for resource allocation predictions or other reasons discussed in Section 5.2.2. Still, reservation splitting is a requirement for other features. Additionally, its main anticipated benefit is to reduce the impact of reoccurring collisions and thus increase the cooperative awareness. Therefore, a value of five will be used. These results also indicate that the impact of reservation splitting on the PDR and cooperative awareness with standard LTE-V2X should be further investigated. Further studies that assess the impact of the number of sub-reservations will be presented in Chapter 8.

Table 7.5.: Sign Table and Results for the Candidate Resource Selector Experimental Design

I	A	B	C	D	AB	AC	AD	BC	BD	CD	ABC	ACD	E	F	G	Mean $\bar{y}$
1	-1	-1	-1	-1	1	1	1	1	1	1	-1	-1	-1	-1	1	0.602
1	1	-1	-1	-1	-1	-1	-1	1	1	1	1	1	1	-1	-1	0.698
1	-1	1	-1	-1	-1	1	1	-1	-1	1	1	-1	1	1	-1	0.601
1	1	1	-1	-1	1	-1	-1	-1	-1	1	-1	1	-1	1	1	0.602
1	-1	-1	1	-1	1	-1	1	-1	1	-1	1	1	-1	1	-1	0.601
1	1	-1	1	-1	-1	1	-1	-1	1	-1	-1	-1	1	1	1	0.602
1	-1	1	1	-1	-1	-1	1	1	-1	-1	-1	1	1	-1	1	0.697
1	1	1	1	-1	1	1	-1	1	-1	-1	1	-1	-1	-1	-1	0.697
1	-1	-1	-1	1	1	1	-1	1	-1	-1	-1	1	1	1	-1	0.601
1	1	-1	-1	1	-1	-1	1	1	-1	-1	1	-1	-1	1	1	0.602
1	-1	1	-1	1	-1	1	-1	-1	1	-1	1	1	-1	-1	1	0.697
1	1	1	-1	1	1	-1	1	-1	1	-1	-1	-1	1	-1	-1	0.698
1	-1	-1	1	1	1	-1	-1	-1	-1	1	1	-1	1	-1	1	0.723
1	1	-1	1	1	-1	1	1	-1	-1	1	-1	1	-1	-1	-1	0.698
1	-1	1	1	1	-1	-1	-1	1	1	1	-1	-1	-1	-1	-1	0.698
1	1	1	1	1	1	1	1	1	1	1	1	1	1	1	1	0.602
10.42	-0.023	0.165	0.217	0.217	-0.167	-0.218	-0.217	-0.025	-0.024	0.027	0.025	-0.026	0.025	-0.601	-0.168	Total/16
0.651	-0.001	0.010	0.014	0.014	-0.010	-0.014	-0.014	-0.002	-0.002	0.002	0.002	-0.002	0.002	-0.038	-0.010	Total/16
	0.083	4.289	7.378	7.409	4.353	7.450	7.412	0.096	0.092	0.117	0.096	0.106	0.101	56.594	4.425	% of var.

7.2.4. Optimal Value for the Minimum Candidate Resource Rating

The previous analysis of the experimental design showed that the minimum rating of a candidate resource, i.e. the parameter $\mathrm{crs}_{\mathrm{min\_rating}}$, has a strong influence on the PDR and should be further investigated. This is done in a separate study, which is shown in this section. According to the previous results, $\mathrm{crs}_{\mathrm{reservation\_weight}}$, $\mathrm{crs}_{\mathrm{ack\_penalty}}$, $\mathrm{crs}_{\mathrm{ack\_weight}}$, and $\mathrm{crs}_{\mathrm{reservation\_weight}}$ have been set to 100, while $\mathrm{crs}_{\mathrm{reservation\_penalty}}$ is set to zero. Additionally, $\mathrm{num}_{\mathrm{sub\_res}}$ has been set to five.

The purpose of these experiments is to find the optimal value for $\mathrm{crs}_{\mathrm{min\_rating}}$. This is done by using a single-factor, multi-level $(8^1 \times 32)$ design. From the previous results, it is clear that a minimum rating of 800 performs better than 400. For this multi-level design, $\mathrm{crs}_{\mathrm{min\_rating}}$ is varied from 200 to 900 in increments of 100, and an additional value of 950 is used. The PDR along with $95\,\%$ confidence intervals is shown in Table 7.6 and Figure 7.3. It can be seen that there is a step-like trend of the PDR, which strongly increases with a minimum candidate resource rating above 600. After this step, it slightly increases until $\mathrm{crs}_{\mathrm{min\_rating}}$ is 900. There is no statistically significant change when $\mathrm{crs}_{\mathrm{min\_rating}}$ is set to 950. Hence, 900 seems to be the best choice.

7.3. Reactive Hidden Terminal Mitigation

The purpose of this experimental design is to find configuration parameters for the reactive hidden-terminal mitigation, i.e. the reaction to low acknowledgement ratios.

7.3.1. Factor Levels and Level Combinations

This design is configured according to the results of the previous studies. Hence, the parameter $\mathrm{crs}_{\mathrm{reservation\_penalty}}$ is set to zero, while $\mathrm{crs}_{\mathrm{reservation\_weight}}$, $\mathrm{crs}_{\mathrm{ack\_penalty}}$, $\mathrm{crs}_{\mathrm{ack\_weight}}$, and $\mathrm{crs}_{\mathrm{rssi\_weight}}$ are set to one hundred. The minimum rating $\mathrm{crs}_{\mathrm{min\_rating}}$ is set to 900. A difference to the previous experimental design is that reactions to low acknowledgement ratios are now enabled. The factor $\mathrm{ack}_{\mathrm{avg},\alpha}$ is considered to be secondary. It should generally include portions of about five measurements, so that all different subchannels contribute to the average acknowledgement ratio. Hence, $\mathrm{ack}_{\mathrm{avg},\alpha}$ is set to $2 \div (N+1) = 2 \div (5+1) = 1/3$. Other secondary factors are set like in the previous design in Section 7.2.

The number of sub-reservations is varied during this experiment. The other primary factors can be seen in Table 7.7. The parameter $\mathrm{ack}_{\mathrm{avg},\delta}$ should neither be set to zero, nor should it be so high that the comparison cannot trigger. Hence, a value of 0.1 has been set as low value and 0.3 as high value. Similarly, the minimum acknowledgement ratio $\mathrm{ack}_{\mathrm{min}}$ cannot be zero, as this would completely disable the mechanism. If the value is to high, the reaction to low acknowledgement ratios will likely trigger too often. The values of 0.4 and 0.7 have been chosen based on preliminary investigations. The hysteresis period has been limited to $5\,\mathrm{s}$ at maximum as this is the mean reuse time period of SAFE when using five sub-reservations.

7.3.2. Analysis of the Design

As the number of primary factors for this design is only four, a full-resolution $2^4 \times 32$ design (i.e. with 32 replications for each configuration) is feasible. This also means that there are no

Table 7.6.: Packet Delivery Ratio for Different Minimum Candidate Resource Ratings

crs_{min_rating}	PDR [%]
200	60.16 ± 0.08
400	60.16 ± 0.08
500	60.14 ± 0.08
600	70.28 ± 0.07
700	69.68 ± 0.09
800	72.26 ± 0.07
900	72.94 ± 0.09
950	72.88 ± 0.08

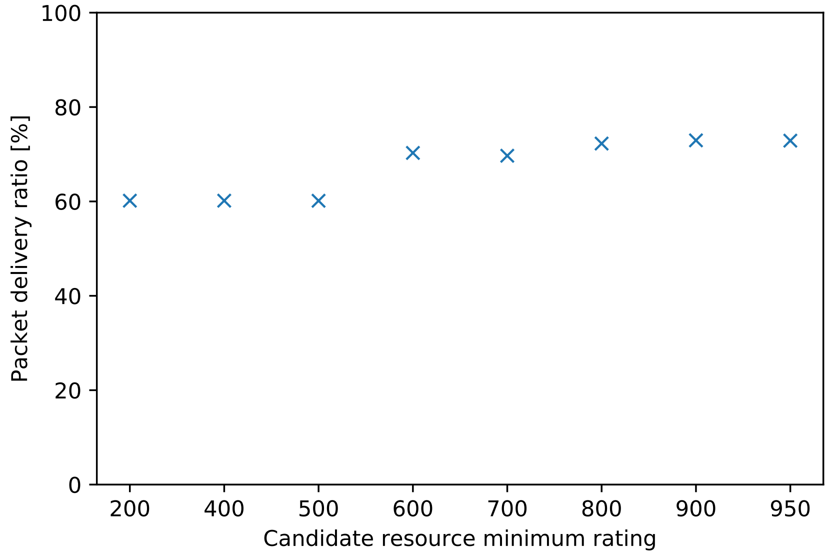

Figure 7.3.: Packet Delivery Ratio for Different Minimum Candidate Resource Ratings.

confounding factors or factor level combinations and an analysis of the confoundings is not necessary.

The model makes the same assumptions about the statistical distribution of the residuals like the design in Section 7.2. As expected, the range of the lowest and highest response is small, i.e. the residuals are multiple orders of magnitudes smaller than the responses. In order to validate that the residuals are normally distributed, the same visual tests like before are performed. As in the previous design, the scatter plot of the residuals versus the predicted responses (Figure 7.4) does not show any trend. The normal-quantile quantile plot has a slight S-shape at the very extremes. This means that the residuals have slightly shorter tails than the normal distribution. However, the residuals appear to be approximately normally distributed. The model seems to be a good choice for the optimisation of configuration parameters.

7.3.3. Analysis and Discussion of the Results

Table 7.8 shows the effects that the different primary factors and combinations thereof had on the mean response. The most important observations are the mean effect (*total/16* column)

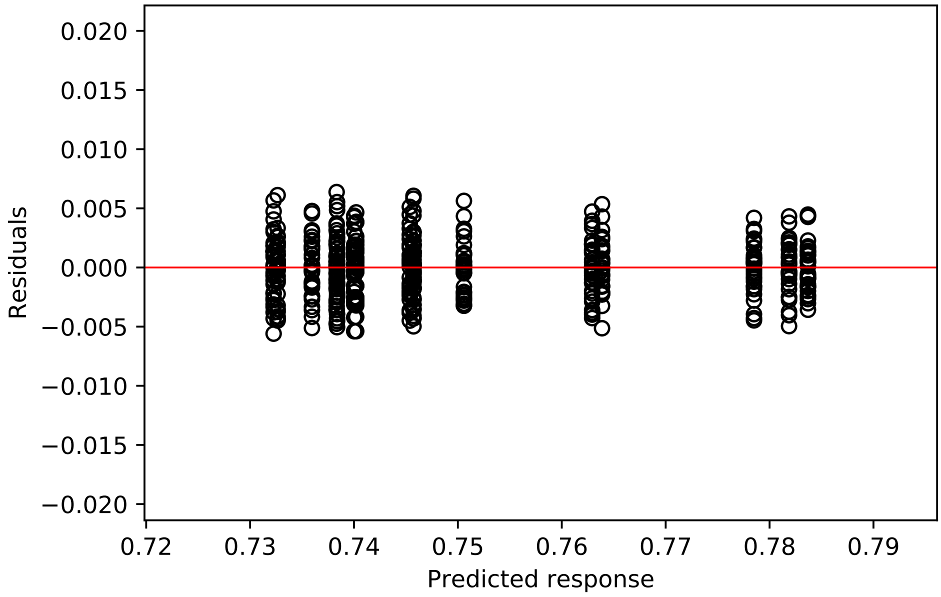

Figure 7.4.: Scatter plot of the residuals versus the predicted responses for the reactive hidden-terminal mitigation experimental design.

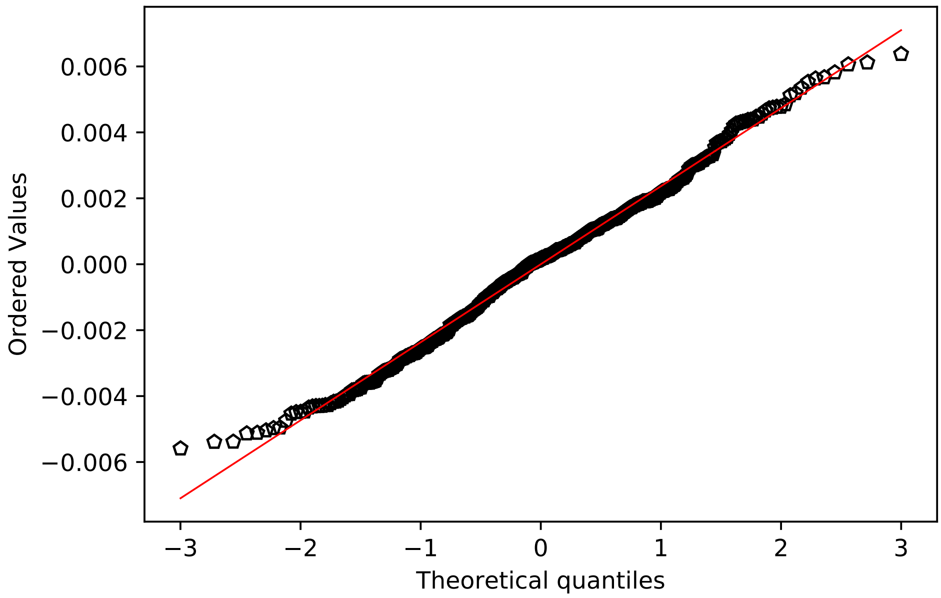

Figure 7.5.: Normal quantile quantile plot of the residuals for the reactive hidden-terminal mitigation experimental design.

Table 7.7.: Mappings for Reactive Hidden Terminal Mitigation

Mapping	Parameter	Low Value (-1)	High Value (1)
A	$\mathrm{num}_{\mathrm{sub\_res}}$	1	5
B	$\mathrm{ack}_{\mathrm{avg},\delta}$	0.1	0.3
C	$\mathrm{ack}_{\mathrm{min}}$	0.4	0.7
D	$\mathrm{ack}_{\mathrm{hysteresis}}$	1	5

and whether this effect is positive or negative. The percentage of variation gives an indication as to the strength of the effect.

SSE, the sum of squared errors, is approximately $0.002\,856$. The confidence intervals for the effects are then calculated with the t-distribution:

$$q_i \pm t_{[1-0.5\,\alpha;\;2^2\,(r-1)]} \times s_{q_i} \approx q_i \pm 1.62 \times 10^{-8}$$

In this calculation, a confidence level of $95\,\%$ was used ($\alpha = 0.05$). For each row, the confidence interval does not include the number zero. Hence, each effect, i.e. any row, is statistically significant.

The following conclusions can be drawn from Table 7.8:

- Factor A ($\mathrm{num}_{\mathrm{sub\_res}}$) explains about $10.3\,\%$ of the total variation. Unlike in the previous design, the influence is positive. This means that an increased number of sub-reservations leads to an increased PDR in this design. In the previous design, it had a small negative influence. As the mechanisms from the previous design are also incorporated into this design, the benefits of a higher number of sub-reservations when enabling the reactions to low acknowledgement ratios outweighs the disadvantages that it normally has. This can be explained with the fact that SAFE uses multiple different radio resources instead of only one. Hence, the exponential moving average of the acknowledgement ratio is more representative of the true mean, i.e. *achievable*, acknowledgement ratio. Consequently, the use of five sub-reservations is justified.
- Factor B ($\mathrm{ack}_{\mathrm{avg},\delta}$) has the smallest influence on the performance. However, the influence is negative. This simply means that the low value, i.e. 0.1, should be used.
- Factor C ($\mathrm{ack}_{\mathrm{min}}$) is the second-most important parameter and explains about $14.7\,\%$ of the total variation. The influence is positive. Hence, the high value, i.e. 0.7, should be used. Further studies would be justified, but do not seem to be a requirement for good performance.
- Factor D ($\mathrm{ack}_{\mathrm{hysteresis}}$) is by far the most important parameter and explains about $43.7\,\%$ of the total variation. This influence is negative, which means that a hysteresis period of one second performs significantly better than one of five seconds. Further multi-level studies regarding this parameter seem to be justified. However, it has to be considered that this mechanism acts as a *safety-component* by preventing the MAC layer from dropping radio resources and selecting new ones too often. This ensures some degree of periodicity of the radio resource allocation. As it could be seen from the conclusions of the first experimental design, the candidate resource selection mechanisms that require periodicity become less important with the introduction of the acknowledgement feedback for radio resources. However, in scenarios with a lower number of available padding bits, this hysteresis period might be more important since other factors, such as the average RSSI, become more important inputs to the candidate resource selection process. Hence, care should be taken when choosing very low hysteresis periods.

Table 7.8.: Sign Table and Results for the Reactive Hidden Terminal Mitigation Experimental Design

I	A	B	C	D	AB	AC	AD	BC	BD	CD	ABC	ACD	ABD	BCD	ABCD	Mean $\bar{y}$
1	-1	-1	-1	-1	1	1	1	1	1	1	-1	-1	-1	-1	1	0.751
1	1	-1	-1	-1	-1	-1	-1	1	1	1	1	1	1	-1	-1	0.782
1	-1	1	-1	-1	-1	1	1	-1	-1	1	1	-1	1	1	-1	0.738
1	1	1	-1	-1	1	-1	-1	-1	-1	1	-1	1	-1	1	1	0.738
1	-1	-1	1	-1	1	-1	1	-1	1	-1	1	1	-1	1	-1	0.764
1	1	-1	1	-1	-1	1	-1	-1	1	-1	-1	-1	1	1	1	0.784
1	-1	1	1	-1	-1	-1	1	1	-1	-1	-1	1	1	-1	1	0.763
1	1	1	1	-1	1	1	-1	1	-1	-1	1	-1	-1	-1	-1	0.779
1	-1	-1	-1	1	1	1	-1	1	-1	-1	-1	1	1	1	-1	0.736
1	1	-1	-1	1	-1	-1	1	1	-1	-1	1	-1	-1	1	1	0.746
1	-1	1	-1	1	-1	1	-1	-1	1	-1	1	1	-1	-1	1	0.732
1	1	1	-1	1	1	-1	1	-1	1	-1	-1	-1	1	-1	-1	0.733
1	-1	-1	1	1	1	-1	-1	-1	-1	1	1	-1	1	-1	1	0.740
1	1	-1	1	1	-1	1	1	-1	-1	1	-1	1	-1	-1	-1	0.745
1	-1	1	1	1	-1	-1	-1	1	1	1	-1	-1	-1	-1	-1	0.740
1	1	1	1	1	1	1	1	1	1	1	1	1	1	1	1	0.746
12.02	0.088	-0.078	0.105	-0.180	-0.045	0.005	-0.046	0.067	0.046	-0.055	0.037	-0.003	0.026	-0.032	-0.018	Total
0.751	0.005	-0.005	0.007	-0.011	-0.003	0.000	-0.003	0.004	0.003	-0.003	0.002	0.000	0.002	-0.002	-0.001	Total/16
	10.34	8.21	14.71	43.71	2.70	0.03	2.80	6.03	2.81	4.09	1.81	0.02	0.93	1.40	0.41	% of var.

- There is a significant interaction between factor B ($\mathrm{ack}_{\mathrm{avg},\delta}$) and C ($\mathrm{ack}_{\mathrm{min}}$), and C and D ($\mathrm{ack}_{\mathrm{hysteresis}}$), explaining $6.0\,\%$ and $4.1\,\%$ of the total variation, respectively. The BC interaction is positive, while the CD interaction is negative.

  A positive BC interaction means that B has a positive effect if C is also at its high level, i.e. a high $\mathrm{ack}_{\mathrm{avg},\delta}$ leads to additional advantages if $\mathrm{ack}_{\mathrm{min}}$ is also high, or vice versa. Intuitively, it can be said that if the exponential moving average has less weight, the definite threshold $\mathrm{ack}_{\mathrm{min}}$ becomes more important and should be raised, and vice versa.

  For the BD interaction, it can be said that a higher required acknowledgement ratio is less beneficial if a reaction to low acknowledgement ratios may occur less often. This is intuitively comprehensible.

7.3.4. Optimal Value for the Hysteresis Time Period

The previous results lead to the conclusion that a multi-level study on the hysteresis time period ($\mathrm{ack}_{\mathrm{hysteresis}}$) should be performed. Hence, five additional experiments with 32 runs each have been performed. For this study, $\mathrm{ack}_{\mathrm{hysteresis}}$ has taken the values of $0.5\,\mathrm{s}$, $1\,\mathrm{s}$, $2\,\mathrm{s}$, $3\,\mathrm{s}$, and $4\,\mathrm{s}$.

The results can be seen in Table 7.9. It can be observed that an hysteresis period of $0.5\,\mathrm{s}$ performs even better than an interval of one second. The trend of the PDR appears to be strictly monotonic increasing if the hysteresis time is lowered. At this point, the conclusion might be drawn that this mechanism fails to meet its expectations and should be disabled by setting it to zero.

However, when considering system knowledge to interpret the results, another conclusion can be drawn. Whenever radio resources are dropped due to low acknowledgement ratios, the current packet will be dropped as well. This is because it does not make sense to transmit packets that would be subject to collisions anyway and would hence even disturb another transmission. This packet dropping happens more often if the hysteresis time is lower. Hence, the number of transmitted packets will be slightly lower. As this results in a lower channel load, and it is easier to reach high PDR with lower load, some of the performance benefits of a low hysteresis time can be attributed to this effect. Another reason to keep this mechanism is that the RSSI-based mechanism for the exclusion of candidate resources still expects some form of periodic resource reuse. In scenarios with less accurate acknowledgement feedback, i.e. less available padding bits, this periodicity might be more important. When considering these arguments and the results, an hysteresis time $\mathrm{ack}_{\mathrm{hysteresis}}$ of one second seems to be the best compromise.

Table 7.9.: Packet Delivery Ratio for Different Hysteresis Time Periods

$\mathrm{ack}_{\mathrm{hysteresis}}$ [s]	PDR [%]
0.5	79.48 ± 0.08
1	78.37 ± 0.08
2	76.70 ± 0.08
3	75.64 ± 0.09
4	74.90 ± 0.09

7.4. Distributed Congestion Control

The last experimental design is used to find optimal configuration parameters for the DCC components of SAFE. An increased traffic load of $150\,\%$ has been used in order to increase the channel load and to ensure that DCC is necessary in the scenario. This means that the results cannot directly be compared to the previous ones.

7.4.1. Factor Levels and Level Combinations

The parameters not related to DCC are set according to the previous results. Like in the previous design, $\mathrm{crs}_{\mathrm{reservation\_penalty}}$ is set to zero, while $\mathrm{crs}_{\mathrm{reservation\_weight}}$, $\mathrm{crs}_{\mathrm{ack\_penalty}}$, $\mathrm{crs}_{\mathrm{ack\_weight}}$, and $\mathrm{crs}_{\mathrm{rssi\_weight}}$ are set to one hundred. The minimum rating $\mathrm{crs}_{\mathrm{min\_rating}}$ is set to 900. The hidden-terminal mitigation based on acknowledgement feedback is enabled and the related factors are set as follows: $\mathrm{ack}_{\mathrm{avg},\alpha}$ is set to $1/3$, $\mathrm{ack}_{\mathrm{avg},\delta}$ to 0.1, $\mathrm{ack}_{\mathrm{min}}$ to 0.7, and $\mathrm{ack}_{\mathrm{hysteresis}}$ to 1. As in all of the experiments in this chapter, $\mathrm{ack}_{\mathrm{sep\_pkts}}$ is disabled.

Of the DCC-related factors, $\mathrm{dcc}_{\mathrm{min\_subres}}$ is considered to be secondary and set to two. The main reason for this parameter is not the improvement of the PDR, which is used as metric for this experimental design. Instead, its purpose is to ensure fairness and reliability even when DCC has to impose restrictions on terminals. Setting this parameter to two appears to be the best choice due to the following reasons. Firstly, this ensures that the terminal is still able to distribute at least $40\,\%$ of the messages of this packet flow in case five sub-reservations are used, i.e. at least two of the five sub-reservations are enabled. Secondly, if one of the sub-reservations is subject to reoccurring collisions or half-duplex effects, there is still another sub-reservation that has a high probability of a successful transmission.

The other factors related to DCC are considered primary and can be seen in Table 7.10. The parameter $\mathrm{crs}_{\mathrm{min\_rating}}$ is boolean. Hence 0 and 1 is the low and high value, respectively. The CBR target $\mathrm{dcc}_{\mathrm{cbr\_target}}$ has been set to 0.8. This allows for headroom for other, more important messages and quantisation effects due to the subchannel allocation. The low value is 0.6, which is seen as a relatively restrictive configuration of DCC. The margin $\mathrm{dcc}_{\mathrm{cbr\_margin}}$ can only be very small, as the DCC component would trigger too early otherwise. Hence, 0.05 and 0.1 has been chosen as low and high value, respectively. The disable time $\mathrm{dcc}_{\mathrm{disable\_time}}$ takes the same values as the acknowledgement hysteresis period $\mathrm{ack}_{\mathrm{hysteresis}}$.

7.4.2. Analysis of the Design

As with the previous design, a full resolution $2^4 \times 32$ design is used. Hence, there are no confounding factors or factor level combinations.

Table 7.10.: Mappings for Distributed Congestion Control

Mapping	Parameter	Low Value (-1)	High Value (1)
A	$\mathrm{crs}_{\mathrm{min\_rating\_dcc}}$	0	1
B	$\mathrm{dcc}_{\mathrm{cbr\_target}}$	0.6	0.8
C	$\mathrm{dcc}_{\mathrm{cbr\_margin}}$	0.05	0.1
D	$\mathrm{dcc}_{\mathrm{disable\_time}}$	1	5

As with any previous experimental design, the assumptions underlying the used model for the errors should be validated. The residuals are multiple orders of magnitude smaller than the responses. The scatter plot of the residuals versus the predicated responses (Figure 7.6) does not show any trend. Additionally, the normal-quantile quantile plot (Figure 7.7) indicates that a normal distribution is a good fit as a model for the errors.

7.4.3. Analysis and Discussion of the Results

Table 7.11 shows the experimental design and its results.

The SSE (sum of squared errors) is approximately $0.001\,095$. The confidence intervals for the effects are then calculated with the t-distribution:

$$q_i \pm t_{[1-0.5\,\alpha;\; 2^2\,(r-1)]} \times s_{q_i} \approx q_i \pm 6.22 \times 10^{-9}$$

In this calculation, a confidence level of $95\,\%$ was used ($\alpha = 0.05$). For each row, the confidence interval does not include the number zero. Hence, each effect, i.e. any row, is statistically significant.

The following conclusions can be drawn from Table 7.11:

- The CBR target $\mathrm{dcc}_{\mathrm{cbr\_target}}$ has a very high influence on the PDR. It explains about $71\,\%$ of the variation. The influence is negative. This means that the high value of the CBR target leads to a worse PDR and vice versa. These results is very pleasant, because it means that the more active the developed DCC component is, the higher the PDR will be. More studies regarding the optimal value of the CBR target should be performed. However, other metrics than solely the PDR should be used as a low CBR target might always lead to a better PDR, but the cooperative awareness might be significantly lower. This will further be investigated in Section 7.4.4.

- Factor A has the second highest influence on the PDR. It explains about $15\,\%$ of the total variation. The influence of factor A is positive. Hence, $\mathrm{crs}_{\mathrm{min\_rating\_dcc}}$ should be set to 1, i.e. the DCC component of the candidate resource selector should be enabled.

- The factors C and D have a similar impact, although the percentage of variation of factor C is lower. The influence of the factors is positive, indicating that the CBR margin $\mathrm{dcc}_{\mathrm{cbr\_margin}}$ should be set to 0.1 and the time interval for disabling of sub-reservations should be set to $5\,\mathrm{s}$.

- There is a significant and comparatively high single-level interaction between factors A and B. Hence, the CBR target interacts with the DCC component of the candidate resource selector. The influence of this interaction is positive. This can be explained as follows. Firstly, a lower CBR target (Factor $\mathrm{B} = -1$) makes the DCC component of the candidate resource selector less important. Secondly, if the DCC component of the candidate resource selector is enabled (Factor $\mathrm{A} = 1$), lowering the CBR target has a slightly smaller effect. Both of these interpretations are plausible. Nevertheless, the interaction is outweighed by the individual influences of the factors A and B.

- There is a significant, but very small interaction between the factors B and D, explaining about $1\,\%$ of the total variation. The influence of this interaction is negative, indicating that a combination of a lower CBR target (Factor $\mathrm{B} = -1$) and a higher sub-reservation disabling time (Factor $\mathrm{D} = 1$) is even more preferential.

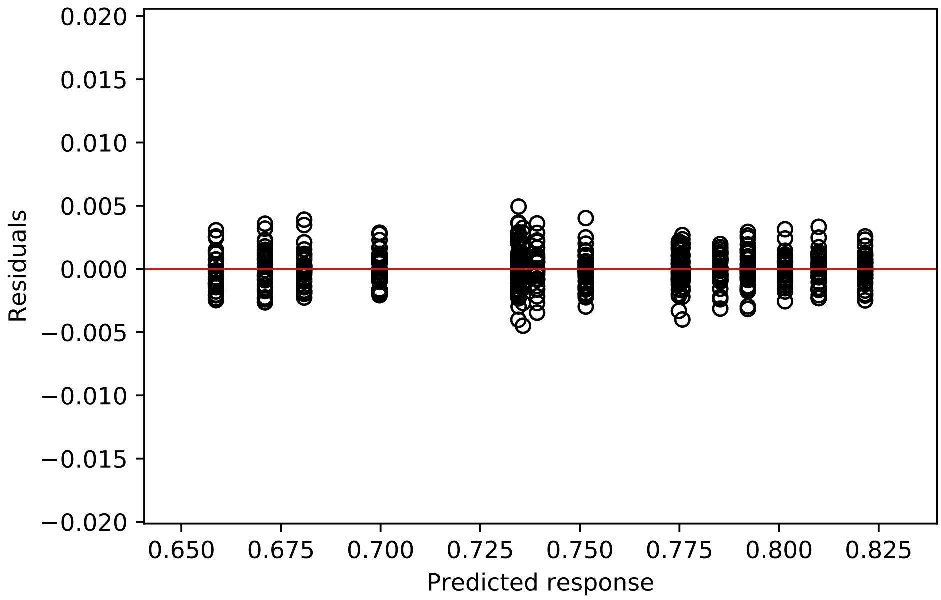

Figure 7.6.: Scatter plot of the residuals versus the predicted responses for the DCC experimental design.

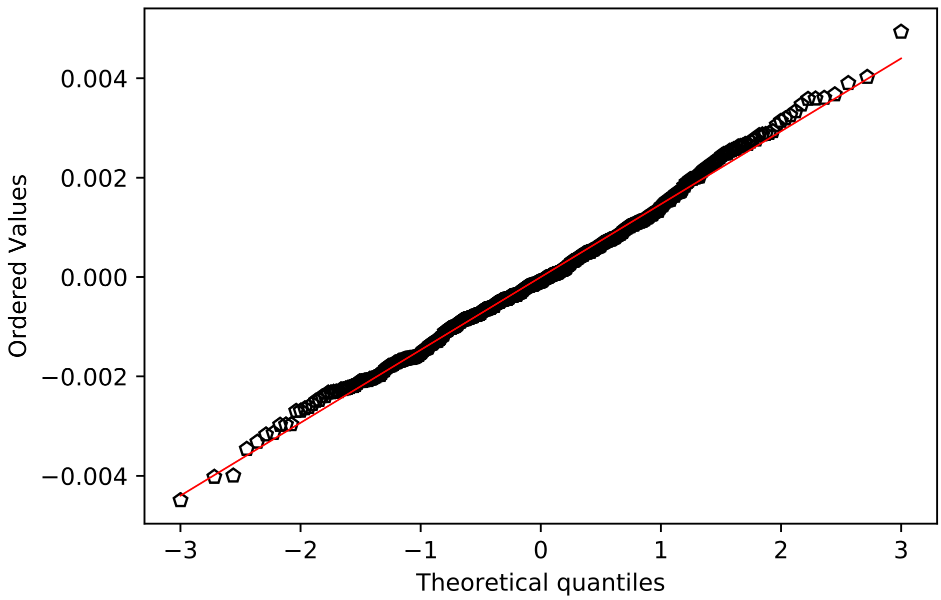

Figure 7.7.: Normal quantile quantile plot of the residuals for the DCC experimental design.

Table 7.11.: Sign Table and Results for the Distributed Congestion Control Experimental Design

I	A	B	C	D	AB	AC	AD	BC	BD	CD	ABC	ACD	ABD	BCD	ABCD	Mean $\bar{y}$
1	-1	-1	-1	-1	1	1	1	1	1	1	-1	-1	-1	-1	1	0.751
1	1	-1	-1	-1	-1	-1	-1	1	1	1	1	1	1	-1	-1	0.776
1	-1	1	-1	-1	-1	1	1	-1	-1	1	1	-1	1	1	-1	0.659
1	1	1	-1	-1	1	-1	-1	-1	-1	1	-1	1	-1	1	1	0.735
1	-1	-1	1	-1	1	-1	1	-1	1	-1	1	1	-1	1	-1	0.775
1	1	-1	1	-1	-1	1	-1	-1	1	-1	-1	-1	1	1	1	0.792
1	-1	1	1	-1	-1	-1	1	1	-1	-1	-1	1	1	-1	1	0.681
1	1	1	1	-1	1	1	-1	1	-1	-1	1	-1	-1	-1	-1	0.736
1	-1	-1	-1	1	1	1	-1	1	-1	-1	-1	1	1	1	-1	0.785
1	1	-1	-1	1	-1	-1	1	1	-1	-1	1	-1	-1	1	1	0.801
1	-1	1	-1	1	-1	1	-1	-1	1	-1	1	1	-1	-1	1	0.671
1	1	1	-1	1	1	-1	1	-1	1	-1	-1	-1	1	-1	-1	0.735
1	-1	-1	1	1	1	-1	-1	-1	-1	1	1	-1	1	-1	1	0.810
1	1	-1	1	1	-1	1	1	-1	-1	1	-1	1	-1	-1	-1	0.822
1	-1	1	1	1	-1	-1	-1	1	1	1	-1	-1	-1	-1	-1	0.700
1	1	1	1	1	1	1	1	1	1	1	1	1	1	1	1	0.739
11.97	0.303	-0.658	0.141	0.159	0.165	-0.057	-0.041	-0.028	-0.089	0.015	-0.034	-0.001	-0.014	0.005	-0.005	Total
0.748	0.019	-0.041	0.009	0.010	0.010	-0.004	-0.003	-0.002	-0.006	0.001	-0.002	0.000	-0.001	0.000	0.000	Total/16
	15.03	70.68	3.26	4.11	4.42	0.52	0.28	0.13	1.30	0.04	0.18	0.00	0.03	0.00	0.00	% of var.

7.4.4. Optimal Value for the CBR Target

The previous experimental design showed that the CBR target of the DCC algorithm should be further investigated as it has a large influence on the PDR. This is carried out in this section. Unlike in previous studies, the cooperative awareness will also be used as metric. Table 7.12 shows a summary of the results, while Figure 7.8 shows a quantile function plot of the percentage of time with ideal awareness for all vehicles during the simulation, and Figure 7.9 shows the mean PDR for different transmission distances.

It can be seen that the PDR increases with a lower CBR target, especially in higher communication distances. However, the percentage of time with ideal awareness is reduced. This is expected because the robustness of the communication can be decreased by disabling sub-reservations as a lower number of different radio resources is used. However, the drop of the awareness with this very strict metric is comparatively low.

The CBR target parameter $\mathrm{dcc}_{\mathrm{cbr\_target}}$ does not mean that it is the goal to have a median CBR of the same value across all vehicles. Along with $\mathrm{dcc}_{\mathrm{cbr\_margin}}$, it determines the CBR range in which the DCC algorithm becomes active for an individual vehicle. The median CBR is lower than the CBR target for multiple reasons. Firstly, DCC regulates the cases with extreme channel loads more restrictively. Some of the vehicles in the scenario might not be subjected to high channel loads at all, or at all times. This means that outliers with high channel load are removed, and the median is pushed towards lower CBR values. Secondly, the resource allocation scheme tries to avoid using resources that even affect one of the two subchannels. As the size of CAM messages is two subchannels and five subchannel per subframe are available, a single subchannel is left unoccupied in many subframes. In fact, an ideal, collision-free allocation of radio resources might therefore not reach CBR values over $80\,\%$. It can be seen in Table 7.12 that a DCC target of $80\,\%$ does hardly influence the median CBR, PDR, or even cooperative awareness. This indicates that DCC has hardly been active with this configuration. Thirdly, the DCC component has a margin parameter $\mathrm{dcc}_{\mathrm{cbr\_margin}}$ which enables it to restrict the usage of radio resources even before the CBR target is exceeded.

These results would justify the use of either $70\,\%$ or $80\,\%$ as CBR target. A CBR target lower than this restricts terminals too much. As the PDR is significantly increased with a lower target, there is more space for high-priority messages and more available space for larger packets, etc., a value of $70\,\%$ has been chosen for the subsequent evaluation of SAFE.

Summary

In this chapter, many experiments have been carried out in order to find optimal values for the configuration parameters of SAFE. Some of the parameters that are part of the LTE

Table 7.12.: Simulation Results for Different CBR Target Values

$\mathrm{dcc}_{\mathrm{cbr\_target}}$	Median CBR [%]	PDR [%] ($d \leq 100\,\mathrm{m}$)	PDR [%] ($d \leq 300\,\mathrm{m}$)	Time with $100\,\%$ Awareness [%]
$60\,\%$	$46.72\ [46.69, 46.79]$	98.27 ± 0.02	82.16 ± 0.04	$17.33\ [17.33, 18.00]$
$70\,\%$	$51.58\ [51.54, 51.66]$	97.76 ± 0.02	77.95 ± 0.04	$18.17\ [17.67, 19.33]$
$80\,\%$	$54.86\ [54.78, 54.92]$	97.26 ± 0.02	73.93 ± 0.05	$38.67\ [38.00, 39.00]$
No DCC	$55.12\ [55.03, 55.25]$	97.22 ± 0.02	73.47 ± 0.06	$41.00\ [40.50, 41.17]$

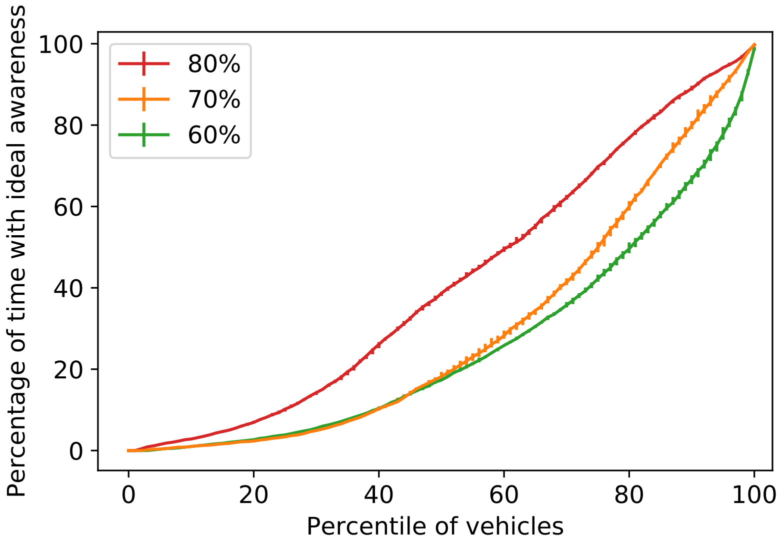

Figure 7.8.: Quantile function plot: percentage of time with ideal awareness for the range of $0\,\mathrm{m}$ to $300\,\mathrm{m}$ and for different CBR targets $\mathrm{dcc}_{\mathrm{cbr\_target}}$. (Vertical lines indicate asymmetric confidence intervals with at least $95\,\%$ confidence level. Horizontal connecting lines cross the confidence interval bars at the median, but are for visualisation purposes only in between.)

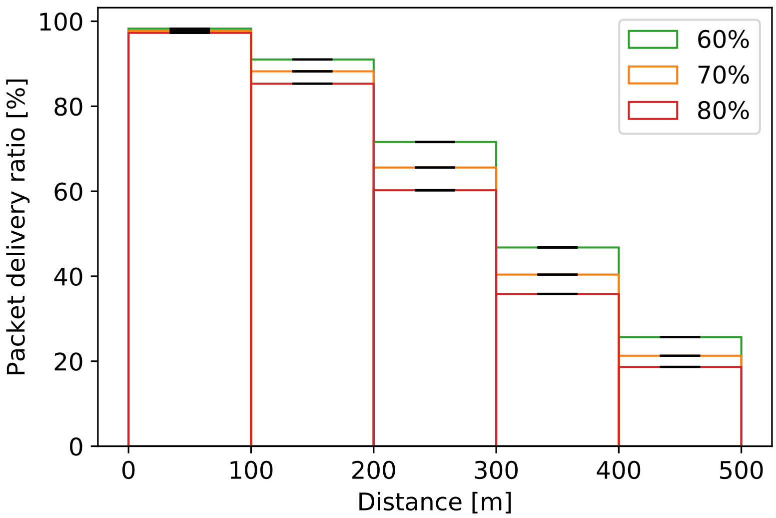

Figure 7.9.: Mean PDR depending on transmission distance for different CBR targets $\mathrm{dcc}_{\mathrm{cbr\_target}}$. (Error bars indicate confidence intervals with a confidence level of $95\,\%$.)

standard or related to the simulation setup have been considered to be secondary. Then, three different experimental designs have been created. The motivation for this approach was firstly to reduce the number of primary factors, and secondly that the individual components can work independently from each other to a certain extent. For example, the candidate resource selector needs to select the best radio resources regardless of whether there is a reaction to low acknowledgement ratios or whether the DCC component is enabled.

The purpose of the first design was to determine the optimal set of parameters for the candidate resource selector. The analysis of the results showed that $\mathrm{crs}_{\mathrm{reservation\_penalty}}$ should not be used. Instead, $\mathrm{crs}_{\mathrm{reservation\_weight}}$, $\mathrm{crs}_{\mathrm{ack\_penalty}}$, $\mathrm{crs}_{\mathrm{ack\_weight}}$, and $\mathrm{crs}_{\mathrm{rssi\_weight}}$ should be set to equal values, i.e. one hundred. The minimum rating of a candidate resource has been determined to be the most influential parameter of the candidate resource selector. A subsequent study showed that it should be set to 900. Using a higher number of sub-reservations lead to a small decrease of the PDR. However, other considerations related to additional components of the resource allocation or metrics other than the PDR justify the use of five sub-reservations.

The second design was about the configuration of the reaction to low acknowledgement ratios, which acts as reactive hidden-terminal mitigation. When enabling this functionality, a higher number of sub-reservations has a positive influence. This is because the average acknowledgement ratio is closer to the true mean performance on the channel because it can be built using multiple, interleaved and different radio resources. The experimental design showed that a higher value (0.7) of the minimum acknowledgement ratio $\mathrm{ack}_{\mathrm{min}}$ should be used. The most important parameter was the acknowledgement hysteresis period. A subsequent study indicated that a value of $1\,\mathrm{s}$ is preferable.

The goal of the third design was to find optimal configuration parameters for the DCC component. The developed DCC component is able to significantly increase the PDR, especially if a low target CBR is configured. As the PDR is not the only optimisation criteria relevant in practice and a lower CBR almost always leads to a higher PDR, an additional analysis of the impact of the target CBR has been presented. This resulted in a chosen CBR target $\mathrm{dcc}_{\mathrm{cbr\_target}}$ of $70\,\%$. Among others, the experimental design additionally indicated that the rating-based DCC mechanism in the candidate resource selector should be enabled and that sub-reservations should be disabled for a relatively long time interval ($5\,\mathrm{s}$).

Chapter 8.

Evaluation

The purpose of the previous chapter was to find good values for the parameters of SAFE This chapter deals with the actual performance evaluation, while being configured with the previously determined parameters.

This chapter is divided into five main parts. At first, the research questions and goals for evaluation will be presented in Section 8.1. Then, a qualitative discussion will take place in Section 8.2. Next, an analytic evaluation of selected aspects of SAFE is presented in Section 8.3. The evaluation by system-level simulation is a major part of this chapter and takes place in the following two sections. Of those, Section 8.4 quantifies the performance of the individual components and determines whether each component of SAFE is necessary and beneficial. The performance of SAFE with all of its components is assessed in Section 8.5 and compared to standard LTE-V2X Mode 4.

8.1. Evaluation Methodology and Research Questions

The part of the evaluation that is carried out by simulation uses the setup and metrics described in Chapter 6. Unless noted otherwise, the configuration parameters determined in Chapter 7 are used for SAFE. They are summarised in Table 8.1. The default simulation parameters have also already been specified in Section 6.7, along with other details about the simulator in Chapter 6.

Before the actual evaluation, a set of research questions should be stated. These questions enable a focused and systematic approach to the selection of the different traffic scenarios, system configurations, and evaluation metrics. In the following, various research questions are stated, which will be answered in subsequent sections.

At first, analytic models will be used in Section 8.3 to address the following research questions:

RQ1. Acknowledgement feedback addresses radio resources, not individual packets or transmissions. Is it possible that a terminal receives feedback for resources that it used, even though this feedback was intended for a different terminal? If so, how likely is it and what are the consequences?

RQ2. What are the chances of complete blindness for extended periods of time with standard LTE-V2X Mode 4 and SAFE?

Subsequently, the individual components are of interest. The following research questions addressed in Section 8.4 using system-level simulations:

RQ3. Is every component of SAFE necessary and beneficial? Are there mechanisms or components that are superfluous?

Table 8.1.: Default Configuration Parameters for SAFE in System-Level Simulations

Parameter Name	Explained in Section	Default Value
$\mathrm{num}_{\mathrm{sub\_res}}$	5.2 (p. 73)	5
$\mathrm{ack}_{\mathrm{avg},\alpha}$	5.3 (p. 78)	1/3
$\mathrm{ack}_{\mathrm{avg},\delta}$	5.3 (p. 78)	0.1
$\mathrm{ack}_{\mathrm{min}}$	5.3 (p. 78)	0.7
$\mathrm{ack}_{\mathrm{hysteresis}}$	5.3 (p. 78)	1 s
$\mathrm{ack}_{\mathrm{sep\_pkts}}$	5.3 (p. 78)	disabled
$\mathrm{crs}_{\mathrm{min\_rating}}$	5.4 (p. 81)	900
$\mathrm{crs}_{\mathrm{min\_rating\_dcc}}$	5.4 (p. 81)	if DCC enabled
$\mathrm{crs}_{\mathrm{rssi\_weight}}$	5.4 (p. 81)	100
$\mathrm{crs}_{\mathrm{reservation\_penalty}}$	5.4 (p. 81)	0
$\mathrm{crs}_{\mathrm{reservation\_weight}}$	5.4 (p. 81)	100
$\mathrm{crs}_{\mathrm{ack\_penalty}}$	5.4 (p. 81)	100
$\mathrm{crs}_{\mathrm{ack\_weight}}$	5.4 (p. 81)	100
$\mathrm{dcc}_{\mathrm{cbr\_target}}$	5.5 (p. 82)	70 %
$\mathrm{dcc}_{\mathrm{cbr\_margin}}$	5.5 (p. 82)	0.1
$\mathrm{dcc}_{\mathrm{disable\_time}}$	5.5 (p. 82)	5 s
$\mathrm{dcc}_{\mathrm{min\_subres}}$	5.5 (p. 82)	2

RQ4. What is the performance impact of each component if it is used by itself (if possible)?

RQ5. Are there synergy effects if all components are enabled at the same time?

RQ6. Does the DCC component of SAFE ensure that the CBR is lowered? Can the DCC component of SAFE effectively limit the channel load even in extreme scenarios? Which impact does it have on the cooperative awareness and the PDR? How does the DCC of SAFE compare to the DCC version of LTE-V2X Mode 4?

Lastly, the performance of the complete system is of importance. The research questions addressed in Section 8.5 are stated as:

RQ7. How is the performance compared to standard LTE Mode 4 in configurations that are beneficial towards standard LTE? This means that a fixed rate of equally sized packets is used, while the channel load is low enough that DCC would not make a huge difference. Additionally, DCC will be disabled for both technologies for this investigation, as DCC has been shown to lead to only small or no performance gains for standard LTE.

RQ8. Is the hidden-terminal mitigation working? This could be answered by looking at the impact of SAFE on the performance in higher transmission distances.

RQ9. Is the effect of repeating collisions mitigated, i.e. does SAFE lead to a more robust communication?

RQ10. How does SAFE perform compared to LTE-V2X Mode 4 if a channel model that explicitly and deterministically models obstacle shadowing is used?

RQ11. How many padding bits, i.e. acknowledgement overhead, are necessary for SAFE? How does it perform in situations with low amounts of available padding bits?

RQ12. How well does SAFE handle packet flows with different packet sizes and rates? How does SAFE compare to standard LTE-V2X Mode 4 in such situations?

Most of these questions will be investigated using traditional metrics such as the PDR, and application-oriented metrics such as the cooperative awareness. The importance of those application-oriented metrics has been motivated in Chapter 4.

8.2. Qualitative Discussion

In Chapter 3, many functional requirements for resource allocation and congestion control have been outlined. In this section, it will be discussed whether SAFE is able to fulfil these.

8.2.1. Functional Requirements

The following functional requirements were identified both for the MAC protocol and DCC:

Coordination of resource allocation and scheduling: Like standard LTE-V2X, SAFE leverages SC-FDMA and is able to allocate the radio resources to terminals in a distributed way with the same granularity as LTE-V2X. Through the introduction of sub-reservations, SAFE is even able to support packet flows with lower packet rates while retaining the periodicity of the resource allocation.

Detection of collisions by the transmitter itself: As hardware restrictions and the broadcast communication makes a collision detection like in wired networks (e.g. carrier sense multiple access/collision detection (CSMA/CD)) infeasible, a more efficient heuristic had to be used to fulfil this requirement. Using the acknowledgement ratio of their own used radio resources, terminals can now detect to which extend their transmissions were successful.

Reaction to detected collisions: If the terminals detect that their transmission was not received by a large number or part of the potential receivers, SAFE reacts by dropping the resources early and selecting new ones ahead of time to prevent further repeating collisions. Hence, this requirement is fulfilled.

Restriction of radio resource use in high load scenarios: The DCC component of SAFE disables sub-reservations of packet flows if the current CBR is above a pre-configured threshold. Hence, the packet rate of all packet flows can be restricted with the granularity of the sub-reservation scheme.

8.2.2. Non-Functional Requirements

Many non-functional requirements were stated in Chapter 3. Of those, the PDR, application performance, scalability (i.e. operation in extreme scenarios), generality (performance in different traffic scenarios), reliability and robustness (despite difficulties in the vehicular scenario) are implicitly or explicitly evaluated in Section 8.4 and 8.5. The qualitative discussion includes the following remaining non-functional requirements:

Overhead and throughput: The only additional protocol overhead of SAFE is related to the acknowledgement feedback. SAFE is designed to use the available padding bits for the transmission of this information. This feedback can be of arbitrary size. The necessity for additional radio resources needs to be quantified in Section 8.5.

Latency: As SAFE uses the same selection window for the initial selection of candidate resources as LTE-V2X does, it does not lead to any additional latency from a transmitter's perspective. From the perspective of the receivers, the introduction of sub-reservations can lead to heavily decreased time periods until a message can be successfully received. This is because the impact of repeating collisions is reduced by the sub-reservations.

Quality of service: SAFE does not use the QoS mechanism of the MAC layer that LTE-V2X uses, i.e. the consideration of explicit reservations depending on the priorities and the RSRP. This is motivated by the findings in Section 4.1.1.1, which indicated that this feature has negative effects on the overall performance and might lead to increased collision probabilities even for packets with higher priorities. QoS aspects from the physical layer, i.e. the use of more radio resources with a lower MCS index and a more robust modulation scheme, remain possible. The DCC part of SAFE currently focuses on the sub-reservations that are likely to be affected by collisions anyway, but it ensures that at least some of the sub-reservations per packet flow will be transmitted. If necessary, it could be implemented that packet flows with a certain priority, e.g. high-priority DENMs, will not be restricted by DCC. Moreover, if additional QoS measures are necessary, the minimum rating of candidate resources $\mathrm{crs}_{\mathrm{min\_rating}}$ could be set for different packet priorities.

Fairness: Two different mechanisms of SAFE can prevent terminals from transmitting a packet: the minimum rating feature of the candidate resource selector, and the DCC component itself. SAFE ensures that each terminal is able to transmit a minimum number of messages despite both of these mechanisms. The minimum rating of a resource is not relevant if the terminal is currently using less than 0.0024 of the radio resources of the last second. This equals twelve single-subchannel resources per second. The DCC component does not restrict packet flows any further if it already uses two or less of its sub-reservations.

Autonomous operation: SAFE is a distributed and autonomous protocol by design. No base station or central entity is involved. Moreover, there is no single terminal that is detrimental to the performance of SAFE, as every terminal has the same role.

Compatibility: It was required that SAFE does not deviate substantially from LTE-V2X Mode 4 and keeps the compatibility with SC-FDMA and the resource grid. SAFE uses SC-FDMA and even leverages some of its features such as the subchannels or slotted subframe structure. Moreover, it uses the resource grid without modification. The introduction of sub-reservations merely changes the typical reuse intervals of resources. Terminals only need to consider the lengthened interval between resource reuses. The fact that sub-reservations are interleaved is implicitly respected. SAFE can only work to its full potential if every terminal that uses the communication channel also follows the same protocol. Hence, acknowledgement feedback should be exchanged and the candidate resource selector and DCC component of SAFE should be used by every terminal. The size of this acknowledgement feedback is variable and it is transmitted in the padding bit area, which is not interpreted in LTE-V2X Mode 4 implementations.

8.3. Analytic Evaluation of Selected Aspects

Due to the complexity of LTE-V2X Mode 4 and the amount of state that each terminal has to carry, an analytic evaluation of the complete access technologies is impractical. Nevertheless, some selected aspects are evaluated with simplified analytic models in this section.

8.3.1. Interpretation of Acknowledgment Feedback by Different Terminals

This section aims to answer the question whether acknowledgement feedback could be interpreted by the wrong transmitter. Intuitively, this could happen as the acknowledgement feedback addresses used radio resources and not transmitters or specific packets.

The following analysis investigates whether this can occur in idealised conditions. The following assumptions are made about the scenario:

- The vehicles do not significantly change their relative position until a radio resource is acknowledged.
- The interference pattern is consistent and only depends on the distance between the terminals.
- If a receiver is inside the transmission range of two transmitters that use the same radio resource, there is a collision, and the receiver is unable to receive any of the messages. Hence, the capture effect does not occur.

The following discussion will be split into two parts. These parts are formulated as:

Lemma 1: If a terminal sends a negative acknowledgement, it will always reach the correct transmitters.

Lemma 2: If a terminal sends a positive acknowledgement, it will not reach any other transmitter that used the same radio resource.

If these two lemmas are shown to be correct, it follows that acknowledgement feedback cannot reach the wrong transmitters under the assumptions mentioned previously. Both of these lemmas are proven by assuming the opposite and producing a contradiction.

For the case of Lemma 1, assume that a terminal T_1 sends a negative acknowledgement. If Lemma 1 is negated, it follows that there is at least one transmitter T_2 that receives this negative acknowledgement even though it should have received a positive acknowledgement. However, if this transmitter T_2 is supposed to receive a positive acknowledgement, T_1 is also supposed to have received the transmission of this transmitter in this exact radio resource. This is a contradiction towards the assumption: if T_1 would have successfully received any message on this radio resource, it would have sent a positive acknowledgement. Hence, Lemma 1 correct.

Lemma 2 is also shown to be correct by contradiction: Assume that a terminal R sends a positive acknowledgement due to a packet from transmitter T_1 that it received successfully. From the negation of Lemma 2 follows that this acknowledgement reaches a different transmitter T_2 that used the exact same radio resource. This transmitter T_2 must be inside the transmission range of R or the acknowledgement would not have been received by T_2. As R has sent a positive acknowledgement to T_1, it must have received its transmission. Hence, R is in the transmission range of both T_1 and T_2. As both T_1 and T_2 used the same radio resource for their transmissions, it follows that there must have been a collision at R. However, in this case, R would not have received any of the transmissions and would have sent a negative acknowledgement. This is a contradiction of the assumption and hence, Lemma 2 is correct.

The assumptions made prior to this proof could be violated in corner cases in practice. A positive acknowledgement could be received in the following conditions:

- There are influences that can change the reception power of the noise or desired signal for the acknowledgement feedback, which is sent at a later point in time. For example, additive background interference might change as other interferers choose different radio resources. The vehicles can also slightly change position until the acknowledgements are sent. Typically, this time interval is less than $200\,\mathrm{ms}$. Longer report intervals would require more than one thousand padding bits. In this short time period, only fast fading effects are relevant. Other external influences like external emitters or thermal noise could contribute to a change of reception power as well.
- The capture effect could contribute to situations in which acknowledgement feedback reaches the wrong terminal. Due to the capture effect, a receiver might be able to receive a transmission despite being inside the transmission range of two different transmitters that are currently active. This receiver can later distribute positive acknowledgements to both of them as they are inside the transmission range. The capture effect is dependent on the performance of the actual transceiver hardware.

The previous considerations showed that it is impossible under idealized conditions that an acknowledgement reaches the wrong terminal. In practice, positive acknowledgements could reach the wrong terminal due to fast fading influences or the capture effect.

This raises the question: what are consequences of positive acknowledgements that reach the wrong terminals? Only the reaction to acknowledgements is relevant for this case. A terminal that received positive acknowledgements for resources that it used for transmission itself might be incorrectly influenced to keep re-using this sub-reservation if the reselection counter is still above zero. Hence, the reactive component of the acknowledgement feedback might not be triggered in this case. This effect is limited in time until the reselection counter reaches zero or the enough negative acknowledgements reach the terminal. The consequences of this are small. Hence, addressing radio resources instead of individual transmissions with acknowledgement feedback is a efficient and sufficiently reliable method to enable hidden-terminal mitigation for periodic broadcast traffic.

8.3.2. Probability of Collisions with All Sub-Reservations

Section 4.2.1 showed that repeating collisions pose a risk to traffic safety by reducing the cooperative awareness when using LTE-V2X Mode 4. SAFE was specifically designed to reduce the likelihood and impact of those repeating collisions. This is realized through reservation splitting and the reaction to acknowledgement feedback. The goal of this section is to determine analytically how successful reservation splitting is.

As the transmission reliability depends on the access technology, traffic scenario, and transmission distance, this analysis should be performed with multiple values for the reception probabilities of a packet. The reselection counter range is also between 5 and 15 for SAFE even when reservation splitting is used. Hence, the number of resource reuses stays the same. Using five sub-reservations, the time interval until a sub-reservation is reused is increased by five times. Therefore, unless a reaction to acknowledgement feedback triggers the selection of new radio resources ahead of time, the time interval of repeating collisions can actually be longer. However, all five sub-reservations need to be affected by repeating collisions for the specified duration of blindness.

The following analysis is performed under the assumption that the safety-critical reaction time is $500\,\mathrm{ms}$. This contrasts with the awareness metric used in the simulations, which is influenced by the CAM lifetime of one second.

8.3.2.1. SAFE

During the observation time, there are no resource reuses when using SAFE. The probability to choose an unoccupied resource p_r is fixed, but different values will be used. The formula to determine the probability of complete blindness during the observation period will be derived in this section. Example calculations for SAFE and LTE-V2X Mode 4 are performed in Section 8.3.2.3. The terminal under observation has a chance of $1 - p_r$ to occupy a resource that is already occupied and cause a collision. This analysis does not consider possible advantages of the reaction to acknowledgement feedback. As the acknowledgement feedback can only shorten the reuse interval of resources with bad performance, this analysis serves as an upper boundary to the performance of SAFE. All of the messages in the $500\,\mathrm{ms}$ time period are affected by collisions with the following probability:

$$P_{\text{blind,SAFE}}\left(p_r\right) = \left(1 - p_r\right)^5$$

This is because all five sub-reservations need to choose radio resources that are already occupied.

8.3.2.2. LTE-V2X Mode 4

For standard LTE-V2X Mode 4, resources are repeated at most five times in the $500\,\mathrm{ms}$ window. In order to determine the probability of total overlap, the probability of selecting an already occupied resource needs to be multiplied with the probability that the two resources overlap for the complete observation interval of $500\,\mathrm{ms}$. The second probability is under the precondition that the terminal under observation has chosen a resource that is already occupied.

In Section 4.2.1, the lower boundary of the average overlapping of resources if a collision happened was determined to be approximately 4.88. As this number is not precisely five and the median might be different from this mean value, it cannot be assumed that resources overlap at least five times if a collision happened with a probability of about $50\,\%$. Thus, the exact probability should be determined more precisely.

Figure 8.1 shows the different configurations of the two radio resources. One resource or reuse of the resource is represented in a quadratic box. The boxes are filled with a number which indicates at which randomly chosen reselection counter the reuse of that resource ends. The different rows in Figure 8.1 indicate different start positions for the transmitter that is affected by collisions. It can be seen that the later the start position is, the more reselection counter values lead to a complete overlap. Resource reselection counter values that lead to a complete overlap are coloured grey. The last possible start position is $t = 10$ because of the aforementioned precondition that the radio resource is already occupied at the time of the first use.

The start position of a transmitter and the chosen value of the reselection counter are independent random variables. The probability of total overlap under the precondition can hence be determined by counting the number of configurations in which a total overlap happens and dividing it through the number of total configurations valid according to the precondition.

As it can be seen in Figure 8.1, for $t = 0$, only one configuration leads to a complete overlap. If the reselection counter is less than 15, the last slots in the observation period are not affected

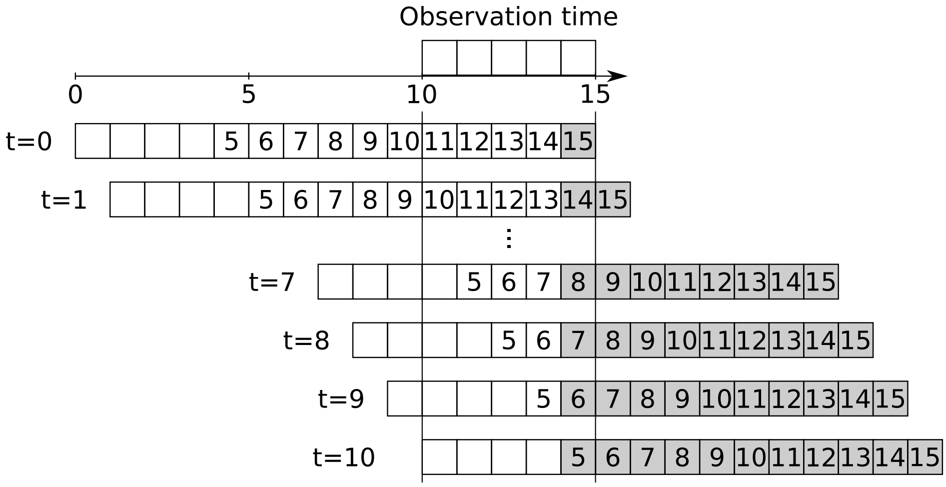

Figure 8.1.: Visualisation of configurations with collisions and overlap in the $500\,\mathrm{ms}$ observation period, depending on different start times and reselection counter values of the other terminal.

by collisions. With each step towards a later t, the number of configurations with collisions as well as the number of configurations with total overlap in the observation period increases. At $t = 7$, a new situation arises. The smallest possible reselection counter value is after the start of the observation period. Hence, the number of possible configurations that cause collisions cannot get past eleven. Each of the start positions t are equally likely. There are eleven of them. Hence, the probability to choose a specific t is $1/11$.

With the previous considerations, the probability for total overlap during $500\,\mathrm{ms}$ if the transmitter under observation chose a resource that is already occupied is:

$$\begin{aligned} P_{\text{overlap,LTE}} &= \frac{1}{11} \times \frac{|[15]|}{|[11,\ldots,15]|} + \frac{1}{11} \times \frac{|[14,15]|}{|[10,\ldots,15]|} + \cdots \\ &+ \frac{1}{11} \times \frac{|[8,\ldots,15]|}{|[5,\ldots,15]|} + \frac{1}{11} \times \frac{|[7,\ldots,15]|}{|[5,\ldots,15]|} + \cdots + \frac{1}{11} \times \frac{|[5,\ldots,15]|}{|[5,\ldots,15]|} \\ &= \frac{1}{11} \times \left(\frac{1}{5} + \frac{2}{6} + \frac{3}{7} + \frac{4}{8} + \frac{5}{9} + \frac{6}{10} + \frac{7}{11} + \frac{8}{11} + \frac{9}{11} + \frac{10}{11} + \frac{11}{11} \right) \\ &\approx 60.99\,\% \end{aligned}$$

Hence, the probability for total blindness for a LTE-V2X Mode 4 terminal that selects a new unoccupied resource with probability p_r is:

$$P_{\text{blind,LTE}}\left(p_r\right) = \left(1 - p_r\right) \times P_{\text{overlap,LTE}} \approx \left(1 - p_r\right) \times 60.99\,\%$$

8.3.2.3. Examples and Conclusion

Using the equations derived in the previous sections, the probability of total blindness for a terminal will be determined. The values $90\,\%$, $95\,\%$, and $99\,\%$ will be used as possible values for the probability to choose a free radio resource (p_r). The results can be seen in Table 8.2.

With $p_r = 90\,\%$, the probability of total blindness for a LTE terminals is about $6\,\%$. This risk is certainly too high for safety-critical applications such as vehicular traffic. As all five sub-reservations of SAFE need to be affected simultaneously, the probability is orders of magnitudes lower. Using this analysis, it is shown that reservation splitting by itself already ensures that SAFE is by far more applicable as technology for the exchange of safety-critical information.

Table 8.2.: Analytically Derived Probability of Total Blindness

p_r [%]	LTE	SAFE
90	0.0610	10^{-5}
95	0.0305	3.13×10^{-7}
99	0.0061	10^{-10}

8.4. Quantitative Evaluation of Individual Components

The goal of this section is to determine the performance impact of each individual component by using simulations as evaluation methodology. Additionally, potential synergy effects of a combined system are quantified. The reservation splitting, candidate resource selection, and reaction to acknowledgement feedback components are individually evaluated in Section 8.4.1, while DCC is evaluated separately in Section 8.4.2. Please see the default simulation parameters in Section 6.7 (p. 102) and the configuration parameters of SAFE in Table 8.1 (p. 128)

8.4.1. Reservation Splitting, Resource Selection, and Acknowledgment Feedback

The design of SAFE is motivated by the assumption that its individual components (reservation splitting, reaction to acknowledgement feedback, a candidate resource selector that considers acknowledgement feedback, and a DCC algorithm) work best in conjunction. This means that there should be synergy effects when using all the components of SAFE. Nevertheless, as stated in Chapter 5, some of its components can also be deployed individually. For some of the components, the lack of complementing mechanisms means that they operate with a limited functionality. For example, the candidate resource selector cannot consider acknowledgement feedback if acknowledgements are not enabled. However, it can still calculate the rating of the candidate resources using the other criteria.

In this section, reservation splitting, the reaction to acknowledgement feedback, and the candidate resource selector are evaluated individually. Additionally, the candidate resource selector is evaluated in conjunction with acknowledgement feedback in order to quantify possible synergy effects. Those configurations are compared to standard LTE-V2X Mode 4 and the complete system (SAFE). As DCC is evaluated in a subsequent section, it is disabled for all of the configurations in this subsection. The Luxembourg scenario at 8:00 has been used for this evaluation.

Table 8.3 summarizes the results for these configurations. Figure 8.2 shows the mean PDR for different transmission ranges and Figure 8.3 shows a quantile function plot of the percentage of time with ideal awareness for the vehicles in the simulation. The only component with no significant influence on the PDR is reservations splitting. This is expected, as this mechanism is not designed to increase the PDR by itself, but rather to make it less likely that a vehicle is unable to distribute status updates for extended periods of time. This is reflected in the results for the cooperative awareness. Reservation splitting is responsible for most of the improvement of the cooperative awareness that SAFE can reach. Still, SAFE, i.e. the combination of the components, outperforms reservations splitting itself. This indicates that the components perform better in conjunction.

The other components lead to comparatively small increases of the cooperative awareness by themselves. However, the goal of those is to increase transmission reliability for each transmitted packet. Hence, the effects are more clearly visible under the PDR metric in Figure 8.2. The reaction to acknowledgements only leads to a small increase of the PDR. This is not plotted in Figure 8.2 because it almost completely overlaps with the configuration of the candidate resource selector without acknowledgements. This configuration also leads to very small improvements of the performance. However, if the acknowledgements and the candidate resource selector is enabled in conjunction, a large increase of the PDR can be seen, especially in larger transmission distances. This indicates that the proactive hidden-terminal mitigation, i.e. penalizing candidate resources that already have been acknowledged by terminals further away, plays a major role for the performance of SAFE. When additionally enabling the reaction to low acknowledgement ratios and reservation splitting, all of the components of SAFE are active, with the exception of DCC. This leads to additional gains that are larger than the sum of the individual gains of the components. There are two possible reasons for this, both of which might be valid at the same time. Firstly, it might indicate that the reaction to acknowledgements benefits from reservation splitting. An explanation for this is that the average acknowledgement ratio is built using five *different* radio resources. It is thus more representative of the true mean acknowledgement ratio in the current situation. Secondly, the reactive hidden-terminal mitigation, i.e. the selection of new radio resources when low acknowledgement ratios are reported, now happens only for a subset of the radio resources that are currently used. This means that the periodicity of the other sub-reservations is retained while preventing reoccurring collisions of only one sub-reservation.

In conclusion, it can be said that each of the components of SAFE leads to an increased PDR or cooperative awareness when used individually. However, the full potential can only be realized when they work in conjunction.

8.4.2. Distributed Congestion Control

The DCC component cannot be evaluated without also using the other components of SAFE. Reservation splitting is necessary to semi-persistently disable resources, the candidate resource selector has a DCC component by considering the minimum candidate resource rating, and the acknowledgement feedback is used to identify sub-reservations with bad performance, which will be preferentially disabled by DCC. However, SAFE can be used with or without DCC. Hence, the impact of DCC can still be quantified.

Table 8.3.: Simulation Results: Reservation Splitting, Resource Selection, and Acknowledgement Feedback

Approach	PDR [%] ($d \leq 100\,\mathrm{m}$)	PDR [%] ($d \leq 300\,\mathrm{m}$)	Time with 100 % Awareness [%]
SAFE without DCC	98.34 ± 0.05	88.62 ± 0.31	92.7 [92.3, 92.8]
Acknowledgement Reaction	97.24 ± 0.08	80.97 ± 0.42	44.5 [42.6, 46.6]
Reservation Splitting	96.43 ± 0.09	78.72 ± 0.44	87.0 [86.7, 87.9]
CRS with Ack.	96.52 ± 0.11	84.53 ± 0.38	56.9 [55.0, 59.0]
CRS without Ack.	95.05 ± 0.14	79.59 ± 0.36	41.6 [39.8, 43.2]
LTE without DCC	96.46 ± 0.10	78.70 ± 0.36	40.2 [37.8, 41.7]

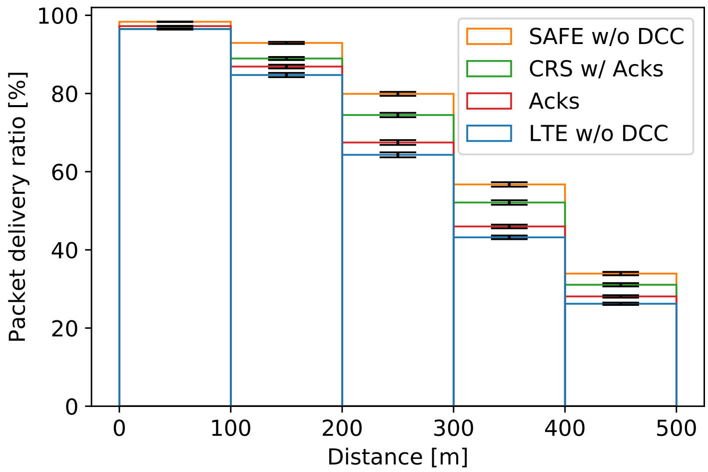

Figure 8.2.: Evaluation of individual components: mean PDR depending on transmission distance. Reservation splitting has no visually distinguishable effect on the PDR and is not plotted. The candidate resource selector without acknowledgements leads to similar results as the acknowledgement configuration itself and is also not plotted. (Error bars indicate confidence intervals with a confidence level of $95\,\%$.)

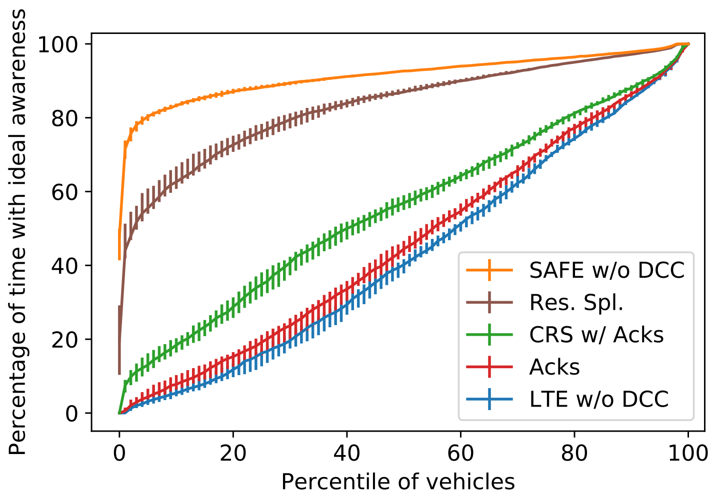

Figure 8.3.: Evaluation of individual components: quantile function plot of the percentage of time with ideal awareness for the range of $0\,\mathrm{m}$ to $300\,\mathrm{m}$. (Vertical lines indicate asymmetric confidence intervals with at least $95\,\%$ confidence level. Horizontal connecting lines cross the confidence interval bars at the median, but are for visualisation purposes only in between.)

Traffic scenarios with a high traffic load need to be selected for the evaluation of DCC. In this section, the Luxembourg scenario at 08:00, the Autobahn scenario with a traffic jam, and the Manhattan grid scenario with $150\,\%$ traffic load have been used. The results of the simulations are summarized in Figure 8.4 and 8.5, and Table 8.4.

Looking at the PDR, it can be seen that SAFE heavily profits from its DCC component. This is unlike standard LTE, which sees marginal improvement only in the Autobahn scenario with a traffic jam. This is the scenario that leads to the highest channel load. The performance of LTE is decreased even with shorter transmission distances, but most noticeably in larger ones. Even when enabling DCC, the channel load is still high enough to cause the MAC protocol to fail often, resulting in low PDR values. This indicates that the DCC component of LTE is not restrictive enough and fails to meet the most important functional requirement of DCC. The reason for this is the static mapping of CR values to CBR values, making a dynamic reaction to extreme situations impossible. In this case, the static configuration of this mapping is not suitable for this scenario, causing the DCC component to be too relaxed. Similar conclusions could be drawn in the other scenarios, although with less severity.

SAFE is able to keep the PDR higher in general, but also the performance improvement of DCC is more distinct. This might be due to the following features: Firstly, a CBR target is set, and SAFE can react to different situations more dynamically. Secondly, the DCC component of SAFE prioritizes on limiting sub-reservations that already cause collisions. This means that it not simply reduces the channel load, but actively reduces the number of radio frame collisions.

The DCC component of standard LTE does not have any significant effect on the cooperative awareness. This is because even though the communication performance is already reduced due to high channel load, DCC does not become active very often to restrict terminals. Naturally, DCC restrictions of SAFE decrease the cooperative awareness to some extent. This is caused by sub-reservations being disabled, limiting the number of different radio resources that a terminal can use and therefore limiting the probability of having one or more sub-reservations that are completely collision-free even for receivers further away. SAFE is still able to maintain a large advantage over LTE with regard to the cooperative awareness.

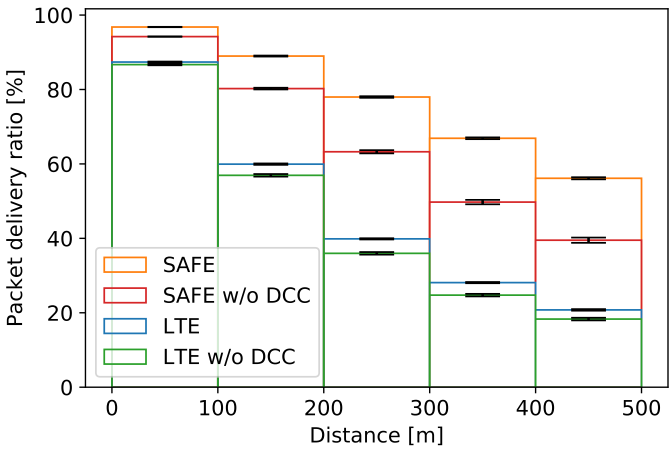

(a) Autobahn with traffic jam

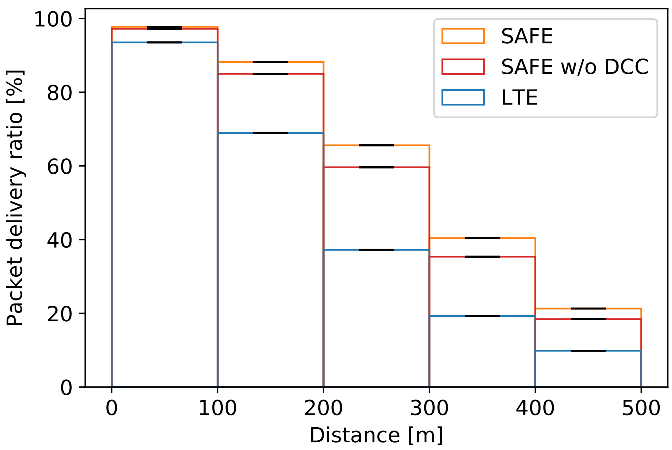

(b) Manhattan with 150 % traffic load

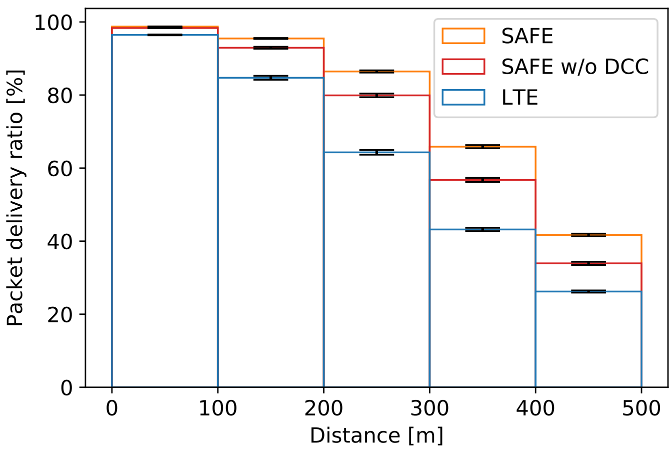

(c) Luxembourg at 8:00

Figure 8.4.: Evaluation of DCC: mean PDR depending on transmission distance. Non-DCC configurations missing from the plots are not visually distinguishable from their DCC counterpart. (Error bars indicate confidence intervals with a confidence level of 95 %.)

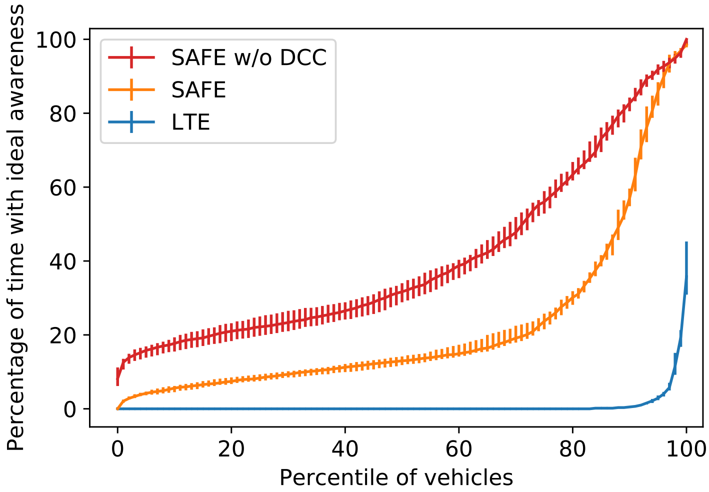

(a) Autobahn

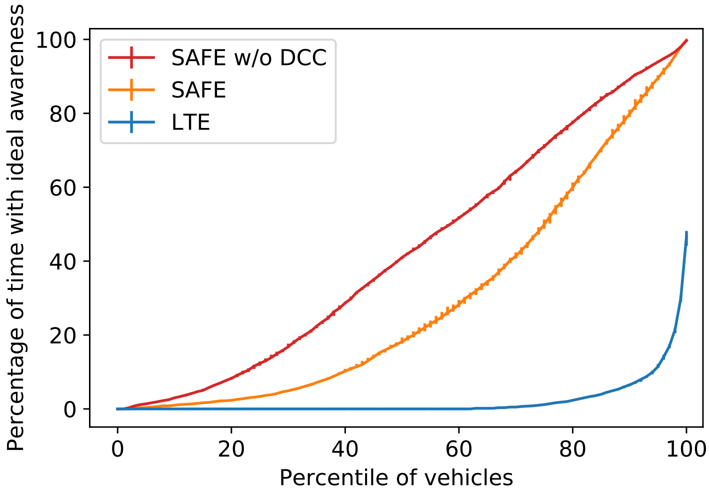

(b) Manhattan

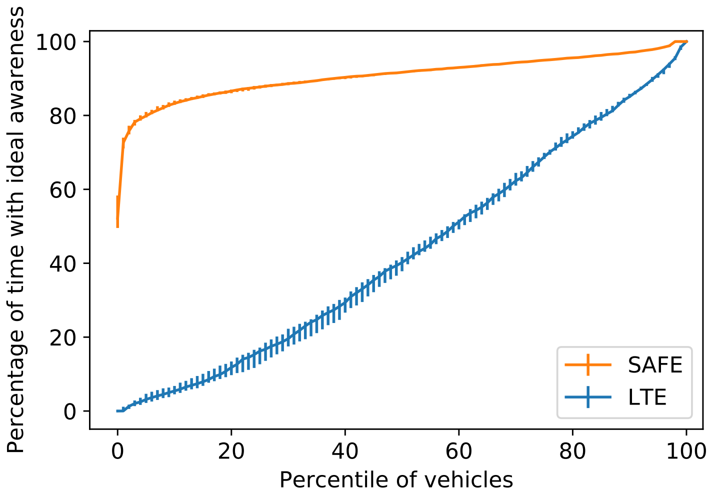

(c) Luxembourg at 08:00

Figure 8.5.: Evaluation of DCC: quantile function plot of the percentage of time with ideal awareness for the range of $0\,\mathrm{m}$ to $300\,\mathrm{m}$. Non-DCC configurations missing from the plots are not visually distinguishable from their DCC counterpart. (Vertical lines indicate asymmetric confidence intervals with at least $95\,\%$ confidence level. Horizontal connecting lines cross the confidence interval bars at the median, but are for visualisation purposes only in between.)

Table 8.4.: Simulation Results: DCC

Scenario	Approach	PDR [%] ($d \leq 100\,\mathrm{m}$)	PDR [%] ($d \leq 300\,\mathrm{m}$)	Time with $100\,\%$ Awareness [%]
Autobahn (traffic jam)	LTE	87.38 ± 0.13	63.39 ± 0.17	$0.0\,[\;0.0,\;\;0.0]$
	LTE w/o DCC	86.69 ± 0.19	60.83 ± 0.31	$0.0\,[\;0.0,\;\;0.0]$
	SAFE	96.79 ± 0.05	88.46 ± 0.12	$13.0\,[11.8, 14.2]$
	SAFE w/o DCC	94.21 ± 0.07	79.87 ± 0.24	$31.7\,[28.8, 34.0]$
Luxembourg (08:00)	LTE	96.46 ± 0.10	78.70 ± 0.45	$40.2\,[37.8, 41.7]$
	LTE w/o DCC	96.46 ± 0.10	78.70 ± 0.45	$40.2\,[37.8, 41.7]$
	SAFE	98.73 ± 0.03	92.40 ± 0.18	$91.7\,[91.4, 91.8]$
	SAFE w/o DCC	98.34 ± 0.05	88.62 ± 0.31	$92.7\,[92.3, 92.8]$
Manhattan ($150\,\%$ traffic)	LTE	93.51 ± 0.05	55.72 ± 0.06	$0.0\,[\;0.0,\;\;0.0]$
	LTE w/o DCC	93.49 ± 0.05	55.47 ± 0.07	$0.0\,[\;0.0,\;\;0.0]$
	SAFE	97.76 ± 0.02	77.95 ± 0.04	$18.2\,[17.7, 19.3]$
	SAFE w/o DCC	97.22 ± 0.02	73.47 ± 0.06	$41.0\,[40.5, 41.1]$

8.5. Quantitative Evaluation of the Complete System

In this section, SAFE with its default configuration that was determined in Chapter 7 will be evaluated in different scenarios. The standard-compliant implementation of LTE-V2X Mode 4 will be used for comparison. Different aspects and special scenarios will be evaluated in the following sections.

8.5.1. Evaluation Under Conditions Favourable for Standard LTE-V2X

In this section, an evaluation under conditions that are rather favourable for the standard LTE-V2X will be performed. This means that a fixed CAM rate of $10\,\mathrm{Hz}$ will be used. All CAMs have a size of $200\,\mathrm{B}$. This is in line with the assumption of LTE-V2X that V2V communication predominantly exchanges periodic messages. In Europe, this might not be realized in practice (see Section 2.3.2.2). Additionally, DCC has been disabled in both configurations, as it leads to no or only small improvements for standard LTE-V2X Mode 4. Configurations with DCC have been performed in Section 8.4.2.

As traffic scenarios, the Luxembourg scenario at 08:00 and 11:30, the Manhattan grid scenario, and the Autobahn without a traffic jam have been chosen. The results are summarized in Table 8.5. Additionally, Figure 8.6 shows the PDR subject to the transmission distance, while Figure 8.7 shows a quantile function plot of the percentage of time with ideal awareness.

The results show that SAFE performs better than standard LTE-V2X Mode 4 in every traffic scenario and under every metric. Figure 8.6 shows that SAFE is able to reach significantly more vehicles that are further away. This improved performance at larger transmission

Table 8.5.: Simulation Results: Conditions Favourable for LTE-V2X

Scenario	Approach	PDR [%] ($d \leq 100\,\mathrm{m}$)	PDR [%] ($d \leq 300\,\mathrm{m}$)	Time with 100 % Awareness [%]
Autobahn	LTE	97.50 ± 0.12	95.41 ± 0.43	84.7 [82.2, 87.2]
	SAFE	98.84 ± 0.04	98.29 ± 0.14	95.8 [95.2, 96.2]
Luxembourg (11:30)	LTE	98.54 ± 0.06	94.94 ± 0.10	94.7 [94.3, 95.2]
	SAFE	99.08 ± 0.03	96.75 ± 0.06	98.3 [98.2, 98.3]
Luxembourg (08:00)	LTE	96.46 ± 0.10	78.70 ± 0.45	40.2 [37.8, 41.7]
	SAFE	98.34 ± 0.05	88.62 ± 0.31	92.7 [92.3, 92.8]
Manhattan	LTE	96.27 ± 0.03	68.65 ± 0.09	7.3 [7.2, 7.5]
	SAFE	98.53 ± 0.02	85.54 ± 0.06	93.8 [93.5, 94.0]

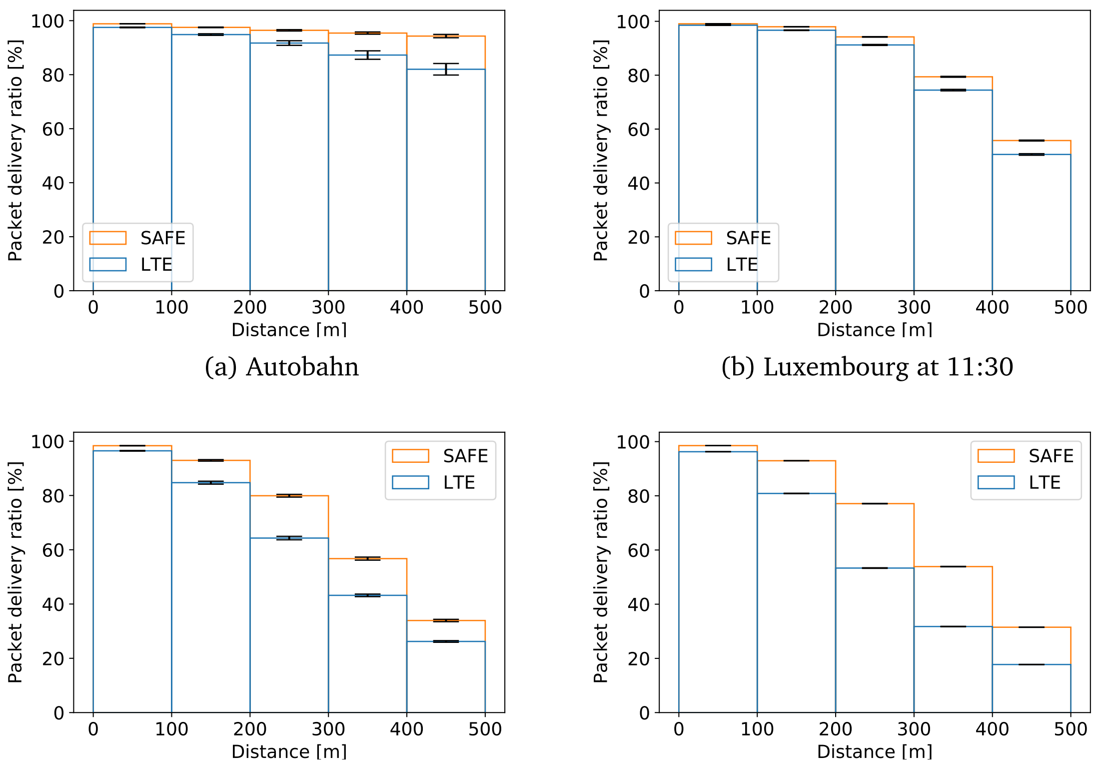

(a) Autobahn

(b) Luxembourg at 11:30

(c) Luxembourg at 08:00

(d) Manhattan

Figure 8.6.: Evaluation under conditions favourable for LTE-V2X: mean PDR depending on transmission distance. (Error bars indicate confidence intervals with a confidence level of 95 %.)

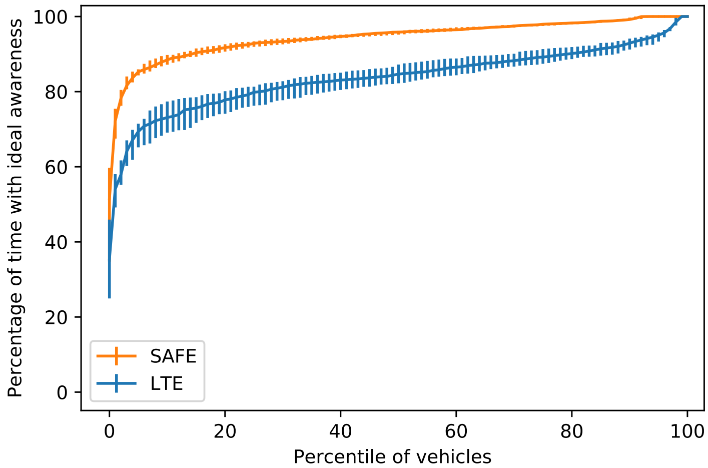

(a) Autobahn

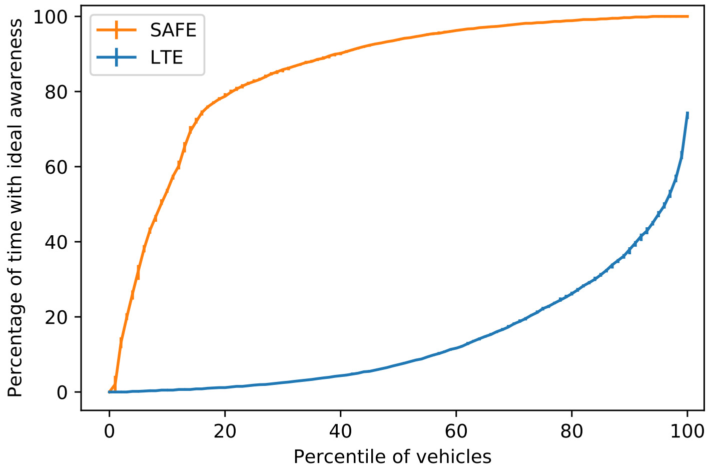

(b) Manhattan

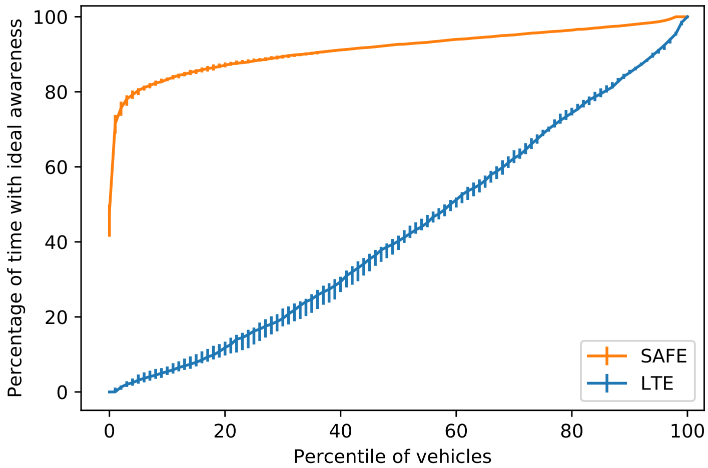

(c) Luxembourg at 08:00

Figure 8.7.: Evaluation under conditions favourable for LTE-V2X: quantile function plot of the percentage of time with ideal awareness for the range of $0\,\mathrm{m}$ to $300\,\mathrm{m}$. (Vertical lines indicate asymmetric confidence intervals with at least $95\,\%$ confidence level. Horizontal connecting lines cross the confidence interval bars at the median, but are for visualisation purposes only in between.)

distances might be a direct result of the acknowledgement feedback. It is an indicator that the acknowledgement feedback indeed leads to an increase of the effective sensing range because collisions with radio frames of transmitter further away are more effectively mitigated with SAFE. SAFE leads to the most impressive improvements of the PDR compared to standard LTE-V2X in the Manhattan grid scenario at larger distances, e.g. between $200\,\mathrm{m}$ to $300\,\mathrm{m}$. Of the used traffic scenarios, the Manhattan scenario leads to the highest average channel utilisation. The results of SAFE indicate that it can reach a higher PDR and spatial reuse in such conditions.

The results regarding the cooperative awareness are even more interesting. Various components of SAFE aim at making the communication more robust. For example, the reservation splitting makes it less likely that there are time periods in which all of the transmitted radio frames of a terminal collide with other packets. Moreover, the acknowledgement feedback enables the terminals to quickly react to disadvantageous radio resource allocations. These mechanism lead to high increases of the percentage of time with ideal awareness (Figure 8.7).

The results of the Autobahn scenario and the Luxembourg scenario at 11:30 are very similar. Hence, only the Autobahn scenario is shown. Standard LTE-V2X Mode 4 is already able to reach a robust awareness in these low-load scenarios. However, SAFE is able to consistently and significantly increase the time with ideal awareness for almost any vehicle in the scenario.

The results of the traffic scenarios with a higher channel load show the largest differences in performance between LTE-V2X mode and SAFE. Especially in the Manhattan grid scenario, the percentage of time with ideal awareness when using LTE-V2X is so low that its deployment can hardly be justified. For example, the $50\,\%$ of the best performing vehicles have ideal awareness about their surrounding cars only for $7\,\%$ or more of the time when using standard LTE-V2X Mode 4. When using SAFE, these vehicles have ideal awareness $94\,\%$ or more of the time.

8.5.2. Performance with Explicit Shadowing by Buildings and Vehicles

The performance of LTE-V2X and SAFE could be influenced by the variability that occurs due to shadowing of radio signals by obstacles. Hence, a study with channel models that consider shadowing effects of vehicles and buildings deterministically should be performed. The obstacle shadowing model used for this analysis has been presented in Section 6.5.2. A simple free-space path loss model has been used as complementary model for non-obstructed fading. Due to the computational complexity of the shadowing model, a smaller area of Luxembourg without border areas has been used as described in Chapter 6.

The results of this analysis are summarized in Table 8.6. The detailed awareness results can be seen in Figure 8.9, while the PDR statistics are visualized in Figure 8.8. The awareness results have been restricted to $95\,\%$ because the *ideal awareness* requirement cannot be reached in longer distances regardless of the MAC performance. Moreover, the obstacle shadowing model

Table 8.6.: Simulation Results: Explicit Shadowing by Buildings and Vehicles

Approach	PDR [%] ($d \leq 100\,\mathrm{m}$)	PDR [%] ($d \leq 300\,\mathrm{m}$)	Time with $100\,\%$ Awareness ($100\,\mathrm{m}$) [%]
LTE	91.50 ± 0.35	53.22 ± 0.65	$74.4\,[72.9, 75.5]$
SAFE	94.16 ± 0.29	56.81 ± 0.70	$80.2\,[79.5, 82.2]$

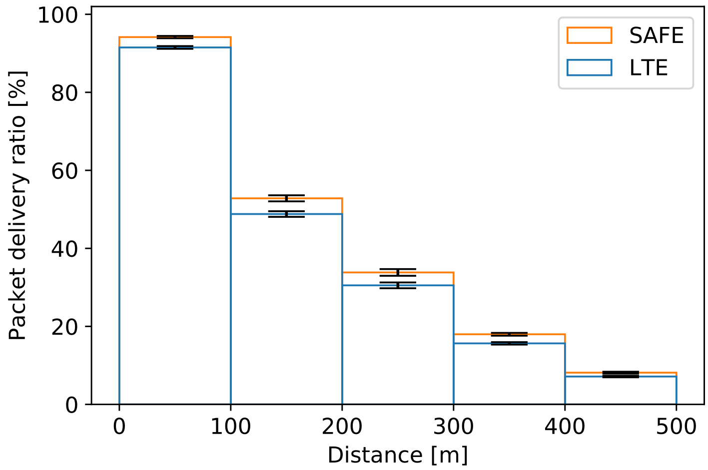

Figure 8.8.: Evaluation with explicit shadowing by buildings and vehicles: mean PDR depending on transmission distance. (Error bars indicate confidence intervals with a confidence level of $95\,\%$.)

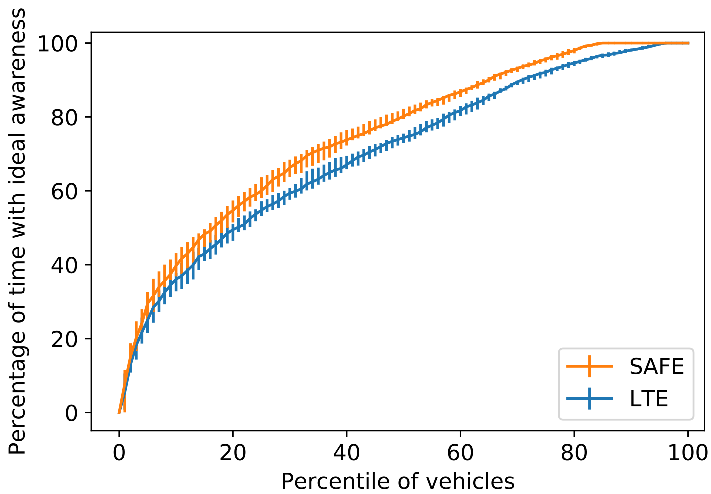

Figure 8.9.: Evaluation with explicit shadowing by buildings and vehicles: quantile function plot of the percentage of time with ideal awareness for the range of $0\,\mathrm{m}$ to $100\,\mathrm{m}$. (Vertical lines indicate asymmetric confidence intervals with at least $95\,\%$ confidence level. Horizontal connecting lines cross the confidence interval bars at the median, but are for visualisation purposes only in between.)

seems to reduce the transmit power across longer distances more than the other channel model, which was also based on measurements in urban areas. Hence, the channel load is lower and the impact that the MAC protocol can have becomes smaller. Still, for many vehicles, SAFE leads to a small, but significant increase of the percentage of time with ideal awareness. Additionally, SAFE leads to substantial improvements of the PDR up to transmission distances of $400\,\mathrm{m}$. Many transmissions with a transmission distance of more than $100\,\mathrm{m}$ are likely impossible due to almost complete shadowing.

8.5.3. Performance Subject to Available Padding Bits

In all of the previous performance evaluations, a fixed message size of $200\,\mathrm{B}$ has been used, resulting in $488\,\mathrm{bit}$ of padding that can be used for the acknowledgements. However, there might be situations in which fewer padding bits are necessary to fill the TB. In these situations, SAFE has less space available to transmit the acknowledgement bitmap. Hence, the information upon which scheduling decisions are made might be less accurate. It is detrimental to understand the impact of this on the performance of SAFE. In this section, many different packet sizes and resulting padding sizes will be configured and evaluated with SAFE. Table 8.7 gives an overview of the packet sizes used in this section as well as the resulting padding sizes.

The Luxembourg scenario at 08:00 has been chosen as scenario for this evaluation. SAFE has been used in its final configuration. This means that all components of SAFE have been enabled, including DCC, which also makes use of the acknowledgement feedback. The performance of SAFE with different amounts of available padding is summarized in Table 8.8. The results of selected configurations is visualized in Figure 8.10 and 8.11.

The results of this evaluation show that only a very small amount of padding is necessary for SAFE to perform adequately. Even with only $32\,\mathrm{bit}$ of padding or acknowledgement feedback, the performance both under the PDR and application-oriented awareness metric is very similar to configurations with more available padding bits. The low amount of necessary overhead of SAFE even makes a non-padding-based deployment feasible, for example with a mandatory acknowledgement field. For padding-based approaches, the amount of acknowledgement feedback is still variable and there might not be any padding available at all. Even though this situation is very unlikely in practice, the results of the configuration with no available padding bits show that this situation should be prevented. A possible mitigation would be to extend SAFE so that an additional subchannel is used whenever a terminal has sent less than $32\,\mathrm{bit}$ of padding during the last second. This extension has no effect on the other, previous evaluation results as enough padding bits have been available with these configurations.

Table 8.7.: Packet Sizes and Resulting Padding Bits

Packet size [B]	Amount of Padding [bit]
261	0
257	32
253	64
245	128
229	256
197	512

Table 8.8.: Simulation Results: Performance Subject to Available Padding Bits

Amount of Padding [bit]	PDR [%] ($d \leq 100\,\mathrm{m}$)	PDR [%] ($d \leq 300\,\mathrm{m}$)	Time with $100\,\%$ Awareness [%]
0	94.94 ± 0.14	79.43 ± 0.35	89.5 [89.9, 90.0]
32	98.12 ± 0.03	91.08 ± 0.15	91.1 [91.0, 91.7]
64	98.38 ± 0.02	91.68 ± 0.15	91.3 [91.2, 91.4]
128	98.59 ± 0.02	92.08 ± 0.15	91.5 [91.3, 91.7]
256	98.69 ± 0.02	92.34 ± 0.16	91.6 [91.5, 91.7]
512	98.73 ± 0.03	92.41 ± 0.16	91.6 [91.4, 92.0]

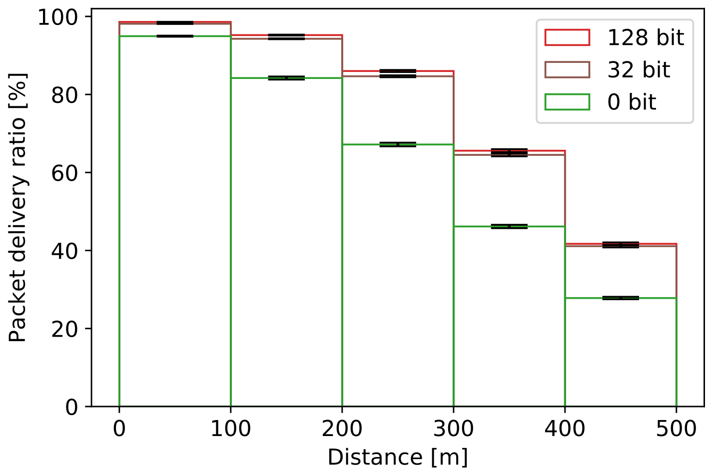

Figure 8.10.: Performance relative to available padding bits: mean PDR depending on transmission distance. Larger amounts of padding are not visually distinguishable and are not plotted. (Error bars indicate confidence intervals with a confidence level of $95\,\%$.)

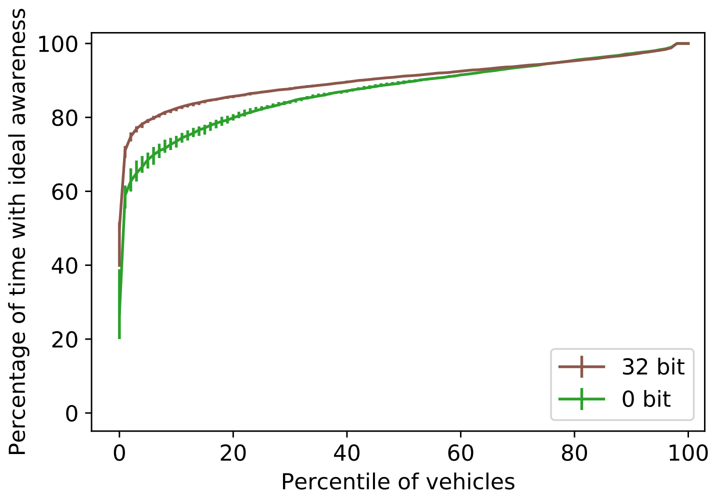

Figure 8.11.: Performance relative to available padding bits: quantile function plot of the percentage of time with ideal awareness for the range of $0\,\mathrm{m}$ to $300\,\mathrm{m}$. Larger amounts of padding are not visually distinguishable and are not plotted. (Vertical lines indicate asymmetric confidence intervals with at least $95\,\%$ confidence level. Horizontal connecting lines cross the confidence interval bars at the median, but are for visualisation purposes only in between.)

8.5.4. Performance with Variable CAM Sizes and Rates

As seen in Section 2.3.2.2, the rate and sizes of CAMs may vary in practice. The size depends on the presence and length of the *lowFrequencyContainer*, which contains the path history of the vehicle, and the presence of additional security information. The packet rate depends on the current change in position, heading, or velocity of the vehicle. Standard LTE-V2X is not suited for both of these non-periodic properties of packet flows. This might be reason enough to disable the variable CAM rate and use a fixed rate of $10\,\mathrm{Hz}$ for this access technology. However, this is only due to lack of support by LTE-V2X.

One of the advantages of SAFE that has been outlined in Chapter 5 is that it supports packet flows with varying size and rates at least to some extent. Those rates and sizes should follow the granularity of the sub-reservations, so that the periodicity can be retained. For example, one of five sub-reservations can be used to transmit a larger CAM that contains security, path history information, or both. Additionally, up to four of the sub-reservations can be disabled if the current movement pattern of the vehicle does not indicate the need for increased packet rates. These sub-reservations can be enabled and used on-demand, but should be so for some time, so that each sub-reservation can be used semi-persistently and the chance of other terminals have an increased chance of receiving these safety-critical messages.

For this evaluation, one long CAM with a size of $550\,\mathrm{B}$ is sent every $500\,\mathrm{ms}$. This message occupies all five subchannels in a subframe with a MCS index of six. The resulting TB size is $5160\,\mathrm{bit}$, resulting in $760\,\mathrm{bit}$ of padding. The other messages are $200\,\mathrm{B}$ long, and are only enabled throughout the duration of $2\,\mathrm{s}$ if one of the C-ITS triggering conditions becomes active. Two traffic scenarios have been evaluated: the Luxembourg scenario to represent a heterogeneous traffic scenario with moderate channel load, and the Manhattan grid scenario with $150\,\%$ traffic load for increased channel load.

Table 8.9 summarizes the simulation results in these scenarios, while the PDR for different transmission distances is plotted in Figure 8.12 and the results for the awareness metric can be seen in Figure 8.13. In the Luxembourg scenario, SAFE has a significantly higher PDR than standard LTE. The difference is especially pronounced in the ranges between $100\,\mathrm{m}$ to $400\,\mathrm{m}$. Interestingly, unlike in configurations with fixed packet rates and sizes, LTE-V2X is unable to achieve a PDR close to $100\,\%$ even in the lower transmission distances, i.e. between $0\,\mathrm{m}$ to $100\,\mathrm{m}$. The same cannot be said about SAFE, which is very close to optimal PDR values in shorter transmission distances.

The percentage of time with ideal awareness in the Luxembourg scenario shows that SAFE is able to have a significant lead over standard LTE-V2X, despite the fact that not all sub-reservations are continuously active. Compared to the results with fixed packet sizes and rates (Figure 8.7c on page 142), LTE-V2X is able to even lead to a slightly increased awareness. This is likely due to the increased randomness in the resource allocation scheme. As some terminals will stop using their resources for some time, others can use those resources without causing a repeating collision.

The PDR in the Manhattan scenario shows even more distinct differences in the PDR for the two approaches. In the transmission distance from $200\,\mathrm{m}$ to $300\,\mathrm{m}$, it is almost twice as high, while it is more than twice as high in larger distances. SAFE is again able to almost reach a perfect PDR in the $0\,\mathrm{m}$ to $100\,\mathrm{m}$ range, while LTE-V2X has a worse performance than in the Luxembourg scenario. One possible explanation for the bad performance of LTE-V2X in this scenario is that too many radio resources are reserved for the shorter packets. Depending on the parameter $\mathrm{sl{-}reselectAfter}$ and the current packet rate, the radio resources that have been reserved for the large CAM will also be used for the subsequent smaller ones. This means that there are many terminals that are likely to have a reservation of a complete subframe (five subchannels) but will only use the first two. Hence, the last three subchannels of many subframes will often be unused and there is a significantly higher probability for collision at the first two subchannels.

The Manhattan scenario with increased traffic load brings both approaches to the limit regarding the cooperative awareness. While SAFE is still able to outperform LTE-V2X substantially, neither approach is able to achieve outstanding results. This indicates that the long CAMs should not be sent in high-load scenarios. This should be enforced in the facilities layer, as the MAC layer has no knowledge about the contents of a message and the importance thereof.

Summary

SAFE has been evaluated and compared to LTE-V2X Mode 4 in this chapter. In the first part, the evaluation methodology and research questions have been established. The main part of the evaluation is carried out using a system-level simulation approach. The simulation framework and metrics have already been described in Chapter 6.

Before the evaluation, a set of research questions is stated. The first research questions target special situations and properties of SAFE. The next questions try are about the performance impact of the individual components of SAFE in order to determine whether each component of SAFE is necessary and beneficial. Moreover, it was investigated if the combined operation of the components of SAFE leads to additional advantages. The performance of the DCC component is also of interest. The next research questions target the performance of the complete system compared to LTE-V2X Mode 4. The performance at larger communication distances is especially important because hidden-terminal effects primarily occur at longer distances. The robustness of the communication is investigated with application-oriented metrics. Different scenarios are used to probe the performance of SAFE under more difficult conditions. These include channel models that explicitly consider obstacle shadowing, lower amounts of available padding bits, and varying packet rates and sizes.

The evaluation begins with a qualitative discussion. Functional requirements like the distributed resource scheduling, the detection of collisions and reaction to it, and the restriction of radio resource use in high load scenarios can be fulfilled by SAFE. By leveraging the padding bits, the overhead of the acknowledgement feedback is small or even negligible. SAFE does not influence the latency compared to LTE-V2X mode as it also respects the application-layer latency requirements when selecting radio resources. QoS aspects can be realized by selecting different modulation and coding schemes, which increases the robustness of the transmission. Moreover, QoS can easily be integrated into the DCC component or into the candidate

Table 8.9.: Simulation Results: Variable CAM Size and Rate

Scenario	Approach	PDR [%] ($d \leq 100\,\mathrm{m}$)	PDR [%] ($d \leq 300\,\mathrm{m}$)	Time with $100\,\%$ Awareness [%]
Luxembourg (08:00)	LTE	91.67 ± 0.24	69.67 ± 0.46	$55.3\ [53.4, 57.5]$
	SAFE	98.69 ± 0.03	91.76 ± 0.17	$87.1\ [86.7, 87.6]$
Manhattan ($150\,\%$ traffic)	LTE	87.08 ± 0.07	49.67 ± 0.06	$0.3\ [0.2, 0.3]$
	SAFE	97.56 ± 0.02	77.82 ± 0.04	$12.0\ [11.8, 12.7]$

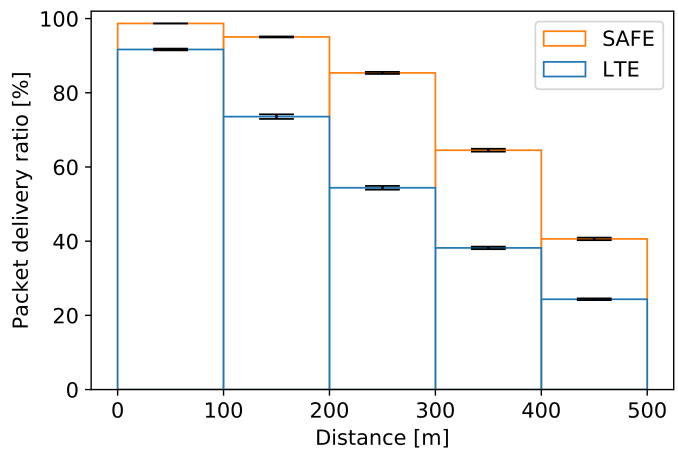

(a) Luxembourg at 8:00

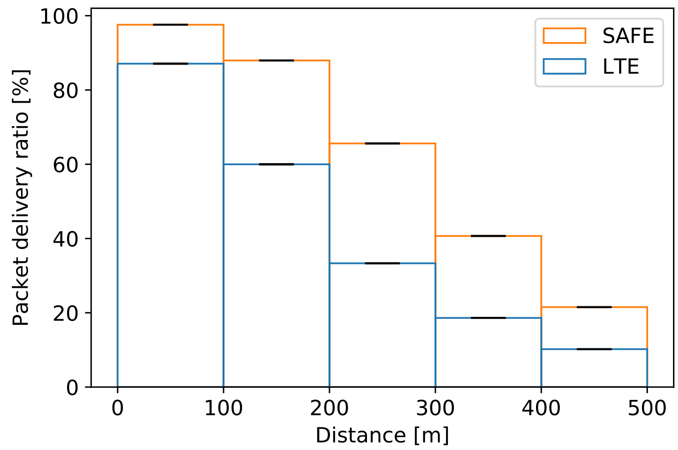

(b) Manhattan with $150\,\%$ traffic load

Figure 8.12.: Evaluation with variable CAM size and rate: mean PDR depending on transmission distance. (Error bars indicate confidence intervals with a confidence level of $95\,\%$.)

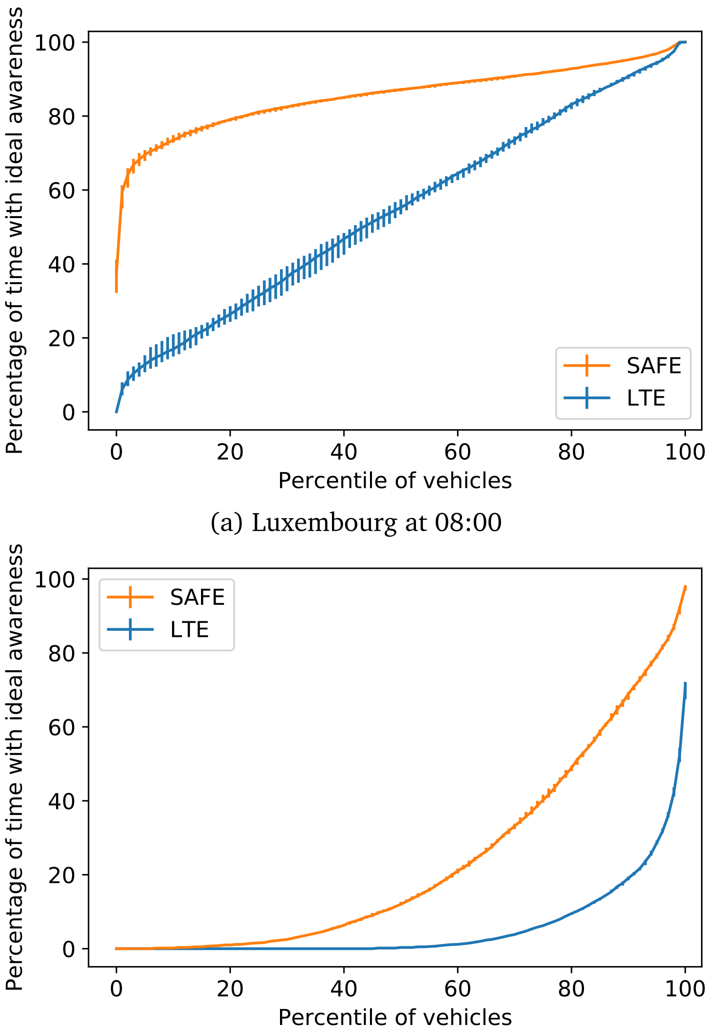

(a) Luxembourg at 08:00

(b) Manhattan

Figure 8.13.: Evaluation with variable CAM rate and size: quantile function plot of the percentage of time with ideal awareness for the range of $0\,\mathrm{m}$ to $300\,\mathrm{m}$. (Vertical lines indicate asymmetric confidence intervals with at least $95\,\%$ confidence level. Horizontal connecting lines cross the confidence interval bars at the median, but are for visualisation purposes only in between.)

resource selection, e.g. by introducing different minimum ratings for candidate resources depending on the priority of the packet. The DCC component does not restrict terminals past a threshold, which ensures fairness. The protocol works autonomously without the need for central scheduling instances and is compatible with physical layers based on SC-FDMA.

In the next section, important aspects have been investigated using analytic models. This includes the addressing of the acknowledgement feedback. The analysis showed that the acknowledgement feedback, although it references radio resources and not packets or transmitters, can only reach the wrong recipient under special conditions. These can be channel conditions changed in the meantime or the capture effect. The effect of this incorrect addressing or interpretation is limited.

Additionally, the probability of total blindness for a period of $500\,\mathrm{ms}$ has been determined for SAFE and LTE-V2X Mode 4. As all sub-reservations have to be affected by collisions for this to occur with SAFE and likely only one reservation is used with LTE-V2X Mode 4 in this period, SAFE can reach a significantly lower probabilities for total blindness.

The quantitative evaluation begins with a focus on the individual components of SAFE. As expected, reservation splitting itself does not have a large influence on the PDR. However, it leads to a large increase of the cooperative awareness as it increases the communication robustness and reduces the impact of repeating collisions. As SAFE is able to reach even higher awareness values than reservation splitting itself, it can be concluded that other components and/or synergy effects lead to an additional increase of the cooperative awareness. Similarly, the reaction to low acknowledgement ratios itself and the candidate resource selector without acknowledgements only leads to comparatively small increases of the PDR. If the new candidate resource selector is able to use the acknowledgement feedback as input, a large increase of the PDR is seen, especially at higher distances. This indicates that the acknowledgement feedback is an important input for the candidate resource selector that likely mitigates hidden-terminal problems effectively. If enabling every feature of SAFE at once, the best performance is reached both in terms of the PDR and the cooperative awareness.

The evaluation of the DCC component shows that SAFE is able to reach significantly higher PDR values. The DCC mechanism of LTE-V2X Mode 4 either does not lead to increased PDR or only to marginally improved performance. DCC can reduce the cooperative awareness by disabling sub-reservations with SAFE, but it still outperforms LTE-V2X.

SAFE proves itself also in configurations that are favourable towards LTE-V2X Mode 4. The performance is higher in all scenarios and under every metric. The differences in performance are lower if channel models that explicitly model obstacle shadowing are used. Due to the higher attenuation and the smaller scenario that had to be chosen because of the computational complexity, the channel utilisation is lower. Thus, the MAC protocol becomes less important and has less influence on the result. Moreover, the obstacles make some communication attempts impossible, which impacts the achievable cooperative awareness regardless of the MAC performance.

Additional studies show that SAFE requires a low amount of padding bits or transmitted acknowledgement feedback. In particular, SAFE shows significant performance increases if $30\,\mathrm{bit}$ to $50\,\mathrm{bit}$ of acknowledgement feedback is transmitted per packet. Due to the incompatibilities between SPS and packet flows with varying rates or sizes, LTE-V2X Mode 4 struggles to achieve acceptable performance in these situations. As these requirements have been considered in the design of SAFE, it can reach a large performance advantage over LTE-V2X.

Chapter 9.

Conclusion and Future Research

This chapter summarizes the thesis and presents possibilities for further research.

9.1. Summary

Traffic accidents play a major role when it comes to premature deaths or severe injuries. This impacts all generations, but especially 5- to 20-year-olds where traffic accidents are the leading cause of death. While the need for mobility is unprecedented, various technological advances have made traffic accidents both less likely and less severe. Vehicular communication is a future trend that promises a further reduction of the number of accidents. One of the most important applications of this technology is cooperative awareness, which is realised by broadcasting information about the position, speed, heading, etc., of a vehicle. Vehicular communication has new requirements and unusual communication patterns. For example, most of the communication is broadcast locally and of periodic nature, as the neighbouring vehicles need to be constantly updated with new information and the constellation of communication partners constantly changes due to the high terminal mobility. IEEE 802.11p was the first contender for an access technology designed for vehicle-to-vehicle (V2V) communication. It is based on WLAN but operates outside of the context of a base station. The request-to-send/clear-to-send (RTS/CTS) protocol is not used due to the overhead for broadcast communication. Special roadside units (RSUs) need to be deployed in order to support communication with the infrastructure.

The effort that is necessary for the deployment of the roadside equipment is very high. Years after the developments around IEEE 802.11p, the 3GPP developed long term evolution vehicle-to-everything (LTE-V2X), which was included in Release 14 of LTE. It also includes Mode 4, which is a distributed MAC protocol. Unlike the carrier sense multiple access/collision avoidance (CSMA/CA) protocol of IEEE 802.11p, semi-persistent scheduling (SPS) is introduced. As the physical layer uses single-carrier frequency division multiple access (SC-FDMA), the radio resources are divided into a fixed time and frequency grid. The MAC protocol requires transmitters to reuse radio resources several times. This reuse of radio resources is used to predict allocations of radio resources in the future. The creators of LTE-V2X therefore leverage the periodic nature of the messages typically exchanged in V2V communication.

However, additional investigations [WST19b] and other related work showed that while the general performance is good, this novel idea leads to new disadvantages that might be safety-critical. For example, due to SPS, collisions reoccur multiple times, and incompatibilities with packet flows with variable packet rates or sizes exist. This has been identified with a new application-oriented awareness metric, which is a methodical contribution of this dissertation. It is important to evaluate the system under consideration of the requirements of the intended application. Traditional metrics such as the packet delivery ratio (PDR) consider every packet as equally important, but it is a severe risk if there is a single vehicle that is unable to distribute status updates for extended periods of time.

The distributed congestion control (DCC) mechanism of LTE-V2X rarely leads to increased performance, and if so, only marginally. Like IEEE 802.11p, LTE-V2X Mode 4 does not deploy mitigations against hidden-terminal situations. Due to the recent release of the technology, only a limited amount of research that targets the improvement of the technology is available. Hence, there is an urgent and huge need for further improvements of this otherwise promising MAC protocol.

After the problem analysis in Chapter 4, an improved MAC protocol and DCC mechanism called SAFE was proposed. SAFE consists of four major components, some of which depend upon one another.

The first component of SAFE, reservation splitting [WST19a], alters the resource allocation by subdividing one reservation of resources into multiple sub-reservations that use different radio resources. These sub-reservations have a longer interval between reuses and are interleaved. This means that all of the sub-reservations need to be affected by collisions in order to completely prevent the dissemination of messages from a terminal.

SAFE uses a heuristic to acknowledge successfully and unsuccessfully received radio resources [WS20]. The broadcast nature of the communication system makes it necessary to use an efficient way to acknowledge transmissions as each receiver must propagate this information back to every transmitter. The acknowledgement feedback acknowledges radio resources instead of packets or transmitters. As transmitters can remember which radio resources they used in the past, they can determine whether the currently reused radio resource is subject to repeating collisions. If so, they select new radio resources ahead of time. This can work as reactive mitigation against reoccurring hidden-terminal problems, but also as remedy from incorrectly chosen radio resources in general.

The candidate resource selector additionally leverages this acknowledgement feedback. The acknowledgement feedback also indicates that a radio resource has been used in the past [WS20]. As it is transmitted by other terminals, it is from the view of these terminals. Hence, it can serve as range extension to the sensing mechanism and prevent hidden-terminal effects proactively. The candidate resource selector of SAFE also considers the explicit reservations of LTE-V2X Mode 4 and the average received signal strength indicator (RSSI). However, it eliminates interdependencies for the reasons to exclude candidate resources and instead calculates a rating for each candidate resource which is influenced by the predicted collision probability. The candidate resource selector has several configuration parameters that can be used to fine-tune SAFE.

The DCC component also leverages the acknowledgement feedback by predominantly disabling sub-reservations with low acknowledgement ratios [WST19a]. This ensures that the channel busy ratio (CBR) is lowered and additionally that a terminal stops using the resources that are more likely to be causing collisions. By semi-persistently disabling sub-reservations if the channel load is above a certain threshold, the periodic use of the sub-reservations is not disturbed. This helps the candidate resource selection process to make more accurate predictions.

A detailed system-level simulation framework has been designed and implemented for this dissertation. The simulation models every vehicle, i.e. terminal separately and independently and is based on different existing software components. These include SUMO and OMNeT++ along with various modules. Different channel models with varying simulation speed and modeling precision are available. A range of traffic scenarios, such as a part of the Luxembourg scenario as well as specifically designed artificial scenarios can be used. Various measures are taken in order to ensure that statistics are meaningful and significant. A special awareness metric can be used to assess the knowledge of the vehicles in the simulation in addition to the global PDR.

As SAFE has a number of configuration parameters, Chapter 7 uses the experimental designs and analysis of variance after Raj Jain [Jai91] to find optimal values for these parameters. Three different experimental designs have been created and multiple additional studies have been performed in order to find a set of good configuration parameters.

In the subsequent evaluation, SAFE has been assessed in a qualitative discussion, with a system-level simulation approach, and an analysis of selected aspects. SAFE showed that it can outperform LTE-V2X Mode 4 in all evaluated scenarios in the simulation, even if parameters that are beneficial for LTE-V2X Mode 4 have been chosen. Using the PDR and a custom, strict awareness metric, a major benefit of SAFE is the better communication reliability especially at high distances, as well as the significantly increased cooperative awareness. Most of the increase of this awareness can be attributed to reservation splitting, as multiple sub-reservations have to be affected by collisions in order prevent a terminal from successfully transmitting status updates. However, an investigation of the individual components of SAFE showed that each component is beneficial by itself, while the best performance can only be reached with a combined operation. The DCC component of SAFE is able to limit the channel load more effectively in extreme scenarios. Moreover, the PDR increase is significantly higher compared to LTE-V2X Mode 4. Additional simulations show that the required overhead for the acknowledgement feedback is very low. It can be of variable length and should fit inside the padding bits to fill the subchannels in most cases, so that it does not lead to additional overhead in practice. SAFE also leads to large benefits when packet flows with variable rate and packet sizes are used. This is because they can be mapped to sub-reservations, which can be enabled or disabled depending on application-layer requirements in order to reach the required packet rate. Moreover, they can reserve different numbers of subchannels for larger packets without breaking the periodic resource allocation. A subsequent analysis showed that it is unlikely that all sub-reservations are affected by collisions at the same time. Moreover, the acknowledgement feedback can only be interpreted by the wrong terminals in special conditions. These include sudden changes of the channel conditions or the capture effect.

9.2. Future Research and Enhancements

SAFE has been developed with Mode 4 of LTE-V2X, i.e. a distributed MAC protocol, in mind. Mode 3, i.e. the centrally scheduled mode of LTE-V2X, requires base stations to carry out the scheduling and signalling. These base stations must schedule radio resources for local broadcast with a lower range. Some of the interfering terminals or external interferers might be located far away from the base station, so that it might not be able to pick up the interference situation at the location of the terminals. The acknowledgement feedback has been shown to be an efficient heuristic to report the currently successful and unsuccessful transmissions, as well as the occupation of the resource grid as observed by the reporting terminal. It could also benefit from this condensed information in such cases.

SAFE allows for a prioritisation of packets using more robust modulation and coding schemes. The DCC component can use different CBR targets depending on the packet priority. As the impact of different CBR targets has already been investigated, this measure could be quickly implemented. Additional QoS measures are currently not part of SAFE. As indicated in previous Chapters, additional prioritisation could easily be integrated in the candidate resource selector, e.g. by setting different minimum ratings for resources. Radio resources with a very good rating could also be reserved for packets with a higher priority. The details of the implementation, mapping of resources, and effectiveness of this measure could be investigated in future work.

It is hard or even impossible to prevent malicious attacks on wireless systems as a simple jamming setup could potentially disrupt the complete communication. However, more sophisticated attacks might target only certain terminals or weaknesses. For examples, traffic accidents could be provoked for the purpose of subsequent insurance fraud by attacks that only target single terminals. Any distributed MAC protocol needs to trust each terminal at least to some extent. However, the security implications of new protocols of SAFE, e.g. the acknowledgement feedback, are not researched yet. This could be performed in future research.

Due to the lack of V2V hardware, SAFE has been developed solely using analytic evaluation and simulations. Real-world testing should be performed to assess potential problems that do not occur in these evaluation methods. These measurement campaigns might also require some of the configuration parameters of SAFE that have been determined in Chapter 7 to be altered.

The evaluation in Chapter 8 showed that only a surprisingly low number of padding bits is necessary for the acknowledgement feedback in order for SAFE to reach a good performance. This result also depends on the simulated scenario. In scenarios with fewer vehicles, less messages will be transmitted in total. This means that there are larger gaps between two transmissions, which could lead to a higher amount of required acknowledgement feedback. If the channel load is low, additional protocol overhead is not problematic because the radio resources would be unused otherwise anyway. However, a dynamic minimum threshold for the transmitted acknowledgement feedback might need to be investigated and implemented.

SAFE might also be used in scenarios other than vehicular traffic. Whenever a periodic stream of packets has to be locally broadcast via a wireless medium, SAFE or components of it might be applicable. This could include safety communication at sea, train depots, etc. SAFE might also be useful in wireless sensor networks in internet-of-things scenarios, e.g. in manufacturing. This leads to other possible modifications that might be necessary in this context.

Appendix A.

Acronyms

3GPP 3rd Generation Partnership Project

5G fifth generation

OMNeT++ Objective Modular Network Testbed in C++

A-MPR advanced maximum power reduction

ADAS advanced driver assistance system

AIFS arbitration inter-frame spacing

ARP address resolution protocol

ARQ automatic repeat request

ASN.1 abstract syntax notation one

BLER block error rate

BPSK binary phase shift keying

BSM basic safety message

BSS basic service set

BTP basic transport protocol

C-ITS cooperative intelligent transport systems

C-V2X cellular vehicle-to-everything

CALM communications access for land mobiles

CAM cooperative awareness message

CAV connected and autonomous vehicle

CBR channel busy ratio

CDMA code-division multiple access

CEN Comité Européen de Normalisation

CENELEC Comité Européen de Normalisation Électrotechnique

CPCL cooperative passive coherent location

CPM collective perception message

CR channel occupancy ratio

CRC cyclic redundancy check

CSMA/CA carrier sense multiple access/collision avoidance

CSMA/CD carrier sense multiple access/collision detection

D2D device-to-device

DCC distributed congestion control

DENM decentralized environmental notification message

DMRS demodulation reference symbol

DoS denial-of-service

DSRC dedicated short range communication

EDCA enhanced distributed coordination access

EIRP effective isotropic radiated power

eNodeB evolved node B

ETSI European Telecommunications Standards Institute

FCC Federal Communications Commission

FEC forward error correction

GNSS global navigation satellite system

GPU graphics processing unit

GUI graphical user interface

I2V infrastructure-to-vehicle

IDE integrated development environment

IEEE Institute of Electrical and Electronics Engineers

IP internet protocol

IPv4 internet protocol version 4

IPv6 internet protocol version 6

ITS intelligent transport systems

LDM local dynamic map

lidar light detection and ranging

LTE long term evolution

LTE-V2X long term evolution vehicle-to-everything

MAC media access control

MCS modulation and coding scheme

MIMO multiple-input and multiple-output

MPLS multi-protocol label switching

MPR maximum power reduction

NAS non-access stratum

OFDM orthogonal frequency division multiplex

OFDMA orthogonal frequency division multiple access

OSI Open Systems Interconnection

OTA over-the-air

P2P peer-to-peer

PAPR peak-to-average power ratio

PCL passive coherent location

PDCP packet data convergence protocol

PDR packet delivery ratio

PDU protocol data unit

PER packet error ratio

PIEV perception-intellection-emotion-volition

PLMN public land mobile network

PPPP proximity services per-packet-priority

PSCCH physical sidelink control channel

PSSCH physical sidelink shared channel

QAM quadrature amplitude modulation

QoS quality of service

QPSK quadrature phase shift keying

radar radio detection and ranging

RB resource block

RLC radio link control

RRC radio resource control

RSRP reference signals received power

RSSI received signal strength indicator

RSU roadside unit

RTS/CTS request-to-send/clear-to-send

SAE Society of Automotive Engineers

SAFE scheduling based on acknowledgement feedback exchange

SAP service access point

SC-FDMA single-carrier frequency division multiple access

SCI sidelink control information

SINR signal-to-interference-plus-noise ratio

SNR signal-to-noise ratio

SPS semi-persistent scheduling

SUMO Simulation of Urban Mobility

TB transport block

TCP transmission control protocol

TR technical report

TraCI traffic command interface

UDP user datagram protocol

UE user equipment

V2I vehicle-to-infrastructure

V2P vehicle-to-pedestrian

V2V vehicle-to-vehicle

V2X vehicle-to-everything

VANET vehicular ad hoc network

Veins vehicles in network simulation

WAVE wireless access in vehicular networks

WiMAX worldwide interoperability for microwave access

WLAN wireless local area network

WSN wireless sensor network

Appendix B.

Bibliography

[ASKT15] Taimoor Abbas, Katrin Sjöberg, Johan Karedal, and Fredrik Tufvesson. A measurement based shadow fading model for vehicle-to-vehicle network simulations. *International Journal of Antennas and Propagation*, 2015, 2015.

[Baz19] A. Bazzi. Congestion control mechanisms in IEEE 802.11p and sidelink C-V2X. In *2019 53rd Asilomar Conference on Signals, Systems, and Computers*, pages 1125–1130, 2019.

[CFFE17] L. Codeca, R. Frank, S. Faye, and T. Engel. Luxembourg SUMO traffic (LuST) scenario: traffic demand evaluation. *IEEE Intelligent Transportation Systems Magazine*, 9(2):52–63, 2017.

[CHS+07] L. Cheng, B. E. Henty, D. D. Stancil, F. Bai, and P. Mudalige. Mobile vehicle-to-vehicle narrow-band channel measurement and characterization of the 5.9 GHz dedicated short range communication (DSRC) frequency band. *IEEE Journal on Selected Areas in Communications*, 25(8):1501–1516, Oct 2007.

[CJLL07] Erik Coelingh, Lotta Jakobsson, Henrik Lind, and Magdalena Lindman. Collision warning with auto brake: a real-life safety perspective. *Innovations for Safety: opportunities and Challenges*, 2007.

[CMR+19] Claudia Campolo, Antonella Molinaro, Francesco Romeo, Alessandro Bazzi, and Antoine O. Berthet. Full duplex-aided sensing and scheduling in cellular-V2X Mode 4. In *Proceedings of the 1st ACM MobiHoc Workshop on Technologies, Models, and Protocols for Cooperative Connected Cars*, TOP-Cars '19, pages 19–24, New York, NY, USA, 2019. Association for Computing Machinery.

[Cor19] Intel Corporation. Outcome of offline discussion #2 for NR-V2X AI - 7.2.4.1.4 resource allocation mechanism. 3GPP Working Group Document R1-160284, Third Generation Partnership Project (3GPP), 2019.

[EGEK19a] Mohamed A. Abd El-Gawad, Mahmoud Elsharief, and HyungWon Kim. A comparative experimental analysis of channel access protocols in vehicular networks. *IEEE Access*, 7:149433–149443, 2019.

[EGEK19b] Mohamed A. Abd El-Gawad, Mahmoud Elsharief, and HyungWon Kim. A cooperative V2X MAC protocol for vehicular networks. *EURASIP Journal on Wireless Communications and Networking*, 2019(1):65, 2019.

[ESAKAND16] Fathi E. Abd El-Samie, Faisal S. Al-Kamali, Azzam Y. Al-Nahari, and Moawad I. Dessouky. *SC-FDMA for mobile communications*. CRC press, 2016.

[ETS09] ETSI. Intelligent transport systems (ITS); vehicular communications; basic set of applications; definitions. Technical Report 102 638, European Telecommunications Standards Institute (ETSI), June 2009. Version 1.1.1.

[ETS10] ETSI. Intelligent transport systems (ITS); communications architecture. European Standard (Telecommunications series) 302 665, European Telecommunications Standards Institute (ETSI), September 2010. Version 1.1.1.

[ETS11a] ETSI. Intelligent transport systems (ITS); decentralized congestion control mechanisms for intelligent transport systems operating in the 5 GHz range; access layer part. Technical Specification (TS) 102 687, European Telecommunications Standards Institute (ETSI), July 2011. Version 1.1.1.

[ETS11b] ETSI. Intelligent transport systems (ITS); vehicular communications; basic set of applications; part 2: specification of cooperative awareness basic service. Technical Specification (TS) 102 637-2, European Telecommunications Standards Institute (ETSI), March 2011. Version 1.2.1.

[ETS11c] ETSI. Intelligent transport systems (ITS); vehicular communications; GeoNetworking; part 4: geographical addressing and forwarding for point-to-point and point-to-multipoint communications; sub-part 1: media-independent functionality. Technical Specification 102 636-4-1, European Telecommunications Standards Institute (ETSI), June 2011. Version 1.1.1.

[ETS12a] ETSI. Intelligent transport systems (ITS); OSI cross-layer topics; part 1: architecture and addressing schemes. Technical Specification 102 723-1, European Telecommunications Standards Institute (ETSI), November 2012. Version 1.1.1.

[ETS12b] ETSI. Intelligent transport systems (ITS); OSI cross-layer topics; part 3: interface between management entity and access layer. Technical Specification 102 723-3, European Telecommunications Standards Institute (ETSI), November 2012. Version 1.1.1.

[ETS13a] ETSI. Intelligent transport systems (ITS); vehicular communications; GeoNetworking; part 2: scenarios. European Standard 302 636-2, European Telecommunications Standards Institute (ETSI), November 2013. Version 1.2.1.

[ETS13b] ETSI. Intelligent transport systems (ITS); vehicular communications; GeoNetworking; part 4: geographical addressing and forwarding for point-to-point and point-to-multipoint communications; sub-part 2: media-dependent functionalities for ITS-G5. Technical Specification 102 636-4-2, European Telecommunications Standards Institute (ETSI), October 2013. Version 1.1.1.

[ETS14a] ETSI. Intelligent transport systems (ITS); vehicular communications; basic set of applications; local dynamic map (LDM). European Standard 302 895, European Telecommunications Standards Institute (ETSI), September 2014. Version 1.1.1.

[ETS14b] ETSI. Intelligent transport systems (ITS); vehicular communications; GeoNetworking; part 1: requirements. European Standard 302 636-1, European Telecommunications Standards Institute (ETSI), April 2014. Version 1.2.1.

[ETS14c] ETSI. Intelligent transport systems (ITS); vehicular communications; GeoNetworking; part 3: network architecture. European Standard 302 636-3, European Telecommunications Standards Institute (ETSI), March 2014. Version 1.2.1.

[ETS14d] ETSI. Intelligent transport systems (ITS); vehicular communications; GeoNetworking; part 6: internet integration; sub-part 1: transmission of IPv6 packets over GeoNetworking protocols. European Standard 302 636-6-1, European Telecommunications Standards Institute (ETSI), May 2014. Version 1.2.1.

[ETS16] ETSI. Intelligent transport systems (ITS); OSI cross-layer topics; part 3: interface between management entity and access layer. Technical Specification 102 723-8, European Telecommunications Standards Institute (ETSI), April 2016. Version 1.1.1.

[ETS18a] ETSI. Intelligent transport systems (ITS); access layer specification for intelligent transport systems using LTE vehicle to everything communication in the 5,9 GHz frequency band. Technical Specification (TS) 103 613, European Telecommunications Standards Institute (ETSI), November 2018. Version 1.1.1.

[ETS18b] ETSI. Intelligent transport systems (ITS); access layer specification for intelligent transport systems using LTE vehicle to everything communication in the 5,9 GHz frequency band. Technical Specification (TS) 103 613, European Telecommunications Standards Institute (ETSI), November 2018. Version 1.1.1.

[ETS18c] ETSI. Intelligent transport systems (ITS); congestion control mechanisms for the C-V2X PC5 interface; access layer part. Technical Specification (TS) 103 574, European Telecommunications Standards Institute (ETSI), November 2018. Version 1.1.1.

[ETS19a] ETSI. Intelligent transport systems (ITS); ITS-G5 access layer specification for intelligent transport systems operating in the 5 GHz frequency band. European Standard (Draft) 302 663, European Telecommunications Standards Institute (ETSI), May 2019. Version 1.3.0.

[ETS19b] ETSI. Intelligent transport systems (ITS); vehicular communications; basic set of applications; analysis of the collective perception service (CPS); release 2. Technical Report (TR) 103 562, European Telecommunications Standards Institute (ETSI), December 2019. Version 2.1.1.

[ETS19c] ETSI. Intelligent transport systems (ITS); vehicular communications; basic set of applications; part 2: specification of cooperative awareness basic service. European Standard 302 637-2, European Telecommunications Standards Institute (ETSI), April 2019. Version 1.4.1.

[ETS19d] ETSI. Intelligent transport systems (ITS); vehicular communications; GeoNetworking; part 5: transport protocols; sub-part 1: basic transport protocol. European Standard 302 636-5-1, European Telecommunications Standards Institute (ETSI), May 2019. Version 2.2.1.

[ETS19e] ETSI. Intelligent transport systems (ITS); vehicular communications; GeoNetworking; part 7: amendments for LTE-V2X; sub-part 1: amendments to ETSI EN 302 636-4-1 (media-independent functionality). Technical Specification 102 636-7-1, European Telecommunications Standards Institute (ETSI), January 2019. Version 1.1.1.

[ETS19f] ETSI. Intelligent transport systems (ITS); vehicular communications; GeoNetworking; part 7: amendments for LTE-V2X; sub-part 2: amendments to ETSI

EN 302 636-5-1 (basic transport protocol). Technical Specification 102 636-7-2, European Telecommunications Standards Institute (ETSI), January 2019. Version 1.1.1.

[ETS19g] ETSI. LTE; evolved universal terrestrial radio access (E-UTRA) and evolved universal terrestrial radio access network (E-UTRAN); overall description; stage 2 (3GPP TS 36.300 version 14.10.0 release 14). Technical Specification (TS) 136 300, European Telecommunications Standards Institute (ETSI), July 2019. Version 14.10.0.

[ETS19h] ETSI. LTE; evolved universal terrestrial radio access (E-UTRA); multiplexing and channel coding (3GPP TS 36.212 version 14.10.0 release 14). Technical Specification (TS) 136 212, European Telecommunications Standards Institute (ETSI), July 2019. Version 14.10.0.

[ETS19i] ETSI. LTE; evolved universal terrestrial radio access (E-UTRA); packet data convergence protocol (PDCP) specification (3GPP TS 36.323 version 15.4.0 release 15). Technical Specification (TS) 136 323, European Telecommunications Standards Institute (ETSI), July 2019. Version 15.4.0.

[ETS19j] ETSI. LTE; evolved universal terrestrial radio access (E-UTRA); physical channels and modulation. Technical Specification (TS) 136 211, European Telecommunications Standards Institute (ETSI), May 2019. Version 14.9.0.

[ETS19k] ETSI. LTE; evolved universal terrestrial radio access (E-UTRA); physical layer; measurements (3GPP TS 36.214 version 15.3.0 release 15). Technical Specification (TS) 136 214, European Telecommunications Standards Institute (ETSI), October 2019. Version 14.10.0.

[ETS19l] ETSI. LTE; evolved universal terrestrial radio access (E-UTRA); physical layer procedures. Technical Specification (TS) 136 213, European Telecommunications Standards Institute (ETSI), May 2019. Version 14.9.0.

[ETS19m] ETSI. LTE; evolved universal terrestrial radio access (E-UTRA); radio link control (RLC) protocol specification (3GPP TS 36.322 version 15.2.0 release 15). Technical Specification (TS) 136 322, European Telecommunications Standards Institute (ETSI), July 2019. Version 15.2.0.

[ETS19n] ETSI. LTE; evolved universal terrestrial radio access (E-UTRA); radio resource control (RRC); protocol specification (3GPP TS 36.331 version 14.8.0 release 14). Technical Specification (TS) 136 331, European Telecommunications Standards Institute (ETSI), October 2019. Version 14.8.0.

[ETS19o] ETSI. LTE; evolved universal terrestrial radio access (E-UTRA); user equipment (UE) radio transmission and reception (3GPP TS 36.101 version 14.10.0 release 14). Technical Specification (TS) 136 101, European Telecommunications Standards Institute (ETSI), May 2019. Version 14.10.0.

[ETS19p] ETSI. Universal mobile telecommunications system (UMTS); LTE; 5G; non-access-stratum (NAS) protocol for evolved packet system (EPS); stage 3 (3GPP TS 24.301 version 15.7.0 release 15). Technical Specification (TS) 124 301, European Telecommunications Standards Institute (ETSI), July 2019. Version 15.7.0.

[ETS20] ETSI. LTE; evolved universal terrestrial radio access (E-UTRA); medium access control (MAC) protocol specification (3GPP TS 36.321 version 14.12.0 release 14). Technical Specification (TS) 136 321, European Telecommunications Standards Institute (ETSI), January 2020. Version 14.12.0.

[Eur06] European Commission. Communication from the commission to the council, the European parliament, the European economic and social committee and the committee of the regions – on the intelligent car initiative "raising awareness of ICT for smarter, safer and cleaner vehicles". Communication COM(2006) 59 final, European Commission, February 2006.

[Eur08] European Commission. Commission decision of 5 august 2008 on the harmonised use of radio spectrum in the 5875-5905 MHz frequency band for safety-related applications of intelligent transport systems (ITS). Commission Decision 2008/671/EC, European Commission, August 2008.

[Eur09] European Commission. Standardisation mandate addressed to CEN, CENELEC and ETSI in the field of information and communication technologies to support the interoperability of co-operative systems for intelligent transport in the European community. Mandate M/453 EN, European Commission, October 2009.

[Eur16] European Commission. Communication from the commission to the European parliament, the council, the European economic and social committee and the committee of the regions – a european strategy on cooperative intelligent transport systems, a milestone towards cooperative, connected and automated mobility. Communication COM(2016) 766 final, European Commission, November 2016.

[Eur19] European Commission. Commission delegated regulation (EU) .../... of 13.3.2019 supplementing directive 2010/40/EU of the european parliament and of the council with regard to the deployment and operational use of cooperative intelligent transport systems. Delegated Regulation C(2019) 1789 final, European Commission, March 2019.

[Fed20] Federal Communications Commission. Modernizing the 5.9 GHz band - first report and order, further notice of proposed rulemaking, and order of proposed modification. Report FCC-CIRC2011-01, Federal Communications Commission, October 2020.

[fSoT17] National Highway Traffic Safety Administration – National Center for Statistics and Analysis – U.S. Department of Transportation. Traffic safety facts 2015. A compilation of motor vehicle crash data from the fatality analysis reporting system and the general estimates system, 2017.

[GFG+09] E. Giordano, R. Frank, A. Ghosh, G. Pau, and M. Gerla. Two ray or not two ray this is the price to pay. In *2009 IEEE 6th International Conference on Mobile Adhoc and Sensor Systems*, pages 603–608, Oct 2009.

[GMT+16] H. Günther, B. Mennenga, O. Trauer, R. Riebl, and L. Wolf. Realizing collective perception in a vehicle. In *2016 IEEE Vehicular Networking Conference (VNC)*, pages 1–8, 2016.

[Gol05] Andrea Goldsmith. *Wireless communications*. Cambridge University Press, 2005.

[Gre00] Marc Green. "How long does it take to stop?" Methodological analysis of driver perception-brake times. *Transportation Human Factors*, 2(3):195–216, 2000.

[GRWF16] H. Günther, R. Riebl, L. Wolf, and C. Facchi. Collective perception and decentralized congestion control in vehicular ad-hoc networks. In *2016 IEEE Vehicular Networking Conference (VNC)*, pages 1–8, 2016.

[GTW15] H. Günther, O. Trauer, and L. Wolf. The potential of collective perception in vehicular ad-hoc networks. In *2015 14th International Conference on ITS Telecommunications (ITST)*, pages 1–5, 2015.

[HCZ+17] Jinling Hu, Shanzhi Chen, Li Zhao, Yuanyuan Li, Jiayi Fang, Baozhu Li, and Yan Shi. Link level performance comparison between LTE V2X and DSRC. *Journal of Communications and Information Networks*, 2(2):101–112, 2017.

[HH16] Huawei and HiSilicon. DMRS enhancement of V2V. 3GPP Working Group Study R1-160284, Third Generation Partnership Project (3GPP), 2016.

[HH19] Amir Haider and Seung-Hoon Hwang. Adaptive transmit power control algorithm for sensing-based semi-persistent scheduling in C-V2X Mode 4 communication. *Electronics*, 8(8):846, Jul 2019.

[HM11] Gerald J. Hahn and William Q. Meeker. *Statistical intervals: a guide for practitioners*, volume 92. John Wiley & Sons, 2011.

[HTFZ18] J. He, Z. Tang, Z. Fan, and J. Zhang. Enhanced collision avoidance for distributed LTE vehicle to vehicle broadcast communications. *IEEE Communications Letters*, 22(3):630–633, 2018.

[Jai91] Raj Jain. *The Art of Computer Systems Performance Analysis: Techniques for Experimental Design, Measurement, Simulation, and Modeling*. Wiley professional computing. Wiley, 1991.

[JCK19] S. Jung, H. Cheon, and J. Kim. Reducing consecutive collisions in sensing based semi persistent scheduling for cellular-V2X. In *2019 IEEE 90th Vehicular Technology Conference (VTC2019-Fall)*, pages 1–5, 2019.

[JKK18] Yongseok Jeon, Seungho Kuk, and Hyogon Kim. Reducing message collisions in sensing-based semi-persistent scheduling (SPS) by using reselection lookaheads in cellular V2X. *Sensors*, 18(12):4388, Dec 2018.

[JR71] Gunnar Johansson and Kåre Rumar. Drivers' brake reaction times. *Human Factors*, 13(1):23–27, 1971. PMID: 5542208.

[KJB18] B. Kang, S. Jung, and S. Bahk. Sensing-based power adaptation for cellular V2X mode 4. In *2018 IEEE International Symposium on Dynamic Spectrum Access Networks (DySPAN)*, pages 1–4, 2018.

[Kra98] Stefan Krauß. *Microscopic modeling of traffic flow: investigation of collision free vehicle dynamics*. PhD thesis, Deutsches Zentrum für Luft-und Raumfahrt eV, Hauptabteilung Mobilität und Systemtechnik, 1998.

[KWG97] S. Krauss, P. Wagner, and C. Gawron. Metastable states in a microscopic model of traffic flow. *Phys. Rev. E*, 55:5597–5602, May 1997.

[LBB+18] P. A. Lopez, M. Behrisch, L. Bieker-Walz, J. Erdmann, Y. Flötteröd, R. Hilbrich, L. Lücken, J. Rummel, P. Wagner, and E. Wießner. Microscopic traffic simulation using SUMO. In *2018 21st International Conference on Intelligent Transportation Systems (ITSC)*, pages 2575–2582, Nov 2018.

[LD12] Robert Layton and Karen Dixon. Stopping sight distance, April 2012.

[Luc20] Lucas Pförtner. Untersuchung der Auswirkungen von DENM Nachrichten auf die Fahrzeug zu Fahrzeug Kommunikation im LTE Modus 4. Master's thesis, Technische Universität Ilmenau, Germany, 2020.

[MB18] Vincent Martinez and Friedbert Berens. Survey on ITS-G5 CAM statistics. Technical report, Car 2 Car Communication Consortium, 2018.

[MBSP19] V. Mannoni, V. Berg, S. Sesia, and E. Perraud. A comparison of the V2X communication systems: ITS-G5 and C-V2X. In *2019 IEEE 89th Vehicular Technology Conference (VTC2019-Spring)*, pages 1–5, 2019.

[MG17] R. Molina-Masegosa and J. Gozalvez. System level evaluation of LTE-V2V Mode 4 communications and its distributed scheduling. In *2017 IEEE 85th Vehicular Technology Conference (VTC Spring)*, pages 1–5, June 2017.

[MGS18a] R. Molina-Masegosa, J. Gozalvez, and M. Sepulcre. Configuration of the C-V2X mode 4 sidelink PC5 interface for vehicular communication. In *2018 14th International Conference on Mobile Ad-Hoc and Sensor Networks (MSN)*, pages 43–48, 2018.

[MGS18b] R. Molina-Masegosa, J. Gozalvez, and M. Sepulcre. An IEEE 802.11p-assisted LTE-V scheduling for reliable multi-link V2X communications. In *2018 IEEE 88th Vehicular Technology Conference (VTC-Fall)*, pages 1–5, 2018.

[MMH19] A. Mansouri, V. Martinez, and J. Härri. A first investigation of congestion control for LTE-V2X mode 4. In *2019 15th Annual Conference on Wireless On-demand Network Systems and Services (WONS)*, pages 56–63, 2019.

[MSG19] R. Molina-Masegosa, M. Sepulcre, and J. Gozalvez. Geo-based scheduling for C-V2X networks. *IEEE Transactions on Vehicular Technology*, 68(9):8397–8407, 2019.

[NKDM18] A. Nabil, K. Kaur, C. Dietrich, and V. Marojevic. Performance analysis of sensing-based semi-persistent scheduling in C-V2X networks. In *2018 IEEE 88th Vehicular Technology Conference (VTC-Fall)*, pages 1–5, 2018.

[NSS$^+$17] T. V. Nguyen, P. Shailesh, B. Sudhir, G. Kapil, L. Jiang, Z. Wu, D. Malladi, and J. Li. A comparison of cellular vehicle-to-everything and dedicated short range communication. In *2017 IEEE Vehicular Networking Conference (VNC)*, pages 101–108, 2017.

[oES16] Institute of Electrical and Electronics Engineers Computer Society. Part 11: Wireless LAN Medium Access Control (MAC) and Physical Layer (PHY) Specifications. IEEE Standard 802.11-2016, Institute of Electrical and Electronics Engineers Standards Association, 2016.

[Off09] Official Journal of the European Union. Directive 2010/40/EU of the European parliament and of the council of 7 july 2010 on the framework for the deployment of intelligent transport systems in the field of road transport and for interfaces with other modes of transport. Directive 2010/40/EU, European Parliament and Council, October 2009.

[Pro19a] Third Generation Partnership Project. Final report of 3GPP TSG RAN WG1 #97 v1.0.0, August 2019.

[Pro19b] Third Generation Partnership Project. Final report of 3GPP TSG RAN WG1 #98 v2.0.0, October 2019.

[Pro19c] Third Generation Partnership Project. Final report of 3GPP TSG RAN WG1 #98bis v2.0.0, November 2019.

[Pro20] Third Generation Partnership Project. Final report of 3GPP TSG RAN WG1 #99 v1.0.0, March 2020.

[Rap96] Theodore S. Rappaport. *Wireless communications: principles and practice*, volume 2. Prentice Hall PTR, 1996.

[RGFW15] R. Riebl, H. Günther, C. Facchi, and L. Wolf. Artery: extending Veins for VANET applications. In *2015 International Conference on Models and Technologies for Intelligent Transportation Systems (MT-ITS)*, pages 450–456, June 2015.

[ROGLA03] Venkatesh Rajendran, Katia Obraczka, and J. J. Garcia-Luna-Aceves. Energy-efficient collision-free medium access control for wireless sensor networks. In *Proceedings of the 1st International Conference on Embedded Networked Sensor Systems*, SenSys '03, page 181–192, New York, NY, USA, 2003. Association for Computing Machinery.

[SAW+19] A. Schwind, C. Andrich, P. Wendland, M. Döbereiner, G. Del Galdo, G. Schaefer, R. S. Thomä, and M. A. Hein. Bi-static delay-Doppler emulation of cooperative passive vehicle-to-X radar. In *2019 13th European Conference on Antennas and Propagation (EuCAP)*, pages 1–5, 2019.

[Sch18] Michael Schubert. Simulation von Wellenausbreitung mittels Raytracing für Car-to-Car-Kommunikation. Master's thesis, Technische Universität Ilmenau, Germany, 2018.

[SD11] Christoph Sommer and Falko Dressler. Using the right two-ray model? A measurement based evaluation of PHY models in VANETs. In *The 17th Annual International Conference on Mobile Computing and Networking*, 2011.

[SDA+20] Andreas Schwind, Michael Döbereiner, Carsten Andrich, Philip Wendland, Giovanni Del Galdo, Guenter Schaefer, Reiner S. Thomä, and Matthias A. Hein. Bi-static delay-doppler reference for cooperative passive vehicle-to-X radar applications. *IET Microwaves, Antennas & Propagation*, 14:1749–1757(8), November 2020.

[SGD11] Christoph Sommer, Reinhard German, and Falko Dressler. Bidirectionally coupled network and road traffic simulation for improved IVC analysis. *IEEE Transactions on Mobile Computing*, 10(1):3–15, January 2011.

[Sin10] T. L. Singal. *Wireless communications*. Tata McGraw-Hill Education, 2010.

[SJD12] C. Sommer, S. Joerer, and F. Dressler. On the applicability of two-ray path loss models for vehicular network simulation. In *2012 IEEE Vehicular Networking Conference (VNC)*, pages 64–69, Nov 2012.

[SJS+15] C. Sommer, S. Joerer, M. Segata, O. K. Tonguz, R. L. Cigno, and F. Dressler. How shadowing hurts vehicular communications and how dynamic beaconing can help. *IEEE Transactions on Mobile Computing*, 14(7):1411–1421, July 2015.

[SLL+10] R. K. Schmidt, R. Lasowski, T. Leinmüller, C. Linnhoff-Popien, and G. Schäfer. An approach for selective beacon forwarding to improve cooperative awareness. In *2010 IEEE Vehicular Networking Conference*, pages 182–188, 2010.

[SSA+19] S. Schieler, C. Schneider, C. Andrich, M. Döbereiner, J. Luo, A. Schwind, P. Wendland, R. S. Thomä, and G. Del Galdo. OFDM waveform for distributed radar sensing in automotive scenarios. In *2019 16th European Radar Conference (EuRAD)*, pages 225–228, 2019.

[SSH18] A. Schwind, R. Stephan, and M. A. Hein. Simulations and measurements of the bistatic radar cross section of vulnerable road users between 2 GHz and 6 GHz. In *2018 IEEE MTT-S International Conference on Microwaves for Intelligent Mobility (ICMIM)*, pages 1–4, 2018.

[SSW19] S. Sabeeh, P. Sroka, and K. Wesołowski. Estimation and reservation for autonomous resource selection in C-V2X mode 4. In *2019 IEEE 30th Annual International Symposium on Personal, Indoor and Mobile Radio Communications (PIMRC)*, pages 1–6, 2019.

[Sum00] Heikki Summala. Brake reaction times and driver behavior analysis. *Transportation Human Factors*, 2:217–226, September 2000.

[TAG+19] R. S. Thomä, C. Andrich, G. D. Galdo, M. Döbereiner, M. A. Hein, M. Käske, G. Schäfer, S. Schieler, C. Schneider, A. Schwind, and P. Wendland. Cooperative passive coherent location: a promising 5G service to support road safety. *IEEE Communications Magazine*, 57(9):86–92, Sep. 2019.

[TSFM19] B. Toghi, M. Saifuddin, Y. P. Fallah, and M. O. Mughal. Analysis of distributed congestion control in cellular vehicle-to-everything networks. In *2019 IEEE 90th Vehicular Technology Conference (VTC2019-Fall)*, pages 1–7, 2019.

[TSG20] G. Thandavarayan, M. Sepulcre, and J. Gozalvez. Generation of cooperative perception messages for connected and automated vehicles. *IEEE Transactions on Vehicular Technology*, 69(12):16336–16341, 2020.

[TSM+18] B. Toghi, M. Saifuddin, H. N. Mahjoub, M. O. Mughal, Y. P. Fallah, J. Rao, and S. Das. Multiple access in cellular V2X: performance analysis in highly congested vehicular networks. In *2018 IEEE Vehicular Networking Conference (VNC)*, pages 1–8, Dec 2018.

[TSMF19] B. Toghi, M. Saifuddin, M. O. Mughal, and Y. P. Fallah. Spatio-temporal dynamics of cellular V2X communication in dense vehicular networks. In *2019 IEEE 2nd Connected and Automated Vehicles Symposium (CAVS)*, pages 1–5, 2019.

[VBM+18] Vladimir Vukadinovic, Krzysztof Bakowski, Patrick Marsch, Ian Dexter Garcia, Hua Xu, Michal Sybis, Pawel Sroka, Krzysztof Wesolowski, David Lister, and Ilaria Thibault. 3GPP C-V2X and IEEE 802.11p for vehicle-to-vehicle communications in highway platooning scenarios. *Ad Hoc Networks*, 74:17–29, 2018.

[VLL15] A. Vinel, L. Lan, and N. Lyamin. Vehicle-to-vehicle communication in C-ACC/platooning scenarios. *IEEE Communications Magazine*, 53(8):192–197, 2015.

[Wor18] World Health Organization. Global status report on road safety 2018, 2018.

[WS20] P. Wendland and G. Schaefer. Feedback-based hidden-terminal mitigation for distributed scheduling in cellular V2X. In *2020 IFIP Networking Conference (Networking)*, pages 549–553, 2020.

[WST19a] P. Wendland, G. Schaefer, and R. S. Thomä. LTE-V2X mode 4: increasing robustness and DCC compatibility with reservation splitting. In *2019 IEEE International Conference on Connected Vehicles and Expo (ICCVE)*, pages 1–6, 2019.

[WST19b] Philip Wendland, Guenter Schaefer, and Reiner Thomä. An application-oriented evaluation of LTE-V's Mode 4 for V2V communication. In *Proceedings of the 34th ACM/SIGAPP Symposium on Applied Computing*, SAC '19, pages 165–173, New York, NY, USA, 2019. ACM.

[YK20] Y. Yoon and H. Kim. Balancing power and rate control for improved congestion control in cellular V2X communication environments. *IEEE Access*, 8:105071–105081, 2020.

[Zaj12] Alenka Zajić. *Mobile-to-mobile wireless channels*. Artech House, 2012.

[ZHW+19] J. Zhao, X. He, H. Wang, X. Zheng, J. Lv, T. Luo, and X. Hou. Cluster-based resource selection scheme for 5G V2X. In *2019 IEEE 89th Vehicular Technology Conference (VTC2019-Spring)*, pages 1–5, 2019.